

Emerging mosquito-borne viruses: transmission and modulation of host defence

Jelke J. Fros



Emerging mosquito-borne viruses: transmission and modulation of host defence

Jelke J. Fros

Thesis committee

Promotors

Prof. Dr J.M. Vlak
Personal chair at the Laboratory of Virology
Wageningen University

Prof. Dr W. Takken
Personal chair at the Laboratory of Entomology
Wageningen University

Co-promotor

Dr G.P. Pijlman
Assistant professor, Laboratory of Virology
Wageningen University

Other members

Prof. Dr B.P.H.J. Thomma, Wageningen University
Prof. Dr H.F.J. Savelkoul, Wageningen University
Dr A. Kohl, University of Glasgow, United Kingdom
Dr B.E.E. Martina, Erasmus Medical Center, Rotterdam

This research was conducted under the auspices of the Graduate School of Production Ecology and Resource Conservation.

Emerging mosquito-borne viruses: transmission and modulation of host defence

Jelke J. Fros

Thesis

submitted in fulfilment of the requirements for the degree of doctor
at Wageningen University
by the authority of the Academic Board,
in the presence of the
Thesis Committee appointed by the Academic Board
to be defended in public
on Friday 5 June 2015
at 11 a.m. in the Aula.

Jelke J. Fros
Emerging mosquito-borne viruses: transmission and modulation of host defence
192 pp

PhD Thesis, Wageningen University, Wageningen, NL (2015)
With references, list of abbreviations and summaries in Dutch and English

ISBN 978-94-6257-424-3

Chapter 1	General Introduction	12
Chapter 2	West Nile virus: High transmission rate in north-western European mosquitoes indicates its epidemic potential and warrants increased surveillance	28
Chapter 3	Usutu virus, highly transmissible by northern house mosquitoes and a prelude to West Nile virus activity in Europe	40
Chapter 4	Mosquito Rasputin interacts with chikungunya virus nsP3 and determines the infection rate in <i>Aedes albopictus</i>	52
Chapter 5	Chikungunya virus nsP3 blocks stress granule assembly by recruitment of G3BP into cytoplasmic foci	74
Chapter 6	Chikungunya virus nonstructural protein 2 inhibits type I/II interferon-stimulated JAK-STAT signaling	86
Chapter 7	The C-terminal domain of chikungunya virus nsP2 independently governs viral RNA replication, cytopathicity, and inhibition of interferon signaling	108
Chapter 8	Chikungunya virus nsP2-mediated host shut-off disables the unfolded protein response	120
Chapter 9	General Discussion	138
References		158
Summary / Samenvatting		172
Abbreviations		180
Dankwoord		184
Curriculum Vitae		190

1 Chapter

General Introduction

“Mr President and Gentlemen –

- What I propose studying is the medium by which the pathogenic material of yellow fever is carried from the bodies of the infected to be implanted in the bodies of the non-infected.”

On August 14, 1881, this is how Dr. Carlos Juan Finley introduced his hypothesis to the Royal Academy of Sciences in Havana. At that time, Yellow fever virus (YFV) transmission was thought to occur through the air or via physical contact. With a series of keen observations and a rather barbaric experiment, Finley was the first to describe that mosquitoes are responsible for the transmission of YFV (1). Numerous species of mosquitoes and other haematophagous arthropods like ticks, sand flies and midges are now widely implicated in the transmission of pathogenic agents from protozoan, bacterial, nematode and viral origin. Arthropod-borne viruses (arboviruses) are the causative agents of many diseases in humans, animals and plants. Arboviruses have RNA genomes and belong to the families *Togaviridae*, *Flaviviridae*, *Bunyaviridae*, *Reoviridae*, *Rhabdoviridae*, or *Orthomyxoviridae*, with the exception of the dsDNA virus African swine fever virus (2). Arboviruses actively replicate in vertebrate as well as in invertebrate hosts. Most arboviruses infect wild animals and ‘spillover’ from their enzootic cycle occurs incidentally when an infected invertebrate feeds on humans. Some arboviruses, however, have developed urban transmission

cycles, in which humans have become the main amplifying hosts (Figure 1.1). In humans, arbovirus infections often cause febrile illness, the more severe infections can result in arthritogenic, encephalitic or haemorrhagic disease and sometimes death (3–5). YFV still infects thousands of people each year, with a case fatality rate of 20% to 50% (6). In addition, Japanese encephalitis virus (JEV) causes encephalitic disease in over 50,000 people resulting in 15,000 deaths annually (7). Dengue virus (DENV) infects 50 to 100 million people each year, with 250 to 500 thousand

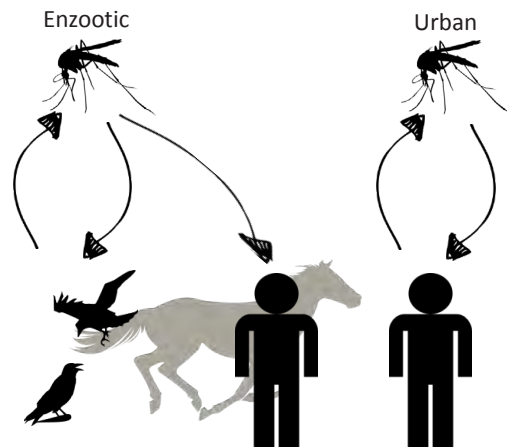


Figure 1.1. Arbovirus transmission cycles. Left, enzootic arbovirus transmission (e.g. WNV). In this example, the virus cycles between mosquitoes and avian amplifying hosts, with incidental infections in humans and horses. Right, urban arbovirus transmission (e.g. CHIKV). The virus is transmitted to humans by urban mosquitoes. The infected individual develops viral titres which are sufficient to infect blood feeding mosquitoes.

suffering from potentially lethal haemorrhagic disease (8). Outbreaks of arboviral disease continue to emerge as global travel and trade constantly relocates arboviruses and their vectors. Two highly pathogenic arboviruses, West Nile virus (WNV) and chikungunya virus (CHIKV), recently (re-)emerged in both Europe and the Americas, resulting in large-scale epidemics of severe encephalitic and arthritogenic disease, respectively.

WNV and CHIKV are unrelated viruses and belong to two distinct viral families. Moreover, WNV exists in an enzootic transmission cycle and is transmitted by numerous mosquito species from the *Culex* genus (9). It is unclear whether *Culex* mosquito populations from WNV-free areas can transmit WNV, although this information is imperative to assess the risk levels for outbreaks of WNV disease. The urban transmission cycle of CHIKV is maintained by two *Aedes* mosquito species (Figure 1.1). However, the molecular interactions that determine effective viral replication throughout the mosquito vector are poorly characterized. Currently there are no licensed vaccines or antiviral drugs available for human use against either WNV or CHIKV. Understanding the strategies that WNV and CHIKV employ to counteract cellular antiviral responses will contribute towards the development of safe and efficacious pharmaceuticals.

This thesis describes how effectively potential mosquito vectors transmit the flaviviruses WNV and Usutu virus (USUV) and provides novel insights on the underlying molecular mechanisms that enable the togavirus CHIKV to accomplish successful infections in both the mosquito and human hosts.

West Nile Virus

WNV is a flavivirus from the family *Flaviviridae*. The *Flavivirus* genus contains many tick and mosquito-borne viruses, including: YFV, DENV, and JEV. Flaviviruses are spherical enveloped viruses with a single stranded, positive sense RNA genome (ss(+)RNA) that contains a single open reading frame (ORF), flanked by 5' and 3' untranslated regions (UTR). In the infected cell, the ORF is translated into a single polyprotein that is further processed by viral and cellular proteases into both the viral structural and non-structural proteins (Figure 1.2, top). The 5'- and 3'-UTRs are highly structured and crucial for viral replication (10). WNV is transmitted mainly by *Culex* species mosquitoes and maintained in an enzootic cycle between the vector and susceptible bird species (11–14). Humans and horses are incidentally infected and considered dead-end hosts, as they generally do not develop sufficiently high viral titres to infect the next mosquito vector (Figure 1.1, left). Infection in humans is associated with febrile illness, which may develop into meningitis, encephalitis, myelitis and death (15). WNV was first isolated in 1937, Uganda, and a number of lineages have been described since, from which strains belonging to lineage 1 and 2 WNV have caused severe pathogenesis in humans (16).

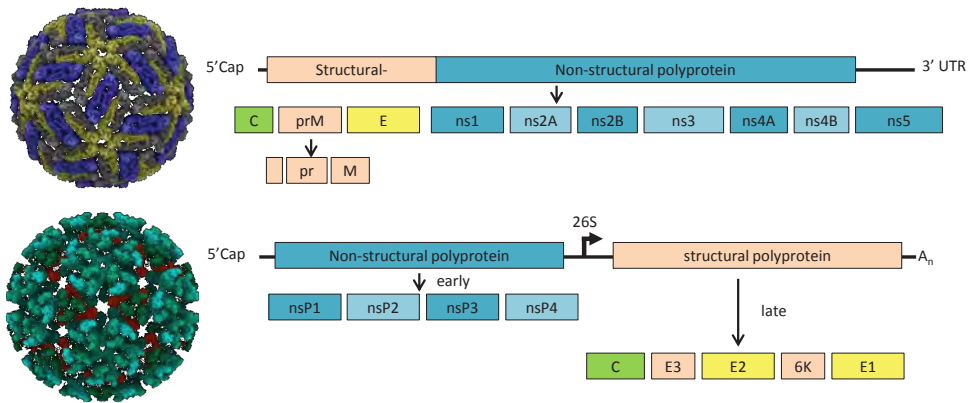


Figure 1.2. Viral particles and genome arrangement. Flavivirus (top) and alphavirus (bottom). Left, typical flavivirus and alphavirus virions. Right, schematic representation of the viral genomes and polyprotein(s). Images of virus particles courtesy of Jean-Yves Sgro.

Lineage 1 WNV has long been endemic in Africa, the Middle East, Asia and southern Europe (16, 17). August 23, 1999, a physician reported two patients with encephalitis in New York City (USA). At the same time, a substantial die-off in New York City birds was being reported. These events led to the first isolation of WNV in the western hemisphere (18). The resulting epidemic swept through North America, reaching the West Coast within three years. From 2008, WNV activity in the USA declined and was expected to reach low-level endemic activity. However, in 2012 WNV resurged and has remained highly active throughout 2013 and 2014 (19, 20). Lineage 1 WNV is now endemic in North America and has evolved into the largest outbreak of neuroinvasive disease to date (Figure 1.3)(18, 19). In addition, neuroinvasive WNV was detected in 2011, in Australia, after it caused disease in horses. This isolate was closely related to the naturally attenuated WNV lineage 1c, Kunjin virus, which is endemic in Australia and not normally associated with overt disease in humans or horses (Figure 1.3)(21).

In 2010, a lineage 2 WNV isolate initiated a large outbreak in Greece, resulting in 262 cases of human disease and 35 deaths (22). Until that moment, lineage 2 WNV strains were considered to be of low pathogenicity (16, 17). Lineage 2 WNV is now endemic in southern Europe and causes annual outbreaks in the region (Figure 1.3)(23, 24). In Central Europe, a related flavivirus, USUV, emerged a few years earlier. Like WNV, USUV is transmitted to birds by *Culex* species mosquitoes. Although pathogenesis in non-avian vertebrates is rare, incidental USUV infections have resulted in neuroinvasive disease in humans and horses (25–27). The emergence of USUV highlights the importance of understanding the transmission dynamics in order to assess potential risk levels and derive intervention strategies for these *Culex*-transmitted flaviviruses.

Chikungunya virus

CHIKV belongs to the *Togaviridae* family and the *Alphavirus* genus. The alphavirus genus contains 30 viruses, such as: Semliki forest virus (SFV), Sindbis virus (SINV), and O'nyong nyong virus (ONNV). The CHIKV ss(+)RNA genome of approximately 11.8 kb contains two ORFs, one of which is directly translated into a polyprotein containing non-structural proteins (nsP) 1234. nsP4 is proteolytically cleaved from this polyprotein. The remaining polyprotein and nsP4 form the replication complex (RC) that produces the (-)RNA. Further cleavage by the protease within nsP2 results in four individual nsPs, which collectively form the RC that produces the (+)RNA genomes and subgenomic messenger RNAs (28). nsP1 is the membrane anchor of the RC and possesses guanine-7-methyltransferase and guanylyl transferase activities necessary for capping of the viral RNA. nsP2 is the protease that cleaves the polyprotein, has helicase activity and causes general host shut-off. The functions of nsP3 are unknown, but it is an essential component of the RC. nsP4 is the RNA-dependent RNA polymerase (29). The subgenomic messengers are translated into the structural polyproteins (Figure 1.2, bottom). Capsid (C) is autocatalytically cleaved and encapsulates (+)sense viral RNA genomes in the cytoplasm forming nucleocapsids. The envelope proteins E1 and E2 mature while they are transported through the endoplasmic reticulum (ER) and Golgi apparatus to the plasma membrane, where the nucleocapsids are met and budding of progeny virus occurs (28).

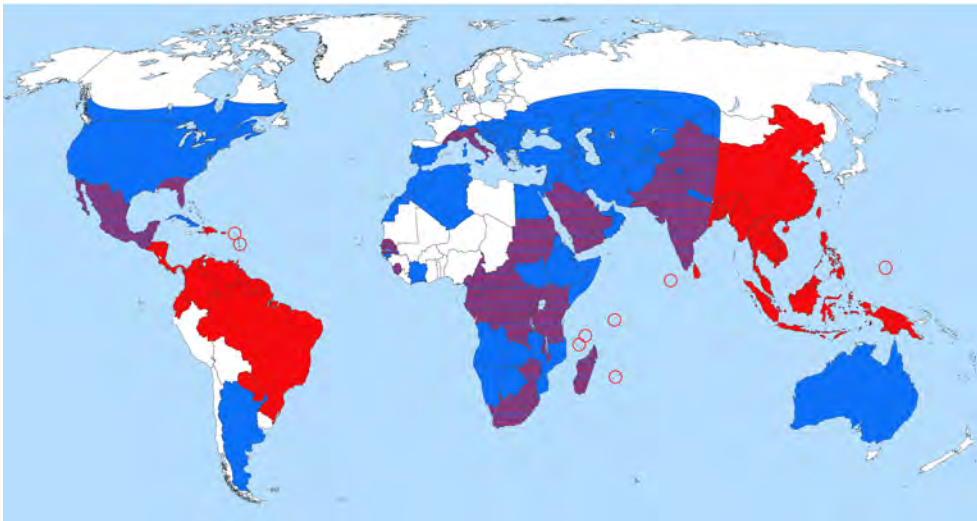


Figure 1.3. Global distribution of CHIKV and pathogenic WNV. Countries and areas with autochthonous transmission of pathogenic WNV (blue) and CHIKV (red). As of February 2015, adapted from (3,4,36,137).

In humans CHIKV infection can cause symptoms of high fever, rash and arthralgia. CHIKV exists in a sylvatic cycle between African, forest dwelling *Aedes* mosquito species and non-human primates. However, in urban areas CHIKV cycles between the more urban *Aedes aegypti* and *Aedes albopictus* mosquitoes and humans (Figure 1.1, right). Since its discovery in 1952, sporadic CHIKV outbreaks have been recorded in Central Africa and Southern Asia (30). However, from 2001 onwards several major outbreaks have occurred affecting the islands of Mauritius, Madagascar, Mayotte and Reunion. On Reunion Island CHIKV affected up to a third of the human population during the outbreak of 2005/2006. In 2006, mainland India suffered a major outbreak resulting in more than 1.4 million infected individuals. CHIKV activity has continued throughout Southern Asia where CHIKV is currently endemic (Figure 1.3) (31). In 2007, the first autochthonous transmission of CHIKV occurred on the European continent, infecting almost 250 people in Italy (32). In 2010 and 2014, CHIKV was again transmitted on European territory in the southeast of France (33, 34). In October 2013, the first cases of autochthonous CHIKV transmission in the western hemisphere were detected in the French Caribbean (35). Within the year, the distribution of CHIKV into the Americas has expanded greatly, affecting countries in South and Middle America as well as the South of the USA (Figure 1.3)(36).

The recent WNV and CHIKV outbreaks in Europe and the Americas illustrate that these viruses can adapt to new environments and different vector populations. The emergence of USUV in Central Europe suggests that more northern *Culex* species mosquitoes are also competent vectors for some flaviviruses. A better understanding of what factors drive arbovirus transmission is therefore necessary to assess the risk for the (re-)emergence of these arboviral diseases.

The mosquito vector

WNV can be transmitted by a long list of *Culex* species, which are present on every continent except Antarctica. Transmission is mostly horizontal i.e. via viraemic vertebrates. However, vertical, trans generational transmission to mosquito offspring has also been observed (37). In North America the most prevalent and effective vector species for WNV are *Culex pipiens*, *Culex tarsalis* and *Culex quinquefasciatus* (38, 39). After its first introduction into the USA, a number of WNV genotypes have evolved, and the currently circulating genotypes all have acquired a mutation in the envelope protein (V159A), which results in more efficient transmission by native *Culex* species (40). In Europe, the main *Culex* species found positive during WNV surveys is the common northern house mosquito *Cx. pipiens* (Figure 1.4)(41, 42).

Until recently CHIKV's only vector in urban areas was *Ae. aegypti*. However, in 2004 a point mutation was discovered in glycoprotein E1 at position

226 which enabled CHIKV to effectively use a second urban mosquito, *Ae. albopictus*, as a vector (Figure 1.4)(43). *Ae. aegypti* originated in Africa but is now widespread as global travel and trade have introduced it into tropical and subtropical regions across the globe. Similarly, the novel vector *Ae. albopictus* is originally from South-East Asia and has been introduced into Africa, the Americas, Europe and Australia where it has established stable populations. *Ae. albopictus* is a highly invasive species and its distribution extends further into more temperate climates. Both mosquito species are well adapted to urban environments and their daytime biting patterns and aggressive biting behaviour can cause intense nuisance.

In Europe, the distribution of the invasive mosquito species *Ae. aegypti* and *Ae. albopictus*, as well as the native species *Cx. pipiens* is well documented. The CHIKV outbreaks in Italy and France were confined to areas where *Ae. albopictus* has established stable populations. Outbreaks of WNV have occurred throughout southern Europe, even though the distribution of its vector *Cx. pipiens* extends into Scandinavia and the United Kingdom (Figure 1.4)(33, 42).

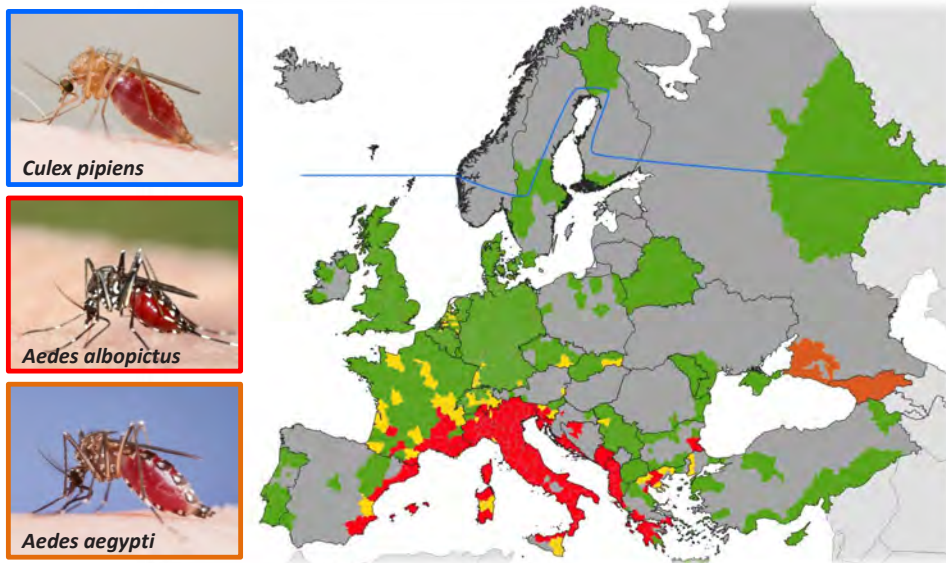


Figure 1.4. Mosquito vectors in Europe. Left, common WNV and CHIKV vectors, *Cx. pipiens* and *Ae. albopictus* and *Ae. aegypti*, respectively. Right, vector distribution as of October 2014. The Blue line represents the northern border of the territory of *Cx. pipiens*. Locations where *Ae. albopictus* or *Ae. aegypti* have established stable populations are coloured red and orange, respectively. Yellow, indicates sites where *Ae. albopictus* has been introduced and green, areas where both *Aedes* species are absent. The presence of these mosquito species in the grey areas has not been investigated. Distribution of *Aedes* mosquitoes adapted from (319) and *Cx. Pipiens* from (42). Images of *Cx. Pipiens* and *Ae. aegypti* courtesy of Hans Smid.

Outbreaks of arboviral disease depend on the presence and abundance of vertebrate amplifying hosts, competent vector species and their capacity to transmit the disease. The vectorial capacity is therefore a function of the vector density in relation to its vertebrate host, the frequency of feeding, the vector's life expectancy, the extrinsic incubation period (EIP), and the vector competence. The vector competence represents the ability of a vector to become infected and successfully transmit the virus to a subsequent vertebrate host. After the mosquito imbibes the blood of a viraemic vertebrate (Figure 1.5a), the virus enters the midgut (Figure 1.5b) and infects the midgut epithelium cells (figure 1.5c). After successful replication in these cells, the virus must infect the haemolymph (Figure 1.5d) and disseminate into other tissues, including the salivary glands (Figure 1.5e). When the virus accumulates in the salivary gland ducts, the mosquito is able to infect the next vertebrate host during a subsequent blood meal, marking the end of the EIP (Figure 1.5f)(38). The vector competence is an evaluation of the vector's capability to transmit a pathogen. The vector competence is often presented as an infection rate at a certain initial virus dose, e.g. percentage of infected mosquitoes, and transmission rate e.g. percentage of mosquitoes with detectable virus in their saliva.

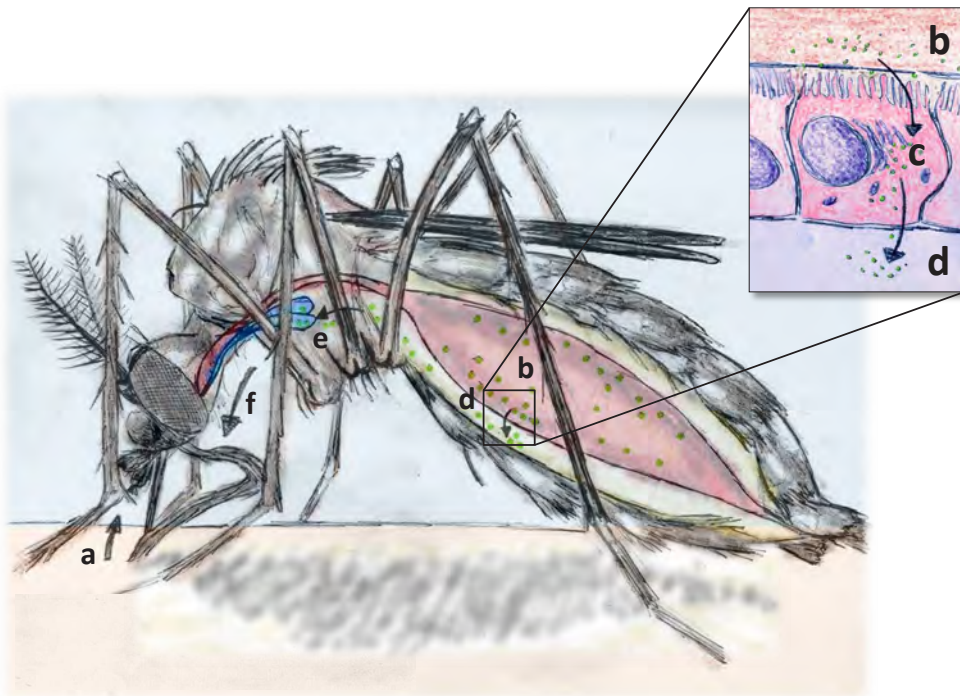


Figure 1.5. Schematic representation of an arbovirus infection in the mosquito vector. A. The mosquito ingests blood from an infected vertebrate. B. The virus (green) enters the midgut and infects the epithelium cells. C. Viral replication is established in the midgut epithelium cells. D. Virus escapes from the midgut epithelium into the haemolymph. E. dissemination into the salivary glands. F. Infected saliva is injected during subsequent blood feeding.

Arboviruses persistently infect their arthropod vector with little to no pathogenesis. This suggests that antiviral responses in the vector control the level of virus replication. Indeed, several mosquito antiviral defence pathways are implicated in the control of arbovirus infections. Insects possess immune pathways that are analogous to those found in humans and other vertebrates (e.g. the Toll pathway, the immune deficiency pathway (IMD) and the Janus kinase signal transducer and activator of transcription (JAK-STAT)) and RNA-mediated gene silencing pathways (reviewed by (44)).

The Toll and IMD pathways detect specific pathogen derived ligands and activate toll-regulated and IMD-regulated gene transcription via their respective intracellular signalling pathways. Both pathways play crucial roles in the invertebrate defence against pathogens. However, their role in fighting off arbovirus infections is less pronounced. The Toll pathway controls DENV infection and activates Toll-regulated gene transcription in the midgut of *Ae. aegypti* (45). Infections with SINV and DENV also upregulate IMD-regulated genes in *Ae. aegypti* (45–47). The invertebrate JAK-STAT pathway is activated by binding of an invertebrate cytokine to the transmembrane receptor dome. Kinases on the cytoplasmic tail of the receptor activate, by phosphorylation, STAT molecules, which then form dimers and translocate to the nucleus to induce antiviral gene transcription (48). The JAK-STAT pathway is also involved in the control of DENV infections in the mosquito midgut (49).

The RNA interference (RNAi) pathway is a predominant innate immune response in plants and insects. Double-stranded viral RNA from replication intermediates or secondary RNA structures are cleaved by the enzyme Dicer 2 (Dcr-2) into short interfering RNAs (siRNA) of usually 21 base pairs. These siRNAs are loaded into a multi-protein RNA silencing complex (RISC) and used as a template to target complementary viral RNA (reviewed in (50)). RNAi controls, among others, WNV and CHIKV infections in mosquitoes (51–54) and affects the infection of the mosquito midgut (51, 55). In addition, larger virus-derived RNAs (24–30 nt) have been found in CHIKV and DENV infected mosquitoes (56, 57). These RNAs suggest the involvement of a Dcr-2-independent RNA-based antiviral defence pathway, the PIWI-interacting RNA pathway. To counteract the RNAi pathway, many plant and insect viruses encode viral suppressors of RNAi (VSRs) (58–60). However, VSRs have not been found in arboviruses (61, 62). Introducing VSRs in arbovirus genomes has resulted in reduced siRNA expression, increased replication and reduced mosquito survival (63).

Additional mosquito host factors that influence viral entry, replication and the modulation of antiviral defences are poorly characterized. However, barriers surrounding the mosquito midgut have been identified. The mesenteron (midgut) infection barrier (MIB) prevents viral entry and replication in these midgut epithelial cells. The mesenteron escape barrier (MEB), prevents the escape of virions from the midgut cells and subsequent dissemination to other

tissues (64, 65). Similarly, salivary gland barriers have also been reported (reviewed in (65)).

The human host

To combat viral infections, higher eukaryotes make use of both innate and adaptive immune responses. The most potent antiviral innate immune response in mammals is the type I interferon (IFN) response. Invading viruses are recognised by cytoplasmic pattern recognition receptors (PRRs) retinoic acid-inducible gene I (RIG-I) and melanoma differentiation-associated gene 5 (MDA5) and/or members of the membrane bound Toll-like (TLR) receptor family. These receptors detect viral dsRNA, ssRNA and CpG DNA ligands and transduce the signal via a number of intracellular pathways to activate NF- κ B and IFN response factors (IRF) 3 and 7. The latter then translocate to the nucleus, inducing the expression of pro-inflammatory cytokines and type 1 IFNs (IFN- α/β) (Figure 1.6, left). Type 1 IFNs are secreted and attach to heterodimeric cell surface receptors IFN alpha receptor (IFNAR) 1 and 2. Tyrosine

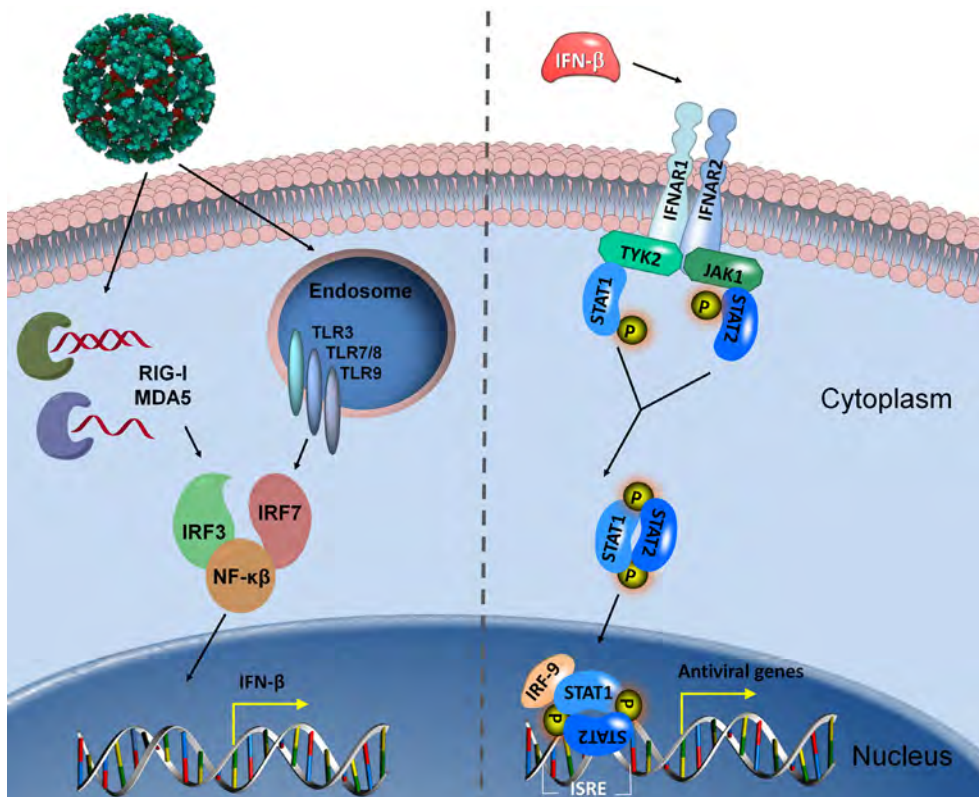


Figure 1.6. Interferon response. Left, Viral replication activates TLRs, RIG-I, and MDA5. Via their respective signalling cascades, IRF3/7 and NF- κ B are activated and subsequently upregulate the transcription of inflammatory cytokines and type 1 IFNs. Right, type 1 IFN binds to IFNAR_{1/2} and transduces the signal through TYK2 and JAK₁ to phosphorylate STAT_{1/2}. The STAT heterodimer translocates to the nucleus and induces expression of antiviral genes.

kinase 2 (Tyk2) is associated with the cytoplasmic tail of IFNAR₁ and is phosphorylated upon IFN binding. This creates a strong docking site for STAT2. STAT2 associates with STAT1 and both STAT1 and STAT2 are phosphorylated by Tyk2 and JAK1. The phosphorylated STAT hetero-dimer is then transported to the nucleus. Together with the protein IRF-9, the STAT hetero-dimer binds to the IFN-stimulated response element (ISRE), resulting in the transcription of many IFN-stimulated genes (ISG)(Figure 1.6, right). ISGs include the above mentioned PRRs and many of the downstream signalling proteins and transcription factors, but also antiviral effector genes e.g. IFIT and mx proteins. The up-regulation of these ISGs renders cells more resistant to viral infection, bringing them in an anti-viral state (reviewed by (66, 67)). During *in vivo* infections, the type 1 IFN response is required to limit CHIKV infection and IFN- α can inhibit CHIKV replication when administered before, but not after infection (68–70). Similarly, WNV infections in inbred mice, lacking crucial components of the type 1 IFN response, were highly pathogenic. However, pre-treatment with IFN- α protected against lethal WNV infection (71–73).

Given the potency of the IFN response and the resulting antiviral state, it is not surprising that most vertebrate viruses have evolved countermeasures. Flaviviruses have evolved a range of mechanisms to suppress the IFN response. The NS5 proteins of WNV, JEV, Langat virus (LGTV) and tick borne encephalitis virus (TBEV) inhibit the phosphorylation of STAT1 (74–77). NS5 of DENV binds and degrades STAT2 (78, 79). Additionally, DENV, WNV and YFV NS4B have been shown to inhibit the IFN response by suppressing STAT1 signalling (80, 81) and the NS2A protein of Kunjin virus inhibits gene transcription driven by the IFN- β promoter (82). In contrast, replication of CHIKV and other alphaviruses in mammalian cells results in dramatic shut-off of host gene expression, which results in cytopathicity (83, 84). A P726S substitution in a conserved region of SINV nsP2 was previously reported to reduce SINV cytopathicity (85). General host shut-off also results in suppression of the innate immune response (28). However, the alphavirus Venezuelan equine encephalitis virus inhibits STAT1 signalling, independent of host cell shut-off (86); for other alphaviruses direct mechanisms to antagonize the IFN response have been suggested (87, 88).

Additional cellular responses, such as the occurrence of stress granules (SGs) may influence the outcome of an arboviral infection as SGs can have diverse pro- or antiviral activities (reviewed by (89)). SGs are non-membranous cytoplasmic focal structures, which rapidly aggregate in response to different types of local environmental stress. In an effort to maintain cellular homeostasis, SGs may function to delay or inhibit mRNA translation or increase mRNA stability during times of cellular stress, e.g. viral infection (90). SGs contain many RNA binding proteins, mRNAs and translation initiation factors (Figure 1.7). Viral products of WNV and DENV have been suggested to interact with SG components, inhibiting the formation of SGs (91). SINV nsP3 interacts with the essential stress granule component Ras-GAP SH3 domain-binding protein

(G3BP)(92, 93), but whether this has a role in the modulation of SGs is unknown.

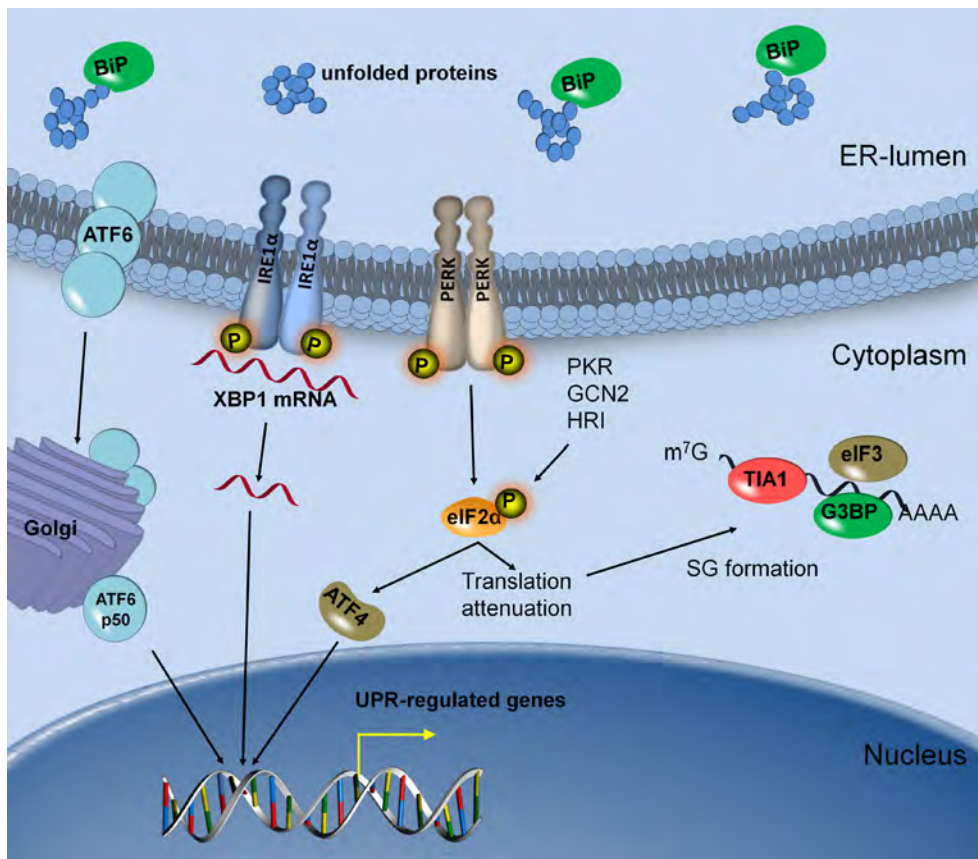


Figure 1.7. Unfolded protein response and stress granule assembly. BiP binds unfolded proteins in the lumen of the ER, activating the three arms of the UPR. ATF6 translocates to the Golgi where it is cleaved resulting in an active transcription factor. IRE1α splices out an intron from XBP1 mRNA, which is now translated as a transcription factor. PERK phosphorylates eIF2α, shutting down general translation whilst ATF4 is still efficiently translated. The phosphorylation of eIF2α by PERK or other kinases may result in the formation of SGs.

Finally, the production of progeny virus requires that the envelope glycoproteins of many viruses including WNV and CHIKV translocate into the ER for post-translational modifications. Large amounts of viral glycoproteins can disrupt the homeostasis within the ER, resulting in the accumulation of misfolded proteins, which activates the unfolded protein response (UPR). The UPR aims to resolve ER-stress by increasing the protein folding capacity of the ER and reducing cellular protein synthesis via the phosphorylation of eukaryotic initiation factor 2α (eIF2α). However, when unsuccessful it will also initiate apoptosis. In the presence of misfolded proteins, three ER-transmembrane proteins; activating transcription factor 6 (ATF6), dsRNA-dependent protein kinase (PKR)-like ER kinase (PERK), and inositol-requiring 1α (IRE1α) detect

misfolded proteins in the ER via the release of ER resident protein Ca^{2+} -dissociated heavy-chain binding protein (BiP). ATF6 translocates via the Golgi apparatus to the nucleus. PERK phosphorylates eIF2 α leading to a general inhibition of cellular translation, whilst the expression of transcription factor ATF4 is upregulated. Active IRE1 α splices out an intron from X-box-binding protein 1 (XBP1) mRNA, to produce a potent transcription factor (reviewed by (94)). The three distinct UPR transcription factors upregulate the transcription of a number of UPR-associated genes (Figure 1.7). In addition, the UPR may also strengthen the IFN response by activating pro-inflammatory transcription factors and cytokine production (reviewed by (95)). WNV NS4A and NS4B regulate ER-stress responses which in turn correlate with the inhibition of JAK-STAT signalling (96). The envelope proteins of SFV induce apoptosis via the activation of the UPR (97), whilst compounds that induce the UPR, reduced infections with SINV and other RNA viruses in mammalian cells (98).

Outline of the thesis

The emerging arboviruses, CHIKV and WNV must replicate in both the vertebrate and invertebrate hosts to complete their respective transmission cycles. This requires both viruses to cope with diverse antiviral responses. In the case of mosquitoes infections lead to relatively high levels of virus production without disease symptoms, whereas in the vertebrate host virus replication initiates strong antiviral responses and disease. This thesis further describes how efficient WNV can be transmitted by potential mosquito vectors and provides novel insights of how CHIKV accomplishes successful transmission via modulation of the invertebrate and vertebrate host-cell responses (Figure 1.8).

In Europe, the presence of invasive *Ae. albopictus* mosquitoes enabled CHIKV transmission in Italy and France (32–34). In contrast, WNV is endemic in the Mediterranean basin, whereas the geographic distribution of its vector *Cx. pipiens* extends North into Scandinavia (41, 42). In **Chapter 2**, the vector competence of north-western European *Cx. pipiens* mosquitoes is determined for two pathogenic WNV lineages, in comparison with American mosquitoes. In addition, this chapter evaluates what influences the current distribution of WNV in Europe to better assess the risk for further spread of both WNV lineages on this continent. USUV has also recently emerged in Europe. Compared to WNV, the distribution of USUV extends more into central and northern parts of Europe. **Chapter 3** thus describes how the vector competence of European *Cx. pipiens* mosquitoes for USUV compares to that for WNV to better understand the transmission dynamics and assess the potential spread of these related flaviviruses.

The molecular mechanisms that determine vector competence are largely unknown. Interestingly, when the genes encoding nsP₃ of CHIKV (vector; *Aedes* mosquitoes) and related alphavirus ONNV (vector; *Anopheles* mosquitoes) were exchanged, CHIKV became infectious for *An. gambiae* (99). Herein lies the hypothesis that a specific interaction between the vector and alphavirus nsP₃ may determine the vector competence. nsP₃ of the alphavirus SINV interacts with the endogenous mosquito protein Rasputin (Rin)(93). **Chapter 4** investigates the potential interaction between CHIKV nsP₃ and mosquito Rin and whether Rin is essential to establish

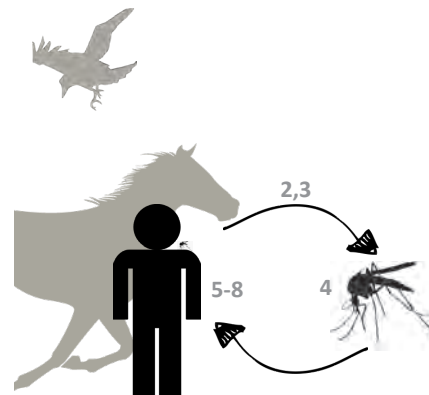


Figure 1.8. Schematic representation of the topics in this thesis. Summary of the arbovirus transmission cycle. Numbers indicate chapters at their respective location within the transmission cycle.

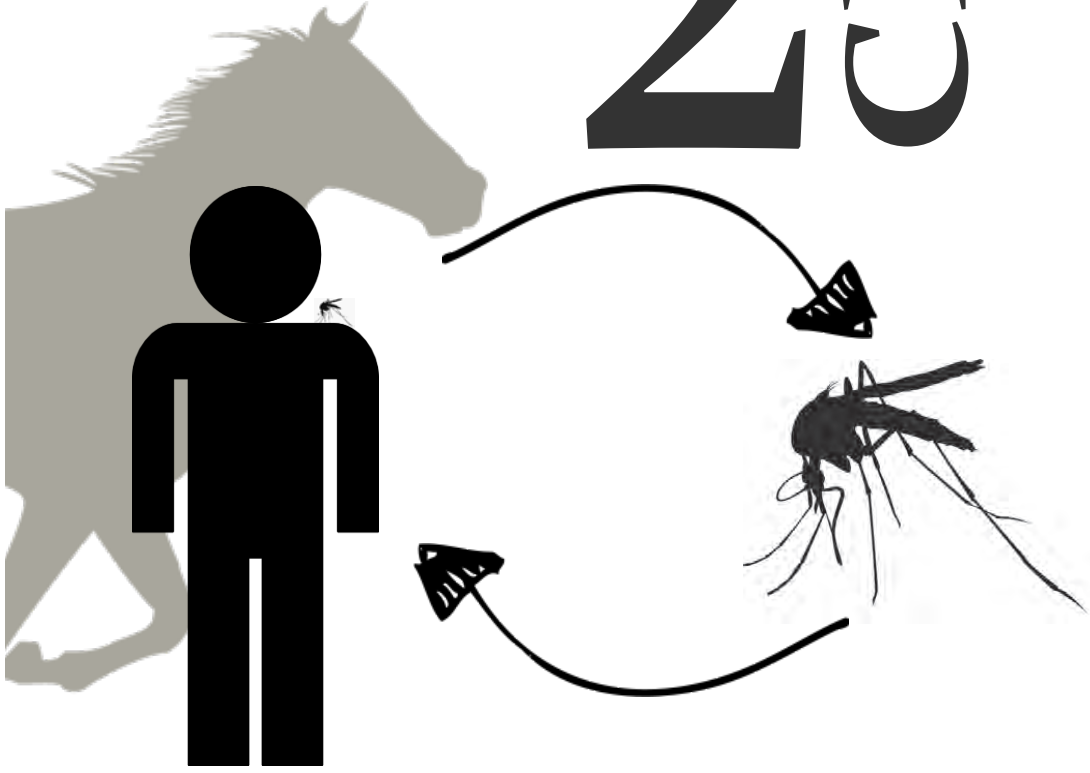
transmissible CHIKV infections in *Ae. albopictus*.

The mammalian homologue to mosquito Rasputin, G3BP also interacts with CHIKV nsP3 in vertebrate cells (93). G3BP itself is a functional and essential component of stress granules. **Chapter 5** describes the first function of alphavirus nsP3 and demonstrates how the interaction between nsP3 and G3BP modulates the formation of SGs. While SGs contribute to a stronger and more specific innate immune response, the IFN response is the most potent antiviral response that vertebrates possess. Flaviviruses have a number of ways to inhibit the IFN-response, whereas alphavirus infection in mammalian cells causes a general host shut-off (84). **Chapter 6** examines CHIKV for additional specific strategies to counteract the IFN response. The results in this chapter identify nsP2 as a specific and potent inhibitor of the JAK-STAT signalling pathway. **Chapter 7** sheds more light on the multifunctionality of nsP2. It presents genetic evidence to identify three distinct functions of nsP2, its role in RNA replication, the inhibition of JAK-STAT signalling and the induction of general host shut-off. In the final phase of viral replication, viral envelope proteins mature in the ER before they translocate to the plasma membrane. **Chapter 8** examines whether this process leads to ER-stress and investigates how CHIKV modulates the resulting unfolded protein response.

Chapter 9 integrates the experimental data presented in this thesis with the most recent insights from the literature. It discusses the risks of further spread of WNV and the intricate relationship between arboviruses and both the arthropod and mammalian host (cell). In addition, chapter 9 provides further insights as to how CHIKV nsP2 inhibits the JAK-STAT signalling pathway.

To put the work presented in this thesis into a wider perspective, the current situation as to the control and prevention of flavi- and togavirus diseases is discussed. Currently there are no licensed vaccines or antiviral drugs available against either WNV or CHIKV for human use. Prevention of WNV and CHIKV disease is therefore limited to mosquito control. A better understanding of how these viruses establish productive infections in vertebrate cells will aid in the search for anti-viral drugs and safe efficacious vaccines. Additionally, understanding the molecular determinants of vector competence may lead to effective intervention strategies at different stages of the transmission cycle. Finally, defining the vector competence will aid in assessing the risk for these emerging arboviral diseases.

Chapter 2



West Nile virus: High transmission rate in north-western European mosquitoes indicates its epidemic potential and warrants increased surveillance

West Nile virus (WNV) is on the rise in Europe, with increasing numbers of human cases of neurological disease and death since 2010. However, it is unknown whether or not WNV will continue to spread to north-western Europe, in a fashion similar to the WNV epidemic sweep in North America (1999-2004). Our study is the first to investigate transmissibility in north-western European *Culex pipiens* for pathogenic lineage 2 WNV, in a systematic, direct comparison with North American *Culex pipiens* and the lineage 1 WNV strain. We demonstrate that European mosquitoes are highly competent for both WNV lineages, which underscores the epidemic potential of WNV in Europe. Significant lower transmission rates for lineage 2 WNV in American mosquitoes indicate different intercontinental risk levels for WNV transmission. We propose that WNV surveillance must be intensified in Europe to allow early detection, timely intervention strategies and better clinical diagnosis of WNV neurological cases.

This chapter has been submitted as:

Jelke J. Fros, Corinne Geertsema, Chantal B. Vogels, Peter P. Roosjen, Anna-Bella Failloux, Just M. Vlak, Constantianus J. Koenraadt, Willem Takken, and Gorben P. Pijlman. *West Nile virus: High transmission rate in north-western European mosquitoes indicates its epidemic potential and warrants increased surveillance*

Introduction

West Nile virus (WNV; family *Flaviviridae*, genus *Flavivirus*) is an important mosquito-borne human pathogen associated with febrile illness, which may develop into severe neuroinvasive disease and death (1). The pathogenic isolates of WNV can be classified into two lineages. Lineage 1 WNV strains have long been endemic in Africa, Australia, the Middle East, Asia and Southern Europe (2,3). In the 1990s, lineage 1 WNV re-emerged in southern Europe and the Middle-East (4–6). In 1999, lineage 1 WNV was unintentionally introduced into New York City from where it spread rapidly across the United States where it is now endemic (7). With an accumulated 17,463 cases of neuroinvasive disease and 1,668 deaths between 1999 and 2013, this outbreak quickly evolved into the largest outbreak of neuroinvasive disease to date (8). Lineage 2 WNV strains have been endemic in sub-Saharan Africa and Madagascar and were previously considered to be of low pathogenicity (2,3). In 2010, a highly pathogenic lineage 2 WNV isolate caused a large outbreak in Greece (9), which resulted in 262 cases of human disease and 35 deaths. Lineage 2 WNV then quickly became endemic in South-East Europe and with annual outbreaks to date WNV activity in the region has increased seven-fold (10,11). At present, WNV activity does not extend into north-western Europe (11).

During enzootic transmission, WNV circulates primarily between *Culex* species mosquitoes and birds. Many avian species in North America (12) and Europe (13,14) are suitable reservoirs/amplifying hosts and can produce high viral titres upon WNV infection. Infected mosquitoes also blood feed on other vertebrate hosts, which leads to frequent infections in humans and horses (15). In Europe, the main *Culex* species found positive during WNV surveys is the common house mosquito *Culex pipiens* (16). In North America the most prevalent and effective vector species for WNV are *Culex pipiens*, *Culex tarsalis* and *Culex quinquefasciatus* (17,18). Laboratory experiments show that American *Culex pipiens* mosquitoes are competent vectors for American isolates of lineage 1 WNV (19). The vector competence of European mosquitoes to lineage 1 WNV has not intensively been studied nor has it been compared directly to competent vectors from NA (20). The vector competence of American and European mosquitoes for transmission of novel European lineage 2 WNV isolates has not yet been determined, but this is of high importance now that a highly pathogenic lineage 2 WNV has emerged in Europe, which appears to be equally neuroinvasive as WNV isolates from lineage 1 (9).

As the global activity of these pathogenic WNV lineages has significantly increased over the past two decades, we set out to assess the potential for virus transmission in areas that are free of either lineage 1 and/or lineage 2 WNV strains.

Materials and methods

Cells and viruses

C6/36 and *Culex tarsalis* cells were grown on Leibovitz L15 and Schneiders (Gibco) medium supplemented with 10% fetal bovine serum (FBS; Gibco). Hela, DF-1 and Vero E6 cells were cultured with DMEM Hepes (Gibco) buffered medium supplemented with 10% FBS containing penicillin (100 IU/ml) and streptomycin (100 µg/ml). When Vero E6 cells were incubated with mosquito lysates or saliva the growth medium was supplemented with fungizone (2,5 µg/ml) and gentamycin (50 µg/ml). P2 virus stocks of the NY'99 and Gr'10 isolates were grown on C6/36 cells and titrated on Vero E6 cells.

Mosquito rearing

The NWE *Culex pipiens* colony originated from Brummen, the Netherlands (°05'23.2"N 6°09'20.1"E) and was established in 2010 and maintained at 23°C. The American *Culex pipiens* colony (19) was maintained at 26°C. Both mosquito colonies were kept in Bugdorm cages with a 16:8 light:dark (L:D) cycle and 60% relative humidity (RH) and were provided with 6% glucose solution. Bovine or chicken whole blood was provided through the Hemotek® PS5 (Discovery Workshops) for egg production. Egg rafts were allowed to hatch in tap water supplemented with Liquifry No. 1 (Interpet Ltd.). Larvae were fed with a 1:1:1 mixture of bovine liver powder, ground rabbit food and ground koi food.

In vivo infections

2-5 day old mosquitoes were infected either via ingestion of an infectious blood meal or via intrathoracic injections. Infectious blood meals: Whole chicken blood was mixed with the respective P2 virus stock to a final concentration of 1.4×10^8 WNV infectious particles per ml. Mosquitoes were allowed to membrane feed, using the Hemotek® system and a parafilm membrane, in a dark climate controlled room (24°C, 70% RH). After 1 hour, mosquitoes were sedated with 100% CO₂ and the fully engorged females were selected. Injections: Mosquitoes were sedated with CO₂ and placed on a semi-permeable pad, attached to 100% CO₂. Mosquitoes were infected by intrathoracic injection using the Drummond nanoject 2 (Drummond scientific company, United States). Infected mosquitoes were incubated at their respective temperatures with a 16:8 L:D cycle and fed with 6% sugar water during the course of the experiment.

Salivation assay

Legs and wings of sedated mosquitoes were removed and their proboscis was inserted into a 200 µl filter tip containing 5 µl of salivation medium (50% FBS and 50% sugar water (glucose, W/V 50%)). Mosquitoes were allowed to salivate for 45 minutes. Mosquito bodies were frozen in individual Eppendorf tubes containing 0.5 mm zirconium beads (Next Advance) at -80°C. The mixture containing the saliva was added to 55 µl of fully supplemented growth medium.

WNV infectivity assay

Frozen mosquito bodies were homogenized in the bullet blender storm (Next Advance) in 100 µl of fully supplemented medium and centrifuged for 90 s at 14000 rpm in a table top centrifuge. 30 µl of the supernatant from the mosquito homogenate or the saliva containing mixture was incubated on a monolayer of Vero cells in a 96-wells plate. After 2-4 hours the medium was replaced by 100 µl of fresh fully supplemented medium. Wells were scored for WNV-specific cytopathic effects (CPE), confirmed with immunofluorescence assay (IFA) against WNV E (31) at three days post infection (dpi). WNV titres were determined using 10 µl of the supernatant from the mosquito homogenate in end point dilution assays on Vero E6 cells. WNV infection was scored by CPE, confirmed with IFA at three dpi.

Temperature maps

Maps displaying the mean diurnal temperature during July and August of the indicated year (32). Human cases of WNV in Europe, during 2011, 2012 or 2013 were projected on the location where they were reported (11). To eliminate potential imported cases, WNV cases were only considered when a country reported more than one case for that year.

Statistical analysis

WNV infections in mosquito bodies and saliva were scored positive or negative and significant differences were calculated using the Fisher's exact test ($P < 0.05$). Differences in WNV titres (TCID₅₀/ml) in infected mosquito bodies and heads were calculated using the Mann Whitney test ($P < 0.05$).

Results

Transmission rate of lineage 2 WNV is higher in European versus American mosquitoes

Culex pipiens mosquitoes from north-western Europe (NWE; the Netherlands), and a North American *Culex pipiens* colony (NA) (19) were infected with either the novel pathogenic lineage 2 WNV isolate (WNV-lin2) from Greece'10 or lineage 1 isolate (WNV-lin1), New York '99. The vector competence of NA mosquitoes for WNV-lin1 has been well-described (19) and serves as a reference for the infection and transmission rates of WNV. The WNV-lin2 and WNV-lin1 isolates displayed similar growth kinetics in human, avian and mosquito cell cultures (Figure 2.1). Infectious blood meals containing 1.4×10^8 TCID₅₀/ml of either WNV-lin2 or WNV-lin1 isolates were fed to the NWE and NA *Culex pipiens* mosquitoes. Fully engorged females were selected and kept at an ambient temperature of 23°C. Immediately after completion of the blood meal, a subset of fully engorged females was tested for the presence of infectious WNV to confirm that both mosquito populations had ingested equal amounts of infectious virus particles (Figure 2.2). Infection with either WNV isolate did not influence mosquito survival during the course of the experiments (data not shown). After 14 days, saliva was collected from the mosquitoes and both the saliva as well as the mosquito bodies were examined for the presence of WNV (schematic representation of the experiment, Figure 2.3A). Both the NWE and NA mosquitoes were equally susceptible to infection, but with significant differences in the infection rates between the WNV-lin2 and WNV-lin1 isolates (Figure 2.3B, Table 1, $P < 0.05$).

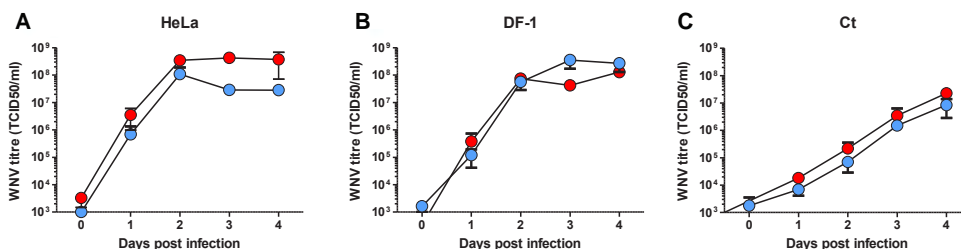


Figure 2.1. Growth kinetics of lineage 1 and 2 WNV strains. A. Human HeLa, B. avian DF-1 (duck fibroblasts), and C. mosquito CT (*Culex tarsalis*) cells infected with WNV-lin2 (red) or WNV-lin1 (blue) isolates at a multiplicity of infection of 1. Medium was harvested at the indicated days post infection and used in end point dilution assays. Error bars represent the standard error of the mean.

Dissemination of WNV into the saliva of a vector is a prerequisite for successful transmission. After consuming a blood meal that contained WNV-lin1, 22% of both the NWE and NA mosquitoes had detectable levels of WNV in their saliva (Figure 2.3C). In contrast, the WNV-lin2 isolate was detectable in the saliva of 24% of the European mosquitoes, but only in 8% of the American

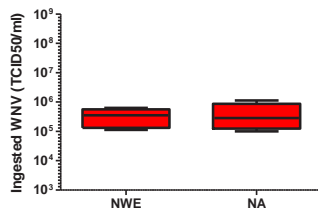


Figure 2.2. Both NWE and NA *Culex pipiens* mosquitoes ingest equal amounts of infectious virus Mosquitoes were infected with WNV-lin2 via an infectious blood meal, homogenized, and the viral titres were determined in end point dilution assays. Results are represented as a Tukey box plot.

mosquitoes (Figure 2.3C, $P < 0.05$) indicative of a strongly reduced susceptibility of the latter for WNV-lin2. The differential transmission rate of the WNV-lin2 isolate is underscored when only WNV-infected mosquitoes are considered. From the population of WNV-infected mosquitoes (Figure 2.3B), successful replication and dissemination of WNV-lin2 into the saliva was found in 59% of the NWE, compared to only 24% of the NA mosquitoes (Table 2 and Figure 2.3D).

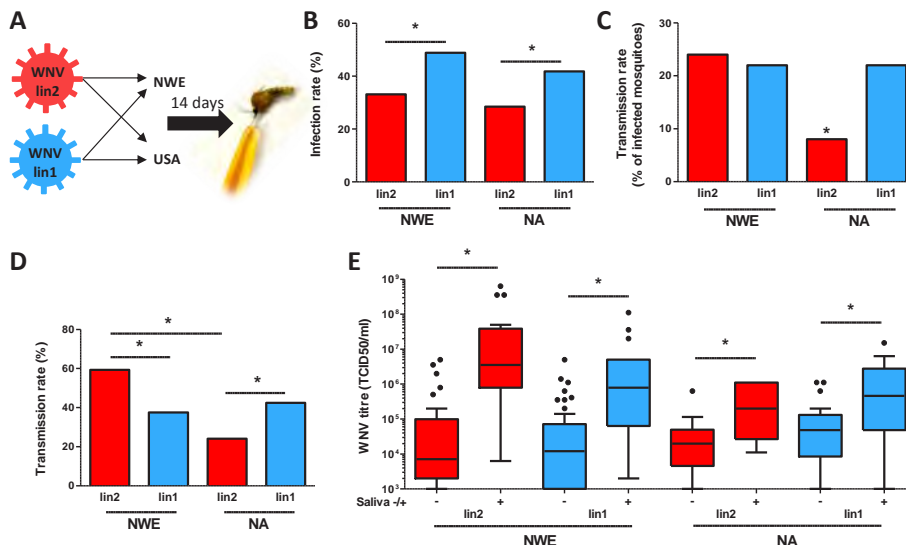


Figure 2.3. European *Culex pipiens* mosquitoes are competent vectors for pathogenic WNV lineages 1 and 2. A. Schematic representation of the experiment. Mosquitoes from NWE or NA were given a blood meal containing virus from either WNV-lin2 or WNV-lin1 isolates. B. NWE or NA mosquitoes were fed an infectious blood meal containing either WNV-lin2 or WNV-lin1 isolates. Fourteen days post infection, saliva was isolated and the presence of WNV in these mosquitoes was assayed. Bars represent the percentage of WNV infected mosquitoes. C. Fourteen days post infection the saliva was harvested and scored for infectious WNV. Bars represent the percentage of mosquitoes with infectious saliva. D. Mosquito saliva was assayed for the presence of WNV. Bars represent the percentage of mosquitoes with WNV positive saliva from the WNV infected population. E. Ten μ l of the homogenized mosquito bodies was titrated in end point dilution assays. For each sample population, the WNV titres of individual mosquito bodies were grouped into saliva negative (left) and positive (right) populations, represented in Tukey box plots. Individual outliers are indicated. Asterisks indicate significant differences ($P < 0.05$, Fisher's exact test (BCD), Man Whitney test (E)).

Table 1. Infection rate of lineage 1 and 2 WNV isolates in NWE and NA *Culex pipiens* mosquitoes.

Mosquito population	WNV lineage	n (#)	Infected (#)	Infection rate (%)
NWE	lin2	154	51	33
NA	lin2	102	29	28
NWE	lin1	131	64	49
NA	lin1	87	36	42

In an effort to understand these differences in transmissibility we first determined the tissue culture infectious dose of WNV present in each positive mosquito body by end point dilution assays. The viral titres in individual mosquito bodies were highly variable and could reach up to 10^9 TCID₅₀/ml for WNV-lin2 infected NWE mosquitoes, compared to a three logs lower maximum titre of only 10^6 TCID₅₀/ml in NA mosquitoes (Figure 2.3E). Comparison between the WNV titres of saliva-positive and saliva-negative mosquitoes within the same sample population showed that significantly more infectious WNV particles were present in the bodies of mosquitoes with positive saliva than with negative saliva (Figure 2.3E). This indicates that the level of WNV replication in the mosquito body determines the dissemination into the salivary glands.

Table 2. Transmission rate of lineage 1 and 2 WNV isolates in NWE and NA *Culex pipiens* mosquitoes.

Mosquito population	WNV lineage	n (#)	Infected (#)	Transmissible (#)	Transmission rate (%)	Positive saliva (% of positive mosquitoes)
NWE	lin2	79	32	19	24	59
NA	lin2	102	29	7	8	24
NWE	lin1	67	40	15	22	38
NA	lin1	74	33	14	22	42

Differential transmission rates of WNV-lin2 attributed to infection barriers

Efficient infection and escape from the midgut epithelial cells is necessary for dissemination of the virus to other tissues, including the salivary glands (21–23). When the midgut was circumvented by injecting WNV-lin2 directly into the thorax, all mosquitoes from both NWE and NA became readily infected (Figure 2.4A, open symbols) and up to 100% of injected individuals were able to transmit WNV at day 8 post injection (Figure 2.4B, open symbols). In contrast, infectious blood meals resulted in differential proportions of the NWE and NA mosquitoes being able to transmit WNV-lin2 (Figure 2.4B, closed symbols), again with NWE as a more competent vector. Strikingly, as early as eight days post infection, the WNV-lin2 isolate was detected in the saliva of 14% of NWE mosquitoes, compared to 3% of NA mosquitoes (Figure 2.4B, closed symbols). Thus, infection with the WNV-lin2 isolate results in better dissemination and a shorter mean extrinsic incubation period, suggesting that WNV-lin2 escapes more effectively from the midgut epithelial cells in mosquitoes from

NWE compared to those from NA. Taken together, transmission of both WNV lineages is intrinsically possible in north-western Europe whereas there is no evidence to suggest that WNV-lin2 can utilize American mosquitoes as effective vectors due to limited dissemination to the salivary glands.

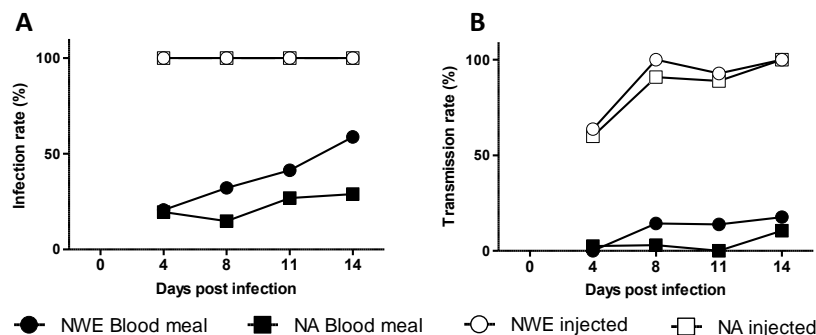


Figure 2.4. Mesenteron infection barriers determine the transmission rate of WNV-lin2. *Culex pipiens* from either NWE (spherical symbols) or NA (square symbols) were infected with the WNV-lin2 isolate via infectious blood meals (closed symbols) or intrathoracic injections (open symbols). At the indicated times post infection, the percentages of effectively infected mosquitoes (A) or successive infectious saliva (B) were determined.

Higher temperatures increase WNV infection rate

As the mosquito colonies used in this laboratory study are representatives of their respective populations from the described areas, the experiments presented here show that highly WNV-competent *Culex pipiens* mosquitoes are present in north-western Europe. Vector competence is, however, not only attributed to intrinsic factors, but also subjective to extrinsic factors, most notably the ambient temperature (19,24). Because indigenous WNV activity is currently absent in north-western Europe (11,25), but competent European bird species are present (13,14), we hypothesized that temperature limits the vector competence of European mosquitoes for WNV transmission. To test this hypothesis, we infected both NWE and NA mosquitoes with the WNV-lin2 isolate via a WNV-containing blood meal and incubated the mosquitoes at three different temperatures. Two of which matched the average temperatures

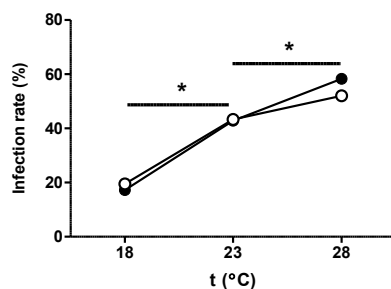


Figure 2.5. Higher temperatures increase WNV infection rate in *Culex pipiens*. Both NA (open symbols) and NWE (closed symbols) mosquitoes were orally infected with the WNV-lin2 isolate via a blood meal. Engorged mosquitoes were separated into three groups which were incubated at either 18, 23 or 28°C. The infection rate was determined 14 days post oral infections. Asterisks indicate significant differences (Fisher's exact test $P < 0.05$).

at the origin of our NWE mosquito colony (the Netherlands; 18°C) and the WNV-lin2 isolate (Greece; 28°C) (26) during the warmest period of the year (July and August) which also corresponded with the peak in WNV amplification and transmission⁸. The third incubation temperature was an intermediate of 23°C. Higher temperatures significantly increased the percentage of WNV-infected mosquito vectors, with no apparent difference between NWE and NA mosquitoes (Figure 2.5, $P < 0.05$). At 18°C, 17% and 19% of mosquitoes were infected with WNV-lin2, whereas incubation at 28°C increased the infection rates to 58% and 52% for NWE and NA mosquitoes, respectively.

Comparison between the spatial arrangement of recent WNV outbreaks in Europe per annum and the corresponding mean temperature during peak transmission season strengthens this hypothesis by displaying a strong correlation between WNV outbreaks and the mean diurnal summer temperature throughout Europe (Figure 2.6A, B and C). The mean temperatures at which WNV outbreaks occurred in 2011, 2012 and 2013 were 24.6°C, 25.3°C, and 23.5°C, with standard deviations of 2.4°C, 2.7°C, and 2.1°C, respectively (Figure 2.6D). Together, the mean temperatures at the respective locations of individual outbreaks give an indication of the average summer temperatures at which there is an elevated risk for WNV activity.

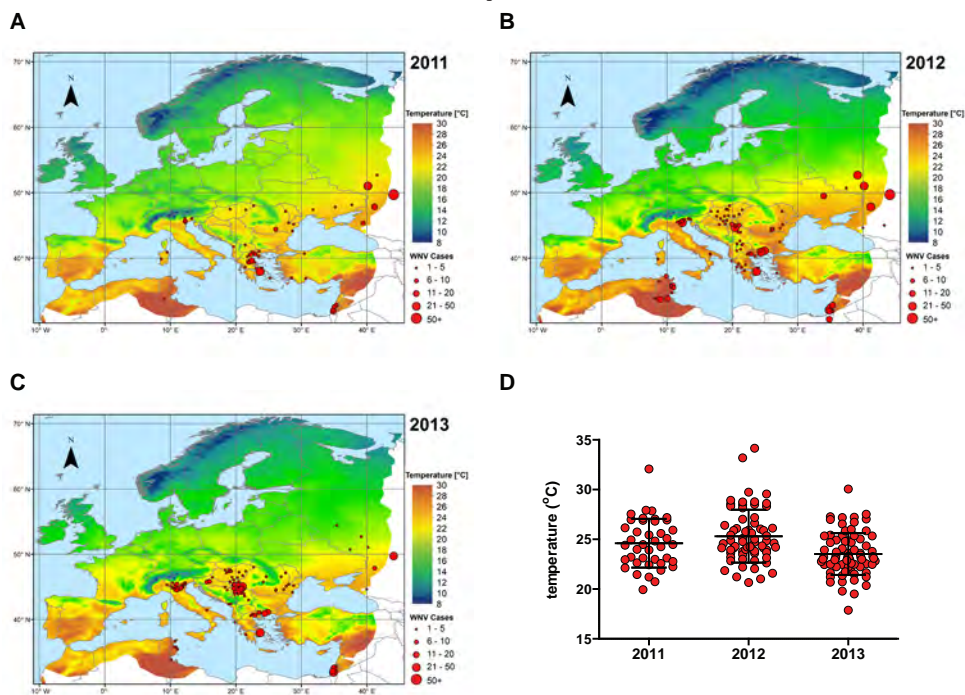


Figure 2.6. Mean diurnal summer temperature correlates with European WNV outbreaks. Mean diurnal temperature during July-August of (A) 2011, (B) 2012 and (C) 2013. Dots represent human WNV cases reported in the respective year. D. Scatter plot displays the mean temperature during July and August of the indicated year at each individual location with WNV activity. The mean temperatures and standard deviations are indicated.

Discussion

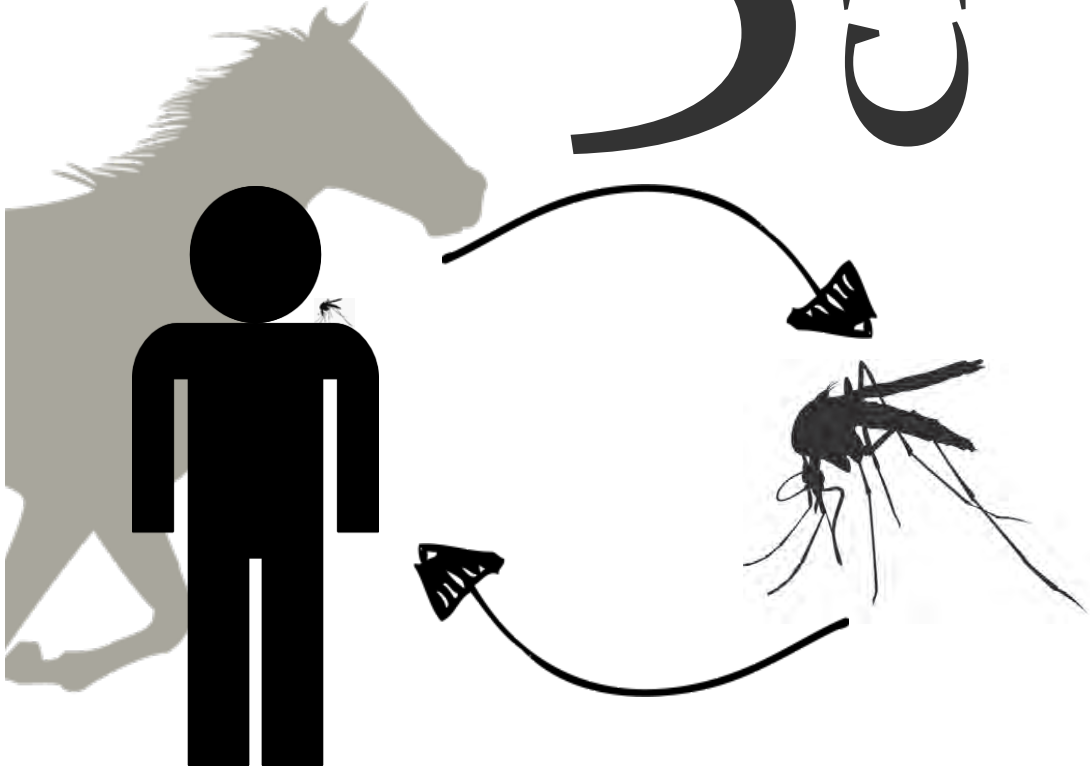
Here we show that both pathogenic lineages of WNV can effectively infect mosquitoes from NWE. Our finding that two geographically separated *Culex pipiens* populations (NWE and NA) have a markedly different vector competence for WNV-lin2, indicates a high degree of genotype-genotype specificity in the interaction between virus and vector. As the differential infection rate is only apparent when WNV is infected orally and not via intrathoracic injections, this suggests that WNV-lin2 escapes more effectively from the midgut epithelial cells in mosquitoes from NWE compared to those from NA. The presence of highly competent vector species in WNV-free areas suggests that extrinsic factors such as temperature play an essential role in the current distribution of WNV. In Europe, the lower average summer temperature (<20°C) may provide a possible explanation for the current WNV epidemics, which remain restricted to southern Europe. However, other extrinsic factors can shape the vectorial capacity and may compensate for a reduced vector competence at low temperature by facilitating larger mosquito populations. The recent resurgence of WNV disease in the United States was most likely fuelled by climatic conditions that were favourable for local vector populations (27,28). In addition, hybrids between two closely related *Culex pipiens* forms may increase the incidence of human WNV disease, as these 'bridge-vectors' are considered less ornithophilic and more likely to feed on other vertebrates, including humans. These hybrids are relatively common in North America, but not in north-western Europe (29). Additionally, viral adaptations that increase the replication efficiency at lower temperatures could further facilitate and enhance transmission of WNV throughout Europe. Indeed, the WNV-lin1 isolate has already proven to be able to adapt to the different climatic conditions in the Americas (19), while other flaviviruses, including a close relative of WNV, Usutu virus, are already endemic in parts of north-western Europe (30). Finally, global warming or temporary weather extremes will likely favour the vectorial capacity of *Culex pipiens* and increase the risk of future WNV outbreaks worldwide. Based on our results and experimental evidence by others that European birds are suitable amplifying hosts (14), we propose that WNV surveillance in mosquitoes and birds should be intensified to allow early detection and the implementation of effective mitigation and intervention strategies. Furthermore, awareness in the clinic throughout Europe is warranted in order to more effectively diagnose cases of human WNV (neurological) disease.

Acknowledgments

We thank Els Roode for technical support concerning the BSL3 laboratory, Byron Martina for sharing the WNV isolates, Aaron Brault for the *Culex tarsalis* cells, the Cell Biology and Immunology group of Wageningen University for the Hela and DF-1 cells, Laura Kramer for providing egg rafts of the North American *Culex pipiens* mosquitoes, and Roy Hall for antibodies against the

WNV envelope. We acknowledge the E-OBS dataset from the EU-FP6 project ENSEMBLES and the data providers in the ECA&D project. This work is supported by the European 195 Community's Seventh Framework Programme (FP7 VECTORIE project number 261466).

Chapter 3



Usutu virus, highly transmissible by northern house mosquitoes and a prelude to West Nile virus activity in Europe

Originating from Africa, Usutu Virus (USUV) first emerged in Europe in 2001. This mosquito-borne flavivirus displayed high mortality rates in its bird reservoirs, which strongly resembled the introduction of West Nile virus (WNV) in 1999 in the United States. Mosquitoes infected with USUV incidentally infect other vertebrates, including humans which can result in neuroinvasive disease. USUV and WNV co-circulate in parts of southern Europe, but the distribution of USUV extends into central and northwestern Europe. In the field, both viruses are most often detected in the northern house mosquito *Culex pipiens*. To understand the transmission dynamics and assess the potential spread of USUV, we determined how effective *Culex pipiens* is as a vector for USUV. We compared the vector competence for USUV with that for the better studied WNV. We show for the first time that European mosquitoes are highly effective vectors for USUV. Interestingly, at higher temperatures USUV was able to infect mosquitoes more effectively than WNV, which could be attributed to barriers present in the mosquito midgut. As both viruses utilize the same vector and reservoir species and only display differences in temperature dependent vector competence, this suggests that USUV may precede WNV transmission in Europe.

This chapter is in preparation for submission as:

Jelke J. Fros, Pascal Miesen, Chantal B. F. Vogels, Paolo Gaibani, Vittorio Sambri, Constantianus J. M. Koenraadt, Ronald P. van Rij, Just M. Vlak, Willem Takken and Gorben P. Pijlman. *Usutu virus, highly transmissible by northern house mosquitoes and a prelude to West Nile virus activity in Europe*

Introduction

The last two decades a number of clinically significant arthropod-borne (arbo) viruses have (re-)emerged in continental Europe. Autochthonous transmission of dengue virus has occurred in France in 2014 (115) and chikungunya virus transmission has been recorded in Italy (2007) (32) and France (2010, 2014)(34)(33). Both these viruses are transmitted by the invasive Asian tiger mosquito *Aedes albopictus*, which has colonized parts of Europe (116). Alternatively, native *Culex* mosquitoes are the main vector for two pathogenic lineages of West Nile virus (WNV), which are now endemic in southern Europe (chapter 2)(23). The enzootic transmission cycle of WNV is maintained by mosquitoes and birds. Infected mosquitoes, however, may also feed on other vertebrates resulting in frequent infections in humans and horses (104). In 1999, WNV was introduced in the United States. The outbreak that followed was characterized by high mortality rates in various American bird species and resulted in the largest outbreak of human neuroinvasive disease to date (10).

In Austria (2001), a sudden and substantial die-off in Eurasian blackbirds closely resembled the WNV outbreak in the United States. Not WNV, but another related flavivirus (family *Flaviviridae*), Usutu virus (USUV), was identified. This was the first isolation of USUV on the European continent (117). The virus was first discovered in South Africa in 1959 and since then its activity has been observed in a number of African countries (118). After the initial outbreak in Austria, USUV activity has been detected in Spain, Italy, Switzerland, the Czech Republic, Hungary, United Kingdom, Poland, Croatia, Germany and Belgium (119, 120). In some southern European countries USUV co-circulates with WNV (41). The high mortality in a large number of avian species enabled monitoring the spread of USUV via the surveillance of dead birds (121). Most of the USUV positive bird species were blackbirds (*Turdus merula*), which belong to the same genus as the suspected WNV reservoir in the United States, the American robin (*Turdus migratorius*)(122). USUV infected mosquitoes may also feed on other vertebrates, and the virus has been detected in horses (123) and bats (124). Infections in humans have resulted in two diagnosed clinical cases in Africa (118). In Europe, two Italian and three Croatian patients with neuroinvasive disease have been reported (25–27). However, serological evidence suggests that less severe and subclinical cases of human USUV infections occur regularly in USUV-endemic areas (125–127).

Similar to WNV, USUV is mostly transmitted by *Culex* species mosquitoes. In Africa USUV has been isolated from *Culex neavei*, *Culex perfuscus*, *Culex univittatus* and *Culex quinquefasciatus*. Additionally, USUV has also been detected in a number of mosquito species from other genera (118). Among European mosquito species, USUV is mostly found in the northern house mosquito (*Culex pipiens*), which is abundant throughout the northern hemisphere (41).

The presence of competent mosquitoes dictates the potential spread of any arthropod-borne pathogen. Vectors are considered competent when they can transmit the pathogen from one vertebrate host to the next. Arboviruses, like USUV, are ingested via an infectious blood meal, infect the epithelial cells that line the mosquito midgut, escape to the haemolymph, and finally accumulate in the saliva to be transmitted during the next blood meal (64). Determining how competent a vector species is provides insight in the viral transmission dynamics and is essential to assess the risk for future outbreaks. The only laboratory experiments that determined vector competence for USUV were done with the African mosquito, *Culex neavei* (128). To better understand, predict and assess the potential spread of USUV in Europe we investigated how competent the northern house mosquito *Culex pipiens* is as vector for USUV. Here we show for the first time that *Culex pipiens* is a highly effective European USUV vector. We provide insight into the replication dynamics within the mosquito vector and show how the vector competence of USUV relates to that of WNV at different temperatures.

Materials and methods

Cells and viruses

C6/36 cells were grown on Leibovitz L15 (Life technologies, Netherlands) medium which was supplemented with 10% FBS. Vero E6 cells were cultured with DMEM Hepes (Life technologies, Netherlands)-buffered medium supplemented with 10% FBS containing penicillin (100 IU/ml) and streptomycin (100 µg/ml). When Vero E6 cells were infected with mosquito lysates or saliva the growth medium was supplemented with fungizone (2,5 µg/ml) and gentamycin (50 µg/ml). This medium will be referred to as fully supplemented medium. P2 virus stocks of USUV, Bologna '09 and WNV Gr'10 lineage 2 were grown on C6/36 cells and titrated on Vero E6 cells.

Mosquito rearing

The European *Culex pipiens* colony originated from Brummen, the Netherlands (°05'23.2"N 6°09'20.1"E) and was established in 2010 and maintained at 23°C. The mosquito colony was kept in Bugdorm cages with a 16:8 light:dark (L:D) cycle and 60% relative humidity (RH), and provided with a 6% glucose solution as food source. Bovine or chicken whole blood was provided through the Hemotek® PS5 (Discovery Workshops, UK) for egg production. Egg rafts were allowed to hatch in tap water supplemented with Liquifry No. 1 (Interpet Ltd., UK). Larvae were fed with a 1:1:1 mixture of bovine liver powder, ground rabbit food and ground koi food.

In vivo infections

Two-to-five day old mosquitoes were infected either via ingestion of an infectious blood meal or via intrathoracic injections. Oral infections were performed by mixing whole chicken blood with the respective P2 virus stock to the indicated final concentration. Mosquitoes were allowed to membrane feed, using the Hemotek® system, in a dark climate controlled room (24°C, 70% RH). After 1 hour, mosquitoes were sedated with 100% CO₂ and the fully engorged females were selected. During intrathoracic injections the mosquitoes were sedated with CO₂ by placing them on a semi-permeable pad, attached to 100% CO₂. Mosquitoes were infected by intrathoracic injection using the Drummond nanoject 2 (Drummond scientific company, United States). Infected mosquitoes were incubated at the indicated temperatures with a 16:8 L:D cycle and fed with 6% sugar water during the course of the experiment.

Salivation assay

Mosquitoes were sedated with 100% CO₂ and their legs and wings were removed. Their proboscis was inserted into a 200 µl filter tip containing 5ul of salivation medium (50% FBS and 50% sugar water (W/V 50%)). Mosquitoes were allowed to salivate for 45 minutes. Mosquito bodies were frozen in individual Eppendorf tubes containing 0.5 mm zirconium beads at -80°C. The mixture containing the saliva was added to 55 µl of fully supplemented growth medium.

Infectivity assays

Frozen mosquito bodies were homogenized in the bullet blender storm (Next Advance, United States) in 100 µl of fully supplemented medium and spun down for 90 seconds at 14,000 rpm in a table top centrifuge. Thirty µl of the supernatant from the mosquito homogenate or the saliva-containing mixture was incubated on a monolayer of Vero cells in a 96-wells plate. After 2-4 hours the medium was replaced by 100 µl of fresh fully supplemented medium. Wells were scored for virus specific cytopathic effects (CPE) at three days post infection. Viral titres were determined using 10 µl of the supernatant from the mosquito homogenate in an end point dilution assay on Vero E6 cells. Infections were scored by CPE, three days post infection.

Analysis of small RNA libraries

Pools of twelve WNV or USUV infected mosquitoes were lysed in TRIzol (life technologies) reagent and total RNA was isolated. The isolation and sequencing of small RNAs was described previously (129). In short, RNA was size separated by PAGE gel electrophoresis and small RNAs (19-33 nucleotides) were isolated. The small RNA library was prepared with the TruSeq Small RNA Sample Preparation Kit (Illumina) and sequenced on an Illumina HiSeq 2500 by Baseclear (www.baseclear.nl). FASTQ sequence reads were generated with the Illumina Casava pipeline (version 1.8.3) and initial quality assessment was performed by Baseclear using in-house scripts and the FASTQC quality control tool (version 0.10.0). FASTQ sequence reads that passed this quality control were analyzed with Galaxy (130). Sequence reads were clipped from the adapter sequence (TruSeq 3' adapter index #8) and mapped with Bowtie (version 1.1.2) (131) to the WNV (GenBank: HQ537483.1) and USUV (GenBank: HM569263.1). A size profile of the viral small RNAs was obtained from all reads that mapped to their respective genomes.

Results

Culex pipiens is a highly competent vector for USUV.

Recently we showed that *Culex pipiens* from north-western Europe is a highly competent vector for pathogenic WNV isolates (chapter 2). To evaluate how competent this mosquito is as a vector for USUV mosquitoes were offered a blood meal containing a 50% tissue culture infectious dose (TCID₅₀) of 4*10⁷ USUV or WNV per ml. The fully engorged females were kept at 28°C. After fourteen days saliva was isolated from each individual mosquito as a proxy for transmission. Virus in the saliva of a mosquito is a prerequisite for transmission and therefore used as an indication of its transmissibility. The presence of infectious USUV or WNV particles was detected on Vero E6 cells. The blood meal that contained WNV infected 46% of the mosquitoes, whereas the blood meal that contained USUV infected a significantly larger percentage (80%) of mosquitoes (Figure 3.1A, Fisher's exact test, P<0.05). From the mosquitoes that ingested a WNV-containing blood meal, 33% had infectious WNV in their saliva, whereas an USUV containing blood meal resulted in 69% of mosquitoes with infectious saliva (Figure 3.1A, Fisher's exact test P<0.05).

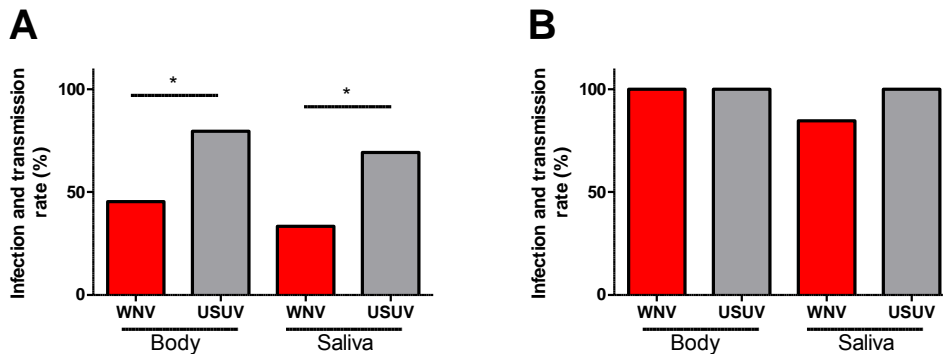


Figure 3.1. *Culex pipiens* is a highly competent vector for USUV. Mosquitoes were offered an infectious blood meal (A) or were injected (B) with either WNV or USUV. Fourteen days post infection mosquito saliva was collected and the mosquito body was homogenized in cell culture medium. The mosquito homogenate and saliva were incubated on Vero E6 cells to detect the presence of either WNV or USUV in the mosquito bodies and saliva. Bars represent the percentage of positive samples. Asterisk indicates significant difference (Fisher's exact test, P<0.05).

As the midgut epithelial cells can form a primary infection barrier (132) mosquitoes were also infected by injecting 5.5*10³ TCID₅₀ directly into the thorax. Injection of either virus into the thorax of *Culex pipiens* mosquitoes clearly circumvents the midgut barrier as it increases the infection rate and transmission rate of both WNV and USUV up to 100% (Figure 3.1B). Taken together, USUV not only infects a large percentage of *Culex pipiens* mosquitoes but also effectively disseminates into their saliva. This indicates that these WNV-competent mosquitoes are even more effective as vector for USUV. In addition, the differential infectivity and transmissibility of both viruses after

an infectious blood meal but not after intrathoracic injection suggests that the midgut epithelial cells play a differentiating role that determines vector competence.

USUV replication in the mosquito vector.

To investigate if the increased dissemination of USUV relates to higher viral titres in the vector, the viral titres present in individual mosquito bodies were determined using end point dilution assays. Interestingly, mosquitoes that were orally infected with either WNV or USUV showed a similar variation in viral titres (Figure 3.2, mean TCID₅₀ of 1.1×10^6 and 1.5×10^6 per ml, respectively). In contrast, intrathoracic injection of either WNV or USUV resulted in significantly different viral titres, with a mean TCID₅₀ of 8.1×10^6 and 2.7×10^5 per ml, respectively (Figure 3.2, student t-test, $P < 0.05$). Interestingly, USUV displayed viral titres that were 30 times lower compared to WNV, but without compromising dissemination to the salivary glands. This suggests that the bottleneck for vector competence is presented by the midgut epithelium, which differentially affects viral replication of WNV as compared to USUV.

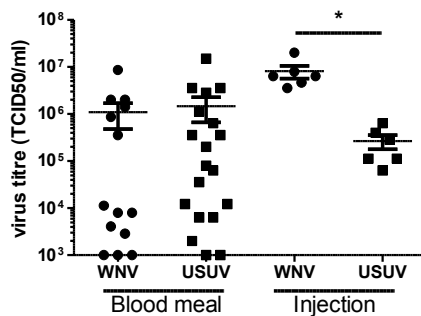


Figure 3.2. USUV and WNV replicate to equally high titres in *Culex pipiens* after an infectious blood meal but not after injection of the viruses. Homogenates from infected mosquitoes were used in end point dilution assays and the tissue culture infectious dose 50% (TCID₅₀)/ml was determined. Data points represent individual mosquitoes infected with either USUV or WNV via the indicated route. Asterisk indicates significant difference (t-test, $P < 0.05$).

WNV and USUV viRNA in infected *Culex pipiens*

Next, we investigated whether both WNV and USUV infections in *Culex pipiens* mosquitoes induced an antiviral response. The activation of the main invertebrate antiviral response, RNA interference (RNAi), occurs via the recognition and cleavage of dsRNA products into small-interfering RNA (siRNA) of usually 21 nucleotides (133). In response to WNV infections virus-derived siRNA (viRNA) has been detected in *Culex quinquefasciatus* (51). To investigate whether the RNAi pathway is activated by WNV and USUV infections in *Culex pipiens*, small RNAs were isolated from pools of WNV or USUV infected mosquitoes and analyzed using deep-sequencing. The small RNA libraries were mapped to the viral genomes and both WNV and USUV infected mosquitoes elicited an RNAi response with the expression of 21 nucleotide viRNA (Figure 3.3).

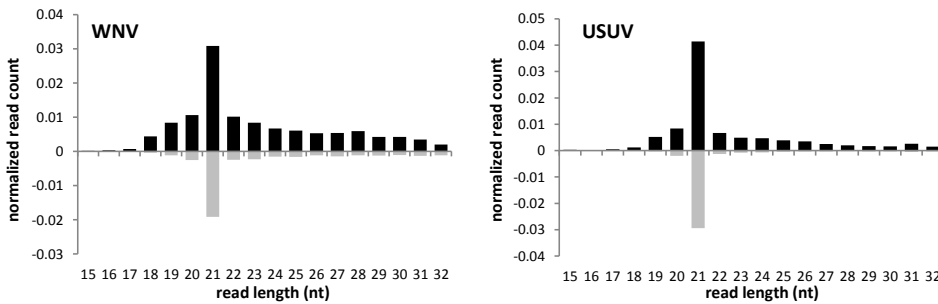


Figure 3.3. RNAi activity in WNV and USUV infected mosquitoes. Size and relative abundance of small RNA reads mapping to the WNV and USUV genomes. Reads mapping to the positive strand (black) are shown above the axis and reads to the negative strand (gray) below the axis.

USUV infection is more effective at higher ambient temperatures.

Culex pipiens mosquitoes are more competent for WNV at higher ambient temperatures (chapter 2). While both USUV and WNV are endemic in parts of Mediterranean Europe, USUV also extends its distribution into the cooler, more central and northern parts of Europe. We hypothesized that the ambient temperature could differentially affect the vector competence to either virus.

Oral infections were performed by offering the mosquitoes a blood meal containing either USUV or WNV, with 3.2×10^7 and 2.2×10^8 TCID₅₀ per ml, respectively. We chose to use higher WNV titres to compensate for the lower vector competence for WNV (Figure 3.1). Fully engorged females were incubated at three different temperatures (18°C, 23°C and 28°C). These temperatures represented the mean diurnal summer (July-August) temperature in northwestern Europe, an intermediate temperature, and the mean diurnal summer temperature for Mediterranean Europe, respectively (iii). After two weeks the mosquitoes were homogenized and the respective viruses were detected. WNV displayed higher infection rates at higher temperatures, infecting 17% at 18°C, 43% at 23°C and 58% at 28°C (Figure 3.4, open symbols).

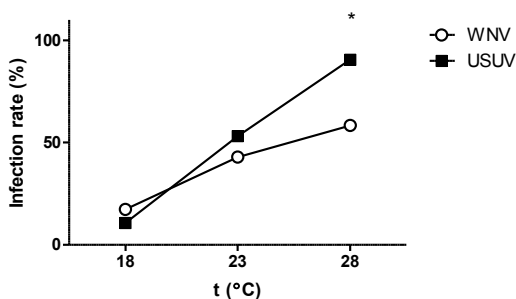


Figure 3.4. USUV is more infectious than WNV at higher temperature. After infectious blood meals, engorged mosquitoes were incubated at three different temperatures for fourteen days, before determining the presence of WNV and USUV. Data points indicate the percentage of infected mosquitoes from the total sample size ($n > 25$). Asterisk indicates significant difference between WNV and USUV ($P < 0.01$, Fisher's exact test).

At lower temperatures USUV infected a similar percentage of mosquitoes (11% at 18°C and 53 % at 23°C). Interestingly, at 28°C, 90% of the mosquitoes were infected with USUV (Figure 3.4, closed symbols), which was significantly more compared to the 58% for WNV (Fisher's exact test, $P < 0.01$). This was especially significant as the titre used for USUV in the infectious blood meals was seven times lower. This indicates that USUV is highly infectious for European *Culex pipiens* mosquitoes and that temperature differentially affects the susceptibility of mosquitoes to either USUV or WNV.

Discussion

Here we show for the first time that USUV not only infects the northern house mosquito *Culex pipiens*, but also effectively disseminates and accumulates in its saliva (Figure 3.1A). In the field USUV is mostly detected in *Culex* species mosquitoes, although it has also been found in mosquitoes from four other genera within the family of *Culicidae*. To what extent mosquitoes from these genera may contribute to the dispersal of USUV is unclear. In southern Europe, USUV was detected in *Culex pipiens*, which is the most abundant mosquito species in Europe and a competent WNV vector (Chapter 2)(41, 118). Northern Europe has a second abundant *Culex* species: *Culex torrentium*. It would be interesting to investigate whether this mosquito species can act as a transmission vector for USUV.

In addition to competent USUV vectors, sufficient vertebrate species are required as amplifying hosts. Susceptible bird species are prevalent in Europe as USUV has been detected in a large number of avian species, most notably within the *Turdus* genus (117, 121). In addition to birds, other vertebrates can become infected with USUV. Like WNV, humans and horses are incidental hosts. Whether bats develop viral titres that are high enough to contribute to the dispersal of USUV is unknown, but if bats are a reservoir this could dramatically influence transmission model predictions (124). Experimental WNV infections in birds can result in viraemia above 10^9 plaque forming units per ml, which is clearly sufficient to infect blood feeding mosquitoes (12). In the experiments presented here, the chicken blood used for infectious blood meals contained USUV titres of maximally 4×10^7 TCID₅₀ per ml. Higher titers in the blood of USUV infected birds may further increase the percentage of vectors able to transmit USUV after blood feeding.

Both USUV and WNV disseminated into the saliva of up to 100% of mosquitoes that were intrathoracically injected with either virus (Figure 3.1B). Interestingly, the viral titres that are present in orally infected mosquitoes were variable, whereas infection by injection displayed only limited variation (Figure 3.2). This indicates that the midgut acts as the major bottleneck for dissemination of the virus. Potentially, the induction of antiviral responses, and/or selective pressure for certain viral quasi species may influence subsequent viral replication and dissemination. Injection of WNV also resulted in titres that were higher than those of blood fed or USUV-injected mosquitoes. Together with the lower vector competence, this suggests that the barriers in the midgut epithelial cells of *Culex pipiens* are more effective against WNV as compared to USUV.

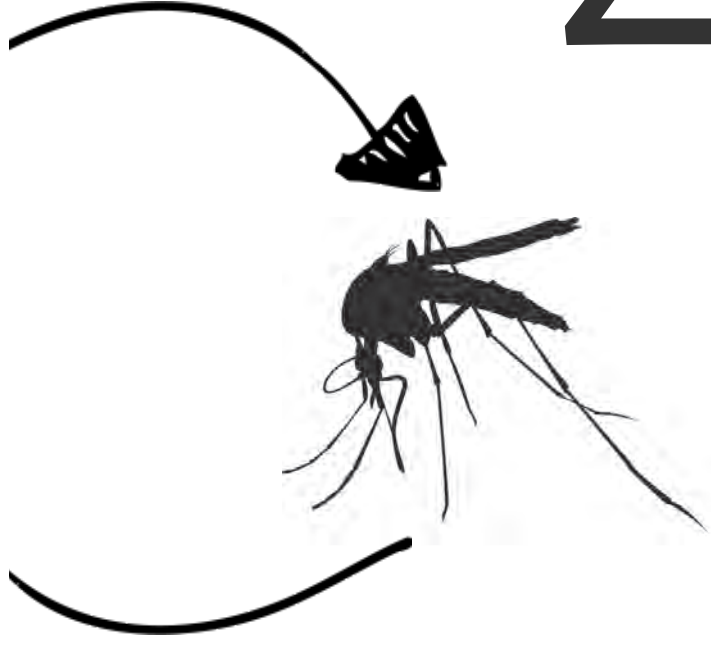
Both viruses elicited an RNAi response by displaying viRNA, with the dicer-2 dependent signature of 21 nucleotides mapping to both the positive genomic RNA strand and the complementary negative strand. There were no apparent differences in viRNA expression that could explain the differential transmission rates between the two viruses.

Despite the observed differences in infectivity and transmissibility, both WNV and USUV can effectively be transmitted by *Culex pipiens*. However, their distribution throughout Europe only has limited overlap. The dispersal of WNV has a strong correlation with mean summer temperatures, which can be explained by the vector competence for WNV at the corresponding temperatures (Chapter 2). USUV activity is also found in more temperate regions, but surprisingly the infectivity in *Culex pipiens* showed a strong temperature dependency, which was more pronounced than for WNV. In the experiments presented here, we used a constant incubation temperature that represented a mean summer temperature. However, diurnal temperature fluctuations around this mean may have additional effects on the vector competence. Indeed, the vector competence of *Aedes aegypti* for dengue virus is influenced by the diurnal temperature range. Fluctuations around lower mean temperatures (<18°C) increased the vector competence in comparison to mosquitoes that were incubated at identical, yet constant, mean temperatures (134). Because *Culex pipiens* is more competent for USUV at higher temperatures, temperature fluctuations above a relatively low mean may still enable USUV to have a higher vectorial capacity compared to WNV, but clearly this needs further experimental evidence.

In conclusion, both USUV and WNV can be transmitted by European *Culex pipiens* mosquitoes and at higher temperatures both the infection rates increase, when infected orally. At higher temperatures, however, *Culex pipiens* is significantly more competent for USUV as compared to WNV. As both viruses utilize the same reservoir species and global temperatures are expected to rise, this suggests that USUV may precede WNV transmission in Europe.

Acknowledgments:

We thank Corinne Geertsema and Els Roode for technical support concerning the BSL3 laboratory and Byron Martina for sharing the WNV isolates. This work is supported by the European Union's Seventh Framework Programme (FP7 VECTORIE project number 261466).



4 Chapter

Mosquito Rasputin interacts with chikungunya virus nsP₃ and determines the infection rate in *Aedes albopictus*

Chikungunya virus (CHIKV) is an arthritogenic alphavirus (family *Togaviridae*), transmitted by *Aedes* species mosquitoes. CHIKV re-emerged in 2004 with multiple outbreaks worldwide and recently reached the Americas where it has infected over a million individuals in a rapidly expanding epidemic. While alphavirus replication is well understood in general, the specific function(s) of non-structural protein nsP₃ remain elusive. CHIKV nsP₃ modulates the mammalian stress response by preventing stress granule formation through sequestration of G₃BP. In mosquitoes, nsP₃ is a determinant of vector specificity, but its functional interaction with mosquito proteins is unclear. In this research we studied the domains required for localization of CHIKV nsP₃ in insect cells and demonstrated its molecular interaction with Rasputin (Rin), the mosquito homologue of G₃BP. The biological involvement of Rin in CHIKV infection was investigated in live *Ae. albopictus* mosquitoes.

In insect cells, nsP₃ localized as cytoplasmic granules, which was dependent on the central domain and the C-terminal variable region but independent of the N-terminal macrodomain. *Ae. albopictus* Rin displayed a diffuse, cytoplasmic localization, but was effectively sequestered into nsP₃-granules upon nsP₃ co-expression. Site-directed mutagenesis showed that the Rin-nsP₃ interaction involved the NTF₂-like domain of Rin and two conserved TFGD repeats in the C-terminal variable domain of nsP₃. Silencing of Rin in cultured mosquito cells did not change nsP₃ localization, CHIKV replication levels, viral glycoprotein expression or virus production. *In vivo*, however, Rin depletion significantly decreased the CHIKV infection rate and transmissibility in *Ae. albopictus*.

We identified the nsP₃ hypervariable C-terminal domain as critical factor for granular localization and sequestration of mosquito Rin. Our study offers novel insight into a conserved virus-mosquito interaction at the molecular level, and reveals a strong proviral role for G₃BP homologue Rin in live mosquitoes, making the nsP₃-Rin interaction a putative target to interfere with the CHIKV transmission cycle.

This chapter is in preparation for submission as:

Jelke J. Fros, Corinne Geertsema*, Karima Zouache, Jim Baggen, Natalia Domeradzka, Daniël van Leeuwen, Jacky Flipse, Just M. Vlak, Anna-Bella Failloux & Gorben P. Pijlman. Mosquito Rasputin interacts with chikungunya virus nsP₃ and determines the infection rate in *Aedes albopictus*

Introduction

Chikungunya virus (CHIKV) is a member of the genus *Alphavirus* (family *Togaviridae*), a group of widely distributed human and animal pathogens. The New world alphaviruses can cause encephalitic disease in humans, while the Old world alphaviruses, including CHIKV, Sindbis virus (SINV), O'nyong nyong virus (ONNV) and Semliki Forest virus (SFV), are associated with rash, fever and (sometimes chronic) arthritis (135). CHIKV is transmitted by vector mosquitoes and actively replicates in mosquitoes of the genus *Aedes*, in particular *Ae. aegypti* and *Ae. albopictus*. CHIKV is endemic in most of Central Africa and South-East Asia. In 2005-2006, major outbreaks of CHIKV occurred on the Indian Ocean islands of Mayotte, Seychelles, Mauritius and La Réunion, where more than one-third of the population was infected and resultant deaths were reported (135) (Schwartz & Albert, 2010). In 2006-2007 CHIKV caused a major outbreak in India (~1.3 million cases), followed by outbreaks in the rest of South-East Asia (136). The first autochthonous CHIKV outbreak in Europe occurred in Italy in 2007, where more than 200 people were infected (32). Likewise, a local CHIKV transmission by *Ae. albopictus* occurred in France in 2010 (2 cases) and 2014 (4 cases) (33, 34). The outbreak that started in the Caribbean in 2013 has spread to the American main land and by December 2014 over a million cases have been reported throughout the Americas (36, 137). No licensed vaccine or antiviral treatment against CHIKV is available at present, but many prototype vaccines are in development (138-144).

CHIKV proteins are translated from a viral single-stranded positive-sense RNA of approximately 11.8kb (29, 145). The four alphavirus non-structural proteins (nsP1-4) are directly translated from genomic RNA and form a replication complex (RC), which is associated with the plasma membrane and endosomal membranes (146). A number of functions have been assigned to alphavirus nsPs: nsP1 is involved in capping of RNA (145) and is the membrane anchor of the RC (146), nsP2 has protease and helicase activity, causes host shut-off and inhibits interferon-induced JAK-STAT signaling and the unfolded protein response (147-150). nsP4 serves as RNA-dependent RNA polymerase (29). The functions of nsP3 are more enigmatic, but the protein is highly phosphorylated on serine and threonine residues (151, 152) and is essential for RNA synthesis (153) as part of the viral RC (146). CHIKV nsP3 can be divided in three regions; the macrodomain (amino acids 1-160) is conserved among alphaviruses, *Coronaviridae*, rubella and hepatitis E viruses and can bind ADP-ribose, RNA and DNA *in vitro* (154). The central, zinc-binding domain (amino acids 161-324) is conserved among alphaviruses, while the C-terminal region is highly variable and even shows substantial dissimilarity between CHIKV strains (155, 156).

SINV nsP3 is found in cytoplasmic granules or foci which are also comprised of various host proteins (92, 93). In both mammalian and mosquito cells the cellular protein Ras-GAP SH3 domain binding proteins (G3BPs) were

found in nsP3-granules (92, 93). G3BPs are ubiquitously expressed proteins conserved among eukaryotes. Mammals have three G3BPs: G3BP1, 2a and 2b, which are expressed from 2 distinct genes, while insects have one, named Rasputin (Rin) (157). Mammalian G3BP is a widely used marker for stress granules (SGs) (158), which are cytoplasmic messenger ribonucleoproteins (mRNPs) that form when translation is impaired in response to several types of cellular stress (90). nsP3-G3BP-granules are the explicit phenotype of the first reported function of alphavirus nsP3, as we have recently shown that CHIKV nsP3-G3BP granule formation prevents the establishment of *bona fide* SGs (159). These nsP3-G3BP-granules did not contain any other SG markers (e.g. eIF3) and cells expressing nsP3 were unable to respond normally to oxidative stress (159). The inhibition of SGs via an interaction between nsP3 and G3BP has now also been confirmed for SFV (160). Details on the interaction between nsP3 and mosquito Rin are currently lacking.

Mosquito vectors display different degrees of vector competence for different CHIKV isolates (161). Vector competence is a complex trait involving an interplay between vectors, pathogens and environmental factors (162) but the molecular details are not well understood. While it has been firmly established that antiviral RNAi pathways play a major role in controlling CHIKV and other arboviral infections in the mosquito (53, 133), other mechanisms of virus-host interactions that influence vector competence and the roles therein of viral (non)structural proteins need to be examined. Recently, however, nsP3 of ONNV (transmitted by *Anopheles* mosquitoes), has been uncovered as an important determinant for vector specificity. CHIKV does not normally infect *An. gambiae*, however, a chimeric virus containing ONNV nsP3 in a CHIKV infectious clone backbone became infectious for *An. gambiae* mosquitoes (99). Thus, it is hypothesized that specific molecular interactions between mosquito host factors and alphavirus nsP3 determine the vector specificity.

In the present study, we investigated the formation of nsP3-granules in insect cells and elucidated the molecular interactions between nsP3 and Rin. Moreover, we studied the effect of Rin silencing on virus replication in mosquito cell culture and on vector competence for CHIKV in mosquitoes. We show that Rin is an important, proviral determinant for CHIKV infection and dissemination in live mosquitoes.

Materials and methods

Cells and viruses

Spodoptera frugiperda Sf21 cells were cultured in Grace's medium (Invitrogen) with 10% fetal bovine serum (FBS; Invitrogen) and Sf9 cells in Sf900 medium (Invitrogen) with 5% FBS. *Aedes albopictus* U4.4 cells and C6/36 cells were cultured in Leibovitz's medium (Invitrogen) supplemented with 10% FBS, 2% tryptose phosphate (Invitrogen) and 1% non-essential amino acids (Invitrogen). All insect cells were cultured at 27°C. Vero E6 and HEK293t mammalian cells were cultured in Dulbecco's modified Eagle medium (Invitrogen) supplemented with 10% FBS at 37°C and 5% CO₂. Infections in cell culture were performed with CHIKV isolate S27 and mosquitoes were infected with CHIKV o6-o21 strain.

Plasmid construction

Cloning of EGFP-nsP3 was described previously and cloned via Gateway technology into pcDNA/Dest40 and pIB-GW plasmid backbones for CMV and OpIE2 driven expression, respectively. Plasmids pIB-EGFP-nsP3.2, pIB-EGFP-nsP3-DDEL, and pIB-EGFP-nsP3-dUGA were generated by PCR from pIB-EGFP-nsP3 using the phosphorylated forward primer attB2-R-phos and reverse primers CHIKVnsP3-2R, CHIKVnsP3-DDEL-R, and CHIKVnsP3-dUGA-R, respectively. Plasmids pIB-EGFP-nsP3.7, pIB-EGFP-nsP3.8, and pIB-EGFP-nsP3.10 were generated from pIB-EGFP-nsP3 and pIB-EGFP-nsP3.2 using the phosphorylated reverse primer EGFP-R-phos and forward primers EcoRI-nsP3-161-F (nsP3.7 and nsP3.8), or EcoRI-nsP3-319-F (nsP3.10). *Ae. albopictus* Rin was amplified by RT-PCR (Invitrogen) from total RNA isolated from U4.4 cells using the Rin forward and reverse primers and cloned into pGEM-T easy (Promega) and sequenced (Genbank accession number KP641128). To obtain pIB-Rin-mCherry, Rin was amplified by PCR from pGEM-Teasy-Rin using primers containing *Hind*III sites and was inserted as a *Hind*III fragment into pIB-mCherry, in frame with and upstream of mCherry. Site-directed mutagenesis of pIB-EGFP-nsP3 and pIB-Rin-mCherry was performed using the forward and reverse primers for nsP3-P398A, nsP3-PRR401AAA, nsP3-FG479AA, nsP3-FG497AA, Rin-F34A and Rin-F34W. All constructs were verified by sequencing and primer sequences are listed in Table 1.

Transient expression of nsP3 and Rin

Insect cells were transfected with the indicated expression plasmids using Fectofly I (Polyplus) or ExpreS2 rt (ExpreS2ion Biotechnologies). Mammalian cells were transfected with lipofectamine 2000 (Invitrogen). Twenty-four hours post transfection the fluorescence of EGFP-nsP3 and/or Rin-mCherry was analysed using a Zeiss Axio Observer Zim inverted microscope in combination with an X-Cite 120 series lamp.

Table 4.1. Oligonucleotides used in this study.

Name	Sequence
attB2-R-phos	TCATACCCAGCTTTCTTGTAC
CHIKVnsP3-2R	TCAGCGTGATGGCACGTTATGG
CHIKV nsP3-DDEL-R	TCATAATTCGTCGTCCTCGTGTC
CHIKV nsP3-dUGA-R	TCACCCACCTGCCCTATCTAGTAATTCGTCGTCCTCGTGCTG
EGFP-R-phos	CTTGTAACAGCTCGTCCATG
EcoRI-nsP3-161-F	CAAGTGGAATTACTAGACGAAC
nsP3-319-F	GTTAGTCCAAGGGAATATAAATC
Aalb-Rin-F	ATGGTAATGGAAGCACAACC
Aalb-Rin-R	CTAACGTCGTCCTCCGTAG
Aalb-Rin-intF	TCCAAGTGTCGCTACC
HindIII-EcoRI-Aalb-Rin-F	GATAAGCTTGAATTCACCATGGTAATGGAAGCACAACC
HindIII-Aalb-Rin-R	GATAAGCTTACGTCGTCCTCCGTAGG
nsP3-FG479AA F	TAACGGCCGCGGATTTTGATGAAGGGGAGA
nsP3-FG479AA R	AATCCGCGGCCGTTATGGGGAAAAGTCTCGT
nsP3-FG497AA F	TGACCGCTGCGGACTTCTCGCCGGGCGAAG
nsP3-FG497AA R	GTCCGCAGCGGTCAGTAACTCAGAGGACAA
Rin-F34A F	GCACCGTGCCTACAACAACCTCGTCGAGCTTC
Rin-F34A R	TGTTGTAGGCACGGTGCAGGTGATCCGGCG
Rin-F34A F	GCACCGTTGGTACAACAACCTCGTCGAGCTTC
Rin-F34A R	TGTTGTACCAACGGTGCAGGTGATCCGGCG
T7-pGEM-Teasy-R	TAATACGACTCACTATAGGGGCCGCGAATTCCTAGTG
Aalb-Rin F2	GTATGCCAACCATTGATCCG
Aalb-Rin R2	GTCCAGTTTCGTTTCATTGACAG
nsP1-int F	CTGACGGAAGGTAGACGAG
nsP1-int R2	GCACGTGAAGCTGAGCTTCCC
S7 F	CCAGGCTATCCTGGAGTTG
S7 R	GACGTGCTTGCCGGAGAAC
nsP3-P398A F	GAATACCGCGGCAGTCGCA
nsP3-P398A R	TGCGACTGCCGCGGTATTC
nsP3-PRR401AAA F	CGCCAGTCGCAGCGGCCGCAAGAAGACGTGGGAA
nsP3-PRR401AAA R	CCCACGTCTTCTTGCGGCCGCTGCGACTGGCGCGGTAT

Rin Knockdown experiments

Linear DNA of *Ae. albopictus* Rin and firefly luciferase was generated by PCR from pGEM-T easy plasmids using the T7 universal primer (New England Biolabs) and T7-pGEM-Teasy-R and double-stranded (ds)RNA was synthesized *in vitro* with T7 RNA polymerase (Invitrogen). Knockdown in cell culture was

performed by transfecting dsRNA into U4.4 cells grown in 24-wells plates (1µg of RNA per well) using Fugene (promega). One day later, cells were transfected with plasmid pIB-EGFP-nsP3 to monitor nsP3-granule formation or infected with CHIKV at a multiplicity of infection (MOI) of five. At the indicated times post infection, the medium was removed from the cells and used in end point dilution assays on Vero E6 cells. The remaining cells were lysed in TRIzol (life technologies) reagent and total RNA was isolated. The RNA was DNase treated (Applied Biosystems) and reverse transcribed using random primers. Rin, S7 and genomic CHIKV cDNA were amplified (primers: Rin F2/R2, S7 F/R and nsP1 int F/R2) and detected with real-time PCR platinum SYBR Green (Invitrogen), in a Rotor Gene RG-3000 (Corbett Research).

In parallel experiments, cells were washed with PBS and lysed in SDS-loading buffer [100 mM Tris-Cl (pH 6.8), 4% (w/v) sodium dodecyl sulfate (SDS), 0.2% (w/v) bromophenol blue, 20% (v/v) glycerol and 200 mM β-mercaptoethanol]. Samples were heated at 95°C for 10 min, clarified by centrifugation for one min at 13 000 r.p.m and loaded on a 12% SDS-Polyacrylamide gel. After electrophoresis, denatured proteins were transferred to an Immobilon membrane (Millipore) for analysis by Western blotting. Membranes were blocked in 3% skimmed milk in PBS with 0.05% Tween 60 (PBST) for 1 h at room temperature. Membranes were washed three times for 5 min each with PBST and subsequently incubated for 1 h at room temperature with rabbit polyclonal anti-E2 (diluted 1 : 20000; (163)) and anti-β-tubulin (diluted 1 : 4000; Abcam) in PBST, respectively. Membranes were washed and treated with alkaline phosphatase conjugated with goat anti-rabbit IgG mAb (Sigma), diluted 1 : 3000 in PBST, for 45 min at room temperature. Membranes were washed twice for 5 min each with PBST and once for 10 min with AP buffer [100 mM NaCl, 5 mM MgCl₂, 100 mM Tris/HCl (pH 9.5), 0.1% Tween 20]. Proteins were detected by nitro blue tetrazolium chloride/BCIP staining (Roche).

In vivo knock down of Rin was performed in *Ae. albopictus* mosquitoes originating from la Reunion island (Providence, F11 generation). 500 ng of dsRin or dsLuc RNA was injected directly in the thorax of female mosquitoes (Drummond nanoject II). Two days post injection mosquitoes were either sacrificed and stored at -80°C or orally infected with an infectious blood meal containing 10⁷ pfu/ml of CHIKV 06-021 strain. Mosquito rearing and preparation of the infectious blood meal was reported previously (162). Fully engorged females were selected and incubated in climatic chambers (Binder) at 28°C, with a light: dark cycle of 16h: 8h and 70% relative humidity. Forced salivation were performed 6 days post-infection as described previously (161). Saliva and mosquitoes were stored at -80°C pending further analysis.

Infectivity assays

Frozen mosquitoes were dissected, separating bodies (abdomen and thorax) from the head. Individual mosquito bodies and heads were homogenized in the bullet blender storm (Next Advance) in 100 μ l of DMEM Hepes (Gibco)-buffered medium supplemented with 10% FBS containing penicillin (100 IU/ml), streptomycin (100 μ g/ml), fungizone (2,5 μ g/ml) and gentamycin (50 μ g/ml) and spun down for 90 seconds at 14,000 rpm in a table top centrifuge. Thirty μ l of the supernatant from the mosquito homogenate or the saliva-containing mixture was incubated on a monolayer of Vero cells in a 96-wells plate. After 2-4 hours the medium was replaced by 100 μ l of fresh cell culture medium, fully supplemented with antibiotics. Wells were scored for virus specific cytopathic effects (CPE) at three days post infection. Viral titres were determined using 10 μ l of the supernatant from the mosquito homogenates in an end point dilution assay on Vero E6 cells. Infections were scored by CPE, three days post infection.

Statistical analysis

CHIKV infections in mosquito bodies and heads were scored positive or negative and significant differences were calculated using the Fisher's exact test ($P < 0.05$). Differences in CHIKV titers (TCID₅₀/ml) in infected mosquito bodies and heads were calculated using the Mann Whitney test ($P < 0.05$).

Results

CHIKV nsP3 displays granular localization in both insect and mammalian cells

Previous studies on the alphaviruses SINV, SFV and CHIKV showed that viral nonstructural protein nsP3, either in its authentic form or fused to markers like EGFP or mCherry, localized to cytoplasmic granules in mammalian cells (93, 159, 164, 165). To investigate if nsP3 has a similar intracellular distribution in insect cells, CHIKV nsP3 was transiently expressed, from an OpIE2 promoter-driven insect expression vector, with a N-terminal EGFP fusion (Figure 4.1A) in cell lines derived from mosquitoes (*Ae. albopictus*, U4.4 and C6/36) (Figure 4.1B, left) and lepidopteran insects (*Spodoptera frugiperda*, Sf21 and Sf9) (Figure 4.1B, middle). As a control, CHIKV nsP3 was also expressed in Vero and HEK293T cells (Figure 4.1B, right). In all cell lines tested, CHIKV nsP3 formed cytoplasmic granules (Figure 4.1B), which indicates that the intracellular localization of nsP3 is conserved in cells of both vertebrate and invertebrate origin.

The gene encoding CHIKV nsP3 contains a natural leaky (opal) stop codon, six codons upstream of the nsP3-4 cleavage site. Two isoforms of nsP3 are likely to be expressed from this gene during viral infections. To investigate whether both isoforms would have the same intracellular localization, two additional EGFP-fusions were made, one with nsP3 lacking the C-terminal six amino acids (CHIKV nsP3-DDEL) and one with nsP3 lacking the leaky stop codon (CHIKV nsP3-dUGA) (Figure 4.1A). When transiently expressed in insect cells, CHIKV nsP3 and the two isoforms displayed an identical granular localization (Figure 4.1C), which shows that the terminal six amino acids of CHIKV nsP3 do not impact its subcellular localization.

The conserved domain of CHIKV nsP3 is sufficient for multimerization but the variable domain is required for the formation of nsP3-granules

In mammalian cells, the C-terminal variable domain was found to be essential for nsP3 granule formation, and upon deletion the localization changed to a filamentous phenotype (159). To determine which domains within nsP3 are responsible for the formation of nsP3-granules, truncated versions of nsP3 fused with EGFP (Figure 4.1A) were expressed in insect cells (Figure 4.1D). Removal of the entire C-terminal variable region (nsP3.2) resulted in the formation of filamentous, cytoplasmic structures. (Figure 4.1D, left). To investigate whether the macrodomain could be eliminated from nsP3 without affecting its localization, it was deleted from EGFP-fused nsP3 and nsP3.2, yielding truncated mutants nsP3.7 and nsP3.8, respectively (Figure 4.1A). When expressed in insect cells, nsP3.7 showed an identical granular phenotype as full-length nsP3, whereas nsP3.8 formed filaments that were very similar to those produced by nsP3.2 (Figure 4.1D, middle). To investigate if the C-terminal,

variable region alone could cause granule formation, it was N-terminally fused to EGFP (nsP_{3.10}) (Figure 4.1A) and expressed in insect cells. The localization of nsP_{3.10} was diffuse, nuclear-cytoplasmic (Figure 4.1D, right), showing that the C-terminal region of CHIKV nsP₃ is required, but not sufficient for the formation of nsP₃ granules.

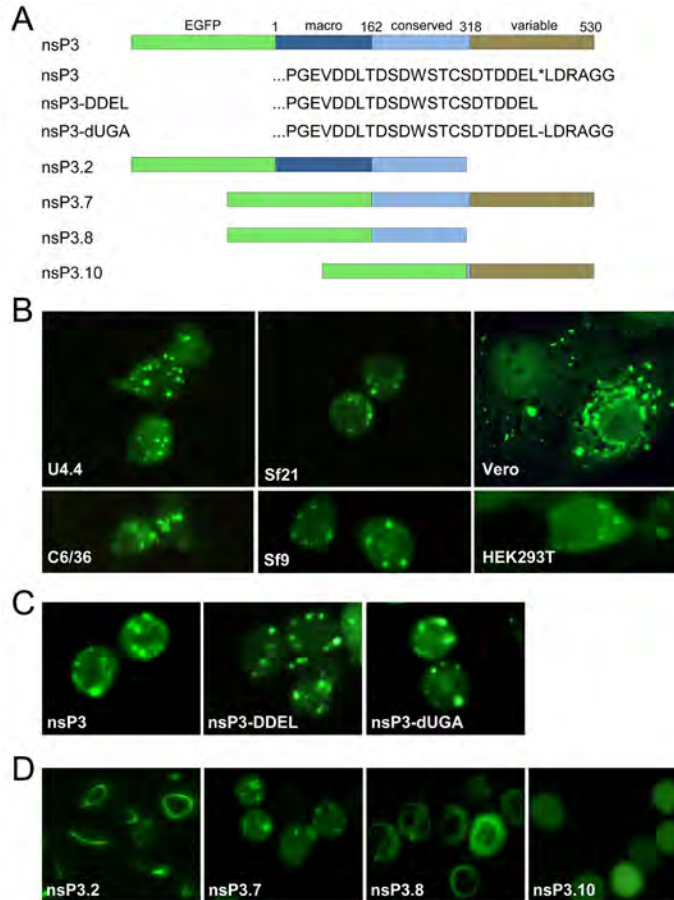


Figure 4.1. CHIKV nsP₃ forms granules in insect cells. **A.** Schematic representation of CHIKV nsP₃ variants used in this study. Representing either the full length protein N-terminally fused to EGFP (nsP₃), nsP₃ isoforms with adapted C-terminal amino acids (nsP₃, nsP₃-DDEL and nsP₃-dUGA) or truncated nsP₃ variants (nsP_{3.2}, 3.7, 3.8 and 3.10). Asterisk indicates opal stop codon between nsP₃ and nsP₄. **B.** Intracellular distribution of wild type CHIKV nsP₃ in cultured insect and mammalian cells. Mosquito and lepidopteran cells were transfected with plasmids that express the nsP₃ variants from OpIE2 insect promoters. In mammalian cells expression of the nsP₃ variants was driven by a cytomegalovirus promoter. **C.** Intracellular distribution of nsP₃-DDEL and nsP₃-dAUG in insect cells. **D.** Intracellular distribution of the truncated nsP₃ variants.

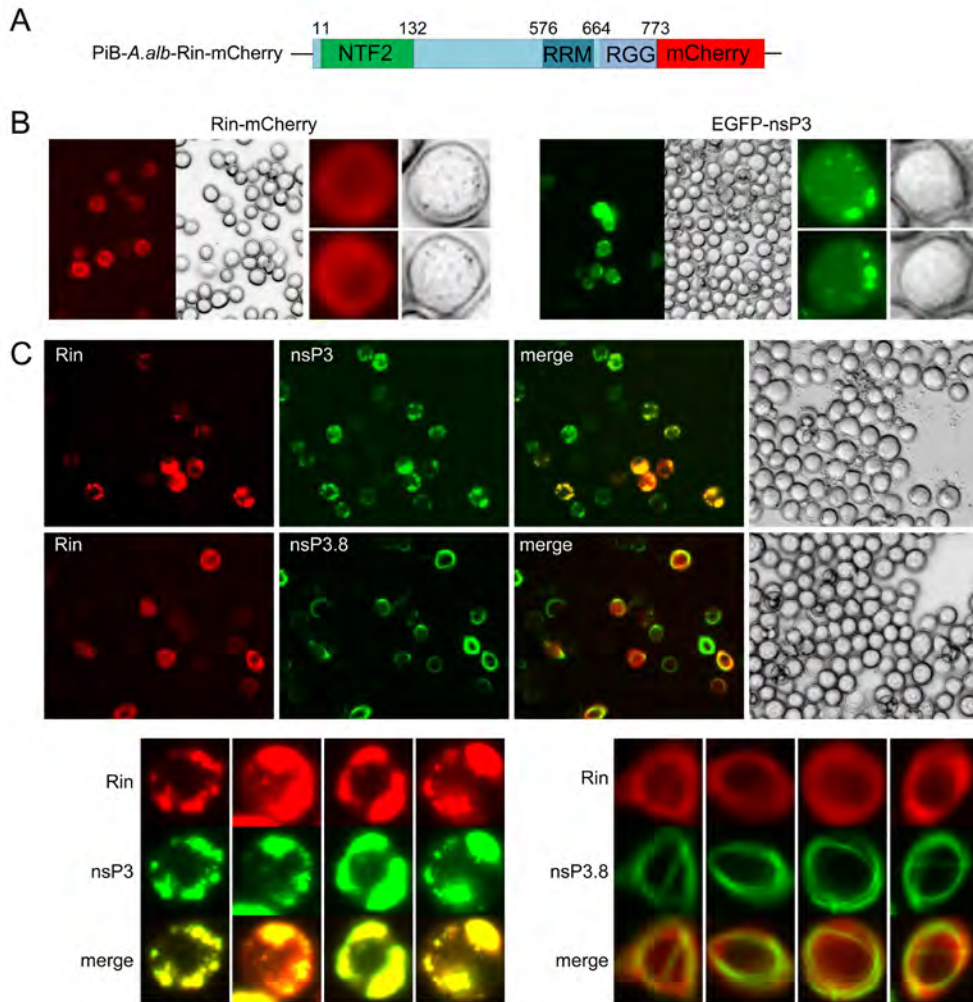


Figure 4.2. CHIKV nsP3 sequesters mosquito Rasputin into cytoplasmic granules. **A.** Schematic representation of *Ae.albopictus*-Rin-mCherry. NTF2; nuclear transport factor 2-like domain, RRM: RNA recognition motif, RGG; arginine-glycine rich box. **B.** *Ae.albopictus*-Rin-mCherry or EGFP-nsP3 were transiently expressed in insect cells and display diffuse and granular intracellular distributions, respectively. **C.** *Ae.albopictus*-Rin-mCherry and EGFP-nsP3 (top) or EGFP-nsP3.8 (bottom) were co-transfected into insect cells. Magnified images are presented.

NsP3 granules co-localize with Rasputin, the insect homolog of mammalian G3BP

In SINV nsP3 pull-down studies, G3BP and its insect homologue Rasputin (Rin) were identified as predominant nsP3-interacting proteins in virus-infected mammalian and mosquito cells, respectively (93). To study a putative interaction of CHIKV nsP3 with mosquito Rin in live cells, the gene encoding *Ae. albopictus* Rin was amplified by RT-PCR from total RNA isolated from U4.4 cells using PCR primers specific for *Ae. aegypti* Rin. We cloned and sequenced

the obtained amplicon. The *Ae. albopictus* Rin sequence (Genbank: KP641128) was 307 amino acids longer than human G3BP1, but the nuclear transport factor 2 (NTF2)-like domain, the RNA recognition motif (RRM) and the arginine glycine-rich (RGG-)box were conserved between these species (Figure 4.2A).

The subcellular localization of Rin was studied by transient expression in insect cells as C-terminal fusion with mCherry, in a similar fashion to a previously described and functional G3BP-EGFP fusion (158). When expressed in insect cells, Rin was evenly distributed throughout the cytoplasm (Figure 4.2B, left). However, when Rin was co-expressed with nsP3, which localized to small nsP3 granules (Figure 4.2B, right), both proteins displayed complete co-localization and formed much larger granules (Figure 4.2C, top). These nsP3- and Rin-positive granules or aggregates were larger and more asymmetrical than normal nsP3-granules. In this experiment, Rin was transiently (over) expressed, which may explain the large size of the granules. In contrast, when mCherry-Rin was co-expressed with the C-terminal truncated, filamentous mutants EGFP-nsP3.8 (Figure 4.2C, bottom) or EGF-nsP3.2 (not shown), Rin did not co-localize with the filaments formed by these mutants and retained its diffuse, cytoplasmic localization (Figure 4.2C). In conclusion, the C-terminal hypervariable domain of nsP3 is important for the interaction with Rin in insect cells.

The C-terminal TFGD repeats in the variable domain of CHIKV nsP3 interact with Rasputin

Previously we showed that transiently expressed CHIKV nsP3 sequesters G3BP into cytoplasmic granules in mammalian cells. Deletion of a conserved SH3-domain binding motif (PVAPPRRRR) in the variable domain of nsP3 resulted in a diffuse nuclear/cytoplasmic localization of nsP3 and abrogated the interaction between nsP3 and G3BP, restoring the potential of the cell to respond to oxidative stress (159). A recent study, however, convincingly showed that the interaction between nsP3 and mammalian G3BP depends on two conserved repeats (with core sequence TFGD) in the variable domain of nsP3 (166). To further investigate which domain(s) of nsP3 are crucial for the interaction between CHIKV nsP3 and Rin, both the SH3-domain binding motif and conserved TFGD repeats in the variable domain of nsP3 were mutated using site-directed mutagenesis (Figure 4.3A). When EGFP-nsP3 and Rin-mCherry were transiently expressed in insect cells, both wild type proteins displayed perfect co-localization. Deletion of the SH3-domain binding motif (nsP3-d398/406) resulted in a diffuse nuclear/cytoplasmic distribution of nsP3 and a diffuse mainly cytoplasmic localization of Rin (Figure 4.3B, second panel), identical to the distribution of nsP3 and G3BP in mammalian cells (159). However, when conserved proline and/or arginine residues from the SH3-domain binding motif were substituted for alanines (nsP3-P398A and nsP3-PRR401AAA) the co-localization of nsP3 and Rin in cytoplasmic nsP3-granules

remained unchanged (Figure 4.3B).

Next, we mutated both domains of the two conserved TFGD repeats separately or together resulting in pIB-EGFP-nsP3-FG479AA, pIB-EGFP-nsP3-FG497AA, and pIB-EGFP-nsP3-FG479AA/FG497AA. The single and double EGFP-nsP3 TFGD mutants were transiently expressed in insect cells together with Rin-mCherry. Both the single FG479AA and FG497AA mutants still sequestered Rin into nsP3-granules (Figure 4.3C, top and middle panels). The double TFGD mutant, however, displayed a completely diffuse intracellular distribution of Rin (Figure 4.3C, bottom panel) but retained a normal granular distribution similar to wildtype EGFP-nsP3 (Figure 4.1B).

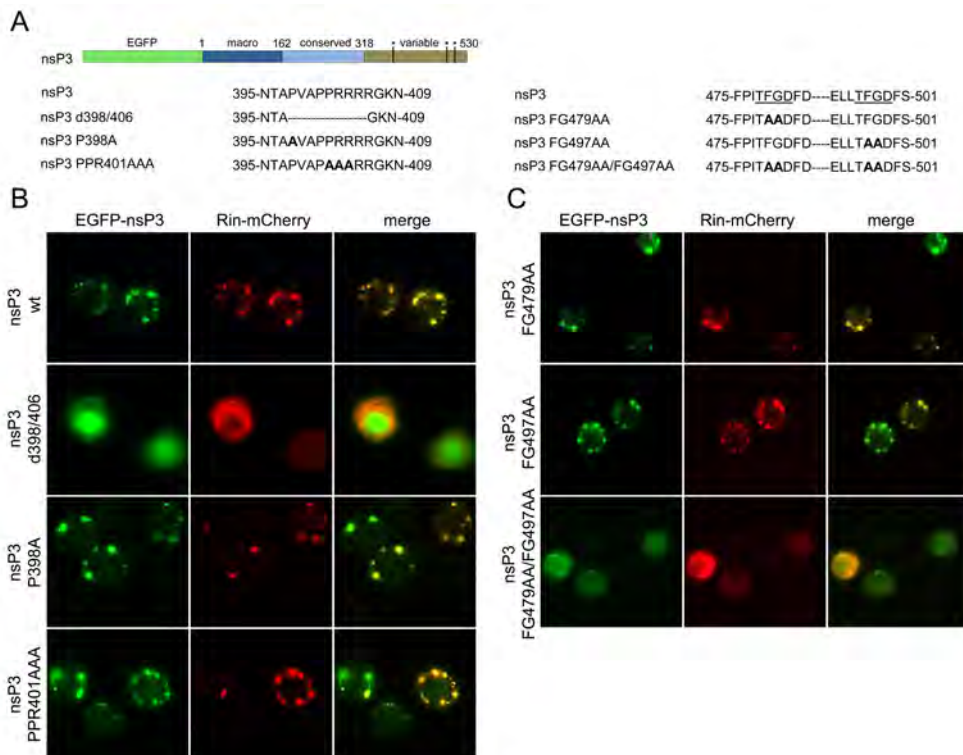


Figure 4.3. The C-terminal TFGD repeats of nsP3 interact with mosquito Rasputin. **A.** Schematic representation of nsP3 and the conserved domains within the C-terminal variable domain. Deletions and mutations are indicated in the amino acid sequence. Insect cells were co-transfected with Rin-mCherry and either one of the EGFP-nsP3 variants. **B.** SH3-domain binding motif, nsP3-d398/406, nsP3-P398A or nsP3-PPR401AAA. **C.** C-terminal repeats, EGFP-nsP3-FG479AA, EGFP-nsP3-FG497AA or EGFP-nsP3-FG479AA/FG497AA.

These results indicate that deletion of the SH3-domain binding motif does abrogate the formation of nsP3 granules, but the formation of nsP3-granules and the interaction with Rin is retained when conserved amino acids within the this domain are substituted for alanines. However, the formation of

CHIKV nsP3-Rin-granules is also abrogated when both the C-terminal conserved TFGD repeats are mutated, suggesting that these motifs are involved in the nsP3-rin interaction.

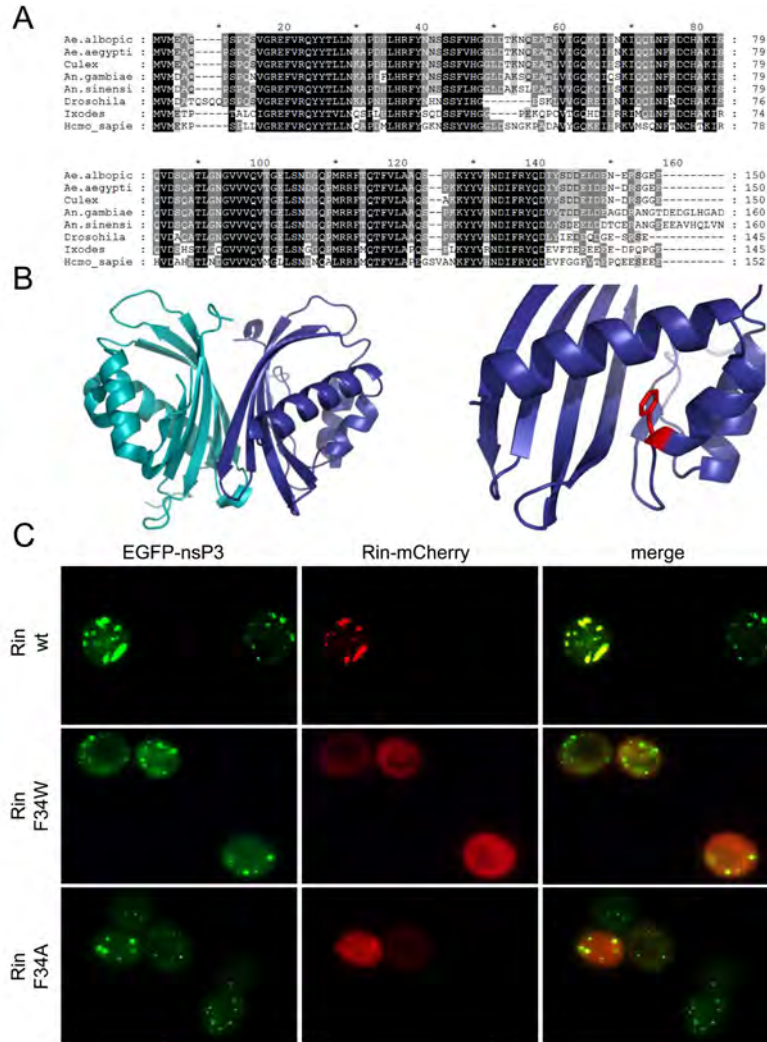


Figure 4.4. nsP3 interacts with the NTF2-like domain of mosquito Rasputin. **A.** Protein alignment of the Rin/G3BP NTF2-like domains from *Ae. albopictus* (KP641128), *Ae. aegypti* (XP_001651045), *Culex quinquefasciatus* (XP_001861860), *Anopheles gambiae* (XP_001688309), *Anopheles sinensis* (KFB40464), *Drosophila melanogaster* (AF231031), *Ixodes ricinus* (GANP01009274), and *Homo sapiens* (CAG38772). Genbank accession numbers in brackets. Alignment made with CLUSTALX and modified using Genedoc. **B.** Structural modeling of *Ae. albopictus*-Rin modeled onto *Drosophila melanogaster* Rin. Modeling was performed using the Phyre2 server (www.sbg.bio.ic.ac.uk/phyre2), results were visualized with PyMOL (www.pymol.org). Left, *Ae. albopictus* Rin (deep blue) is depicted together with *D. melanogaster* Rin (cyan). Right, the FxFG binding pocket is shown and phenyl alanine 34 is highlighted in red. **C.** Insect cells were co-transfected with EGFP-nsP3 and either Rin-mCherry (wild type), Rin-mCherry F34A or Rin-mCherry F34W.

The NTF2-like domain of mosquito Rin interacts with CHIKV nsP3.

The NTF2-like domain of G3BP has been shown to interact with SINV nsP3 in mammalian cells (92). The first 140 amino acids of mosquito Rin show high sequence homology to that of human G3BP and other NTF2-like domains (Figure 4.4A). Protein structure prediction of *Ae. albopictus* Rin revealed a 100% structural homology of the NTF2-like domain with those of G3BP and *Drosophila* Rin (Figure 4.4B, left). Here we mutated a phenylalanine of Rin (F34) that is expected to interact with the phenylalanines of FxFG domains via pi-stacking (Figure 4.4B, right) (167). Indeed, mutations F34W or F34A strongly reduced the sequestration of Rin into nsP3-granules (Figure 4.4C), indicating that this amino acid is essential for nsP3-Rin interaction.

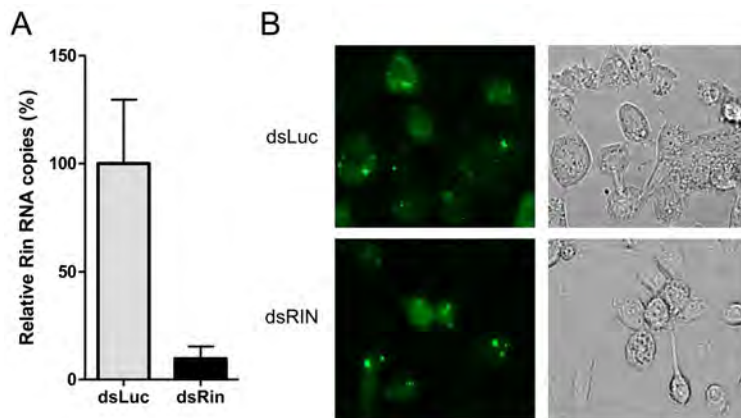


Figure 4.5. Formation of nsP3-granules is independent of mosquito Rasputin. **A.** Rin silencing was determined by semi-quantitative RT-PCR on *Ae. albopictus* Rin mRNA, relative for the internal control S7. Bars represent relative Rin mRNA expression normalized to dsLuc transfected samples. Error bars indicate standard deviation of duplicate samples from a single representative experiment, which is presented in **B.** **B.** U4.4 mosquito cells were transfected with dsRNA against *Ae. albopictus* Rin or luciferase. Twenty-four hours later these cells were transfected with wild type EGFP-nsP3, displaying a granular localization.

Effect of Rasputin silencing on the formation of CHIKV nsP3-granules

So far, we have shown that nsP3 has a granular localization and that Rin has a diffuse cytoplasmic localization when expressed individually. To investigate whether the formation of nsP3-granules requires Rin, localization of EGFP-nsP3 was studied after Rin expression was silenced in mosquito cells using dsRNA-mediated RNAi. U4.4 mosquito cells were transfected with dsRNA from either Rin (dsRin) or firefly luciferase (dsLuc) as a control. Semi-quantitative RT-PCR on *Ae. albopictus* Rin mRNA, normalized by housekeeping gene S7 mRNA, showed a 90% reduction in Rin mRNA when cells were transfected with dsRin RNA (Figure 4.5A). Subsequent transient expression of EGFP-nsP3 displayed clear nsP3-granules in both dsRin and dsLuc transfected cells (Figure 4.5B). This result indicates that mosquito Rasputin is not required for the formation of CHIKV nsP3-granules in mosquito cells.

Effect of Rasputin silencing on CHIKV infection in mosquito cell culture

Next, we examined the effects of Rin knock down on CHIKV infection in mosquito cell culture. U4.4 mosquito cells were transfected with dsRin or dsLuc. Twenty four hours later, cells were infected with CHIKV at an MOI of five. Sixteen and twenty-four hpi, total RNA was isolated, viral structural proteins were detected and viral titers were determined. Semi-quantitative RT-PCR on transcripts purified from CHIKV infected cells showed that Rin silencing was efficient (>70%) (Figure 4.6A). To quantify replication levels of CHIKV in Rin silenced cells the relative levels of CHIKV genomic RNA were measured. CHIKV replication produced equal concentrations of genomic RNA in Rin-depleted versus dsLuc transfected cells at both timepoints (Figure 4.6B).

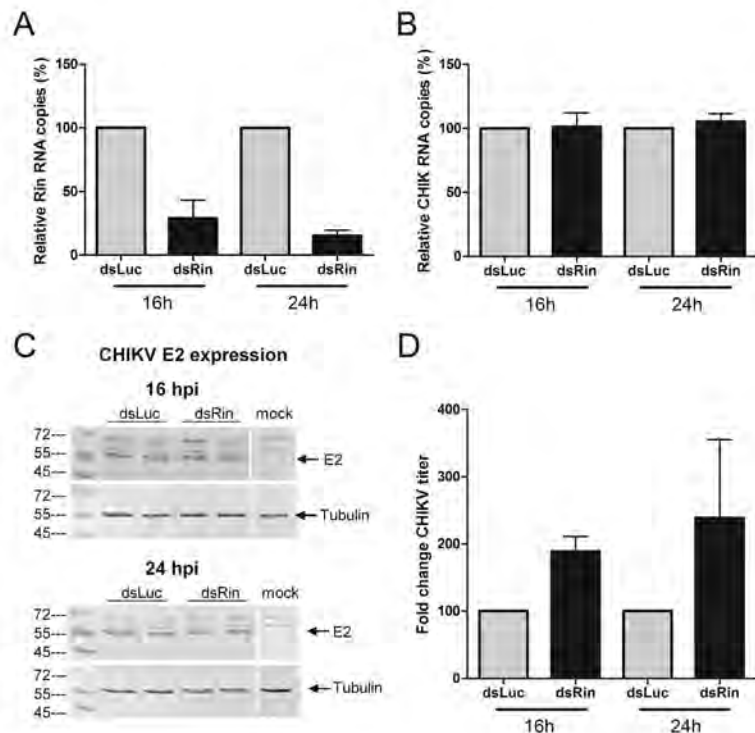


Figure 4.6. CHIKV infection is not affected by Rin depletion in cultured mosquito cells.

In four independent experiments, U4.4 mosquito cells were transfected with dsRNA against *Ae. albopictus* Rin or luciferase. Twenty-four hours later these cells were infected with CHIKV (MOI 5) and total RNA was isolated at 16 or 24 hpi. **A.** Rin silencing was determined by semi-quantitative RT-PCR on *Ae. albopictus* Rin mRNA, normalized for the internal control S7. **B.** CHIKV genomic RNA was quantified with primers that anneal to the nsP1 gene. **C.** CHIKV structural protein expression was determined by immunoblot staining against CHIKV E2 and host cell β -tubulin. Protein sizes indicated in kDa. **D.** At the indicated hpi medium was harvested and the CHIKV TCID₅₀/ml was determined in end point dilution assays. A,B,D. Bars represent the mean of four independent experiments, normalized to the respective value of dsLuc transfected samples in each individual experiment. Error bars represent one standard error of the mean.

Structural protein expression of CHIKV was detected in an immunoblot using E2 polyclonal antiserum, with no apparent differences between dsRin and dsLuc transfected cells, at both time points (Figure 4.6C, arrow). Correspondingly, the CHIKV titer in Rin-depleted cells was similar to the titer in cells transfected with dsLuc RNA (Figure 4.6D). We conclude that Rin depletion in cell culture does not affect CHIKV RNA replication, structural protein expression or virion production.

Rasputin silencing limits the CHIKV infection rate and transmissibility in *Aedes albopictus*

As alphavirus nsP3 is a determinant for vector specificity (99) and specifically interacts with Rin, we finally investigated the putative role for Rin during CHIKV infection in live mosquitoes. *Ae. albopictus* females (5-day old, 200 per group) were intrathoracically injected with 500 ng dsRNA against Rin or Fluc (day -2). Two days later (day 0), the mosquitoes were offered a blood meal containing 10^7 pfu/ml CHIKV. Six days after blood feeding saliva was isolated and the mosquitoes were sacrificed (Day 6) (Figure 4.7A). Silencing of Rin mRNA was confirmed in mosquitoes on the day of the blood meal, two days post dsRNA injections. Total RNA was isolated and relative Rin mRNA copies were quantified. Mean values in relative Rin mRNA copies in the dsRin injected mosquitoes were 60% of the dsLuc injected mosquitoes (Figure 4.7B).

On day six, mosquito saliva was obtained and the mosquito heads were separated from their thorax and abdomen, to distinguish between infections that were transmissible, fully disseminated or limited to the mosquito body, respectively. Mosquito saliva or homogenate from either heads or bodies were incubated on Vero cells to determine the presence of CHIKV. CHIKV infected 75% of the mosquitoes that were injected with dsLuc RNA. In these mosquitoes the infection had also disseminated into the head of the mosquito. In addition, it resulted in two mosquitoes with infectious saliva (Figure 4.7C, red symbols). Injection with dsRin significantly reduced ($P < 0.05$) the number of infected mosquito bodies to 40% with identical percentages in mosquito heads and no mosquitoes with infectious saliva (Figure 4.7C). In addition, Rin silencing also reduced the viral titers in the infected mosquitoes, with significant reductions in the mosquito heads ($P < 0.05$, Figure 4.7D). Together, these results show a significant effect of Rin silencing on the infection rate and dissemination of CHIKV in *Ae. albopictus*.

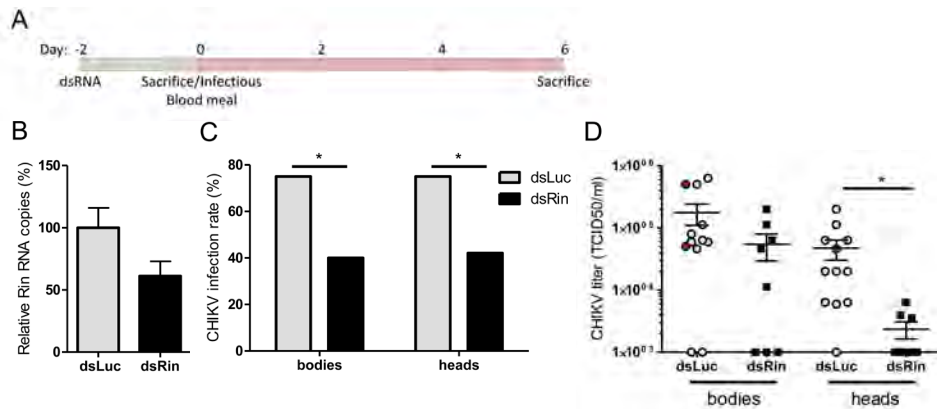


Figure 4.7. Rin silencing reduces the CHIKV infection rate in live *Aedes albopictus* mosquitoes. **A.** Schematic representation of the experiment. Mosquitoes were injected with 500ng of dsRin or dsLuc two days prior to blood feeding. On day 0, a subset of mosquitoes was sacrificed to determine the level of Rin depletion. Remaining mosquitoes were orally infected with CHIKV (10⁷ pfu/ml) and sacrificed six days post infection. **B.** Total RNA was isolated and Rin silencing was determined by semi-quantitative RT-PCR on *Ae. albopictus* Rin mRNA, normalized for the internal control S7. Bars represent mean Rin mRNA values normalized to dsLuc injected mosquitoes. Error bars indicate one standard error of the mean (n=5). **C.** Heads and bodies from the blood fed mosquitoes were separated, homogenized and the presence of CHIKV was determined by incubating the homogenate on Vero E6 cells. Bars represent the percentage of CHIKV positive mosquito bodies and heads from both dsLuc and dsRin injected mosquitoes. Asterisk indicates significant difference (P<0.05 Fisher's exact test). **D.** From all the CHIKV positive mosquito heads and bodies the viral titers (TCID₅₀/ml) were determined. Data points represent one individual mosquito head or body. Asterisk indicates significant difference between dsLuc and dsRin injected mosquitoes (P<0.05, Mann Whitney test) and red data points indicate mosquitoes with positive saliva.

Discussion

In this study we investigated the localization of CHIKV nsP3 and its interaction with mosquito Rin in insect cells and live mosquitoes. Our results show that the intracellular distribution of CHIKV nsP3 is conserved in cells from mammalian and insect origin. In mosquito cells, CHIKV nsP3 forms cytoplasmic granules, which are highly similar to the nsP3-G3BP granules that inhibit the formation of SGs in mammalian cells (159). Removal of the variable domain results in the formation of filaments and both the granular or filamentous distribution of nsP3 is independent of the N-terminal macrodomain. This indicates that multimerization of nsP3 is attributed to the central conserved domain. How nsP3 multimerizes into these two diverse cytoplasmic phenotypes is unknown, however, removal of the C-terminal variable domain may cause a conformational change or affect interactions with host factors which allows nsP3 to form long cytoplasmic filaments. Whereas Rin is clearly sequestered into nsP3-granules and transient overexpression of Rin may increase the size of the nsP3-granules, silencing of Rin and reducing its co-localization with nsP3 by mutagenesis shows that Rin is not required for the formation of nsP3-granules (Figures 4.3, 4.4 and 4.5). The exact structural composition of these nsP3 granules and filaments, however, needs further experimentation.

In mammalian cells, nsP3-granule formation and the inhibition of SGs is lost when the conserved SH3-domain binding motif is removed from the variable domain of nsP3 (159). Similarly, nsP3-d398/406 was diffuse throughout insect cells. Amino acid substitutions within the SH3-domain binding motif, however, did not affect the formation of nsP3-granules or the sequestration of mosquito Rin into granules. Apparently, the amino acid substitutions were not sufficient to abrogate the interaction between nsP3 and Rin. Alternatively, deletion of the complete SH3-domain binding motif may have disrupted the folding of nsP3, rendering a dysfunctional protein that no longer can execute its normal function. Indeed, deletion of the entire SH3-domain binding motif from a CHIKV replicon yielded a replication-negative phenotype (159).

G3BP and nsP3 were also shown to interact via two conserved repeats in the C-terminal variable domain of nsP3 (166). When we replaced the phenylalanine and glycine from either one of the nsP3 C-terminal TFGD repeat with alanines there was no apparent change in the co-localization of nsP3 and Rin. However, the interaction between nsP3 and Rin was completely lost when both TFGD repeats were mutated (Figure 4.3C). This suggests a direct interaction between these amino acid repeats and Rin and shows that both repeats interact with Rin but are exchangeable for the observed phenotype. *Ae. albopictus* Rin was isolated from U4.4 cells. Sequence analysis revealed that the N-terminal NTF2-like domain has high homology with other NTF2-like domains including human G3BP (Figure 4.4A). The three-dimensional crystal structures of the NTF2-like domains from *Drosophila* Rin and human G3BP have recently been resolved, and contain a binding pocket for FxFG containing

peptides (167, 168). The NTF2-like domain from *Ae. albopictus* Rin was modelled onto that of *Drosophila*, showing high resemblance (Figure 4.4B). As expected from this model, point mutations in the binding pocket of the Rin NTF2-like domain (position F34) greatly reduced the interaction between nsP₃ and Rin (Figure 4.4C). Although Rin still partly localized to nsP₃-granules, this result does provide evidence of an interaction between nsP₃ and the NTF2-like FxFG binding pocket. A recent study has confirmed that this interaction is conserved between homologue sites in SFV nsP₃ and vertebrate G₃BP (169). Additional interactions were predicted between FxFG peptides and residues in the NTF2-like binding pocket of G₃BP (167), which could explain the strongly reduced, but not completely abolished, interaction with nsP₃.

Rasputin silencing did not affect CHIKV infection in cultured mosquito cells (Figure 4.6). This is in agreement with *in vitro* studies with SINV and siRNA-mediated G₃BP_{1/2} silencing (170). However, a recent study that shows effective simultaneous knock down of both G₃BP₁ and G₃BP₂ resulted in decreased CHIKV replication rates, with severely reduced minus strand RNA replication (171). Similarly, depletion of Rin during oral, *in vivo* infections resulted in a marked decrease in CHIKV infected mosquitoes and disseminated virus particles in the heads (Figure 4.7). This suggests that Rin is involved in the establishment of a productive infection and/or affects CHIKV infections in specific tissues. It also suggests that results obtained in cell lines are not always a good proxy for results *in vivo*. Indeed, midgut barriers have been described in arthropods that limit arbovirus replication and/or dissemination through the organism (64, 65). The interaction between nsP₃ and Rin may play a significant role in modulating the midgut antiviral responses. Interestingly, exchanging the nsP₃ genes of CHIKV and ONNV made CHIKV infectious for *An. gambiae* (99). Moreover, replacing only the C-terminal end of CHIKV nsP₃, which is required for Rin interaction, with that of ONNV was sufficient to orally infect *An. gambiae* with CHIKV. This fragment encompasses the variable domain of CHIK nsP₃, suggesting a strong role for the C-terminal domain of nsP₃ in facilitating oral infection in specific vector species.

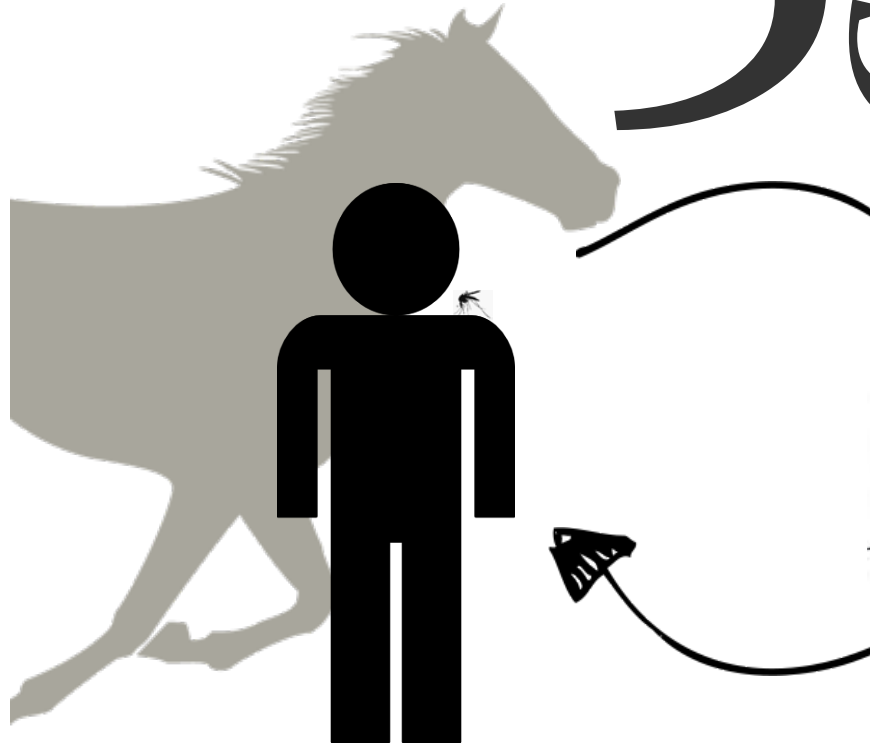
The decreased infectivity of CHIKV in Rin depleted mosquitoes suggests a proviral role for Rin. In *Drosophila*, Rin is involved in Ras and Rho-mediated signaling, cell proliferation and oogenesis (172–174). In mammalian cells, G₃BP is essential for assembly of SGs, which display many antiviral characteristics (89, 175). In response, viruses often inhibit the formation of *bona fide* SGs (reviewed in (89)). Poliovirus 3C cleaves G₃BP (176), whereas others, including alphaviruses, induce viral granules that sequester G₃BP and/or other SG factors (91, 159, 160, 177, 178). This suggests that viral-granules inhibit *bona fide* SG formation while at the same time utilizing SG components (e.g. G₃BP/Rin) for their own replication. Indeed, flavivirus and hepatitis C virus infections bind SG components which increases their replication efficiency (177, 179). In *Drosophila*, Rin has been suggested to form RNase inhibitor complexes (173),

which could protect CHIKV RNA replication during the initial infection in the mosquito midgut. Clearly, the molecular details of nsP3 and Rin in live mosquitoes should be examined in follow up studies to uncover the exact mechanism.

The interaction of nsP3 with Rin is highly homologous to that of nsP3 with G3BP in mammalian cells, which suggests that, in addition to the inhibition of SGs, nsP3-G3BP-granules formation can have additional roles to increase the infectivity of CHIKV or to evade antiviral responses. Disruption of this nsP3-Rin interaction could be of interest as a target for the development of compounds that stop the CHIKV transmission cycle.

Acknowledgements

We thank Els Roode for technical support concerning the BSL₃ laboratory in Wageningen. We acknowledge Marie Vazeille for injecting mosquitoes and Anubis Vega Rua and Laurence Mousson for their assistance in forced salivation. JJF and KZ were supported by the European 195 Community's Seventh Framework Programme (FP7 VECTORIE project number 261466) and KZ by the Foundation Inkermann (Fondation de France).



5 Chapter

Chikungunya virus nsP₃ blocks stress granule assembly by recruitment of G₃BP into cytoplasmic foci

Chikungunya virus nonstructural protein nsP₃ has an essential but unknown role in alphavirus replication and interacts with Ras-GAP SH₃ domain-binding protein (G₃BP). Here, we describe the first known function of nsP₃ to inhibit stress granule assembly by recruiting G₃BP into cytoplasmic foci. A conserved SH₃ domain-binding motif in nsP₃ is essential for both nsP₃-G₃BP interactions and viral RNA replication. This study reveals a novel role for nsP₃ as regulator of the cellular stress response.

This chapter has been published as:

Jelke J. Fros, Natalia E. Domeradзка, Jim Baggen, Corinne Geertsema, Jacky Flipse, Just M. Vlak and Gorben P. Pijlman. *Chikungunya virus nsP₃ blocks stress granule assembly by recruitment of G₃BP into cytoplasmic foci*. *J. Virol.* **86**, 10873-9 (2012).

Main text

Chikungunya virus (CHIKV; family *Togaviridae*, genus *Alphavirus*) can severely affect human health by causing debilitating disease with symptoms of high fever, rash, arthralgia and sometimes death (135). CHIKV is endemic in parts of Africa, the Indian Ocean area and Southern Asia (136, 180) and has recently been transmitted by the Asian tiger mosquito, *Ae. albopictus*, in Italy (2007) (32) and France (2010) (34). CHIKV has a positive-sense, single-stranded RNA genome (gRNA) that encodes two polyproteins. The first polyprotein is directly translated from the gRNA and produces nonstructural proteins nsP1 to nsP4, which are essential for viral replication. The structural proteins are translated from a subgenomic RNA, which is transcribed later in infection from the viral 26S promoter. nsP3 is the most enigmatic of all nsPs, with unclear yet essential roles in alphavirus RNA replication (153). nsP3 is highly phosphorylated (151, 152), is part of the viral replication complex (RC) (146) and has been shown to interact with Ras-GAP SH3 domain binding proteins (G3BP1 and G3BP2) in two independent coimmunoprecipitation studies (92, 93). Infection with another *Togaviridae* member; Rubella virus, has been shown to alter the distribution of host-cell G3BP, suggesting that G3BP plays an important role in the outcome of viral infection (181). G3BP is an essential factor in the assembly of stress granules (SGs) (182), which are non-membraneous cytoplasmic focal structures (foci) containing cytoplasmic messenger ribonucleoproteins (mRNPs). SGs rapidly aggregate in response to different types of environmental stress and lead to impaired translation of most mRNAs (90). SGs can have diverse anti- or proviral activities (89, 158, 183).

To investigate the relationship between CHIKV replication and SG formation, Vero cells were transfected with CHIKV replicon RNA, in two independent experiments, as described previously (148). Next, 16 hours post-transfection (hpt) cells were either exposed to oxidative stress by using arsenite to induce SGs or left untreated. Cells were immunostained for double stranded RNA (dsRNA, a replication intermediate of viral RNA replication) and/or G3BP (Figure 5.1). Cells that were treated with only transfection reagent (mock transfected) (Figure 5.1A,) responded to arsenite induced stress with the formation of SGs. G3BP readily localized to these typical SGs, displayed as irregularly shaped granules that converge around the nucleus and extend from there into the cytoplasm, and are often smaller when located farther away from the nucleus (Figure 5.1A, right). In contrast to arsenite-induced SGs, the presence of replicating CHIKV replicon RNA (visualized by the dsRNA signal, Figure 5.1B) caused G3BP to localize into foci that displayed a more punctate morphology and were distributed throughout the cytoplasm in a seemingly random manner (Figure 5.1B, top). Exposing cells that harbor replicating CHIKV replicon RNA to oxidative stress did not affect the morphology of these G3BP foci (Figure 5.1B, bottom left). Cells from the same sample that did not harbor replicating CHIKV replicon RNA after transfection were still able to

respond to arsenite with the formation of SGs (Figure 5.1B, bottom right).

To investigate the interaction between G3BP and the viral protein nsP3, an mCherry reporter protein was incorporated into nsP3 within the CHIKV replicon in a way similar to that described for Sindbis virus (92, 184), creating CHIKrep-nsP3mC-FlucEGFP (Figure 5.2A) (where FlucEGFP is firefly luciferase-enhanced green fluorescent protein)(cloning details are available upon request). Fluc measurements of two independent experiments indicated that CHIKrep-nsP3mC-FlucEGFP RNA was still able to replicate, albeit to lower levels than wild-type CHIKrep-FlucEGFP (Figure 5.2B). Immunofluorescence analysis revealed nearly complete colocalization between nsP3-mCherry and G3BP (Figure 5.2C), indicative of a close interaction between nsP3 and G3BP during CHIKV RNA replication. These nsP3/G3BP-foci were indistinguishable from G3BP-foci observed in Figure 5.1B in both their morphology and unresponsiveness to arsenite-induced stress. Note that only untransfected cells were able to form typical arsenite-induced SGs (Figure 5.2C).

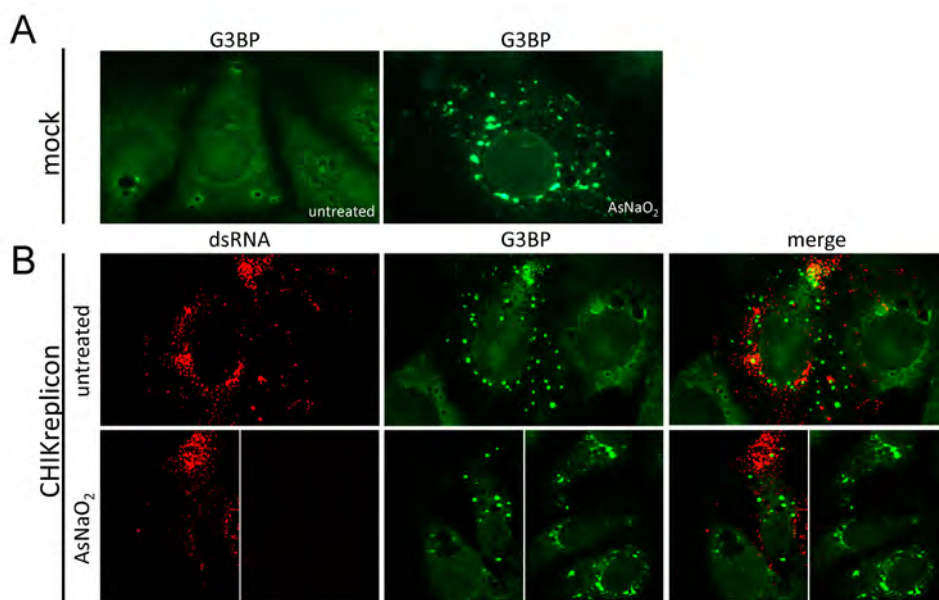


Figure 5.1. During CHIKV RNA replication, G3BP localizes to punctate cytoplasmic foci. A. Mock transfected Vero cells were left untreated or were treated with sodium arsenite (NaAsO₂). Cells were fixed in 4% paraformaldehyde in phosphate buffered saline (PBS) for 10 min at room temperature (RT) and permeabilized with ice-cold acetone-methanol (1:1) for 10 min at -20°C. SGs were stained with anti-G3BP (G6046; Sigma). **B.** Vero cells were transfected with in vitro transcribed CHIK replicon RNA (CHIKrep) and stained with J2 anti-dsRNA and anti-G3BP. **B.** (bottom), displays CHIKrep transfected cells (left) and cells that remained untransfected cells from the same sample (right). Where indicated, samples were treated with sodium arsenire (0.5 mM) for 30 min at 16 hpt.

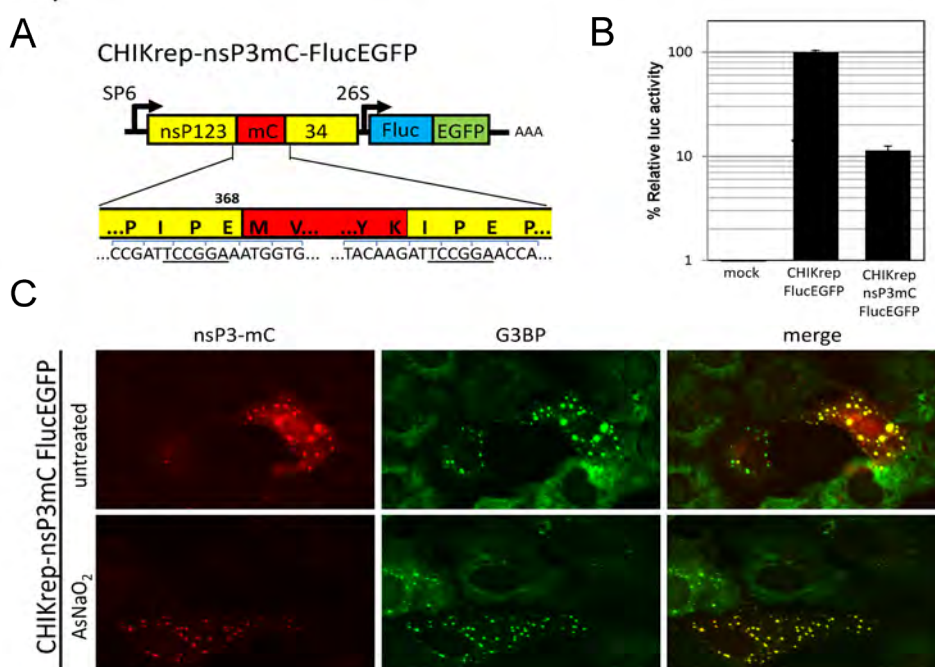


Figure 5.2. During CHIKV RNA replication, nsP3 localizes to punctate cytoplasmic foci concurrently with G3BP. **A.** Schematic representation of the CHIKrep-nsP3mC-FlucEGFP replicon expressing nsP3 with an internal mCherry fusion and an FlucEGFP fusion protein from the subgenomic promoter. **B.** Vero cells were transfected with a pRL-TK plasmid constitutively expressing Rluc together with either CHIKrep-FlucEGFP or CHIKrep-nsP3mC-FlucEGFP in vitro transcribed RNA. Cells were lysed 16 hpt and Fluc/Rluc activities were measured. Luciferase activity in mock transfected cells was also measured. The Fluc measurements were normalized by Rluc to compensate for differences in transfection efficiency. Depicted values are the average of triplicate samples and expressed in the percentage of normalized Fluc activity relative to CHIKrep-FlucEGFP. Error bars represent standard deviation. **C.** CHIKrep-nsP3mC-FlucEGFP in vitro transcribed RNA was transfected into Vero cells, 16 hpt cells were fixed and stained with G3BP antibodies. Where indicated, samples were treated with sodium arsenite (0.5 mM) for 30 min at 16 hpt.

To determine whether nsP3 expressed alone also localizes into foci and which domain(s) in nsP3 is required for its specific subcellular localization, several expression plasmids with an N-terminal EGFP tag fused to nsP3 (Figure 5.3A) were constructed (cloning details are available upon request) and transfected into Vero cells. Expression of EGFP-nsP3 resulted in foci that were indistinguishable from those generated during CHIKV replicon RNA replication, indicating that subcellular localization in cytoplasmic foci is an intrinsic property of nsP3 (Figure 5.3B, top). Deletion of the N-terminal macrodomain (nsP3.7, Figure 5.3A), which is conserved among the *Togaviridae*, *Coronaviridae* and hepatitis E virus (154), did not result in a change in localization (Figure 5.3B, middle). In contrast, deletion of the highly variable, C-terminal domain (nsP3.8 and nsP3.2, Figure 5.3A) resulted in the formation of filaments instead

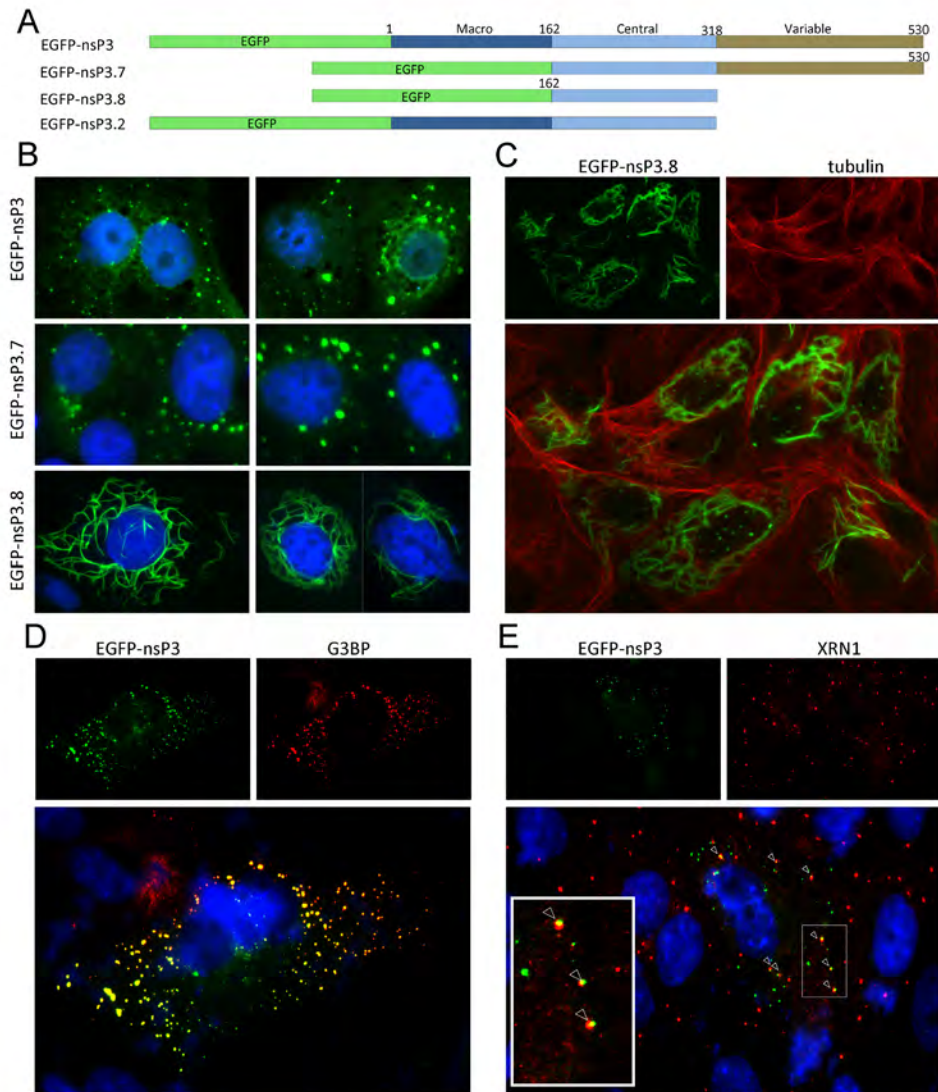


Figure 5.3. Individually expressed CHIKV nsP3 localizes to small punctate cytoplasmic foci that are juxtaposed to P-bodies. **A.** Schematic representation of N-terminal EGFP-nsP3 fusion proteins expressing either full length nsP3 (EGFP-nsP3) or truncations of nsP3 missing only the macrodomain (EGFP-nsP3.7), both the macro- and variable domain (EGFP-nsP3.8) or only the variable domain (EGFP-nsP3.2). **B.** Plasmids expressing these nsP3 variants from a CMV promoter were transfected into Vero cells. Cells were fixed 20 hpt and nuclei were visualized by Hoechst staining. **C.** Vero cells transfected with EGFP-nsP3.8 were fixed 20 hpt and stained for tubulin (14-4502; eBioscience). Vero cells expressing EGFP-nsP3 were fixed and stained with either SG marker G3BP (**D**) or P-body marker XRN1 (A300-443A; Bethyl Laboratories) (**E**) antibodies. Arrowheads indicate juxtaposed SGs and PBs.

of foci (Figure 5.3B, bottom and data not shown). Since these filaments resembled the cytoskeleton, cells expressing nsP3.8 were stained for tubulin (Figure 5.3C). No colocalization between nsP3.8 and the cytoskeleton was observed, indicating that multimerization is an intrinsic property of the conserved, central domain of alphavirus nsP3.

Next, EGFP-nsP3 transfected cells were stained for SG marker G3BP (Figure 5.3D) or a marker for processing bodies (PBs), XRN1 (Figure 5.3E). PBs are small cytoplasmic foci, and have been shown to be modulated by various RNA viruses (91, 158, 183, 185). Here we show for the first time that individually expressed nsP3 displays complete colocalization with G3BP in Vero (Figure 5.3D) and HEK293T (not shown) cells in the absence of viral RNA replication and other CHIKV proteins. XRN1 showed a punctate localization in untransfected cells similar to that in nsP3-transfected cells (Figure 5.3E). Interestingly, the observed PBs did not colocalize but were sometimes juxtaposed to nsP3-foci (Figure 5.3E, arrowheads). Juxtaposition of PBs and SGs is a well-known phenomenon (186). The observations that nsP3-foci include G3BP and are often juxtaposed to PBs, suggest that nsP3/G3BP-foci might be SGs.

Since nsP3/G3BP-foci have a morphology different from that of *bona fide*, arsenite-induced SGs we set out to elucidate whether or not CHIKV nsP3/G3BP-foci are indistinguishable from true SGs. In three independent experiments, cells expressing EGFP-nsP3 or EGFPns-P3.8, were treated with arsenite and subsequently treated with cycloheximide (CHX), before being immunostained for G3BP (Figure 5.4ABC). CHX has been shown to disassemble arsenite-induced, *bona fide* SGs (Figure 5.4A)(182). Cells that remained untransfected in the field (Figure 5.4B) behaved similarly to mock transfected cells (Figure 5.4A), no longer displaying any *bona fide* SGs after CHX treatment. Cells transfected with EGFP-nsP3 displayed typical nsP3/G3BP-foci, which were unaffected by either arsenite or CHX treatment and are therefore different from SGs (Figure 5.4B). In contrast, when the same experiment was performed with EGFP-nsP3.8, arsenite induction resulted in G3BP-containing granules with typical SG morphology (described above)(Figure 5.4C, arrowheads) and CHX treatment led to SG disassembly. This experiment indicated an essential role for the nsP3 C-terminal variable region in inhibiting *bona fide* SG assembly.

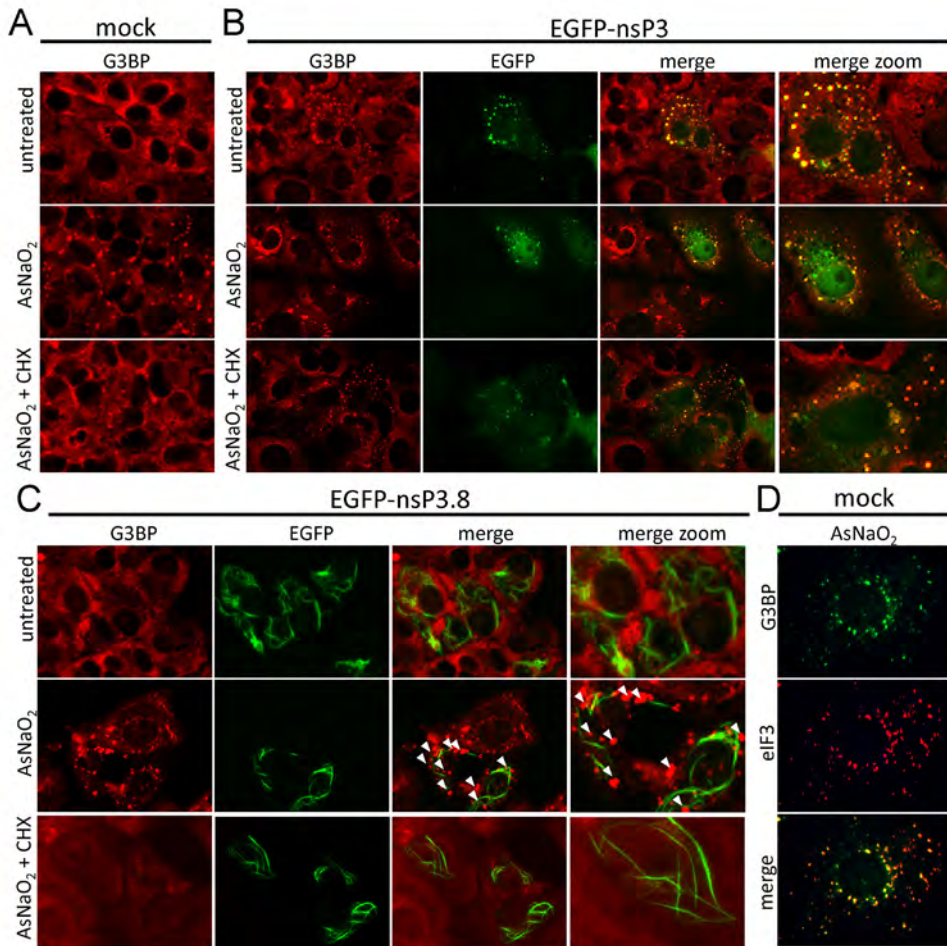


Figure 5.4. nsP3/G3BP-foci do not disassemble upon cycloheximide treatment. Vero cells were either mock transfected (A) transfected with EGFP-nsP3 (B) or EGFP-nsP3.8 (C). After 16 h samples were left untreated (top), treated with arsenite for 30 min (middle) or treated with arsenite for 30 minutes prior to a cycloheximide (CHX)(10 μ g/ml) treatment for 30 min (bottom). After treatment samples were fixed and stained for G3BP. Arrowheads show bona fide SGs in cells transfected with EGFP-nsP3 variants. D. Untransfected Vero cells were mock treated or treated with sodium arsenite, fixed and stained for G3BP and eIF3 (sc-16377; SantaCruz).

In addition to CHX treatment, another well-known SG marker, eIF3 (182), was used to assess the composition of the nsP3/G3BP-foci. Similar to G3BP, eIF3 readily localized to bona fide SGs and colocalized with G3BP in arsenite-treated cells (Figure 5.4D). Cells were transfected with either EGFP-nsP3 alone (Figure 5.5A) or CHIKV replicon RNA expressing FlucEGFP from its subgenomic promoter (Figure 5.5B). Mock-transfected cells (Figure 5.5A, top) and cells that remained untransfected (Figure 5.5B, bottom) readily displayed arsenite-induced, eIF3-containing, SGs. In contrast, cells transfected with either EGFP-nsP3 (Figure 5.5A, bottom) or CHIKrep-FlucEGFP (Figure 5.5B, bottom)

did not show any eIF3-positive granules, strongly suggesting that nsP3/G3BP-foci are different from SGs and that the formation of nsP3/G3BP-foci inhibits assembly of bona fide, eIF3-positive SGs.

Since deletion of the nsP3 C-terminal, variable domain inhibited the formation of foci, and restored the ability of the host cell to form bona fide SGs, we set out to determine the element responsible within this domain. Interestingly, a Src homology-3 (SH3) domain-binding motif (PxxPxR) is conserved within the variable domains of many, if not all, alphaviruses. This element was demonstrated to be important for efficient Semliki forest virus replication (187). Deletion of this element from a CHIKV replicon (CHIKrep-nsP3^{d398/406}-FlucEGFP, Figure 5.6A) rendered it unable to replicate (Figure 5.6B). Cotransfection with a second (wild-type) CHIKV replicon in a trans-complementation experiment, rescued CHIKrep-nsP3^{d398/406}-FlucEGFP replication (Figure 5.6B). This confirmed that the RNA of CHIKrep-nsP3^{d398/406}-FlucEGFP was unable to replicate in the absence of wild-type nsP3. Interestingly, nsP3 expressed with the SH3 domain-binding motif deleted (EGFP-nsP3^{d398/406}) (Figure 5.6A) no longer localized in foci but was diffusely distributed throughout

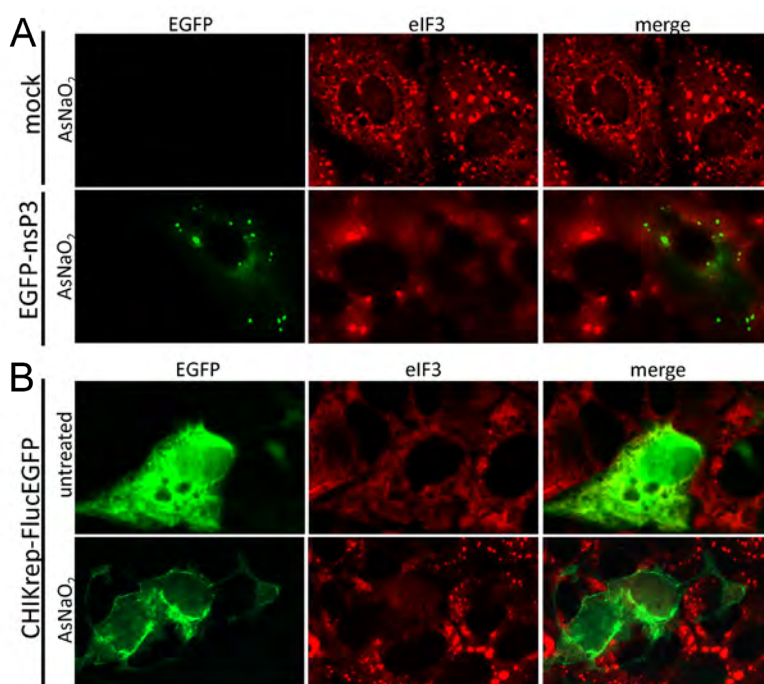


Figure 5.5. nsP3/G3BP-foci do not co-localize with eIF3. A. Vero cells were either mock transfected (A, top) or transfected with EGFP-nsP3 (A, bottom), 16 hpt all samples were treated with arsenite for 30 min before being fixed and stained for eIF3. B. Vero cells were transfected with CHIKrep-FlucEGFP in vitro transcribed RNA and 16 hpt cells were either left untreated (top) or treated with arsenite for 30 min (bottom) before being fixed and stained with anti-eIF3 antibodies.

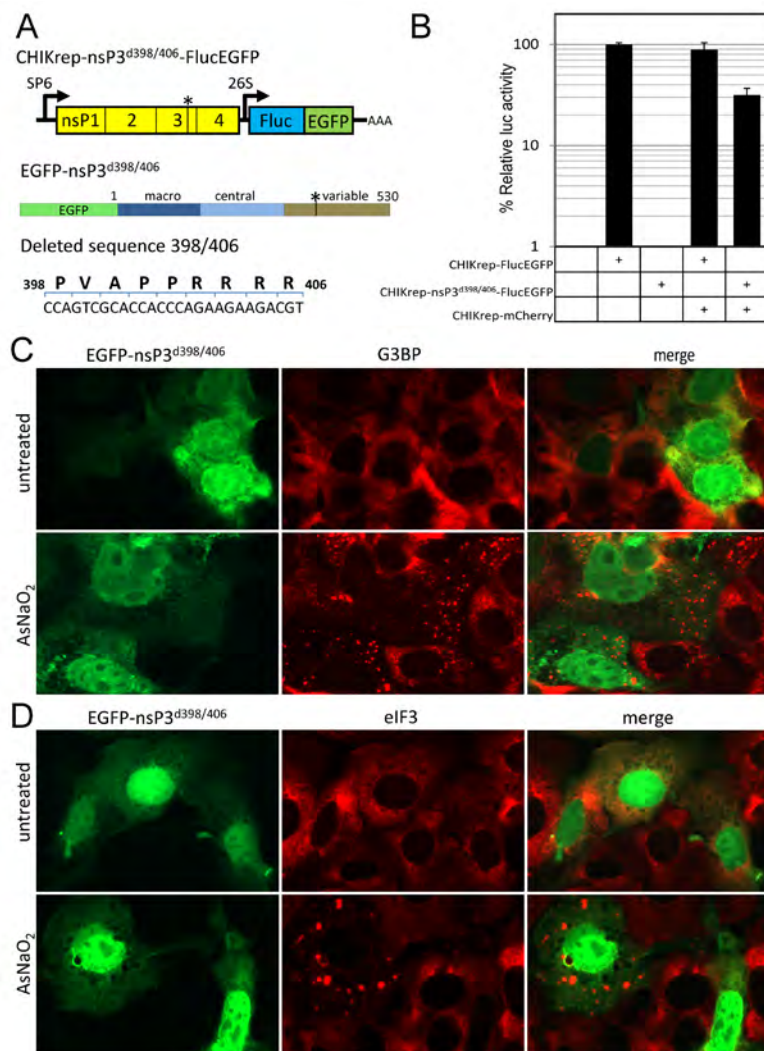


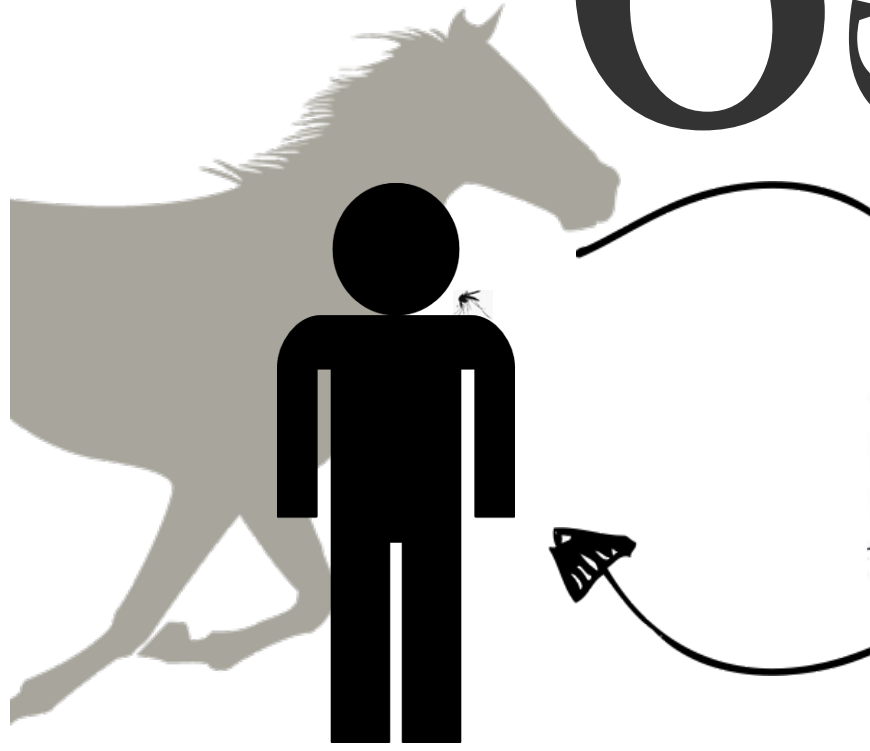
Figure 5.6. SH3 domain-binding motif is necessary for CHIK replicon RNA replication and the formation of nsP3/G3BP-foci. A. Schematic representation of the SH3 domain-binding motif deletion constructs, CHIKrep-nsP3^{d398/406}-FlucEGFP (top) and EGFP-nsP3^{d398/406} (middle). The schematic representation of the deleted sequence (bottom) depicts both the deleted amino acid sequence and the corresponding nucleotides. The numbers indicate the amino acid positions within CHIK nsP3. B. Vero cells were transfected with a pRL-TK plasmid constitutively expressing Rluc together with in vitro transcribed RNA from either CHIKrep-FlucEGFP, CHIKrep-nsP3^{d398/406}-FlucEGFP, CHIKrep-FlucEGFP together with CHIKrep-mCherry or CHIKrep-nsP3^{d398/406}-FlucEGFP together with CHIKrep-mCherry. Cells were lysed 16 hpt and Fluc/Rluc activities were measured. Luciferase activity in mock transfected cells was also measured. The Fluc measurements were normalized by Rluc to compensate for differences in transfection efficiency. Depicted values are the average of triplicate samples and expressed in the percentage of normalized Fluc activity relative to CHIKrep-FlucEGFP. Error bars represent standard deviations. Vero cells were transfected with EGFP-nsP3^{d398/406} and 16 hpt cells were either left untreated (top) or treated with arsenite for 30 min (bottom) before being fixed and stained with anti-G3BP (C) or -eIF3 (D) antibodies.

the cytoplasm and the nucleus, in two independent experiments. Staining with either anti-G3BP (Figure 5.6C) or eIF3 (Figure 5.6D) did not show apparent colocalization with EGFP-nsP3^{d398/406}. Treatment with arsenite readily induced SGs in both untransfected and EGFP-nsP3^{d398/406}-transfected cells. These results indicate that deletion of the SH3 domain-binding motif from nsP3 resulted in the complete loss of association with G3BP.

In conclusion, we show that G3BP localizes to CHIKV nsP3-containing foci, both in the presence and in the absence of CHIKV RNA replication. Although reminiscent of SGs, these nsP3/G3BP-foci differ from bona fide SGs in four ways; i.e., (i) they are morphologically different, (ii) they do not contain the hallmark SG marker eIF3, (iii) they do not disassemble upon CHX treatment, and (iv) they render cells that express these nsP3/G3BP unable to form bona fide SGs in response to oxidative stress. The observation that CHIKV replication inhibits SG assembly may suggest that SGs have antiviral activity. However, it cannot be completely ruled out that G3BP is part of the alphavirus RC, although the limited overlap between viral dsRNA and G3BP does not support this possibility. Furthermore, deletion of the SH3 domain-binding motif from nsP3 restores bona fide SG assembly but abolishes CHIKV RNA replication. We propose that nsP3 blocks SG assembly by the sequestration of G3BP into foci via an interaction with the SH3 domain-binding motif in nsP3. The nature of the binding (direct versus indirect) between G3BP and nsP3 and the relative contributions of other nsP3-binding proteins are important avenues for follow-up studies. This study provides new insights into the function of CHIKV nsP3 at the molecular level and suggests that its C-terminal variable domain plays an important role in modulating SG assembly during CHIKV RNA replication.

Acknowledgements

We thank Martijn Langereis and Frank van Kuppeveld for sharing the eIF3 antibody. This work is supported by the European Community's Seventh Framework Programme (FP7 VECTORIE project number 261466).



6 Chapter

Chikungunya virus nonstructural protein 2 inhibits type I/II interferon-stimulated JAK-STAT signaling

Chikungunya virus (CHIKV) is an emerging human pathogen transmitted by mosquitoes. Like other alphaviruses, CHIKV replication causes general host shut-off leading to severe cytopathicity in mammalian cells and inhibits the ability of infected cells to respond to interferon (IFN). Recent research, however, suggests that alphaviruses may have additional mechanisms to circumvent the host's antiviral IFN response. Here we show that CHIKV replication is resistant to inhibition by interferon once RNA replication has been established and that CHIKV actively suppresses the antiviral interferon (IFN) response by preventing IFN-induced gene expression. Both CHIKV infection and CHIKV replicon RNA replication efficiently blocked STAT1 phosphorylation and/or nuclear translocation in mammalian cells induced by either type I/II IFNs. Expression of individual CHIKV nsPs showed that nsP2 was a potent inhibitor of IFN-induced JAK-STAT signaling. In addition, mutations in CHIKV-nsP2 (P718S) and SINV-nsP2 (P726S), which render alphavirus replicons non-cytopathic, significantly reduced JAK-STAT inhibition. This host shut-off independent inhibition of IFN signaling by CHIKV is likely to have an important role in viral pathogenesis.

This chapter has been published as:

Jelke J. Fros, Wen Jun Liu, Natalie Prow, Corinne Geertsema, Maarten Ligtenberg, Dana L. Vanlandingham, Esther Schnettler, Just M. Vlak, Andreas Suhrbier, Alexander A. Khromykh and Gorben P. Pijlman. *Chikungunya virus non-structural protein 2 inhibits type I/II interferon-stimulated JAK-STAT signalling*. *J. Virol.* **84**, 10877–10887 (2010).

Introduction

Chikungunya virus (CHIKV) is a mosquito-borne, arthrogenic *Alphavirus* (fam. *Togaviridae*) causing current epidemics in the Indian Ocean region (180). The first reported CHIKV outbreak was in 1952-53 in Tanzania. In the local Makonde language, chikungunya means “that which bends up” and refers to the body posture of infected individuals who suffer from associated arthralgia (188). CHIKV is transmitted mainly by *Aedes* mosquito species and is endemic in most of Central Africa and Southern Asia (30). From 2001 onwards several major outbreaks have occurred affecting the islands of Mauritius, Madagascar, Mayotte and Reunion Island. On Reunion Island, CHIKV affected up to one third of the population and CHIKV-associated deaths were recorded (180). Due to an acquired mutation in the viral glycoprotein E1 (43) and the concurrent expanding distribution of its novel mosquito vector *Aedes albopictus*, CHIKV is rapidly spreading to other parts of the world including Europe (189). In 2006, mainland India suffered a major outbreak resulting in more than 1.4 million infected individuals, after which more outbreaks occurred throughout the rest of Southern Asia (31). The first outbreak of CHIKV on the European continent occurred in Italy in 2007 (32). Currently, no licensed CHIKV vaccine or effective antiviral treatment is available.

CHIKV is a plus-strand RNA virus with a genome of almost 12kb and replicates in the cytoplasm of infected cells within virus-induced membranous vesicles (190). CHIKV produces two polyproteins, of which the first encodes nonstructural proteins (nsPs) 1, 2, 3 and 4. The nsP123 precursor and nsP4 function in a complex for viral negative strand RNA synthesis, after which sequential processing of nsP123 into its individual proteins results in positive strand RNA transcription and production of subgenomic RNA (sgRNA). CHIKV nsPs encode functions needed for viral replication, e.g. methyltransferase and guanylyltransferase (nsP1), protease and helicase (nsP2) and RNA-dependent RNA polymerase (nsP4) (191). The second, structural polyprotein is translated from this sgRNA and codes for capsid and envelope glycoproteins that constitute the virus particle (191). In mosquito cells, alphaviruses can replicate in a persistent manner, whereas alphavirus replication in mammalian cells usually results in severe cytopathicity, mainly caused by a dramatic shut-off of host gene expression resulting in the suppression of innate immunity (28).

Cellular sensors including the cytoplasmic RNA helicase MDA5 are able to detect alphavirus replication in infected mammalian cells (88). Downstream signal transduction ultimately leads to interferon regulatory factor (IRF)-3 activation and interferon (IFN)- β production. After secretion from the infected cell, IFN- β binds to the IFN- α/β receptor IFNAR in an auto- or paracrine manner to amplify the signal or to prime uninfected cells to establish an antiviral state, respectively. Subsequently, the Janus kinases JAK1 and TYK2 are phosphorylated, which in turn phosphorylate Signal Transducers and Activators of Transcription (STAT)1 and STAT2 (192). Heterodimers of STAT1/

STAT2 are then translocated from the cytoplasm into the nucleus in an IRF9-dependent manner where they bind IFN Stimulated Response Elements (ISRE). STAT1 activation causes cells to produce and secrete IFN- α to further amplify the signal via the same signaling cascade. In addition, the expression of an array of antiviral proteins, including protein kinase R (PKR), 2',5'-oligoadenylate synthetase (2'5'OAS) and Mx proteins is then induced to ultimately clear the infection (192). In addition to the type I IFNs (IFN α / β) expressed by most cells, type II IFN (IFN- γ) is also produced early in CHIKV infection, probably by NK cells (68), to promote the transition from innate to adaptive immunity. IFN- γ activates STAT1 via binding to the IFN- γ receptor, upon which the latter in the form of homodimers translocates to the nucleus where they bind Gamma Activating Sequence (GAS) elements to transactivate antiviral gene expression (192).

Given the potency of IFNs to fight viral infection many viruses have evolved specific strategies to counteract or evade the antiviral IFN response (192). While alphaviruses are known to cause dramatic host protein synthesis shut-off (28), recent research has shown that this alone is not sufficient to ensure productive infection and that the IFN response is also antagonized in a more direct manner (193). Whether or not CHIKV counteracts the IFN response is unknown, however it is clear that robust IFNAR-dependent type I IFN-signaling is required to limit CHIKV replication in animals (70, 194). IFN- α was recently shown to inhibit CHIKV replication in mice if given before infection, but not when given 3 days after infection (68).

In this paper, we show that CHIKV replication is resistant to IFN treatment and inhibits IFN-induced JAK-STAT signaling and downstream gene transcription independently of host shut-off. We also show for the first time that alphavirus nsP2 alone is sufficient for JAK-STAT inhibition. A P726S substitution in a conserved region of Sindbis virus (SINV) nsP2 was previously reported to reduce SINV cytopathicity (85). Here we show that this substitution and the corresponding P718S in CHIKV reversed the ability of CHIKV and SINV replicons to block the JAK-STAT pathway.

Materials and methods

Cells and virus

African green monkey kidney (Vero) and baby hamster kidney BHK-21J cells were cultured in DMEM (Invitrogen) supplemented with 10% FBS (Invitrogen) at 37°C in an atmosphere with 5% CO₂ in tissue culture flasks (Greiner). Chikungunya virus isolate 06113879 (Mauritius strain) was obtained from the Victorian Infectious Diseases Reference Laboratory (VIDRL) and supplied via Queensland Health Forensic and Scientific Services (QHFSS) and titrated on Vero cells via plaque assay.

Construction of alphavirus replicons and expression plasmids

A CHIKV strain 37997 replicon (CHIKrep-EGFP, Figure 6.4A) expressing EGFP was constructed by removing the structural genes from CHIKV infectious clone 5'-pCHIKic (195) and the insertion of EGFP. Next, a Firefly luciferase (Fluc) gene was generated by PCR (Phusion DNA polymerase, Finnzymes) from pGL3 (Promega) using primers (AscI-Luc-F and BssHII-Luc-R), cloned into CHIKrep-EGFP, in-frame and upstream of the EGFP gene to generate CHIKrep-FlucEGFP (Figure 6.1C). The red fluorescent marker gene mCherry (196) was amplified by PCR using primers (AscI-mCherry-F and EcoRI-mCherry-R) and cloned into CHIKrep-EGFP in place of EGFP to generate CHIKrep-mCherry (Figure 6.5A). A puromycin-acetyltransferase gene fused to the Footh-and-Mouth disease virus (FMDV)2A autoprotease was generated by PCR from repPAC-βGal (197) using primers (MluI-PAC2A-F/R) and cloned into CHIKrep-EGFP in place of EGFP to generate CHIKrep-pac2AEGFP (Figure 6.6A). An *MluI* fragment from CHIKrep-pac2AEGFP was subcloned into pBluescript and reinserted after nsP2 was mutated by QuickChange PCR using primers (CHIK-nsP2-P718S-F/R), generating CHIKrep-pac2AEGFP-nsP2m. Cytopathic, "wildtype" Sindbis replicon was generated from the noncytopathic replicon, SINrepGFP (pHY213; pToto1101-derivative), by mutating the nsP2 serine at position 726 into a proline with primers (SINnsP2-726P-V426/7) to generate SINrepGFP "wt" (Figure 6.6A). Individual CHIKV nsPs were PCR amplified from CHIKrep-EGFP using AttB1/2 primers listed (Table 1) and cloned in expression plasmids downstream of a cytomegalovirus immediate early (CMV) promoter (Figure 6.6A) via traditional cloning or Gateway technology using pDONR207 and pcDNA-DEST40 (Invitrogen). The mCherry gene was fused to FMDV2A using PCR with primers (EcoRI-mCherry-F and EcoRI-2A-mCherry-R) and was cloned as an *EcoRI* fragment in-frame and upstream of CHIKV nsPs for live visualization of transfected cells (Figure 6.5A). Autocleavage of the red fluorescent mCherry2A protein from the nsPs results in expression of CHIKV nsP1-4 with nearly authentic N-termini to retain biological activity. All constructs were verified by sequencing (Eurofins MWG Operon, Germany).

IFN sensitivity assay

CHIKV: For IFN pre-treatment, Vero cells grown in 24 well plates were treated with various doses of IFN-α (I-4276, Sigma), IFN-β (I-4151, Sigma) and IFN-γ (I-1520, Sigma) for 6 h. The cells were washed and infected with CHIKV at a multiplicity of infection (MOI) of 1 plaque forming unit (pfu) per cell. Three hours after viral absorption, the cells were washed and then incubated for an additional 21 h. For IFN post-treatment, Vero cells were infected with CHIKV at an MOI of 1 pfu/cell. Four hours after viral absorption, cells were treated with various doses of IFN as indicated and left for additional 21 h. The supernatants were collected and viral titers were determined by plaque assay on Vero cells. **CHIKV replicon:** *In vitro* transcribed, capped CHIKrep-FlucEGFP

replicon RNA (400 ng/well) was transfected into Vero cells in 96 wells plates, using Lipofectamine 2000 (Invitrogen) and OptiMEM medium (Invitrogen) according to the manufacturer's recommendations. The transfection mix was removed after 4 h of incubation and replaced with DMEM + 10% FBS. Directly after transfection (0 h p.t.) or 24 h p.t., type I IFNs (IFN- α , IFN- β ; Calbiochem, Nottingham, UK) and type II IFN (IFN- γ ; AbD Serotec, Dusseldorf, Germany) were added to the wells in increasing concentrations. Two days after transfection, cells were lysed in 100 μ l passive lysis buffer (Promega Benelux, Leiden, the Netherlands) and luciferase expression was measured on a Fluostar Optima (BMG Labtech, Germany) using D-luciferin (Synchem OHG, Germany) as a substrate basically as described (198).

IFN reporter assay

Vero cells grown in 24-well plates were cotransfected with 40 ng pRL-TK (Promega) plasmid DNA expressing Renilla luciferase (Rluc) and with 200 ng of either the IFN- α/β -responsive (ISRE) firefly luciferase (Fluc) reporter plasmid p(9-27)4th (-39)Lucifer or the IFN- γ responsive (GAS) luciferase reporter plasmid p(IRF-1*GAS)6tk (-39)Lucifer (199), using Genejammer (Stratagene) transfection reagent. Briefly, 24 h p.t., cells were infected with CHIKV at MOI=5 pfu/cell. Four, 8 and 12 hours post infection (p.i.), cells were treated with 1,000 international units (IU) of IFN- α (Intron A Redipen) per ml or 100 ng of IFN- γ (BD Pharmingen) per ml for 6 h and then assayed for Fluc and Rluc activity using the Dual luciferase reporter assay system (Promega) as described (200).

Realtime RT-PCR

Vero cells grown in 24-well plates were infected with CHIKV at MOI=5 pfu/cell. Healthy or infected cells were subsequently incubated at 4, 8, 12 h p.i. with 1,000 IU of IFN- α (Intron A Redipen) per ml (A) or 100 ng of IFN- γ (BD Pharmingen) per ml for 10 h. Total RNA was purified using Trizol reagent (Invitrogen), and realtime RT-PCR was carried out on a Rotor-Gene 3000 PCR machine (Corbett Research) using Superscript III (Invitrogen) and SYBRgreen (Invitrogen) basically as described (68). Primers for amplification of OAS2 transcripts were HuOAS2-F/R, primers for the housekeeping gene RPL13A (201) were HuRPL13A-F/R. Each sample was analyzed in duplicate and normalized to RPL13A mRNA levels. OAS2 mRNA transcription levels were expressed relative to mock-infected, IFN treated samples.

Immunofluorescence and western blot

CHIKV virus: Vero cells grown on glass cover-slips in 24 wells plates were infected with CHIKV at a multiplicity of infection at MOI=1 pfu/cell. Twenty four hours after infection, cells were treated with 1,000 IU/ml of IFN- α (I-4276; Sigma) or 50 ng/ml of IFN- γ (I-1520; Sigma) for 30 min at 37°C. Cells were fixed in 4% formaldehyde in phosphate-buffered saline (PBS) for 10 min at room

temperature, permeabilized with ice-cold acetone-methanol (1:1) for 30 min at -20°C , and stained sequentially with cross reacting monoclonal antibodies specific against CHIKV envelope protein and with polyclonal antibodies against STAT1 (SC-345; SantaCruz Biotechnology, Santa Cruz, USA) or STAT2 (SC-476; SantaCruz) at concentrations of 1 $\mu\text{g}/\text{ml}$ essentially as described by the manufacturer. Secondary antibodies (GaM-AF546 and GaR-AF488) were obtained from Molecular Probes (Invitrogen) and nuclei were stained with DAPI. Microscopy was performed using a Zeiss LSM 510 Meta confocal microscope. For western analysis, Vero cells in 6 well plates were infected with CHIKV at $\text{MOI}=1$ pfu/cell. Twenty four hours p.i., cells were treated with either IFN- α (I-4276; Sigma) or IFN- γ (I-1520; Sigma) for 30 min or untreated as indicated. Western blot was performed on Vero cell lysates as described before (200) using antibodies against phosphorylated STAT1 (pSTAT1) (550428; Pharmingen, San Diego, USA), STAT1 (SC-345; SantaCruz) and tubulin (T2200; Sigma), and analyzed with an Odyssey Infrared Imaging System (LI-COR Biosciences, Lincoln, USA). Replicons and single nsPs: Vero cells grown in 96-well plates were transfected with capped, *in vitro* transcribed CHIKrep-EGFP, CHIKrep-mCherry, CHIKrep-pac2AEGFP or CHIKrep-pac2AEGFP-nsP2m replicon RNA, the four pCMV-nsP constructs or the SINrepGFP construct (400 ng of RNA or DNA per well) using Lipofectamine 2000 (Invitrogen). Twenty four hours later, cells were treated for 30 min with 100 IU IFN- α (Calbiochem), 2.5 ng IFN- β (Calbiochem) or 1 ng IFN- γ (AbD Serotec) per well (100 l). For the host shut-off experiment, cells were transfected with CHIKrep-EGFP replicon in normal medium or medium containing 0.5 $\mu\text{g}/\text{ml}$ cycloheximide. Twelve hours p.t. cells received a similar IFN- β treatment. Cells were fixed with 4% paraformaldehyde in PBS and permeabilized with 0.1%SDS in PBS to retain EGFP and/or mCherry fluorescence. Nuclei were stained with Hoechst 3342. STAT1 nuclear translocation was visualized with primary antibodies anti-pSTAT1 (phospho-Tyr701; SAB Signalway Antibody, Pearland, USA) with secondary antibodies GaR-Rhodamine (Nordic Immunology, Tilburg, the Netherlands) or GaR-AF488 (Molecular Probes, Leiden, the Netherlands) or primary antibody anti-STAT1 (SC-417; SantaCruz) with secondary antibody GaM-AF546 (Molecular Probes), using an Olympus IX71 inverted microscope with an X-Cite 120 series lamp.

Table 6.1. Oligonucleotides used in this study

Name	Sequence 5'-3'
AscI-Luc-F	TTGGGCGCGCCATGGAAGACGCCAAAAACATAA
BssHII-Luc-R	TTGTGCGCGCTCCACGGCGATCTTTCCGCC
MluI-PAC₂A-F	TTGGACGCGTCATGACCGAGTACAAGCCCACG
MluI-PAC₂A-R	TTGTACGCGTTCGGGGCCCTGGGTTGGACTCG
AscI-mCherry-F	CGGGCGCGCCACCATGGTGAGCAAGGGCGAGGAG
EcoRI-mCherry-R	CGGAATTCCTTGTACAGCTCGTCCATG
CHIK-nsP₂-P_{718S}-F	GCTCAAGTCGGGTGGTTCATTACTG
CHIK-nsP₂-P_{718S}-R	CCACCCGACTTGAGCAGTCTCAGGG
SINnsP₂-726P-V₄₂₆	CTGAATTGTTTAAACCCAGGAGGCACCTC
SINnsP₂-726P-V₄₂₇	GAGGGTGCCTCCTGGGTTTAAACAATTGAG
attB1-CHIK-nsP₁	GGGGACAAGTTTGTACAAAAAAGCAGGCTTAGAATTCACCATGGATC CCGTGTACGTGG
attB1-CHIK-nsP₂	GGGGACAAGTTTGTACAAAAAAGCAGGCTTAGAATTCACCATGGGAA TAATTGAAACTCCAAGAG
attB1-CHIK-nsP₃	GGGGACAAGTTTGTACAAAAAAGCAGGCTTAGAATTCACCATGGCAC CGTCGTACCGGGTT
attB1-CHIK-nsP₄	GGGGACAAGTTTGTACAAAAAAGCAGGCTTAGAATTCACCATGTACA TATTCTCATCTGACACC
attB2-CHIK-nsP₁	GGGGACCACTTTGTACAAGAAAGCTGGGTACTATGCCCCAGCTCTGT CTTC
attB2-CHIK-nsP₂	GGGGACCACTTTGTACAAGAAAGCTGGGTACTAGCACCTGCTCGGG TGG
attB2-CHIK-nsP₃	GGGGACCACTTTGTACAAGAAAGCTGGGTACTACCCACCTGCCCTAT CTAG
attB2-CHIK-nsP₄	GGGGACCACTTTGTACAAGAAAGCTGGGTACTATTTAGGACCACCGT ACAG
EcoRI-mCherry-F	CGGAATTCACCATGGTGAGCAAGGGCGAGGAG
EcoRI-2A-mCherry-R	CGGAATTCGGGGCCCTGGGTTGGACTCGACGTCGCCGGCCAACTTGAG CAGGTCAAAGTTAACCTTGTACAGCTCGTCCATG
HuOAS₂-F	CGGTGTATGCCTGGGAACAGG
HuOAS₂-R	GGGTCAACTGGATCCAAGATTAC
HuRPL_{13A}-F	CATCGTGGCTAAACAGGTACTG
HuRPL_{13A}-R	CGCAGGACCTTGAGGGCAGC

Results

CHIKV replication confers resistance to type I/II IFN treatment

Since an intact IFN response is a requirement for limiting CHIKV infection in animals (194), it was first investigated to what degree CHIKV replication could be inhibited in cells by (pre-)treatment with type I and type II IFNs. Vero cells have an intact IFN signaling pathway and respond to IFN treatment, however they cannot produce IFN (202) and thus lack the autocrine IFN amplification loop. These characteristics allow accurate measurement of the effect of different, exogenous IFNs on viral RNA amplification and virus production. When cells were primed for 6 h with IFN prior to virus infection, CHIKV production was decreased in an IFN concentration dependent manner (Figure 6.1A). IFN α was most effectively, followed by IFN- β and IFN- γ . Although pre-treatment with 10,000 U/ml of IFN- α could reduce virus production approximately 25-fold (from 8.1×10^8 to 6.7×10^6 pfu/ml), viral titers were not reduced further than 6.7×10^7 pfu/ml, indicating that CHIKV was rather insensitive to IFN pre-treatment under the experimental conditions used and still replicated to relatively high titers. When IFN was applied 4 h p.i., viral titers were not significantly decreased (maximum reduction from 1×10^8 to 7.7×10^7 pfu/ml) (Figure 6.1B), indicating that virus production was thus not overly affected by high concentrations of IFN when IFN was added after establishment of infection.

Next, the effect of IFN treatment on CHIKV viral RNA replication independent of virus production and/or secondary infection was tested. A CHIKV replicon was constructed with the structural genes replaced by a Firefly luciferase (Fluc)-Enhanced Green Fluorescent Protein (EGFP) fusion gene (CHIKrep-FlucEGFP, Figure 6.1C). In this way, transfected cells could be visualized by fluorescence microscopy and replication measured by luminometry. *In vitro* transcribed, capped CHIKrep-FlucEGFP replicon RNA was transfected into Vero cells. Directly after transfection or 24 h post transfection (p.t.), type I/II IFNs were added to the wells in increasing concentrations and luciferase expression was measured 2 days after transfection. Similarly to the results obtained with CHIKV infection, when IFN was added directly after RNA transfection (pre-treatment), CHIKV replication was negatively affected in a concentration-dependent manner (Figure 6.1D). In the concentrations used, IFN- β was most effective (~10% of transgene expression retained), followed by IFN- α and IFN- γ . This is similar to what was reported for SINV, another Old World alphavirus (203). When IFN was added 24h p.t., however, Fluc expression could not be reduced further than approximately 50%, not even with the highest IFN concentrations (Figure 6.1E). Collectively, these results suggest that CHIKV is insensitive to IFN once viral RNA replication has been established.

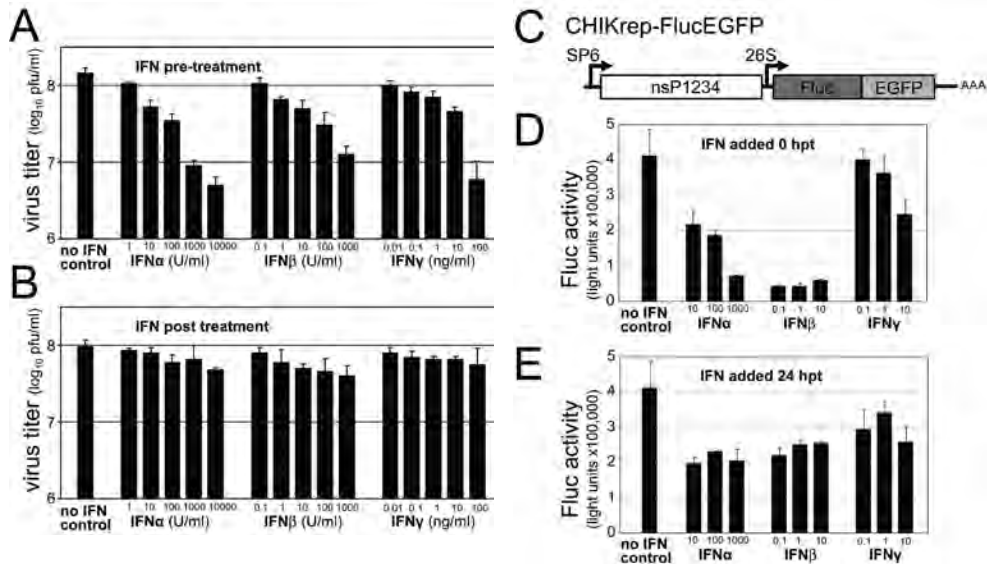


Figure 6.1. Resistance of CHIKV to type I/II IFN treatment. AB. Sensitivity of CHIKV infection to IFN treatment. IFNs were added as indicated to CHIKV infected Vero cells 6 h prior to infection (A) or 4 h p.i. (B). Supernatants were collected 24 h p.i. and virus titers were determined by plaque assay. Error bars represent standard deviations of duplicates. C. Schematic representation of CHIKrep-FlucEGFP replicon expressing an Fluc-EGFP fusion protein. DE. Sensitivity of CHIKV replicon RNA replication to IFN treatment. Different concentrations of IFNs were added to CHIKV replicon transfected Vero cells in 96 wells plates directly post transfection (0 h p.t.) (D) or 24 h p.t. (E), and Fluc activity was measured 48 h p.t. Concentrations of IFN- α are denoted in international units (IU) per ml, and IFN- β/γ in ng per ml. Error bars represent standard deviations.

CHIKV infection inhibits type I/II IFN signaling

Since CHIKV replication is partially sensitive to priming of cells with type I IFNs (and to a lesser extent with type II IFN), but is largely resistant to IFN treatment after viral RNA replication is well underway, it is likely that CHIKV blocks downstream IFN signaling and expression of IFN stimulated genes (ISGs) with antiviral activity. To test this hypothesis the effect of CHIKV RNA replication on downstream IFN-induced gene transcription was investigated. Vero cells were transfected with type I IFN-responsive (ISRE) or type II IFN-responsive (GAS) firefly luciferase (Fluc) reporter plasmids and subsequently infected with CHIKV. Fluc expression was induced by stimulation with type I/II IFNs at 4, 8 and 12 hpi and normalized to Renilla luciferase (Rluc) activity expressed from a constitutive promoter on a co-transfected pRL-TK plasmid (Figure 6.2A and 6.2B). Rluc activity decreased approximately 1.5-fold, 2.5-fold and 4-fold at 4, 8 and 12 hpi, respectively, as compared to mock-infected cells (not shown), indicating that CHIKV infection resulted in some host shut-off within this time frame. However, the inhibition by CHIKV of IFN-stimulated gene transcription was more pronounced. Relative Fluc expression from the ISRE or GAS responsive elements (normalized to Rluc expression) in response

to treatment with IFN- α (Figure 6.2A) and IFN- γ (Figure 6.2B), respectively, was substantially inhibited in Vero cells infected with CHIKV. This inhibition was apparent at 4 hpi (2-fold), 8 hpi (5-8-fold) and was essentially 100% at 12 hpi (Figure 6.2A and 6.2B). In the absence of CHIKV infection, a more than 7-fold or 58-fold induction of normalized Fluc expression in response to treatment with either IFN- α (Figure 6.2A) or IFN- γ (Figure 6.2B), respectively. These results clearly indicated that CHIKV infection efficiently blocks IFN signaling beyond the inhibition mediated by host shut-off.

To illustrate that CHIKV infection also inhibited induction of interferon stimulated gene (ISG) expression, an RT-PCR assay was used to monitor the expression of 2'-5'-oligoadenylate synthetase 2 (OAS) transcripts. As expected (204), large increases in OAS mRNA levels were seen in Vero cells after treatment with IFN- α and IFN- γ (Figures 6.2C and 6.2D, first two bars). However, in cells infected with CHIKV and treated with type I and II IFNs at various time points p.i., OAS mRNA levels were substantially reduced relative to the house keeping gene, RPL13A (Figures 6.2C and 6.2D). These results illustrated that CHIKV infection efficiently blocks ISG expression beyond that mediated by host shut-off.

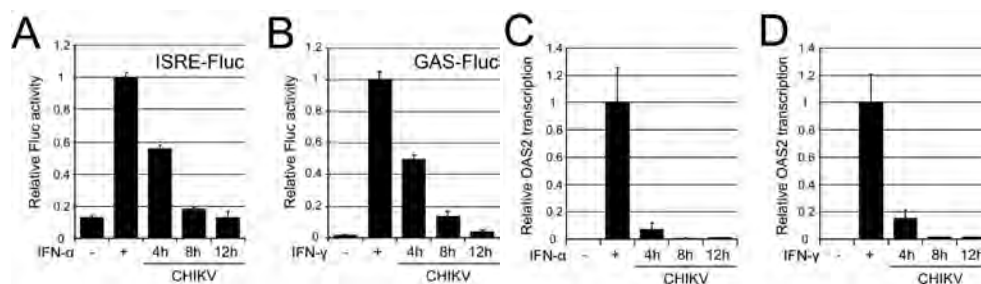


Figure 6.2. Inhibition of type I/II IFN signaling and ISG induction by CHIKV infection. **AB.** Vero cells were transfected with a pRL-TK plasmid expressing Rluc and either type I IFN-responsive (ISRE) or type II IFN-responsive (GAS) Fluc reporter plasmids. 24 h p.t., cells were infected with CHIKV at MOI=5 pfu/ml. At 4, 8 or 12 hours p.i., cells were treated with IFN- α at 1,000 IU/ml (A) or IFN- γ at 100 ng/ml (B) for 6 h and then assayed for Fluc and Rluc activity. Mock-infected (= uninfected) cells with/without IFN induction were also measured. Fluc was divided by Rluc readings to compensate for virus-induced downregulation of transcription/translation and expressed relative to mock-infected, IFN treated samples. Average values from triplicate samples are shown. Error bars represent standard deviations. **CD.** Vero cells, healthy or infected with CHIKV for 4, 8, 12 h were incubated with 1,000 IU of IFN- α (C) or 100 ng of IFN- γ (D) per ml for 10 h. Real-time RT-PCR values for IFN stimulated gene OAS2 were normalized to the housekeeping gene RPL13A. OAS2 mRNA transcription levels were expressed relative to mock-infected, IFN treated samples. Average values from duplicate samples are shown. Error bars represent standard deviations.

CHIKV infection and CHIKV replicon RNA replication block type I/II IFN-induced STAT1 nuclear translocation

In order to investigate whether CHIKV could block IFN signaling by specifically interfering with the JAK-STAT pathway, Vero cells were infected with CHIKV at MOI=1 pfu/cell and subsequently induced with type I IFN. Induction with type I IFNs should result in STAT1/STAT2 phosphorylation/heterodimerization and subsequent nuclear translocation. As expected, STAT1 in normal Vero cells was localized in the cytoplasm, but translocated to the nucleus upon induction with type I IFN (Figure 6.3A). In contrast, when cells were infected with CHIKV 12 h prior to IFN induction, STAT1 nuclear translocation was completely blocked (Figure 6.3A). The same result was obtained for STAT2 (Figure 6.3B). Similarly, type II IFN stimulation should lead to STAT1 phosphorylation/homodimerization and nuclear translocation in normal Vero cells, and this was indeed observed in uninfected cells (Figure 6.3C). Again, CHIKV infection effectively blocked STAT1 nuclear translocation (Figure 6.3C). Taken together, these results indicate that CHIKV infection blocks both type I and type II IFN-induced JAK-STAT signaling.

It is well known that alphavirus replication leads to host protein synthesis shut-off (16). However, based upon the immunofluorescence detection of similar levels of endogenous STAT1 and STAT2 in infected and uninfected cells (Figures 6.3A-C), it is unlikely that CHIKV infection depletes/degrades STAT1/2 proteins. To confirm that the absence of nuclear phospho-STAT1 in cells infected with CHIKV was not the result of depletion of STAT1 protein, western blot immunodetection was performed to detect endogenous STAT1. It is apparent that cells infected with CHIKV (Figure 6.3D, lane 2) have similar levels of endogenous STAT1 as compared to uninfected cells (Figure 6.3D, lane 5), suggesting that CHIKV does not degrade endogenous STAT1 but may act via the inhibition of STAT1 phosphorylation and/or nuclear translocation. As expected, STAT1 was highly upregulated by IFN induction in uninfected cells, likely through signaling via the JAK-STAT pathway (200). In contrast, this was not the case in CHIKV infected cells, suggesting that CHIKV also blocks the IFN-induced upregulation of STAT1. Importantly, western analysis performed with antibodies against phospho-STAT1 showed that CHIKV infection causes a major reduction in the amount of phospho-STAT1 in induced cells (Figure 6.3D, lanes 3 and 4) when compared to IFN induced, uninfected cells (Figure 3D, lanes 6 and 7). These data support the observations from the immunofluorescence experiments and indicate that CHIKV infection inhibits STAT phosphorylation.

Some so-called New World alphaviruses need expression of their capsid gene to modulate the IFN response (205). CHIKV is an Old World alphavirus and therefore is not expected to need capsid expression for suppression of IFN signaling. To determine whether RNA replication and expression of CHIKV nsPs are sufficient to block the JAK-STAT pathway, a CHIKV replicon was constructed in which the structural genes were deleted and replaced by EGFP

(CHIKrep-EGFP, Figure 6.4A). *In vitro* transcribed, CHIKrep-EGFP RNA was transfected into Vero cells and the cells were then stimulated with type I and type II IFNs 24 h p.t. As expected, in untransfected cells, phospho-STAT1 was found in the nuclei of Vero cells after 30 min of induction with IFN- α , and even more efficiently with IFN- β or IFN- γ (Figure 6.4B). In contrast, however, the cells transfected with CHIKrep-EGFP (green; expressing EGFP) and induced with IFN- β or IFN- γ lack nuclear STAT1 (Figure 6.4C, arrowheads), indicating that CHIKV replication blocks type I and type II IFN-induced STAT1 phosphorylation and/or nuclear translocation.

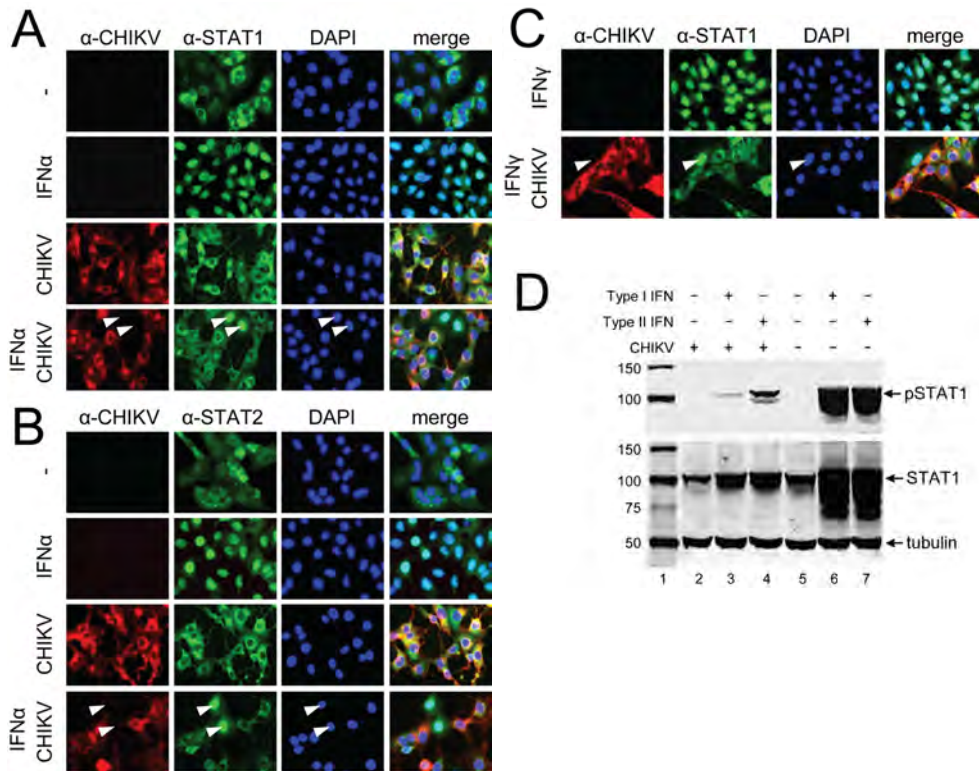


Figure 6.3. CHIKV infection blocks STAT1/STAT2 nuclear translocation without depleting endogenous STAT1 levels. Vero cells were infected by CHIKV and treated with IFN- α (A) or IFN- γ (C) for 30 min. Cells were fixed and stained with monoclonal antibodies specific against CHIKV envelope protein and STAT1 (AC) or STAT2 (B). C. Block in nuclear translocation of STAT1 in CHIKV infection in response to treatment with IFN- γ . Solid arrows show cells negatively infected with CHIKV but with nuclear STAT1/2. D. CHIKV infection blocks STAT1 phosphorylation in Vero cells in response to IFN treatment. Western blot detection of pSTAT1, STAT1 and tubulin in Vero cells infected or mock-infected with CHIKV and untreated or induced with type I or type II IFNs. Lane 1; protein size marker (in kDa).

There is a possibility that the lack of nuclear STAT1 translocation in replicon cells could still be due to host shut-off resulting from CHIKV replicon RNA replication, although Figure 6.3D showed that endogenous STAT1 levels

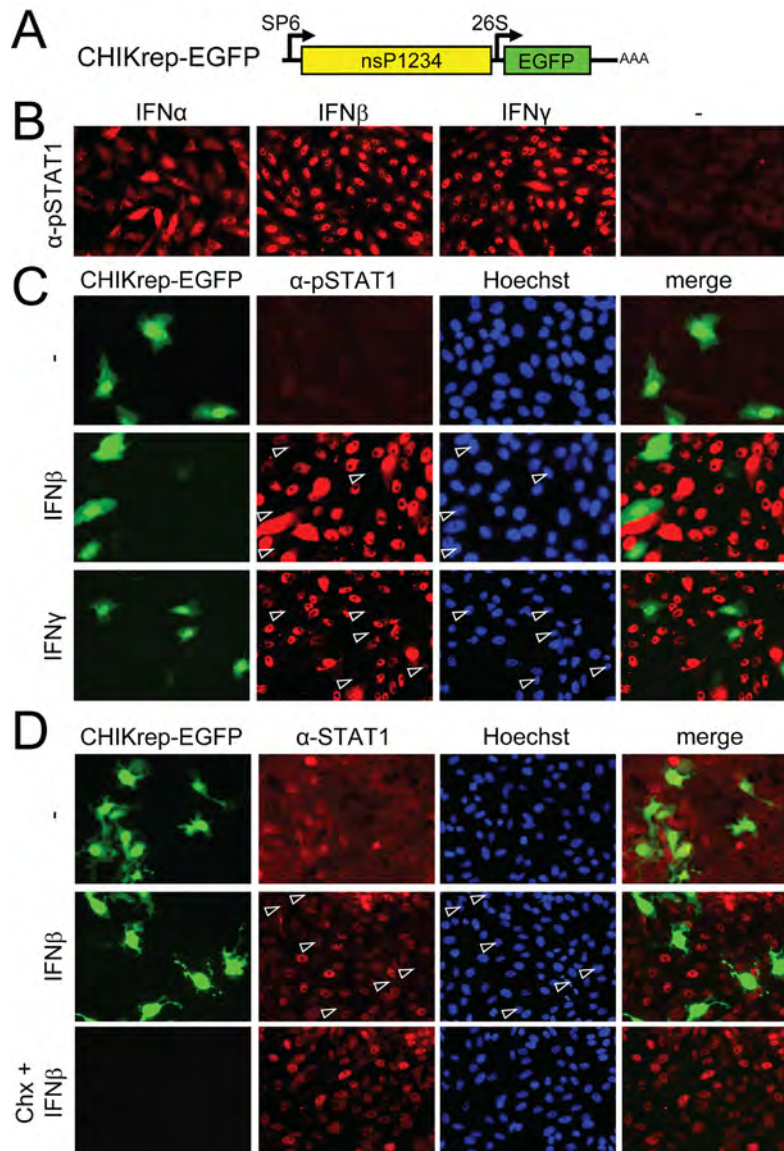


Figure 6.4. CHIKV replicon efficiently inhibits type I/II IFN-induced JAK-STAT signaling independent of host shut-off. **A.** Schematic representation of CHIKrepEGFP expressing EGFP. **B.** pSTAT1 nuclear translocation in Vero cells upon induction with type I and type II IFNs. **C.** CHIKV replicon blocks pSTAT1 nuclear translocation upon type I/II IFN induction. Vero cells were immunostained with anti-pSTAT1 antibody 24 h p.t. **D.** CHIKV RNA replication but not translational shut-off blocks STAT1 nuclear translocation. Vero cells were transfected with CHIKrep-EGFP replicon RNA in the absence or presence of cycloheximide. Cells were induced for 30 min with IFN- β at 12 h p.t. and stained with anti-STAT1 antibody. Open arrows show CHIKV replicon positive cells lacking nuclear STAT1.

were not decreased by CHIKV infection. To nevertheless rule out this possibility, cells were treated with cycloheximide to inhibit translation. This method of pharmacologically induced host cell protein synthesis shut-off was recently used in experiments with Venezuelan Equine Encephalitis virus (VEEV) to show that JAK-STAT signaling was blocked by VEEV and not by host shut-off (193). As expected, STAT1 fluorescence in control cells not treated with cycloheximide was cytoplasmic with no apparent difference in localization or fluorescence intensity between untransfected cells and green CHIKV replicon transfected cells (Figure 6.4D, top row). After IFN- β treatment, STAT1 was translocated into the nucleus in all cells except those expressing the CHIKV replicon (Figure 6.4D, open arrowheads). In cells treated with cycloheximide, CHIKV replicon encoded EGFP was absent due to effective inhibition of protein synthesis (Figure 6.4D, bottom). However, STAT1 nuclear translocation upon IFN- β induction was still clearly apparent despite effective inhibition of translation by cycloheximide (Figure 6.4D, bottom). Taken together, these experiments clearly show that CHIKV infection and replication of CHIKV replicon RNA efficiently inhibit IFN-stimulated JAK-STAT signaling independent of host shut-off.

CHIKV nsP2 inhibits IFN-induced STAT1 nuclear translocation

Since the CHIKV replicon could efficiently inhibit JAK-STAT signaling, the next question was if any of the CHIKV nsPs could be found to be responsible for this activity. Previous reports suggested that alphavirus nsP2 may be an important modulator of the IFN response (87, 206), however, direct inhibition of the JAK-STAT pathway by individual alphaviral nsP2 has not been reported.

In order to identify the CHIKV encoded protein responsible for blocking STAT1 nuclear translocation, Vero cells were transfected with plasmids expressing individual nonstructural proteins fused to self-cleaving mCherry2A and as a control transfection with a CHIKV replicon expressing mCherry (CHIKrep-mCherry) (Figure 6.5A). Two days p.t., cells were incubated with IFN- β and nuclear localization of phospho-STAT1 was visualized using anti-pSTAT1 antibodies (Please note; pSTAT1 in these pictures is green). IFN- β induction of transfected Vero cells showed that STAT1 efficiently translocated to the nucleus in cells expressing nsP1, nsP3 and nsP4 (Figure 6.5B, solid arrowheads). Only very few cells were found to lack nuclear phospho-STAT1 (Figure 6.5B, open arrowheads), suggesting that nsP1, -3 and -4 were not capable of efficiently blocking STAT1 nuclear translocation. In sharp contrast, however, STAT1 nuclear translocation was absent in the vast majority of cells expressing nsP2 (Figure 6.5B, nsP2, open arrowheads) and the positive control CHIKrep-mCherry (Figure 6.5C, open arrowheads). In the few nsP2-expressing cells that did display nuclear pSTAT1, the fluorescence intensity was greatly reduced as compared to untransfected cells (Figure 6.5B, nsP2, closed arrowheads). As expected, the CHIKrep-mCherry transfected cells also showed no nuclear

translocation after IFN- β treatment (Figure 6.5C, open arrowheads). These results clearly indicate that individually expressed CHIKV nsP2 is capable of inhibiting of JAK-STAT signaling.

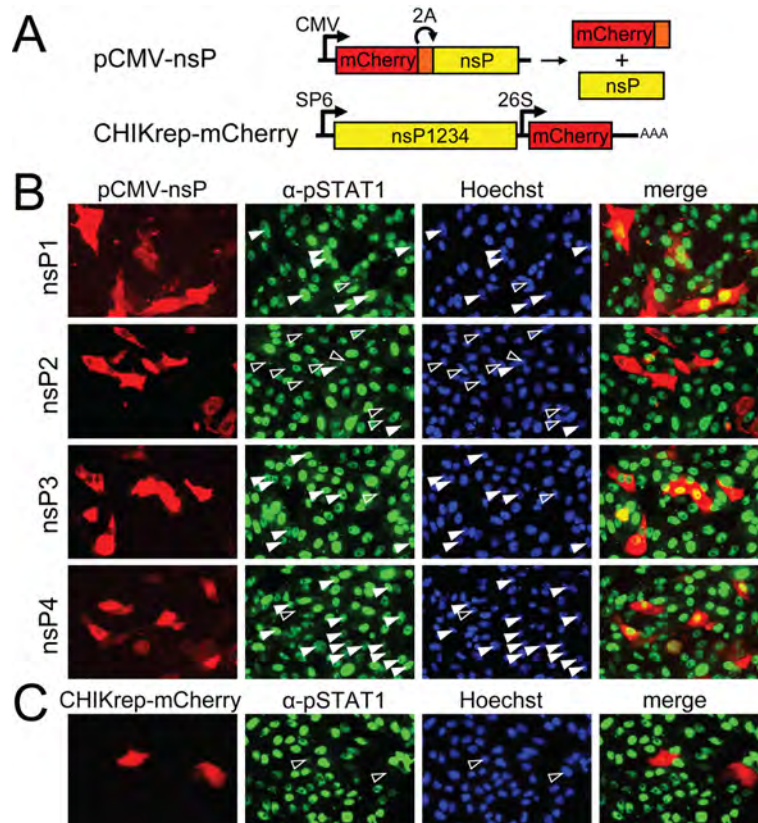


Figure 6.5. Inhibition of IFN- β induced STAT1 nuclear translocation by individual CHIKV nsPs. **A.** Schematic representation of pCMV-nsP1-4 expression plasmids and CHIKrep-mCherry replicon expressing mCherry. CMV; cytomegalovirus immediate early promoter, 2A; Foot-and-Mouth disease virus 2A autoprotease. Bacteriophage SP6 and CHIKV 26S promoters are indicated. **B.** pSTAT1 nuclear translocation upon IFN- β induction in pCMV-nsP1-4 transfected Vero cells. Cells were immunostained with anti-pSTAT1 antibody. **C.** pSTAT1 nuclear translocation upon IFN- β induction in CHIKrep-mCherry transfected Vero cells. Open arrows show nsP1-4 or CHIKV replicon positive cells lacking nuclear pSTAT1, solid arrows show nsP1-4 positive cells with nuclear pSTAT1.

Mutation of a conserved proline in the C-terminus of nsP2 abolishes the inhibitory effect of CHIKV and SINV replicons on JAK-STAT signaling.

Mutations in alphavirus nsP2 can have significant effects on the IFN response (87, 206). For example, a mutation of a conserved proline (Figure 6.6B) at position 726 in SINV was previously shown to result in non-cytopathic RNA replication (85) and reduced viral titers associated with higher IFN production (206). We hypothesized that this mutation could render the

replicon unable to block JAK-STAT signaling. This possibility was investigated by transfecting Vero cells with cytopathic “wildtype” SINrepGFP-wt (with restored proline at position 726) and non-cytopathic SINV replicon SINrepGFP (containing nsP2-P726S mutation) (Figure 6.6A). Transfected cells were induced 24 h p.t. with IFN- β for 30 min and stained with phospho-STAT1 antibodies as before. According to the hypothesis, cytopathic “wildtype” SIN replicon was able to effectively block STAT1 nuclear translocation, whereas the non-cytopathic SIN replicon with nsP2-P726S mutation (85) was not (Figure 6.6C).

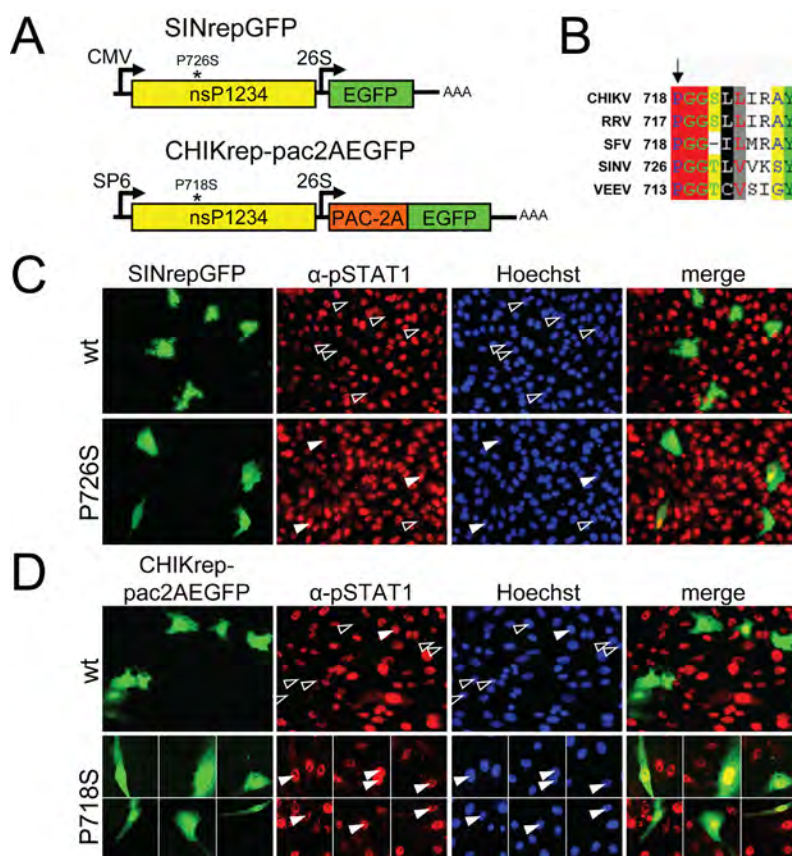


Figure 6.6. Mutation of a conserved proline in nsP2 abolishes inhibitory effect of CHIKV and SINV replicons on JAK-STAT signaling. **A.** Schematic representation of CHIKrep-pac2AEGFP and SINrepLuc replicons. NsP2 mutations P718S and P726S are indicated with an asterisk. PAC; puromycin acetyltransferase. **B.** Partial amino acid alignment of alphavirus nsP2. RRV; Ross River virus, VEEV; Venezuelan equine encephalitis virus. The conserved Proline and amino acid numbers within nsP2 proteins are indicated. **C.** pSTAT1 nuclear translocation upon type IFN- β induction in SINrepGFP (wildtype and mutant nsP2-P726S) transfected Vero cells. Cells were immunostained with anti-pSTAT1 antibody. Open arrows show replicon positive cells lacking nuclear pSTAT1, solid arrows show replicon positive cells with nuclear pSTAT1. **D.** phospho-STAT1 nuclear translocation upon IFN- β induction in CHIKrep-pac2AEGFP (wildtype and mutant nsP2-P718S) transfected Vero cells. Cells were immunostained with anti-pSTAT1 antibody.

We then investigated for CHIKV whether an analogous mutation of the conserved proline in CHIKV-nsP2 at position 718 (Figure 6.6B) could also be linked to a reduced ability to block JAK-STAT signaling. A puromycin-selectable CHIKV replicon designated CHIKrep-pac2AEGFP (Figure 6.6A) and the same construct with a nsP2-P718S mutation (CHIKrep-pac2AEGFP-nsP2m) were constructed and tested for their ability to block the JAK-STAT pathway in transient transfection experiment. The replication efficiency in Vero cells of CHIKrep-pac2AEGFPnsP2m (5-10 EGFP-expressing cells per well in a 96 wells plate) was severely reduced in comparison to CHIKrep-pac2AEGFP (~10% EGFP-expressing cells). In contrast, replication efficiency in BHK-21J cells of CHIKrep-pac2AEGFP-nsP2m as compared to CHIKrep-pac2AEGFP was only slightly reduced (~10% vs. ~20% EGFP-expressing cells), but with notable differences in the induction of cytopathic effect (CPE). BHK-21J cells transfected with CHIKrep-pac2AEGFP-nsP2m retained normal cell morphology, in contrast to cells transfected with CHIKrep-pac2AEGFP, which lost adherence and showed cell rounding 48 h p.t. (data not shown).

In order to investigate the effect of the CHIKV nsP2-P718S mutation on JAK-STAT signaling, Vero cells transfected with CHIKrep-pac2AEGFP or CHIKrep-pac2AEGFP-nsP2m, were induced with IFN- β at 24h p.t. and stained with α -STAT1 antibody as before. Similar to the results obtained with SINV, CHIKV replicon expressing nsP2-P718S was indeed unable of blocking IFN- β induced STAT1 nuclear translocation, in contrast to its parental “wildtype” CHIKV replicon (Figure 6.6D). This observation suggests that SINV and CHIKV most likely employ a similar mechanism of blocking the JAK-STAT pathway, and that the conserved proline in nsP2 at positions 726 and 718, respectively, is essential for this activity.

Discussion

The IFN response is the first line of defense against invading pathogens and therefore it is no surprise that many viruses actively suppress this antiviral mechanism to promote virus replication and spread (reviewed by Randall & Goodbourn, 2008) (192). In this research we have shown that once established, CHIKV replication is largely resistant to treatment with type I and II IFN. While IFN- α has been proposed as an antiviral drug to control CHIKV replication (207), our results suggest that IFN may have limited use in antiviral therapy. Recent experiments in mice support this view illustrating that IFN- α treatment before, but not after CHIKV infection inhibits disease and viraemia (68). Next, we demonstrated that CHIKV infection and CHIKV replicon RNA replication both efficiently blocked IFN-induced JAK-STAT signaling. This activity was mapped to the nsP2 gene by expression of nsP2 alone and in the context of an attenuated CHIKV replicon harboring an nsP2 mutation from a conserved proline to a serine at position 718.

NsP2 had earlier been recognized as an important player in modulating the IFN response associated with host shut-off (208). Recently, it is becoming clear that host shut-off and suppression of the IFN response by alphaviruses can be regarded as separate activities (193). In Old World alphaviruses, nsP2 has been found to be the most important viral protein in modulating the IFN response, with an additional role for the capsid protein in the New World alphaviruses (205, 209). Through the generation of adaptive mutants, nsP2 has been identified as the main viral factor to establish persistent replication in mammalian cells. Non-cytopathic variants of SINV and SFV with different mutations in nsP2 display severe defects in counteracting the IFN response (87, 206) and result in high IFN production. This lead to the hypothesis that nsP2 has an essential role in modulation of the IFN response, likely via interference with downstream JAK-STAT signaling. We show here for the first time that alphavirus nsP2 alone is able to block the JAK-STAT pathway.

Whether or not the other nsPs or their intermediate precursors could possible contribute to the activity displayed by nsP2 was not further investigated. However, given the potency of individual nsP2 to block STAT1 nuclear translocation, any contributory activity by other viral proteins may not be required to establish a productive infection. Selection of Vero or BHK-21J cell lines harboring persistently replicating, attenuated CHIKV replicon RNA was unfortunately not accomplished. It might be possible that for CHIKV replicons additional mutations in nsP2 or other locations are required to support persistent replication in mammalian cells as was previously described for non-cytopathic SINV (85).

Previous research has suggested important roles for nsP2 and a host-encoded, cellular endoribonuclease, RNaseL, to initiate the transition from minus- to plus-strand RNA synthesis (210, 211). Since RNaseL is activated by OAS, which itself is an interferon stimulated gene (ISG), this seems at odds

with the inhibitory role of nsP2 on the JAK/STAT pathway. However, the switch from the minus-strand replication complex (RC-) to RC+ occurs at a later stage during infection and only after cleavage of the nsP2/3 precursor. In CHIKV-infected cells, we have observed inhibition of OAS induction by IFN treatment at later timepoints (>8 hpi). This correlates with the current view that nsP2 is released in its free form after early replication has been established and creates an environment where host transcription/translation is reduced and the IFN response is actively suppressed.

We have shown by several different experimental approaches that CHIKV replication blocks the JAK-STAT pathway, yet the exact mechanism at the molecular level remains to be elucidated in follow up experiments. We have ruled out that the observed blockage of JAK-STAT signaling was due to host shut-off, since signaling in these settings was unaffected in cells treated with cycloheximide. We have also ruled out that CHIKV reduces endogenous STAT1 levels, an observation also reported for VEEV- and SINV-infected cells (203).

During dengue virus infection, STAT1 nuclear translocation is inhibited by dengue virus nonstructural protein NS5 as an indirect result of preventing STAT2 phosphorylation and STAT1-STAT2 heterodimer formation (78, 212). Consequently, dengue virus is not capable of inhibiting IFN- γ induced STAT1 phosphorylation/homodimer formation. In contrast to dengue virus, however, incubation with IFN- γ of cells infected with CHIKV or transfected with CHIKV replicon demonstrates that STAT1 activation is blocked (Figures 6.3C and 6.4C), suggesting that the inhibitory mechanism in the case of CHIKV is different.

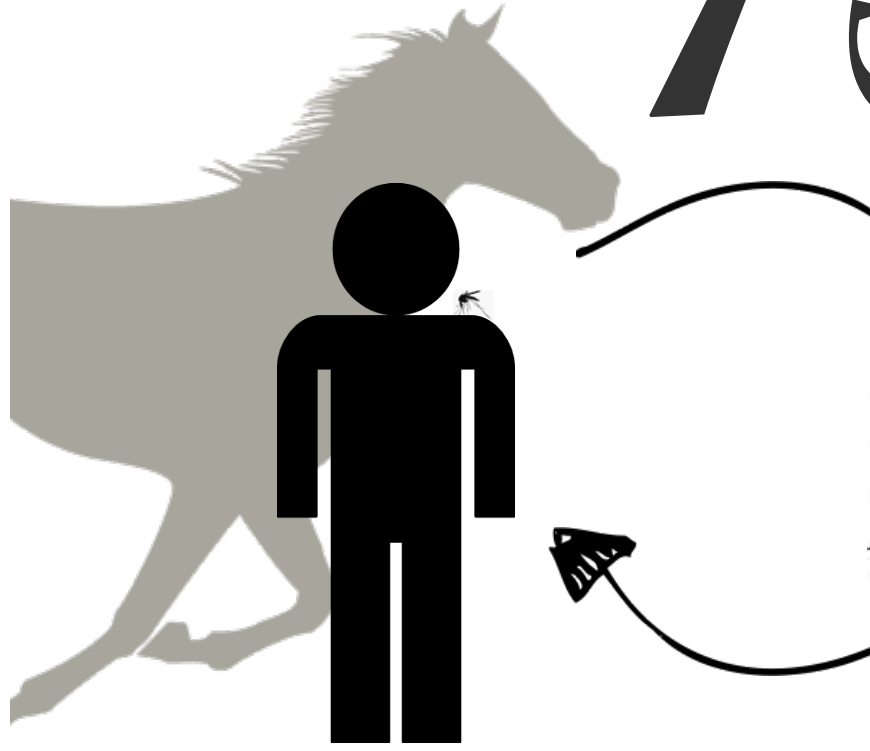
The increased STAT1 levels upon IFN induction in normal but not in CHIKV infected cells (Figure 6.3D) may be the result of signal transduction via JAK-STAT pathway as was suggested earlier (200). In this scenario, STAT1 upregulation in CHIKV-infected cells is prevented by active inhibition of JAK-STAT signaling, which is supported by the observed decreased luciferase production from the IFN responsive plasmids in infected cells (Figure 6.2).

We showed that a SINV replicon containing nsP2 with a serine at position 726 was not able to efficiently block phospho-STAT1 nuclear translocation, in contrast to the “wildtype” SINV replicon containing nsP2 with a restored proline at position 726. Others have previously claimed that wildtype SINV infection does not impair the ability to respond to IFN- α as judged by similar levels of STAT1 phosphorylation in infected as compared to uninfected cells (75). The reason for this apparent discrepancy in results is not clear, but an explanation may be the timing of the experiment or the genetic background of the SINV constructs. In our studies, we induced Vero cells with IFN 24 h p.t. with a pToto1101 derived replicon (213), whereas Lin *et al.* (2006) (75) used a dsTE12Q recombinant Sindbis vector (214) and induced Vero cells with IFN 6 h p.i.. It would be interesting to map the putative differences between these SINV vectors, within nsP2 or elsewhere in the genome, and identify the domain(s) or amino acid(s) responsible.

Taken together, the inability of alphaviruses with mutated nsP2 proteins to efficiently block STAT1 nuclear translocation may now provide an explanation for the reported overall increased IFN production by such mutants. In this light it is interesting to note that in preliminary studies Ross River virus (RRV), another arthrogenic alphavirus and a close relative to CHIKV, does not appear to antagonize STAT1 activation (215) although this awaits confirmation. In future research, it may be interesting to investigate whether this apparent difference between CHIKV and RRV could be due to differences of their respective nsP2 proteins. Mapping the functional domains within CHIKV nsP2 and deciphering the exact mechanism how nsP2 blocks the JAK-STAT pathway, possibly by preventing STAT1 phosphorylation and/or prohibiting nuclear import of phosphorylated STAT1, is the focus of future studies in our laboratories. Our results may also provide insights into the development of live-attenuated vaccines to control CHIKV and other alphavirus infections.

Acknowledgements

We thank the VIDRL (Australia) for supply of the chikungunya virus isolate. We acknowledge Klaske Schippers and Dr. Dirk Martens (dept. of Process Engineering, Wageningen University) for use of the fluorescence microscope. We thank Julia Eekels (AMC, Amsterdam) for sending us the pcDNA-DEST40 plasmid, Dr. Brigitte Biesinger (University of Erlangen-Nürnberg) for sharing native STAT1 antibody, Dr. Peter de Haan (Amarna Therapeutics B.V., Leiden) for the SINrepGFP construct and Dr. Peter Bredenbeek (LUMC, Leiden) for BHK-21J cells. We thank Konstantin Tsetsarkin and Dr. Stephen Higgs for their role in the construction of CHIKrep-EGFP. Joël van Mierlo, Teije Kleikamp, Jason Leung and Jan Vermond were involved in the construction of SINrepGFP-wt, CHIKrep-FlucEGFP, CHIKrep-pac2AEGFP and CHIKrep-pac2AEGFP-nsP2m, respectively.



7 Chapter

The C-terminal domain of chikungunya virus nsP2 independently governs viral RNA replication, cytopathicity, and inhibition of interferon signaling

Alphavirus non-structural protein (nsP)₂ has pivotal roles in viral RNA replication, host cell shut-off and inhibition of antiviral responses. Mutations that individually rendered other alphaviruses non-cytopathic were introduced into chikungunya virus nsP₂. Results show that (i) nsP₂ mutation P718S only in combination with KR649AA or adaptive mutation D711G allowed non-cytopathic replicon RNA replication, (ii) prohibiting nsP₂ nuclear localization abrogates inhibition of antiviral interferon-induced JAK-STAT signaling (iii) nsP₂ independently affects RNA replication, cytopathicity and JAK-STAT signaling.

This chapter has been published as:

Jelke J. Fros, Erika van der Maten, Just M. Vlak and G. P. Pijlman. *The C-terminal domain of chikungunya virus nsP₂ independently governs viral RNA replication, cytopathicity, and inhibition of interferon signalling*. *J. Virol.* **87**, 10394–400 (2013).

Main text

Chikungunya virus (CHIKV) is a member of the Alphavirus genus within the *Togaviridae* family. In humans, infection by this mosquito-borne virus can result in the development of a high fever, rash and incapacitating, sometimes chronic, arthralgia. The last decade CHIKV outbreaks occurred throughout the Indian ocean region, including La Reunion infecting up to one third of the human population, before infecting millions of people in India and Southern Asia (3, 31). CHIKV is a positive-strand RNA virus that replicates in the cytoplasm of infected cells. The genome contains four non-structural proteins (nsP1-4) that are directly translated from the genomic RNA (gRNA). The viral structural proteins are translated later in infection from subgenomic mRNA (sgRNA)(191).

NsP1 is a methyltransferase and is associated with cellular membranes (145), nsP3 is a phosphoprotein that recruits host factor G3BP and consequently inhibits the formation of cellular stress granules (160, 216) and nsP4 is the viral RNA-dependent RNA polymerase (191). NsP2 contains the viral helicase, protease and a putative C-terminal methyltransferase domain, associates with many host proteins and can effectively shut down host cell protein synthesis (217–221). Alphavirus nsP2 also contains a nuclear localization signal (NLS) in its C-terminal domain (CHIKV nsP2 KR649-650) (Figure 7.1A, top). NsP2 from related Semliki Forest (SFV) and Sindbis viruses (SINV) has been shown to translocate to the nucleus (222–224) as specific mutations within the NLS retained SFV nsP2 in the cytoplasm and reduced its cytopathicity (225). In the nucleus, nsP2 of Old World alphaviruses (SFV, SINV, CHIKV) has been reported to inhibit host cell mRNA transcription via degradation of a subunit of DNA-directed RNA polymerase II (RPB1)(149). Mutation of a conserved proline residue in a site homologous to CHIKV nsP2 P718 (Figure 7.1A, bottom) rendered SINV non-cytopathic and alleviated the transcriptional inhibition via RPB1 (85, 149, 226).

In addition, alphavirus nsP2 has been shown to antagonize the hosts main antiviral response, the interferon(IFN)-response in two ways: (i) IFN- β transcription via global host shut-off and (ii) downstream type I/II IFN-induced Janus kinase/signal transducers and activators of transcription (JAK-STAT) signalling (87, 148, 149, 193, 206). Upon activation, phosphorylated STAT1/2 proteins translocate as dimers into the nucleus to activate the transcription of antiviral genes, bringing the cell in an antiviral state (192). Inhibition of STAT1 phosphorylation and/or nuclear translocation are important determinants of alphavirus virulence (193, 227).

Previously, we showed that CHIKV replication is sensitive to pre-stimulation of cells with IFNs, but becomes largely resistant to IFNs once replication has been established (148). In addition, we showed that individually expressed CHIKV nsP2 is a potent inhibitor of IFN downstream signaling by blocking STAT1 nuclear translocation. In the context of CHIKV replicon

RNA replication, the mutation P718S within the nsP2 gene abrogated the inhibitory effects of nsP2, re-allowing STAT1 to translocate to the nucleus upon stimulation with IFN (148). Since the C-terminal domain of nsP2 appears to be highly multifunctional and is associated with host cell shut-off and cytopathic effect (CPE), the inhibition of JAK-STAT signaling, viral replication and with nuclear translocation of nsP2, we set out to determine whether or not these characteristics of nsP2 are intrinsically connected.

We began by investigating the cellular distribution of CHIKV nsP2. EGFP was fused within the N-terminus of nsP2 (essentially as described for SINV (224)), in a CHIKV replicon expressing mCherry from the 26S subgenomic promoter (148) creating CHIKrep-nsP2EGFP-mCherry (Figure 7.1B, bottom). Mutations in the NLS (KR649AA) or P718 (P718S) were introduced creating CHIKrep-nsP2EGFP^{KR649AA}-mCherry and CHIKrep-nsP2EGFP^{P718S}-mCherry, respectively. Transfection of *in vitro* transcribed CHIKrep-nsP2EGFP-mCherry RNA into Vero cells showed that nsP2EGFP not only translocates from the cytoplasm to the nucleus, but also supports functional viral RNA replication and sgRNA expression as indicated by mCherry expression (Figure 7.1C, top panel). Both the mutated replicons were hardly detectable when the same exposure time was used as with wild type CHIKrep-nsP2EGFP-mCherry. However, longer exposure times revealed that nsP2EGFP^{KR649AA} was exclusively localized to the cytoplasm and that the mCherry signal was barely detectable (Figure 7.1C). Although overall protein levels were much lower, nsP2EGFP^{P718S} distribution and the mCherry signal resembled that of the wild type replicon (Figure 7.1C).

Since these mutations in the C-terminus of alphavirus nsP2 clearly affect viral protein expression we introduced both the mutations in the NLS (KR649AA) or P718S into a plasmid that individually expressed nsP2-EGFP from a cytomegalovirus (CMV) promoter (Figure 7.1B, top) creating pnsP2-EGFP, pnsP2-EGFP^{KR649AA} and pnsP2-EGFP^{P718S}, respectively. As expected and similar to expression from replicon (Figure 7.1C), individually expressed nsP2EGFP fusion proteins localized to both the cytoplasm and the nucleus (Figure 7.1D, top panels). In line with what was found for SFV, disruption of the NLS in CHIKV nsP2 blocked nuclear localization and retained nsP2 in the cytoplasm (Figure 7.1D, middle panels)(222, 225). In contrast, the P718S mutation still allowed nuclear translocation and displayed a distribution of the nsP2EGFP fusion protein similar to wild type nsP2 (Figure 7.1D, lower panels). In the context of replicon RNA replication (Figure 7.1C), the fraction of nsP2EGFP in the nucleus was somewhat smaller compared to individually expressed nsP2EGFP (Figure 7.1D). Most likely, more nsP2 is retained in the cytoplasm when it interacts with other nsPs to form replication complexes. These results demonstrate that CHIKV nsP2 is present in the nucleus during RNA replication and upon individual expression but requires an intact NLS for nuclear translocation.

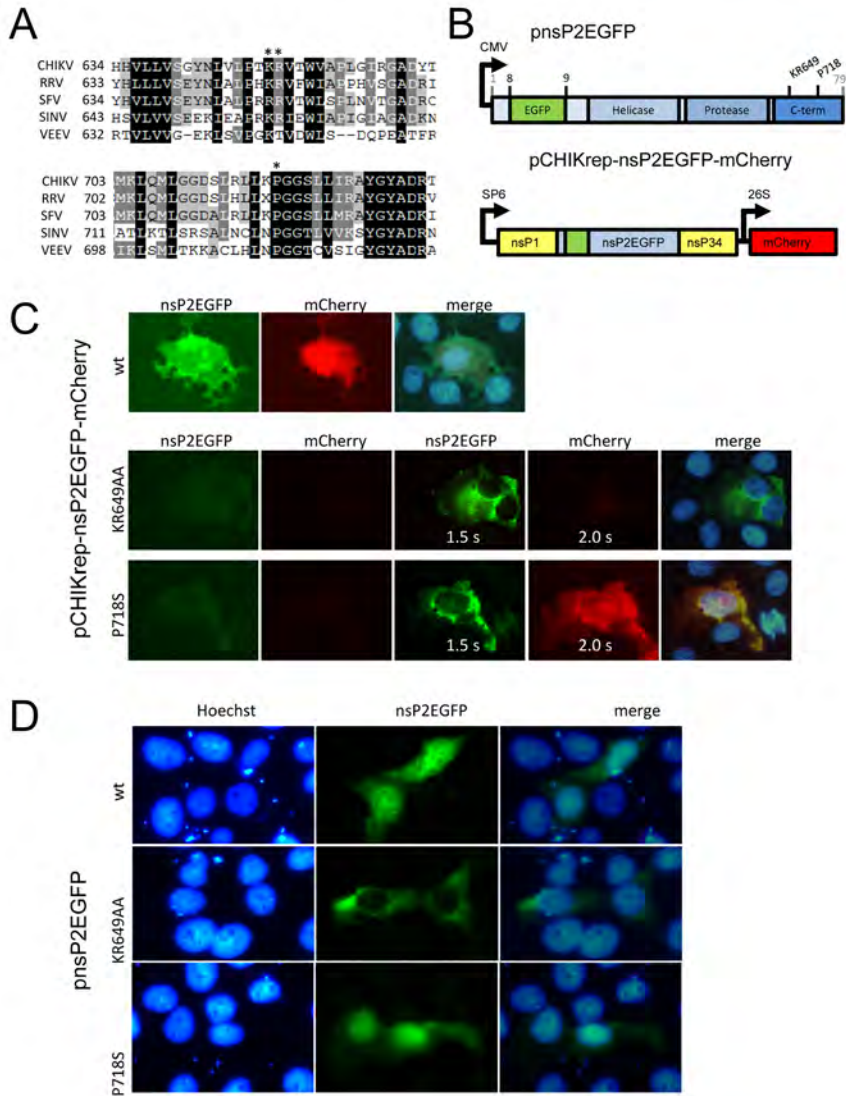


Figure 7.1. CHIKV nuclear localization depends on an intact NLS. **A.** Partial amino acid alignment of alphavirus nsP2s. RRV, Ross River virus; VEEV, Venezuelan equine encephalitis virus. Arrows indicate the conserved amino acids lysine (K) and arginine (R) in the NLS at CHIKV nsP2 position 649 (top) and the conserved proline (P) at position 718 (bottom). **B.** Schematic representation of pnsP2EGFP (top) and pCHIKrep-nsP2EGFP-mCherry (bottom). EGFP has been inserted between amino acid 8/9 as indicated. Asterisks indicate the location of conserved site mutations (KR649 and P718). **C.** Vero cells were transfected with in vitro transcribed CHIKrep-nsP2EGFP-mCherry wild type RNA and the KR649AA and P718S mutants. After 24 h the cells were fixed in 4% paraformaldehyde in phosphate-buffered saline for 10 min at room temperature and nuclei were visualized by Hoechst 33342 staining (10 ng/ml). All samples were visualized with identical exposure times prior to being overexposed. **D.** Vero cells were transfected with pCMV-nsP2EGFP, nsP2EGFPKR649AA or nsP2EGFP718S. After 24 h cells were fixed and stained with Hoechst and visualised with a Zeiss Axio Observer Zim inverted microscope in combination with an X-Cite 120 series lamp.

Since alphavirus nsP2 causes shut down of host cell protein synthesis and is cytotoxic (85, 218, 225) we investigated the effect of the mutations in the C-terminus of CHIKV nsP2 on host cell protein synthesis. CMV promoter-driven expression plasmids (21) encoding nsP2^{KR649AA} and nsP2^{P718S} mutants were transfected into Vero cells together with a plasmid, constitutively expressing Renilla luciferase (Rluc). Cells transfected with a control plasmid expressing EGFP were either left untreated or treated with cycloheximide (CHX), to inhibit protein synthesis. Both CHX treatment and wild type nsP2 expression reduced the amount of translated Rluc considerably, whereas both mutants did not decrease Rluc protein synthesis (Figure 7.2A). Surprisingly, nsP2^{KR649AA} even seemed to increase Rluc synthesis (Figure 7.2A). Although alphavirus nsP2 is known to modulate host cell translation, possible mechanisms that could enhance general translation have not been reported (85, 218, 225, 226, 228).

Subsequently, the level of cytotoxicity induced by CHIKV nsP2 and its mutants was investigated in cell viability and apoptosis assays. Vero cells were transfected with either the control plasmid or with plasmids encoding one of the nsP2 mutants. Cells transfected with the control plasmid were either left untreated or treated with actinomycin D (ActD) to induce CPE through transcriptional inhibition (229). Both treatment with ActD and transfection with nsP2 resulted in severe CPE and thus reduced the total cell viability (Figure 7.2B). In sharp contrast, expression of either the nsP2^{KR649AA} or nsP2^{P718S} mutants did not induce any CPE over the course of the experiment. In a parallel experiment, the level of nsP2-induced apoptosis was determined by measuring effector caspase 3/7 activity (Figure 7.2C). The presence of either ActD or nsP2 resulted in a significant induction of caspase activity compared to the mock. In line with results from the cell viability assay, both mutant nsP2 proteins did not induce any caspase activity. Together, these results indicate that mutation of the NLS (KR649) or the conserved proline at P718 abrogates host cell shut-off and significantly decreases the cytotoxicity of nsP2 and the subsequent induction of apoptosis.

Previously, we reported that in the context of CHIKV RNA replication, nsP2^{P718S} allows STAT1 nuclear translocation, whereas wild type nsP2 is a potent inhibitor of JAK-STAT signalling (148). Because residues P718, but also KR649 are important for viral replication, host cell shut-off and associated CPE, we investigated whether or not there is a connection with the inhibition of JAK-STAT signaling by individually expressed nsP2. Vero cells were transfected with either wildtype pCMV-nsP2, -nsP2^{KR649AA} or -nsP2^{P718S}. Since nsP1 alone did not have any effect on STAT1 nuclear translocation, pCMV-nsP1 was used as a control (Figure 7.2D, left)(148). At 24 h post transfection, STAT1 phosphorylation was induced with IFN- β . Immuno-staining with phosphoSTAT1 antibodies showed that nsP2 wild type clearly inhibits STAT1 nuclear translocation (Figure 7.2D, middle left). The NLS mutant nsP2^{KR649AA} completely lost the ability to inhibit STAT1 nuclear translocation, indicating that a functional NLS in nsP2

may be required for blocking the JAK-STAT pathway (Figure 7.2D, middle right). Unexpectedly, given the previously observed abrogation of JAK-STAT inhibition by a CHIKV replicon with a P718S mutation in nsP2, the individually expressed nsP2^{P718S} mutant still inhibited STAT1 nuclear translocation to the same extent as wild type nsP2 (Figure 7.2D, right).

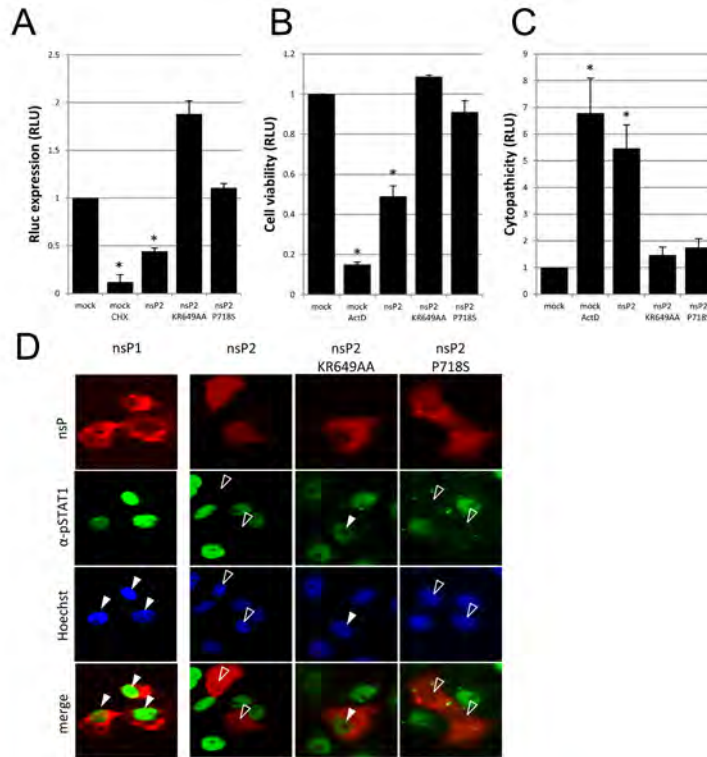


Figure 7.2. Mutations in CHIKV nsP2 differentially influence host shut-off mediated cytopathicity and the inhibition of JAK-STAT signaling. **ABC.** Vero cells were transfected with either a control plasmid pEGFP-N1 (Clontech) or CMV-nsP2, CMV-nsP2KR649AA or CMV-nsP2P718S. **A.** In addition to the nsP2 plasmid cells were co-transfected with plasmid constitutively expressing Renilla luciferase (pRL-TK, Promega). Control cells were either left untreated or treated with CHX (0.5µg/ml) for 24 h, before Rluc expression was measured. Values are depicted as the average duplicate samples from two individual experiments. Error bars represent one standard error and asterisk indicate a significant difference compared to the mock (Tukey HSD test, $P < 0.05$). **BC.** Cells were transfected with the nsP2 variants or control plasmid. Controls were either treated with ActD (2µg/ml) for 48 h or left untreated. After 48 h cell viability (**B**) or caspase activity (**C**) were measured with a luminescent based assays (CelltiterGLO and Caspase-GLO 3/7 assays, Promega). Values are depicted as the average of triplicate samples from three individual experiments and relative to the mock. Error bars represent one standard error and asterisk indicate a significant difference compared to the mock (Tukey HSD test, $P < 0.05$). **D.** Vero cells were transfected with the indicated mutants of pCMV-nsP2. After 24 hours cells were fixed and permeabilized with 0.1% sodium dodecyl sulfate (SDS) in PBS. Nuclei were stained with Hoechst 33342. STAT1 nuclear translocation was visualized with anti-pSTAT1 primary antibody (phospho-Tyr701; SAB Signalway Antibody) and the secondary antibody GaR-AF488 (Molecular Probes). Open arrowheads indicate the nuclei of nsP2 positive cells that lack the signal for pSTAT1. Solid arrowheads indicate nsP2 positive cells with nuclear pSTAT1

We therefore hypothesized that reduced RNA replication of the CHIKV replicon carrying the P718S mutation could explain the observed lack of inhibition of JAK-STAT signaling in our earlier study (148). We set out to determine what the (combined) effects of the NLS and P718S mutations were on CHIKV RNA replication and cytopathicity. In a puromycin selectable CHIKV replicon which was described previously (148), we engineered both mutations either separately or together, creating: CHIKrep-nsP2^{KR649AA}-pac2AEGFP, CHIKrep-nsP2^{P718S}-pac2AEGFP and CHIKrep-nsP2^{KR649-P718S}-pac2AEGFP, respectively. *In vitro* transcribed RNA was transfected into BHK cells and puromycin selection was started 24 hpt (Figure 7.3A). The double mutant (CHIKrep-nsP2^{KR649-P718S}) proved easily selectable (Figure 7.3A, e) and is similar to a recently described non-cytopathic CHIKV replicon that acquired a 5 amino acid insertion of unknown origin that disrupted the NLS (226). However, multiple attempts to select cells that expressed replicons with single nsP2 mutations were unsuccessful (Figure 7.3A, cd). In one of these experiments, however, a single colony of the CHIKrep-nsP2^{P718S}-pac2AEGFP mutant survived and grew out to a stable, CHIKrep-pac2AEGFP expressing cell line. Sequencing of the nsP2 gene revealed that nsP2 had acquired a second-site mutation, D711G. To exclude the possibility that additional adaptive mutations outside nsP2 were acquired we engineered a replicon with only the D711G and P718S mutations (CHIKrep-nsP2^{D711G-P718S}-pac2AEGFP). Transfection into BHK cells displayed a non-cytopathic phenotype and as a result these cells were readily selected with puromycin (Figure 7.3A, f).

To investigate whether reduced cytopathicity was due to nsP2 related host cell modulation and/or affected replication efficiency we measured CHIKrep RNA replication in a time course experiment. BHK cells were transfected with either wild-type CHIKrep-pac2AEGFP (Figure 7.3B, b), a replication-defective variant lacking its 3'UTR (CHIKrep-pac2AEGFP-Δ3'UTR) (Figure 7.3B, a) or one of the above described mutants (Figure 7.3B, c-f). Cells were harvested at different times post transfection and the relative copy numbers of CHIKrep gRNA and sgRNA were quantified by qRT-PCR via amplification of parts of the nsP1 and the pacEGFP genes, respectively. At 15 hpt all replicons had reached peak RNA copy numbers (Figure 7.3C). The transfected cells were not subjected to puromycin selection, making it likely that the observed decrease after 15 h was caused by proliferation of untransfected cells and/or cell death induced by CHIKV RNA replication. At 15 hpt, wild type CHIKrep displayed a ~30-fold increase in relative copy numbers of gRNA (Figure 7.3C, left) and a ~60-fold increase of sgRNA (Figure 7.3C, right). The gRNA levels of the KR649AA mutant were similar to wild type (Figure 7.3C, left). The primers used to amplify sgRNA also amplify the corresponding fragment from the gRNA. Since the level of sgRNA amplification was comparable to that of gRNA, this indicates that the actual production of sgRNA was severely impaired (Figure 7.3C, right). The lack of mCherry production during CHIKrep-nsP2EGFP^{KR649AA}-mCherry

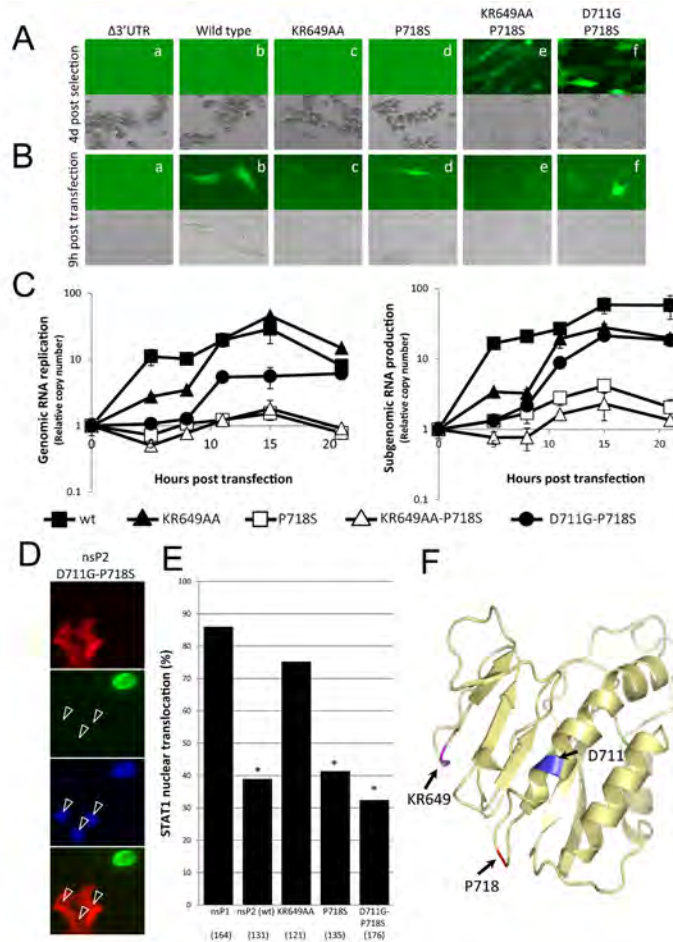


Figure 7-3. CHIKV nsP2 requires multiple mutations to establish non-cytopathic replication, independently of STAT1 nuclear translocation. **AB.** BHK cells were transfected with in vitro transcribed RNA of the various mutants of CHIKrep-pac2AEGFP (a-f). **A.** Twenty four hpt cells were selected for non-cytopathic replicon replication expressing the puromycin resistance gene (pac) by adding puromycin (5 ng/ml) to the medium. Pictures were taken at 9 h (**B**) and 5 d (**A**) post transfection. **C.** Vero cells were transfected with in vitro transcribed RNA of the indicated mutants of CHIKrep-pac2AEGFP. At indicated times post transfection total RNA was harvested (Maxwell, LEV16 simplyRNA cell kit, Promega) and reverse transcribed (SuperScriptIII, Invitrogen) using random primers. Genomic RNA replication was measured using semi-quantitative PCR (IQ SYBRgreen, Bio-rad). Depicted is a representative of 2 independent experiments. Values represent the average from duplicate samples, after being normalized for a non-replicating replicon (lacking the 3'UTR) and relative to input RNA at 0 h post transfection. Error bars represent one standard deviation. **D.** Vero cells were transfected with nsP2D711G-P718S and fixed and stained for pSTAT1. Open arrowheads indicate the nuclei of nsP2 positive cells that lack the signal for pSTAT1. **E.** Vero cells were transfected with the indicated mutants of pCMV-nsP2 and immunostained with pSTAT1 24 hpt. Values represent manual cell counts of STAT1 positive nuclei, relative to nsP1. Values within brackets represents population size. Asterisks indicate significant decrease from nsP1 (binomial test, $P < 0.01$). **F.** Model of the C-terminal domain of CHIKV nsP2. Loop structures 1-4 and residues KR649 (magenta), D711 (blue) and P718 (red) are indicated.

replication confirms the reduction in sgRNA production (Figure 7.1C). The P718S mutant had a very low level of gRNA replication (Figure 7.3C, left) with a respective ~3-fold increase of sgRNA at 15 hpt. (Figure 7.3C, right). Reduced replication rates of both mutant replicons correspond to what was found for other alphavirus replicons that carry mutations at homologous sites (225, 226). The severely diminished sgRNA production of CHIKrep-nsP2EGFP^{KR649AA} has not been reported previously. These observations and those presented by others, indicate that various mutations at these sites can differentially affect the efficiency of alphavirus replicon RNA replication, depending on the alphavirus species (225, 226). The replicon with both the KR649AA and P718S mutations has an intermediate phenotype, resulting in low level production of gRNA and sgRNA (Figure 7.3C). Interestingly, RNA replication of the D711G-P718S replicon was partly rescued by this novel adaptive mutation as observed by increased gRNA (~7-fold) and sgRNA (~12-fold) levels at 15 hpt (Figure 7.3C).

These results indicate that, unlike other alphaviruses, CHIKV replicons require multiple mutations in the C-terminus of nsP2 for establishment of non-cytopathic replication. Since the mutations KR649AA and P718S completely reduced the cytotoxicity of nsP2 when it was individually expressed (Figure 7.2BC), the inability to select both CHIKrep-nsP2^{KR649AA}-pac2AEGFP and CHIKrep-nsP2^{P718S}-pac2AEGFP replicons is likely to be the result of reduced production of sgRNA messenger and gRNA replication, respectively (Figure 7.3C). The reduced replication efficiencies of replicons with the P718S mutation (Figures 7.1C and 7.3C) explain the absence of inhibition of STAT1 nuclear translocation observed in our previous study (148). In addition, we identified a novel combination of mutations (D711G-P718S) that allows non-cytopathic replication combined with relatively high sgRNA levels. This replicon may be an attractive tool for biotechnology applications where high level protein expression from non-cytopathic viral vectors is desired. In addition, this novel replicon carrying combined D711G and P718S mutations allowed us to investigate whether or not the inhibition of JAK-STAT signaling is intrinsically linked to non-cytopathic RNA replication. We introduced the D711G mutation in pCMV-nsP2^{P718S} to create pCMV-nsP2^{D711G-P718S}. When STAT1 localization was assayed in the presence of this novel double mutant it proved to be a potent inhibitor of JAK-STAT signaling (Figure 7.3D). A manual count of cells displaying STAT1 nuclear translocation in the presence of either nsP1, wild type nsP2 or one of the described nsP2 mutants clearly showed that only nsP2^{KR649AA} was no longer able to inhibit STAT1 nuclear translocation (Figure 7.3E). This shows that non-cytopathic RNA replication is independent from JAK-STAT signaling and that a functional NLS is a prerequisite for the inhibition of STAT1 nuclear localization.

In conclusion, we show that host cell shut-off and associated CPE induced by CHIKV RNA replication are caused by CHIKV nsP2 (Summarized in Table 1). The shutoff caused by overexpression of nsP2 has been clearly described by others and is a result of transcriptional arrest via degradation of DNA-directed

Table 7.1. Summary of Data ^a

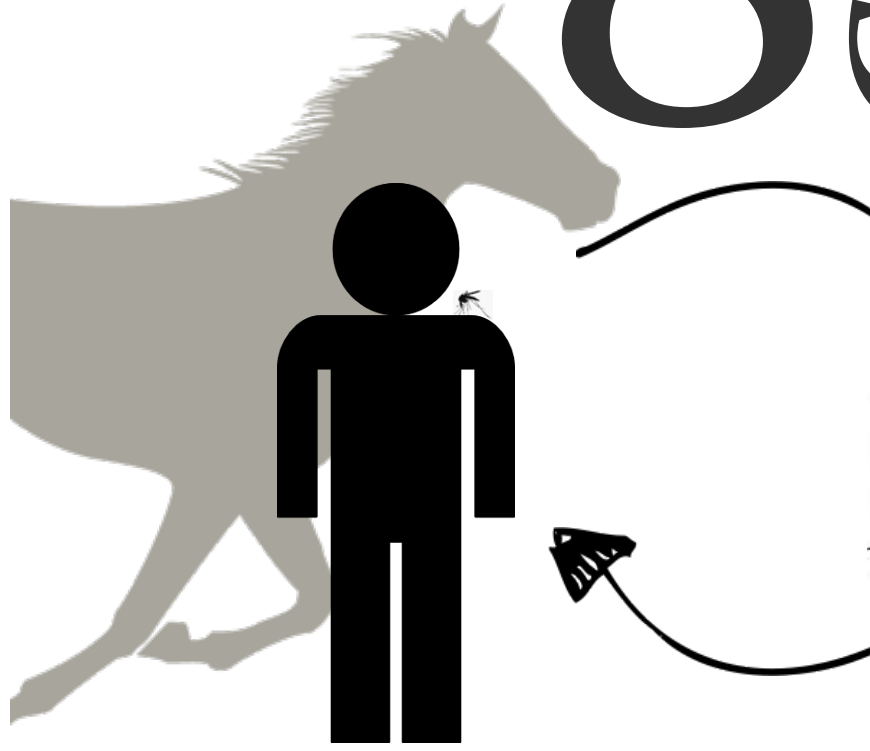
Characteristic	Figure(s)	Level for strain:				
		Wildtype	KR649AA mutant	P718S mutant	KR649AA-P718S mutant	D711G-P718S mutant
Nuclear localization	1C and D	+	-	+	NT	NT
CPE	2B and C	+	-	-	-	-
gRNA replication	3C	+	+	-	-	+/-
sgRNA production	3C	++	-	+/-	-	+
JAK-STAT signaling inhibition	2D, 3D and E	+	-	+	NT	+

^a Symbols and abbreviations: -, negative, +/-, intermediate, +, positive, ++, strongly positive, NT, not tested.

RNA polymerase II (149). Mutations that rendered other alphavirus replicons non-cytopathic (KR649AA, P718S) completely restored host cell protein synthesis and efficiently prevented nsP2-induced CPE. Unlike the situation in other alphaviruses, multiple mutations in the C-terminus of nsP2 are required to establish non-cytopathic CHIKV RNA replication in mammalian cells. Here we show that directed mutagenesis of the NLS (KR649AA) in combination with the P718S mutation is sufficient to sustain non-cytopathic RNA replication and selection of replicon cell lines. Moreover, we also identified a second combination of mutations including a novel adaptive second-site mutation (D711G-P718S) not affecting the NLS and resulting in higher sgRNA synthesis than the other mutations. Interestingly, neither P718S alone, nor in combination with this novel adaptive mutation reverted the inhibition of STAT1 signaling, when nsP2 was individually expressed. Disruption of the NLS, however, abolished the inhibition of STAT1 nuclear translocation, indicating that a functional NLS within nsP2 is a pivotal determinant for inhibition of STAT1 nuclear translocation. Whether the lack of nuclear nsP2 re-allows STAT1 to translocate to the nucleus or that a mutation within the NLS disrupts an additional function of the nsP2 C-terminal domain will be subject of future investigation. The three-dimensional structure of the C-terminal domain of CHIKV nsP2 reveals that the residues KR649-650 and P718 are both located at the tips of externalized loop structures (loop 2 and 4 respectively), whereas the novel adaptive mutation at amino acid D711 is located within the alpha-helix at the base of loop 4 (Figure 7.3F). Interestingly, this region of the C-terminus of nsP2 has been shown to directly bind nsP3 in the viral replication complex of SINV (156). Modifications in the nsP2-nsP3 interaction could explain the differential replication efficiencies of the mutant CHIKV replicons. Taken together, these results show that the C-terminus of nsP2 is a truly multifunctional domain distinctly involved in the regulation of RNA replication, cytopathicity and the inhibition of IFN-induced JAK-STAT signaling.

Acknowledgements

We thank Joeri Kint and the facility services from the Zodiac (building 122, Wageningen University and Research Centre) for allowing experimental work at odd hours. The authors would also like to thank Mark Sterken and Casper van Schaik for help with the Maxwell instrument and Corinne Geertsema for technical assistance and cell culture. This work is supported by the European Community's Seventh Framework Programme (FP7 VECTORIE project number 261466).



8 Chapter

Chikungunya virus nsP2-mediated host shut-off disables the unfolded protein response

The unfolded protein response (UPR) is a cellular defense mechanism against high concentrations of misfolded protein in the endoplasmic reticulum (ER). In the presence of misfolded proteins, ER-transmembrane proteins PERK and IRE1 α become activated. PERK phosphorylates eIF2 α leading to a general inhibition of cellular translation, while the expression of transcription factor ATF4 is upregulated. Active IRE1 α splices out an intron from XBP1 mRNA, to produce a potent transcription factor. Activation of the UPR increases the production of several proteins involved in protein folding, degradation and apoptosis. Herein we demonstrate that transient expression of chikungunya virus (CHIKV) (*Togaviridae*, genus *Alphavirus*) envelope glycoproteins induced the UPR and that CHIKV infection resulted in the phosphorylation of eIF2 α and partial splicing of XBP1 mRNA. However, infection with CHIKV did not increase the expression of ATF4 and known UPR target genes (GRP78/BiP, GRP94 and CHOP). Moreover, nuclear XBP1 was not observed during CHIK infection. Even upon stimulation with tunicamycin, the UPR was efficiently inhibited in CHIKV infected cells. Individual expression of CHIKV non-structural proteins (nsP) revealed that nsP2 alone was sufficient to inhibit the UPR. Mutations that render nsP2 unable to cause host-cell shut-off prevented nsP2-mediated inhibition of the UPR. This indicates that initial UPR induction takes place in the ER, but that expression of functional UPR transcription factors and target genes is efficiently inhibited by CHIKV nsP2.

This chapter has been published as:

Jelke J. Fros, Lee D. Major, Florine E. M. Scholte, Joy Gardner, Martijn J. van Hemert, Andreas Suhrbier and Gorben P. Pijlman. *Chikungunya virus nsP2-mediated host shut-off disables the unfolded protein response. J Gen Virol.* **96**, 580–589 (2015).

Introduction

Many newly translated proteins, including those of viral origin, are translocated into the endoplasmic reticulum (ER) for post-translational modifications (e.g. glycosylation) and proper folding, before being secreted or transported to various cellular organelles. Several stimuli can disrupt the homeostasis in the ER, including viral infections that result in high expression of viral glycoproteins (95). An increase in the concentration of unfolded and misfolded proteins in the ER lumen results in ER stress. To cope with ER stress, eukaryotic cells have the ability to sense unfolded protein levels and regulate the transcriptional and translational machinery to reduce general protein synthesis and to increase the protein folding capacity of the ER. The mechanisms by which cells respond to ER stress are collectively called the unfolded protein response (UPR). The initial responses of the UPR aim to reduce ER stress and aid in cell survival. However, prolonged activation of the UPR results in the induction of apoptosis (230–232). The UPR is initiated when Ca^{2+} -dissociated heavy-chain binding protein (BiP), also known as glucose-regulated protein 78 (GRP78), dissociates from three distinct ER trans-membrane UPR sensors to bind misfolded proteins in the ER lumen (233, 234).

Dissociation of GRP78/BiP from double-stranded RNA-dependent protein kinase (PKR)-like ER kinase (PERK), allows PERK to phosphorylate the alpha subunit of the eukaryotic translation initiation factor-2 (eIF2 α). Phosphorylation renders eIF2 α unable to be recycled back into its active, GTP-bound state, reducing the general level of translation and thereby reducing the protein load in the ER lumen (235). Under conditions of eIF2 α phosphorylation, activating transcription factor 4 (ATF4) is selectively translated (236). ATF4 causes up-regulation of UPR target gene transcription, including redox and metabolism regulatory proteins and pro-apoptotic protein DNA damage-inducible protein C/EBP-homologous protein 10 (CHOP or GADD153) (237).

Dissociation of GRP78/BiP from inositol-requiring α (IRE1 α) results in the oligomerization and *trans*-autophosphorylation of the kinase domain of IRE1 α , which activates its cytoplasmic RNase activity. This results in the removal of a 26 base pair long intron from X-box-binding protein 1 (XBP1) mRNA, allowing translation of the full-length transcription factor (238). In the nucleus XBP1 promotes the transcription of genes that increase (i) protein folding capacity, (ii) chaperone protein entry to the ER, and (iii) ER-associated degradation (239–241).

The third unfolded protein sensor is activating transcription factor 6 (ATF-6). After the ER-luminal domain of ATF-6 has sensed the unfolded protein load and disassociates from GRP78/BiP, ATF-6 is cleaved and acts as a potent transcription factor for the expression of many ER-chaperones as well as XBP1 (242, 243). The three arms of the UPR form a highly cross-linked network, as specific interactions between ATF-6 and XBP1 have been reported and the transcription of CHOP and GRP78/BiP can be induced via all three arms of the

UPR (241, 244, 245).

To facilitate their replication, viruses manipulate many processes within their host cells. Enveloped viruses often rely on the ER for the maturation of their glycoproteins and transport of the glycoproteins to the plasma membrane. Many viruses inhibit, modulate or exploit arms of the UPR. For instance, human cytomegalovirus and Semliki Forest virus (SFV) induce XBP1 mRNA splicing (246, 247), whereas hepatitis C virus and herpes simplex virus induce ATF-6 cleavage (248, 249). West Nile virus infection initiates both XBP1 mRNA splicing and ATF-6 cleavage (250). The induction of the IRE1 α and/or ATF-6 arms of the UPR may help to maintain ER homeostasis by increasing protein folding capacity, thereby facilitating viral glycoprotein maturation and host cell survival. In contrast, most viruses block activation of the PERK pathway and the downstream phosphorylation of eIF2 α , thereby avoiding translational inhibition and the subsequent induction of apoptosis via CHOP (249–251).

Herein we explored the impact of CHIKV on the UPR. CHIKV is a re-emerging mosquito transmitted alphavirus that causes sporadic epidemics of primarily rheumatic disease, with the largest epidemic ever recorded starting in 2004 in Africa and spread across Asia (3) and recently reached Oceania (252) affecting millions of people. The recent explosive outbreak in the Caribbean (35) was the first on the Western Hemisphere and has even reached the United States (253). The structural proteins of CHIKV are expressed as a polyprotein that results from translation of the viral subgenomic RNA. After autocatalytic cleavage of the capsid protein, the remaining polyprotein translocates to the ER. In the ER the polyprotein is cleaved by host signalases into precursor E2 and E1, which are N-linked-glycosylated before being transported to the Golgi network (163, 254). We investigated whether CHIKV envelope glycoproteins induced the UPR and whether CHIKV replication affects UPR target gene expression and the expression of ATF4. Furthermore, we analyzed the activation and localization of XBP1 and conclude that host cell shut-off, mediated by viral non-structural protein (nsP2) was responsible for modulating the UPR.

Materials and methods

Ethics statement

All animals were handled in strict accordance with good animal practice as defined by the National Health and Medical Research Council of Australia. All animal work was approved by the QIMR Berghofer Medical Research Institute animal ethics committee.

Cells and virus isolates

Vero cells (ATCC number CRL-1586) and murine embryonic fibroblasts from C57 BL/6 mice (MEFs) were cultured in RPMI 1640 medium (GIBCO-invitrogen) supplemented with 5% fetal calf serum (FCS) at 37 °C, 5% CO₂. Murine splenic macrophages were obtained by homogenizing a spleen in RPMI 1640 with 10% FCS. Tissue was pelleted and resuspended in 3 ml of ACK lysis solution (150 mM NH₄Cl, 1 mM Na₂-EDTA [pH 7.3]) for 3 minutes to remove any erythrocytes. Cells were washed and pelleted twice with RPMI 1640, 10% FCS, before being plated and left to attach overnight. Medium was replaced by RPMI 1640, 10% FCS containing 30% of Langerhans cell conditioned medium (LCCM). Cells were left to incubate over 3 days before being washed again with RPMI 1640, 10% FCS, 30% LCCM. The chikungunya virus isolate (LR2006-OPY₁) is a primary isolate from the recent outbreak in Reunion Island (268) and CHIKV LS₃ (Scholte *et al.*, 2013) is an infectious clone-derived virus.

Reagents

The UPR reporter constructs consisted of a pGL-3 basic backbone with the promoter region of either GRP78/BiP (pGL-3 basic GRP78P(-132)-luc), GRP94 (pGL-3 basic GRP94P(-363)-luc controls, respectively. CHIKV (S27) envelope cassette was expressed from a pcDNA/Dest40 backbone (pcDNA-envelope) and the plasmids expressing individual nsPs were described previously (147, 148). GeneJammer (Agilent Technologies) and Lipofectamine2000 (Invitrogen) were used as transfection reagents and tunicamycin (tm) (Sigma-Aldrich) was used to activate the UPR in a concentration of 5 µg/ml.

XBP1 mRNA splicing

Activation occurs via the removal of a 26 base pair intron from XBP1 mRNA, which contains a PstI restriction site. Total RNA extraction from cell cultures was performed using Trizol reagent (Invitrogen). Female C57BL/6 mice were inoculated with CHIKV LR2006-OPY₁ (10⁴ CCID₅₀) subcutaneously into the ventral side of each hind foot as described previously (68). For the extraction of total RNA from mouse feet, each foot was placed in a snaplock Eppendorf tube with 1.5 ml Trizol reagent and two, 3 mm tungsten carbide beads (QIAGEN). Tissue was homogenised at 25 HZ in a tissue lyser (QIAGEN). Samples were spun down for 10 min at 12,000 rpm at 4 °C. The supernatant

(1 ml) was used for further Trizol RNA extraction. To remove genomic DNA, all RNA samples were DNase treated (TURBO DNA-free Applied Biosystems). The RNA from murine splenic macrophages and mouse feet was reverse transcribed using random primers. Murine RPL13A, spliced and unspliced XBP1 and CHIKV RNA were quantitated by real-time PCR, using platinum SYBR Green (Invitrogen), using a Rotor Gene RG-3000 (Corbett Research). Primers used in this assay were mXBP1 Fwd, mXBP1 U Rev and mXBP1 S Rev with the respective sequences: 5'-AAACAGAGTAGCAGCGCAGACTGC-3', 5'-GCTGCAGAGGTGCACATAGTCTGA-3' and 5'-GCCTGCACCTGCTGCGGACTC-3'. Murine RPL13A was used as an internal control, mRPL13A Fwd. 5'-GAGGTCGGGTGGAAGTACCA-3' and mRPL13A Rev. 5'-TGCATCTTGGCCTTTTCCTT-3'. CHIKV RNA was detected using Fwd. 5'-AGCTCCGCGTCCTTTACC-3' and Rev. 5'-CAAATTGTCCTGGTCTTCCTG-3' primers. mRNA from Vero cells was reverse transcribed (Superscript III, Invitrogen) using random hexamers (Roche) and XBP1 was PCR amplified using XBP1 F 5'-CCGGAGCTGGGTATCTCAAAT-3' and XBP1 R 5'-CCGTATCCACAGTCACTGTAGCA-3' primers. Amplicons were digested with PstI and loaded on an agarose gel (250).

Dual luciferase assay

One day after transfection with the respective UPR reporter plasmids, Vero cells were infected and/or tm-treated as indicated. At the end point of each experiment cells were lysed in passive lysis buffer (Promega) and cellular debris were pelleted by centrifugation (6 min, 5000 rpm). Fluc and Rluc luminescence was measured using the dual-luciferase reporter assay system (Promega). Supernatants (25 to 50 µl) were transferred into a white Greiner F-bottom 96-wells plate and scanned for luciferase luminescence in a POLARstar OPTIMA (BMG Labtech) plate reader. Significant differences ($P < 0.05$) between two samples were tested using a student's T-test and significant differences between multiple samples with a Tukey honestly significant difference [HSD] test.

Immunostaining

Protein expression of CHIKV E2 and eIF2 α were analysed by sodium dodecyl sulphate polyacrylamide gel electrophoresis (SDS-PAGE). Mock infected and infected cells were washed once with PBS and lysed in RIPA buffer (PBS, 1% NP-40, 0.5% sodium deoxycholate, 0.1% SDS supplemented with Complete Protease Inhibitor Cocktail (Roche), 1 mM NaF and 1 mM Na₃VO₄) and clarified by centrifugation for 10 min at 13,000 rpm. After electrophoresis, denatured proteins were transferred to an Immobilon membrane (Millipore) for analysis by Western blot (WB). Membranes were blocked in 3% skimmed milk in PBS-0.05% Tween-60 (PBST) for 1h at RT. Membranes were washed 3x5 min with PBST and subsequently incubated for 1h at RT with rabbit polyclonal

anti-E2 (1:20,000)(163), anti-P-eIF2 α (ab32157, 1:500) and anti-beta-Tubulin (ab6046, 1:4000) in PBST, respectively. Membranes were washed and treated with alkaline phosphatase (AP) conjugated, goat anti-rabbit IgG monoclonal antibodies (Sigma), 1:3000 times diluted in PBST, for 45 min at RT. Membranes were washed 2 \times 5 min with PBST and 1 \times 10 min with AP-buffer (100 mM NaCl, 5 mM MgCl₂, 100 mM Tris-HCl, 0.1% Tween 20, pH 9.5). Proteins were detected by NBT/BCIP staining (Roche).

To determine the expression of CHIKV-E2, Vero cells were transfected with pcDNA-envelope. After 24 hours, the cells were washed with PBS and fixed with 4% paraformaldehyde in PBS for 10 minutes at room temperature (RT). Cells were washed twice with PBS and permeabilized with 0.1% SDS in PBS for 10 minutes at RT. Samples were washed and incubated with PBS containing 5% FBS and 1:5000 diluted rabbit α -E2 polyclonal antibodies, for 1h at RT. Cells were washed 3 \times with PBS and treated with 1:2000 diluted goat-anti-rabbit Alexa fluor 488 (Invitrogen) for 1h at RT. Finally, cells were washed and treated with 10 μ g/ml Hoechst stain for 5 min at RT. Cells were analyzed using a Zeiss Axio Observer Zim inverted microscope in combination with an X-Cite 120 series lamp.

The subcellular localization of XBP1 was determined with indirect immunofluorescence microscopy as described previously (255). Double-stranded RNA was detected using mouse monoclonal antibody J2 (English & Scientific Consulting, #10010500). Rabbit polyclonal antibody was used to detect XBP-1 (Santa Cruz, #sc-17160). Primary antibodies were detected with Cy3- or Alexa488-conjugated secondary antibodies (Jackson/Life technologies). Nuclei were visualized with Hoechst 33342. The coverslips were analyzed using a Leica TCS SP5 confocal microscope and LAS AF Lite software (Leica).

Results

Effect of Chikungunya virus infection on UPR activation

CHIKV replication in cell culture is relatively fast and cytopathic, with the production of progeny virus and clear expression of structural proteins from 6 hours post infection (255). To determine whether CHIKV infection leads to the activation of the UPR, the induction of three well-known ER-stress related proteins, CHOP, GRP78/BiP and GRP94 (256), was investigated. Vero cells were co-transfected with a plasmid containing the promoter region and 5'untranslated region (UTR) of one of these target genes upstream of a firefly luciferase (Fluc) gene and a plasmid constitutively expressing renilla luciferase (Rluc). Given that CHIKV infection induces host shut-off and reduces RNA polymerase II driven transcription (149, 218), we studied the induction of UPR reporter genes using a luciferase-based assay in which all Fluc values were normalized for constitutive Rluc expression. One day after transfection, cells were infected with CHIKV at a multiplicity of infection (MOI) of 15. Sixteen hours post infection (hpi) the induction of three UPR target genes was measured (Figure 8.1A). As a positive control, uninfected cells were treated with tunicamycin (tm) for 6 hours. Tm is a microbial toxin, commonly used to induce the UPR by blocking N-linked glycosylation. Treatment with tm resulted in a 2, 6 and 2.5-fold upregulation of CHOP, GRP78/BiP and GRP94 reporters, respectively. In contrast, CHIKV infection did not upregulate the activity of any of these UPR reporters (Figure 8.1A). Because prolonged CHIKV infection induces host shut-off, we studied the UPR at an earlier time point as well. However, also at six hours post CHIKV infection additional expression of the UPR reporter genes was not induced (Figure 8.1B).

Both PKR and PERK have been reported to be activated early during alphavirus infection (228, 257–260). To confirm the activation of the PERK-eIF2 α -ATF4 branch of the UPR we analyzed the phosphorylation status of eIF2 α (Figure 8.1C). A time course experiment indicated that CHIKV infection in Vero cells resulted in a marked increase in p-eIF2 α within eight hours post infection. The phosphorylation of eIF2 α was concurrent with the expression of CHIKV envelope proteins, as indicated by the presence of E2 and precursor E3E2 (Figure 8.1C). Phosphorylation of eIF2 α limits general translation and selectively upregulates the translation of transcription factor ATF4 (236). A plasmid containing the promoter and 5'UTR of ATF4 upstream of a Fluc gene was transfected into Vero cells concurrently with a plasmid that constitutively expresses Rluc. Treatment with tm resulted in a respective 4- and 5-fold upregulation of the ATF4 reporter, whereas CHIKV infection for 6 or 16 hours did not induce ATF4 reporter activity (Figure 8.1D), indicating that the expression of viral glycoproteins and the phosphorylation of eIF2 α by CHIKV infection does not effectively stimulate the PERK arm of the UPR.

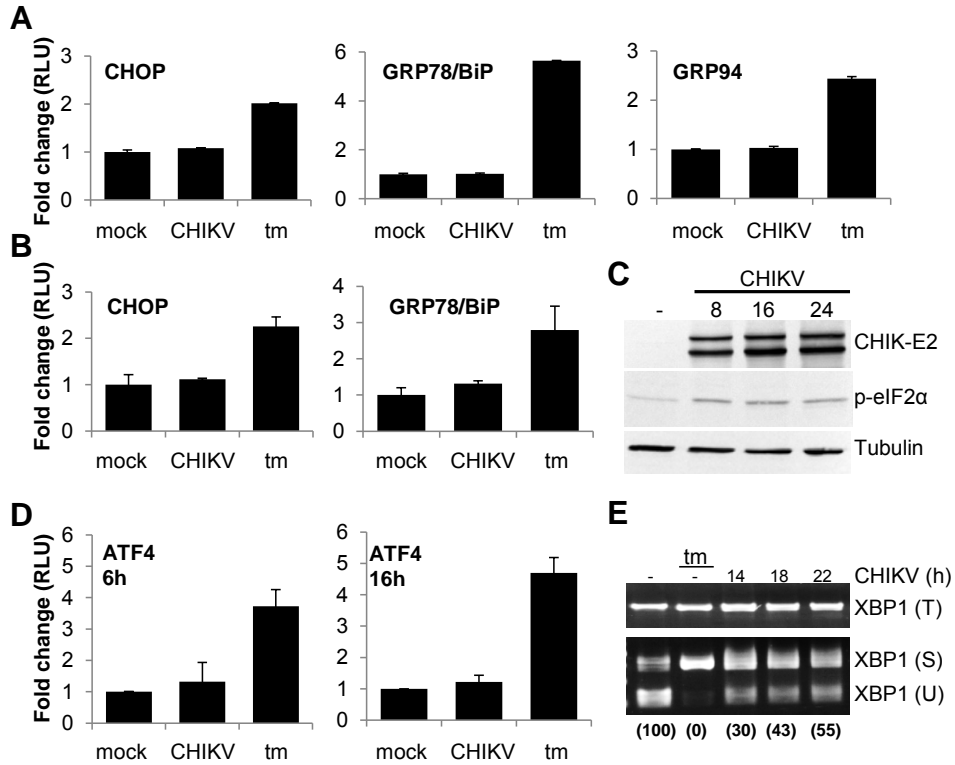


Figure 8.1. CHIKV infection does not activate the UPR. **ABD.** Vero cells were co-transfected with plasmids constitutively expressing Rluc and either CHOP-, GRP78/BiP- or GRP94-Fluc reporter plasmids. Cells were not infected (mock) or infected with CHIKV (MOI 15). The UPR was induced with tunicamycin (tm)(5 µg/ml) for 6 hours. Cells were assayed for dual-luciferase expression sixteen (A and D) or six (B and D) hours hpi. Values are depicted as fold change of Fluc normalized for Rluc relative to the untreated mock. Error bars represent standard deviation. **C.** Vero cells infected with CHIKV (MOI 10) for 8, 16 and 24 hours were harvested and immunostained for CHIKV E2, p-eIF2α and β-tubulin. **E.** Vero cells were not infected (mock) or infected with CHIKV (MOI 10). Total RNA was harvested and XBP1 mRNA was reverse transcribed and PCR amplified. Samples were split into two, from which one subset was digested with PstI. Both digested and undigested amplicons were loaded on a 1.5% agarose gel. Numbers within the brackets are the volume intensity of the XBP1(U), normalized to XBP1(T) and relative to mock.

The IRE1a-XBP1 arm of the UPR has been shown to be activated during infection with other viruses (246, 247, 250). To investigate whether CHIKV infection induces XBP1 mRNA splicing, Vero cells were either mock infected, infected with CHIKV, or treated with tm in a time course experiment. In uninfected cells most of the XBP1 mRNA remained in its unspliced form (U) (Figure 8.1E, left lane). When treated with tm, nearly all XBP1 mRNA was spliced (S) (Figure 8.1E, second lane). During CHIKV infection, part of the XBP1 mRNA was spliced and some remained unspliced between 14 and 22 hours post

infection (Figure 8.1E, lanes 3-5). When the amount of XBP1(U) mRNA was quantified and normalized for total XBP1(T), the relative amount of XBP1(U) during CHIKV infection was 30 to 55% of the mock untreated and tm treated controls (Figure 8.1E). These data suggest that CHIKV infection results in partial XBP1 activation; however, a substantial amount of XBP1 remains in its inactive unspliced form.

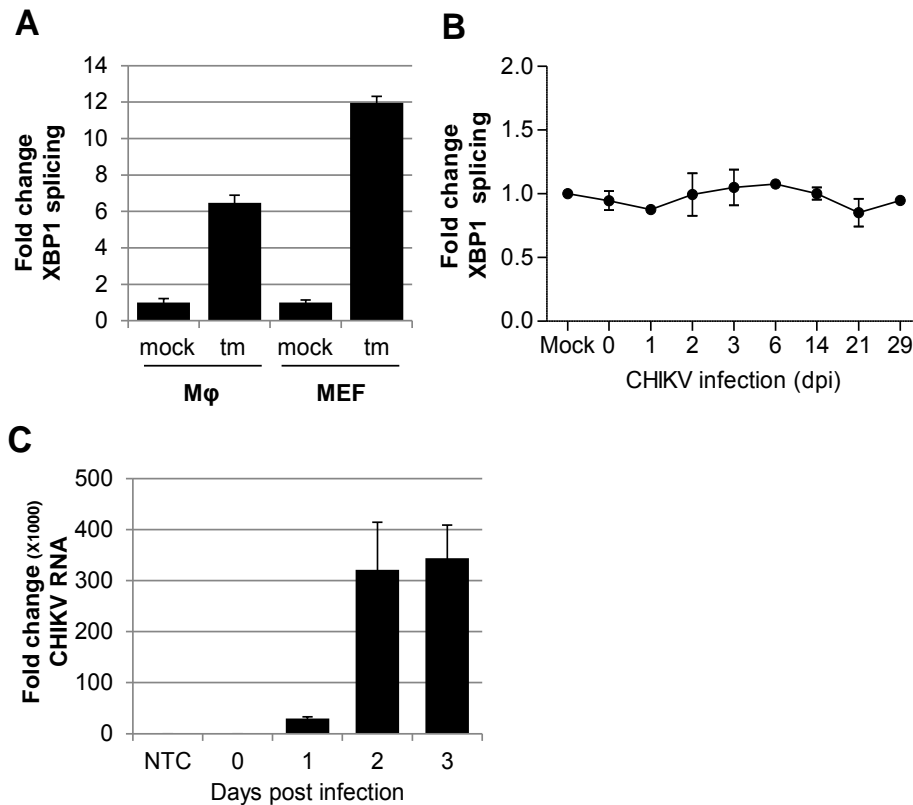


Figure 8.2. XBP1 mRNA splicing in murine cells and in a mouse model. **A.** Isolated murine splenic macrophages and MEFs were mock treated or tm treated. **B.** Mouse feet were infected with CHIKV and harvested at the indicated days post infection. Values are depicted as fold induction of spliced divided by unspliced XBP1 mRNA, normalized to RPL13A and relative to the mock. Error bars represent one standard deviation. **C.** CHIKV RNA copies harvested from infected mouse feet at the indicated days post inoculation.

CHIKV infection does not induce XBP1 splicing in mice

Next, we analyzed XBP1 mRNA splicing *in vivo* in an adult wild-type mouse model of CHIKV arthritis. To increase the sensitivity of the XBP1 splicing assay, we designed a semi-quantitative reverse transcriptase PCR assay to measure the relative levels of spliced and unspliced XBP1 mRNA. To validate the XBP1

mRNA splicing assay in murine cells, XBP1 mRNA splicing was measured in murine splenic macrophages and mouse embryonic fibroblasts (MEF). Treatment with tm resulted in a respective 6- and 12-fold increase in mouse embryonic macrophages and MEFs (Figure 8.2A). In the *in vivo* experiment, C57BL/6 mice were either mock infected or infected with CHIKV as described previously (68). Tissue samples from mouse feet were collected at the indicated days post infection and XBP1 mRNA splicing was measured (Figure 8.2B). The infected mouse feet displayed all the signs of CHIKV specific inflammation, with maximum foot-swelling at day 6 post infection and ample CHIKV RNA replication in the first three days post infection (68, 139, 261, 262)(Figure 8.2C and data not shown). However, XBP1 mRNA splicing could not be detected in these tissues (Figure 8.2B). Taken together, these results indicate that although CHIKV infection did induce XBP1 mRNA splicing in Vero cells *in vitro*, XBP1 splicing remained undetectable in mouse feet during an *in vivo* infection.

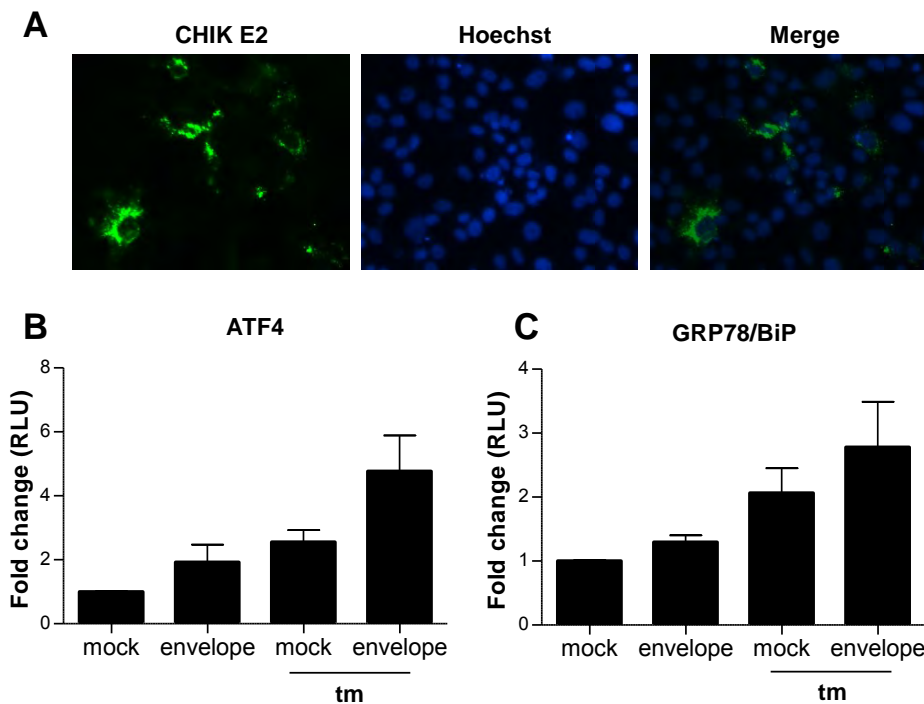


Figure 8.3. Overexpression of CHIKV envelope glycoproteins induces the UPR. Vero cells were transfected with plasmids expressing either EGFP (mock) or CHIKV envelope proteins (E) together with constitutively expressing RLuc and either ATF4-Fluc or GRP78-Fluc reporter plasmids. 24 hours post transfection cells were either fixed, permeabilized and immunostained for CHIKV E2 (A) or lysed in passive lysis buffer and assayed for dual luciferase activity (B and C). Values are depicted as average of three individual experiments. Error bars represent one Standard error of the mean.

Chikungunya virus glycoproteins stimulate the UPR

Since we observed signs of induction during the early steps of the UPR, but no upregulation of the UPR target proteins in response to CHIKV infection, we determined whether overexpression of the CHIKV envelope proteins outside the context of viral replication activates the UPR. Vero cells were transfected with a plasmid expressing either GFP or the CHIKV envelope glycoproteins (E3E26KE1) under the control of a CMV promoter. The expression of CHIKV envelope glycoproteins was confirmed by immunofluorescence microscopy (Figure 8.3A). To measure the effects of the CHIKV envelope glycoproteins on UPR target gene expression and the PERK arm of the UPR, GRP78/BiP and ATF4 Fluc reporter plasmids were co-transfected with constitutive Rluc and either a GFP-expressing plasmid or the plasmid expressing the CHIKV envelope glycoproteins. After 24 hours, the overexpression of CHIKV envelope proteins resulted in a moderate but consistent upregulation of both ATF4 and GRP78/BiP expression (Figure 8.3B and C). Treatment with tm 24 hours post transfection resulted in an enhancement of ATF4 and GRP78/BiP expression compared to tm treatment or CHIKV envelope expression alone (Figure 8.3B and C). These data suggest that CHIKV envelope protein expression results in UPR activation.

Chikungunya virus replication prevents effective activation of the UPR

Since the expression of viral envelope glycoproteins, in the absence of viral RNA replication and non-structural proteins (nsP1-4), induced the UPR, we investigated whether the lack of UPR activation during CHIKV infection was the result of active inhibition by the virus. Vero cells were either mock infected or infected with CHIKV, and 4, 8 or 12 hours later they were treated with tm (10 hours)(Figure 8.4A). The UPR target reporters CHOP, GRP94 and GRP78/BiP were induced by tm in the mock infected cells. However, this induction was reduced in infected cells that were treated with tm at 4 hpi and was completely absent in infected cells that were treated with tm at 8 or 12 hpi (Figure 8.4B). In a similar experiment, tm-mediated induction of ATF4 was also completely inhibited when cells were infected with CHIKV 12 hours prior to tm treatment (Figure 8.4C).

In a time course experiment (Figure 8.4A), UPR induction using tm resulted in the splicing of almost the entire XBP1 mRNA pool (Figure 8.4D, lane 2). Treatment with tm 4 hpi with CHIKV also resulted in the splicing of all XBP1 mRNA (Figure 8.4D, lane 3). However, tm treatment at 8 or 12 hours post CHIKV infection no longer induced complete XBP1 mRNA splicing (Figure 8.4D, lanes 4 and 5). Interestingly, CHIKV infection with (Figure 8.4D) and without (Figure 8.1D) tm treatment resulted in a gradual increase in the total amount of unspliced XBP1 mRNA during these experiments. Next, we determined the subcellular localization of XBP1 protein to investigate whether the spliced XBP1 mRNA was translated in the functional XBP1 transcription factor in CHIKV infected cells. When uninfected Vero cells were treated with tm (6 hours) and

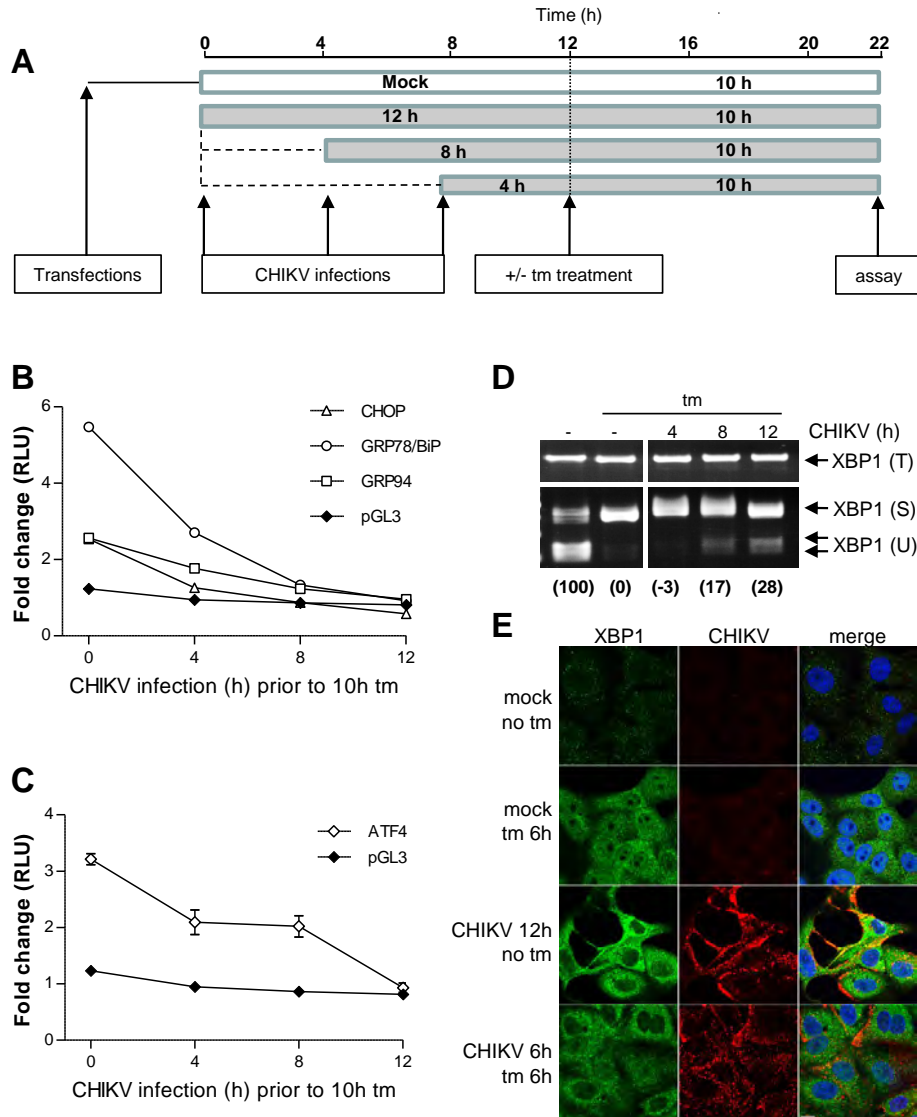


Figure 8.4. CHIKV replication constrains the UPR. **A.** schematic representation of the of the experiment. **BC.** Vero cells were co-transfected with plasmids constitutively expressing Rluc and UPR-Fluc reporter plasmids. Cells were not infected (mock) or infected for with CHIKV (MOI 10) for either 4, 8 or 12 hours prior to an additional 10 hours tm (5 µg/ml) stimulation (**A**). At the end of the time-course experiment cells were lysed and luciferase activity was measured. Values are depicted as fold change of Fluc normalized for Rluc relative to the untreated mock. Error bars represent one standard deviation. **D.** Vero cells were infected with CHIKV (MOI 10) and stimulated with tm in an identical time-course experiment (**A**). Total RNA was harvested and XBP1 mRNA was reverse transcribed and amplified, digested with PstI and loaded on a 1.5% agarose gel. Within brackets is the volume intensity of the XBP1(U) normalized for XBP1(T) and relative to mock. **E.** Vero cells were either mock infected or infected with CHIKV LS3 (MOI 5) and treated with tm as indicated. Cells were fixed and stained for XBP1 (green) and dsRNA (red) as a marker for CHIKV replication.

immunostained for XBP1, XBP1 localized to the nucleus as expected (Figure 8.4E). In contrast, during CHIKV infection XBP1 remained predominantly cytoplasmic even when the cells were treated with tm (Figure 8.4E). Taken together these results demonstrate that CHIKV infection inhibits the functional expression and/or subcellular localization of transcription factors ATF4 and XBP1 respectively, and effectively prevents the induction of UPR target genes.

Non-structural protein 2 inhibits the upregulation of UPR target genes

Overexpression of CHIKV glycoproteins activated the UPR, but CHIKV infection did not (Figures 8.1-8.4), suggesting that one or more of the CHIKV non-structural proteins are able to inhibit activation of the UPR. Plasmids expressing individual CHIKV nsPs (147, 148), were co-transfected with Fluc UPR reporter plasmids and a plasmid constitutively expressing Rluc. Sixteen hours post transfection the cells were treated with tm. CHIKV nsP2 clearly inhibited the tm-mediated induction of both ATF4 and GRP78/BiP reporters (Figure 8.5A and B). Since CHIKV nsP2 is a multifunctional protein, with clear roles in host shut-off (149, 217), nsP2 mutants that do not inhibit cellular protein synthesis were analyzed for their ability to inhibit tm-mediated UPR induction. Mutations in the nuclear localization site (KR649) or proline 718, both known to abolish host transcriptional shut-off activity (147), rendered nsP2 unable to inhibit tm-induced ATF4 and GRP78/BiP reporter activity (Figure 8.5C and D). These data suggest that CHIKV infection inhibits the UPR via nsP2-mediated host shut-off.

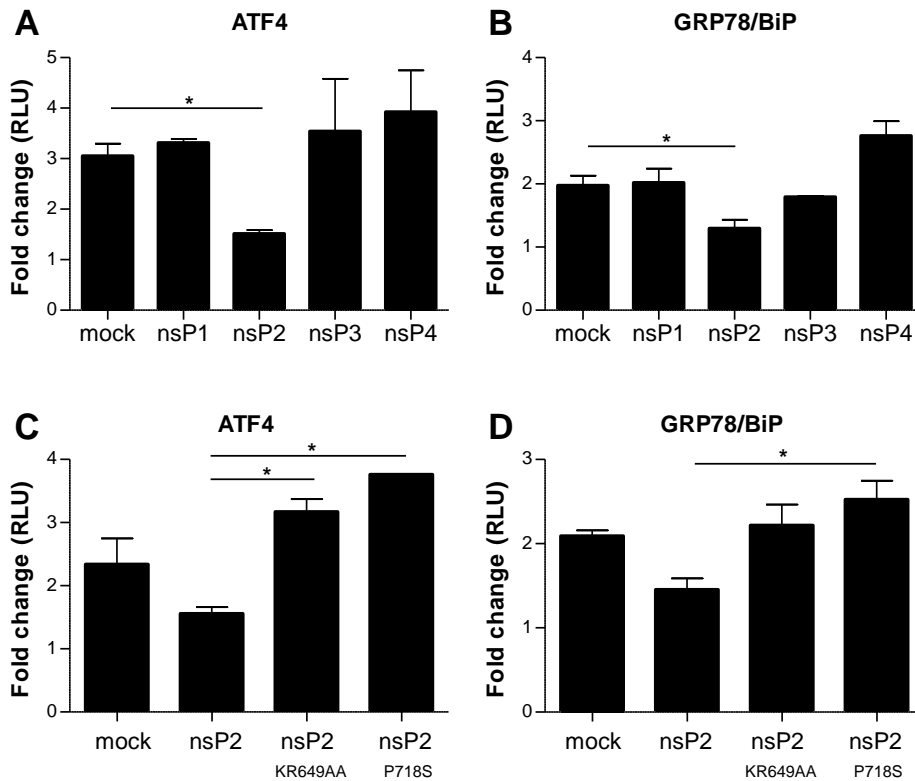


Figure 8.5. CHIKV nsP2-induced host shut-off inhibits the UPR. Vero cells were co-transfected with plasmids expressing individual CHIKV nsPs (A and B) and mutants thereof (C and D), UPR-Fluc reporter plasmids and a plasmid constitutively expressing Rluc. Eighteen hours post transfection cells were either induced with tm (6 hours, 5 μ g/ml) or mock treated, lysed and luciferase activity was measured. Values are depicted as average of 2-4 independent experiments, relative to the corresponding non-induced samples. Error bars represent one Standard error of the mean and an asterisk indicates significant differences ($P < 0.05$).

Discussion

Alphavirus infection has been reported to induce several key components of the UPR. PERK is activated early during SINV and CHIKV infections and XBP1 mRNA splicing is initiated during SFV infection (247, 259, 258). Herein we demonstrate that, although eIF2 α is phosphorylated and part of the XBP1 mRNA pool is spliced, XBP1 is not present in the nucleus and the upregulation of ATF4 and UPR target genes is completely inhibited in CHIKV-infected cells. Transient expression studies of nsPs demonstrated that nsP2 is responsible for preventing an effective UPR. In addition to PERK, eIF2 α can be phosphorylated by a number of other kinases, including PKR, which recognizes (viral) dsRNA (235). To allow the translation of viral proteins, most viruses prevent the phosphorylation of eIF2 α (249–251). Although inhibition of eIF2 α phosphorylation via CHIKV nsP4 has been reported (259), we and others have found that alphaviruses are exceptional in allowing the phosphorylation of eIF2 α during productive infection (228, 263, 264, 258). In our experiments, CHIKV infection resulted in the phosphorylation of eIF2 α within 8 hours post infection (Figure 8.1C). The translation of alphaviral structural proteins from their subgenomic messenger is unaffected by the phosphorylation of eIF2 α . A stable hairpin loop structure in the 26S promoter of the subgenomic mRNA from SINV was shown to stall the ribosome on the correct AUG providing resistance to eIF2 α phosphorylation (263). Surprisingly, the translational shut-off during alphavirus infection has been shown to be independent of eIF2 α phosphorylation, indicative of an additional mechanism by which alphaviruses modulate the translational machinery of the host (228, 264). In agreement with this hypothesis, the phosphorylation of eIF2 α during CHIKV infection did not result in an increased expression of the eIF2 α phosphorylation insensitive transcription factor ATF4 (Figure 8.1D) nor did it upregulate the induction of known UPR target genes GRP78/BiP, CHOP and GRP94 (Figure 8.1A and B). In fact, when the UPR was induced with tm in the context of a CHIKV infection, the expression of UPR target gene reporters and transcription factor ATF4 was clearly inhibited (Figure 8.4B,C and D).

SFV replication was shown to induce the UPR only when the envelope proteins were expressed during RNA replication (247), an observation consistent with our results that shows the ability of CHIKV envelope proteins to induce GRP78/BiP and ATF4. The addition of tm to cells expressing the CHIKV envelope proteins resulted in an enhanced induction of the UPR (Figure 8.3B and C). These results indicate that CHIKV envelope proteins expressed outside the context of viral infection do induce the UPR, with the presence of these glycoproteins markedly increasing tm-mediated activation of the UPR. However, no stimulation of the UPR target genes was observed during CHIKV replication, not even when cells were treated with tm (Figures 8.1 and 8.4). This clearly indicates that, despite the ability of the envelope proteins to activate the UPR, the induction of transcription factor ATF4 and UPR target genes is

effectively inhibited during CHIKV infection.

Previous studies showed that the IRE1 α -XBP1 arm of the UPR was activated during SFV infection (247). In agreement with this finding, our *in vitro* experiments did show a moderate level of XBP1 mRNA splicing during CHIKV infection (Figures 8.1E). A time course experiment (Figures 8.4D) revealed that four hours post infection, tm induction induced complete XBP1 mRNA splicing. Interestingly, XBP1 mRNA splicing upon tm induction at eight hours post CHIKV infection was partly inhibited. In addition, CHIKV infection of mice did not induce detectable levels of XBP1 mRNA splicing (Figures 8.2B). Thus, although CHIKV infection activates the IRE1 α -XBP1 arm of the UPR in certain cell types, progressive CHIKV infection does severely limit the extent to which XBP1 mRNA is spliced. Immunostaining of XBP1 protein at twelve hours post CHIKV infection showed that the nuclear accumulation of XBP1 is completely inhibited, even when cells are treated with tm (Figures 8.4E). These data illustrate that although some XBP1 mRNA splicing is induced by CHIKV infection in certain cell types, XBP1 proteins are absent from the nucleus of an infected cell.

Using a combination of independent PCR-based assays, dual-luciferase reporter systems, immunofluorescence and Western blot, we have shown that the IRE1 α /XBP1 and PERK arms of the UPR are effectively suppressed by CHIKV infection. Expression of individual CHIKV non-structural proteins revealed that nsP2 is responsible for the inhibition of ATF4 and UPR target gene induction (Figures 8.5A and B). NsP2 is a multifunctional protein with an active protease and helicase domain, and NTPase activity (29, 217, 265). In addition, it causes host cell transcriptional shut-off via the degradation of a catalytic subunit of RNA polymerase II (149), and also inhibits the JAK-STAT signaling pathway of the IFN response (147, 148). Here we show that point mutations in nsP2 that render the protein non-cytopathic by eliminating its function in host shut-off (KR649AA or P718S)(147, 149) reversed the nsP2-mediated inhibition of the UPR (Figures 8.5C and D). Alphaviruses carrying these mutations at homologous sites are effectively attenuated in cell culture (85, 225), perhaps in part due to a failure to constrain the UPR. It would be informative to investigate how CHIKV replication and the UPR influence one another in light of these attenuating mutations. We postulate that the host-cell shut-off, which is governed by CHIKV nsP2, is responsible for the inhibition of the UPR, by preventing the upregulated expression of ATF4, active XBP1 and additional UPR target genes.

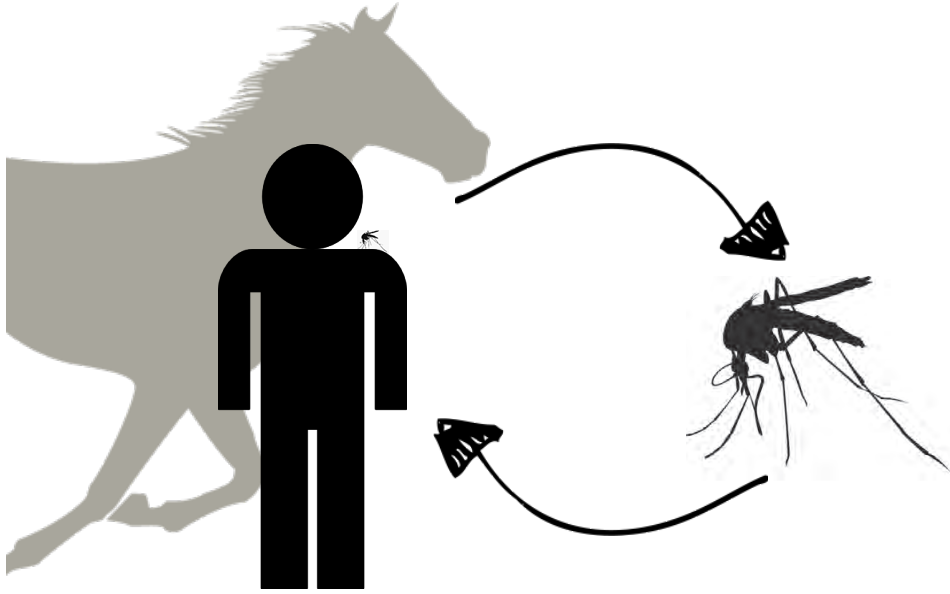
The diminished UPR activation during CHIKV infection suggests that anti-viral effects, elicited by the UPR, could hamper CHIKV propagation. This provides a rationale for why CHIKV induced host shut-off has evolved to also inhibit the UPR. In addition, immune responses directed against viral infections can be augmented by the UPR (reviewed by (266)). Replication of several RNA viruses, including SINV, was shown to be inhibited by a small

molecule deubiquitinase inhibitor that functions via the activation of the UPR (98, 267). This indicates that alphaviruses are sensitive to the effects of the UPR and that activating the UPR may have potential as an antiviral strategy.

Acknowledgements

We thank Corinne Geertsema for technical support. This work is supported by the European Union's Seventh Framework Programme (FP7 VECTORIE project number 261466).

9 Chapter



General Discussion

The outbreaks of arboviruses West Nile virus (WNV) and chikungunya virus (CHIKV) in recent years and their effect on the human population emphasize the need for new strategies to control the transmission of these viruses and to prevent or mitigate the disease they cause (Chapter 1)(3, 100). Classical broad spectrum antivirals (e.g. interferons (IFN)) proved unsuccessful and the need for novel, more specific, compounds has increased. In addition, transmission cycles with alternating vertebrate and invertebrate hosts and possible enzootic cycles complicates arbovirus control and risk assessments, but at the same time provides unique opportunities for innovative novel intervention strategies. This thesis addresses the questions how arboviruses secure effective transmission between invertebrate and vertebrate hosts and how these two biologically very different hosts cope with arbovirus infections.

Arbovirus transmission

The mosquito vector

Most arboviruses are transmitted by a small number of mosquito species. The proximity between susceptible vectors and amplifying hosts and the feeding behaviour of these vectors are important factors that often drive evolution towards a narrow virus-vector host range. CHIKV is transmitted in an urban cycle involving humans and two specific mosquito species *Aedes aegypti* and *Aedes albopictus*, or in a sylvatic cycle involving non-human primates and closely related forest-dwelling *Aedes* species (269). In contrast, WNV is rather unusual as more than 60 mosquito species have been reported as vectors, many of which belong to the *Culex* genus (9, 270, 271). In addition, WNV also replicates in a broad range of vertebrate species. Most amplifying hosts are bird species, but also several reptile and rodent species can develop high viral titers ($>10^6$ pfu/ml) (272–274), which is sufficient to infect *Culex* mosquitoes (275). Interestingly, when WNV infected mice were fed to birds of prey and alligators or when these animals were housed in close vicinity of one another WNV was readily transmitted (273, 276, 277). Although the exact biological relevance of these findings is unknown, it is possible that these alternative transmission routes contribute to sustained endemic WNV activity over time.

During the epidemic sweep of WNV that engulfed North America in the early 2000s, the virus was transmitted by several main *Culex* species: *Culex pipiens*, (38), *Culex quinquefasciatus* (39) and *Culex tarsalis* (278). Southern Europe currently suffers from annual WNV outbreaks and field studies have detected both WNV and the related flavivirus Usutu virus (USUV) in a large number of mosquito species, but most often in the northern house mosquito *Cx. pipiens* (41). Not only southern European mosquitoes can transmit WNV, as *Cx. pipiens* from WNV-free, north-western Europe (NWE) now appears to be a highly competent vector for lineage 1 and 2 WNV, and USUV (Chapter 2 and 3). The species *Cx. pipiens* is further classified into two biotypes (*Cx. pipiens pipiens* and *Cx. pipiens molestus*). For both biotypes, different feeding preferences on either avian or mammalian hosts have been reported (113). Hybrids between both biotypes are considered less ornithophilic and more likely to feed on other vertebrates, including humans, which may contribute to the incidence of human WNV disease. These hybrids are considered to be relatively common in North America, but not in north-western Europe (113). However, a more recent study detected substantial numbers of hybrids in Germany, suggesting that more continuous mosquito surveillance is necessary to determine the exact distribution of these dynamic mosquito populations (279). Other *Culex* species could also contribute to the distribution of WNV and USUV. In North and Central Europe, *Cx. torrentium* is a very common mosquito (42), but it is poorly characterized how effectively these different *Culex* species or *Cx. pipiens* biotypes can vector either WNV or USUV. In southern France, *Cx. modestus*

was found highly competent for a local lineage 1 WNV isolate (106). Thus, in order to establish more reliable risk projections for WNV transmission, the data presented in Chapters 2 and 3 can be augmented by a more detailed picture of the distribution of these *Culex* populations and their competence to circulating arboviruses.

WNV activity in Europe has thus far remained localized to the Mediterranean basin, which could be explained by a higher number of WNV refractory mosquitoes in more northern parts of Europe e.g. *Cx. torrentium* with currently unknown competence to WNV. However, the distribution of USUV does extend further into central and northern Europe (280). The localized activity of WNV is therefore somewhat surprising as *Cx. pipiens* mosquitoes from north-western Europe (NWE) are competent vectors for both lineage 1 and 2 WNV (Chapter 2) as well as for USUV (Chapter 3). In parts of southern Europe, WNV and USUV co-circulate but it is unknown whether these viruses can co-infect the same vector. Laboratory infections of *Cx. quinquefasciatus* with either WNV or St Louis encephalitis virus (SLEV), however, reduced the infectivity of a subsequent second flavivirus infection (281). In addition, insect-specific flaviviruses (e.g. *Culex* flavivirus), which are vertically transmitted among insects without transmission to vertebrates, are widely distributed and infections in mosquito populations can also reduce the vector competence of infected mosquitoes to other flaviviruses (282). Finally, flavivirus activity generally decreases when substantial numbers of amplifying hosts have previously been exposed to a related flavivirus. Thus, infections with related flaviviruses, e.g. SLEV in North America and USUV in Europe, may reduce secondary flavivirus infections in both invertebrate and vertebrate hosts (114). Exactly how co-circulating flaviviruses influence the seroconversion rates in the diverse and dynamic populations of (avian) amplifying hosts is still poorly characterized.

Intrinsic factors that determine vector competence

North American (NA) and NWE *Cx. pipiens* mosquitoes were competent vectors for an American isolate of lineage 1 WNV (NY'99)(Chapter 2). Interestingly, the transmission rate of lineage 2 WNV was significantly lower in NA compared to that in NWE mosquitoes (Chapter 2). That these two geographically separated *Cx. pipiens* populations have a significantly different vector competence for lineage 2 WNV, but not lineage 1 WNV, indicates a high degree of genotype-genotype specificity in the interaction between virus and vector. In North America, lineage 1 WNV has evolved within a few years from the introduced NY'99 isolate into genotypes that all have an adaptive mutation in the viral envelope (V159A). This WNo2 genotype allows more effective transmission by North American *Culex* species and has completely replaced the original NY'99 strain (40). The lower transmission rates of lineage 2 WNV by NA mosquitoes could be explained by purifying selection that takes

place in the mosquito midgut (283). However, sequencing of small RNAs from lineage 2 WNV infected NWE and NA *Cx. pipiens* mosquitoes both resulted in the expression of 21 nucleotide long RNA molecules, suggesting that both viruses are subjected to an antiviral RNAi response. Mapping of these virus-derived RNA molecules to the viral reference genomes resulted in identical distributions when allowing either 0 or 1 mismatch per RNA (data not shown). This suggests that there was no selection for single nucleotide changes in the consensus genome sequences. Thus, the obtained transmission rates are the direct result of infections with the respective WNV isolates in both NWE and NA mosquitoes. The generation of recombinant inbred lines between both mosquito populations may ultimately provide a molecular explanation for the observed differences in vector competence. However, the *Cx. pipiens* genome has not been completely sequenced (yet), and simultaneously maintaining numbers of different mosquito colonies is very time-consuming and elaborate as *Cx. pipiens* eggs cannot be stored for later use. Both these factors complicate this approach. More feasible is to locate the viral elements that are responsible for the differential vector competence using oral infection experiments with chimeric viruses. Once identified, this also allows a more specific search for the host factors that determine vector competence.

Extrinsic factors that directly influence vector competence

The presence of highly WNV competent vector species and susceptible amplifying hosts in WNV-free areas suggests that other, extrinsic factors may play a role in limiting WNV activity. Incubation at higher temperatures significantly increased the infectivity of both WNV and USUV in *Cx. pipiens* (Chapter 2 and 3). While this provides a rationale for the current WNV activity in southern Europe, it fails to explain the more northern distribution of USUV. Infection and transmission rates of lineage 1 WNV in North American *Culex* species were also shown to be influenced by the incubation temperature and in North America, WNV has already adapted to certain climatic conditions (105, 284).

An interesting observation is that the transmission and infection rates of USUV were substantially higher in NWE *Cx. pipiens* mosquitoes compared to those of WNV when incubated at 28°C, but not at temperatures <23°C (Chapter 3). The average summer temperatures in northern and central Europe, however, are generally well below 23°C (108). Both viruses infect the same amplifying hosts; therefore similar vector competence in their main vector would infer that also WNV has the potential to extend its distribution into Central and the North of Europe. However, the influence of daily temperature fluctuations on vector competence should not be neglected. For example, the vector competence of *Ae. aegypti* for dengue virus (DENV) increases or decreases, depending on whether incubation temperatures fluctuate around low or high mean temperatures, respectively (134). Temperatures in North and Central Europe

can reach daily highs that are well above 23°C, and as USUV is more infectious than WNV at these temperatures, this could provide an explanation for the current, more northern, distribution of USUV. To test this hypothesis, USUV and WNV infected mosquitoes can be incubated at fluctuating temperatures that represent the normal diurnal temperature range around a specific mean and can be compared to mosquitoes that are kept at an identical, but constant, mean temperature.

These complex interactions between the virus, vector and environment observed for WNV also introduce large diversity into the vector competence of *Ae. albopictus* for CHIKV. *Aedes albopictus* populations, collected from six separate global sites, have highly diverse transmission rates for two isolates of CHIKV. In some of these mosquito populations, the two CHIKV isolates displayed large differences in transmission rates within one mosquito population and showed a high variation in response to two distinct incubation temperatures (162). The intricate relationships between temperature, virus and vector genotypes that determine vector competence imply that arbovirus outbreaks will remain largely unpredictable.

Vectorial capacity

The multiple ecological traits that should be taken into account when assessing the risk levels of an arbovirus outbreak add one more layer of complexity. The vectorial capacity (VC) includes traits of the vector population, providing a better measure of the capacity of a mosquito population to transmit a pathogen and follows from

$$VC = m \cdot a^2 \cdot b \cdot p^n / -\log_e(P)$$

where **VC** is the vectorial capacity, **m** is the number of female mosquitoes per host, **a** the daily blood feeding rate, **b** the vector competence or transmission rate, **p** the daily mosquito survival rate (from 0-1.0), and **n** the extrinsic incubation period. The lineage 2 WNV transmission rate in European *Culex pipiens* mosquitoes is three times higher as compared to that in North American mosquitoes (Chapter 2). This indicates that under similar environmental circumstances the vectorial capacity is also three times larger. Additionally, the extrinsic incubation period is shorter for lineage 2 WNV, which enhances the VC even further. However, mosquito numbers, blood feeding behavior and the mosquito survival rate can also influence the vectorial capacity significantly. In addition, temperature and rainfall may severely influence mosquito numbers. For example, the resurgence of WNV disease in 2012 in the United States was partly attributed to a wet spring and hot summer, which provided suitable microclimates that led to high numbers of mosquito vectors, coinciding with dense local bird populations (20). Finally, virus-induced behavioral changes, such as the increased locomotive activity and probing behavior of DENV

infected *Ae. aegypti* (285, 286), adds to the already complex interplay between virus, vector, and environmental factors.

Taken together, the presence of WNV and USUV competent mosquitoes in currently WNV-free areas in Europe clearly indicates a risk for WNV transmission in these areas. Climatic conditions that favor mosquito numbers or increase their vector competence are likely the main factors that determine the distribution of these arboviruses. It is clear that vector competence is a highly complex trait and a better understanding of the possible vector species, co-circulating arboviruses, seroconversion rates of amplifying hosts, and environmental risk factors will increase the effectiveness and accuracy of arbovirus surveillance and risk assessments.

Molecular determinants of arbovirus infections

Antiviral RNAi and viral counter defense

Arboviruses establish a permanent infection in the vector and although effects on fecundity have been reported (287) the infection does not obstruct the invertebrate's ability to find and feed on subsequent vertebrate hosts. After the vector has fed on a viraemic vertebrate host, the ingested arbovirus must first infect the midgut epithelial cells. Both WNV and USUV have a high infection rate in *Cx. pipiens*, suggesting limited involvement of a midgut infection barrier (MIB) (Chapter 2 and 3). Once inside the midgut epithelial cells the Toll, immune deficiency (IMD), Janus kinase signal transducer and activator of transcription (JAK-STAT) and RNA-mediated gene silencing pathways can influence arbovirus infections in the midgut (44). Both WNV and USUV infections in *Cx. pipiens* mosquitoes elicit an RNAi response as small (21 nt) viral RNA products are expressed as a result of dicer2/AGO2 dependent cleavage of double stranded RNA replication intermediates (Chapter 3). Larger RNA products (24-30 nt) were detected in CHIKV and DENV infected *Aedes* mosquitoes and suggest antiviral activity of the PIWI-interacting RNA pathway (56, 57). Although reported as an antiviral response in several insect species, the apparent lack of PIWI-interacting RNA pathway specific products suggests that this pathway is not involved in the systemic defense against flaviviruses in *Culex* mosquitoes (Chapter 3).

Although inhibitors of RNAi from an arboviral origin have not been extensively described, introducing strong heterologous viral suppressors of RNAi (VSR) in Sindbis virus (SINV) has resulted in reduced siRNA expression, increased viral replication and reduced mosquito survival (63). This suggests that arboviruses are subjected to the RNAi response only to some extent to ensure an optimal balance between viral replication and antiviral responses that ultimately results in effective arbovirus transmission. Flaviviruses possess a potent RNAi suppressor during *in vitro* replication, which maps to the 3' untranslated region (UTR) (288). The 3'UTR of flaviviruses is highly structured and is able to stall the 5' exoribonuclease (pacman/XRN1) that normally degrades RNA molecules (289, 290). This results in the accumulation of large quantities of short (~500 nt) non-coding subgenomic flavivirus RNA (sfRNA) (289). Besides inhibiting the RNAi response, sfRNA also modulates the mammalian interferon (IFN) response and is essential for the cytopathicity and pathogenicity of WNV (289, 291). The fact that insect-specific flaviviruses also produce sfRNA in high quantities suggests a specific, conserved interaction with the arthropod host. Specific mutations in the pseudoknots of the 3'UTR can abrogate the production of sfRNA (292) by altering the structure that would normally stall the exoribonuclease (293). Introducing mutations in a full-length infectious WNV clone will result in a virus that is unable to produce sfRNA and its infectivity can then be compared to wild type WNV *in vivo*. When sfRNA

also has *in vivo* VSR activity these modified viruses are likely to have reduced infection and/or transmission rates in live mosquitoes. Reducing the activity of the RNAi pathway by silencing crucial components (e.g. AGO2) can potentially restore viral replication and dissemination. Experiments such as these can provide valuable insights into the role of siRNA as an RNAi suppressor *in vivo*.

A recent study showed that knock down of RNAi (e.g. AGO2) increases CHIKV replication in *Ae. aegypti* (53). Although RNAi is likely the most potent antiviral defense strategy invertebrates possess, O'nyong nyong virus (ONNV) infections in *Anopheles gambiae* showed that the exogenous RNAi pathway did not play any role during the initial midgut infection, but only limited systemic viral infections. In contrast, the JAK-STAT and IMD signaling pathways did affect viral infection of the midgut. Moreover, ONNV partly inhibited the IMD and JAK-STAT pathway. Naturally high infection rates also required a natural gut microbiome (294). This suggests that ONNV infection in the mosquito vectors encounters different antiviral responses during the course of infection, which should be taken into account when studying the mosquito antiviral responses against other arboviruses.

Chikungunya virus nsP3 and Rasputin/G3BP

The interactions between viral and host products involved in vector specificity are not well understood, but are beginning to become elucidated. ONNV is effectively transmitted by *Anopheles* mosquitoes. Interestingly, when CHIKV non-structural protein 3 (nsP3) was replaced with nsP3 of ONNV inserted in a chimeric CHIKV infectious clone, it enabled CHIKV to infect *An. gambiae* (99). This suggests that alphavirus nsP3 has a specific function that determines the outcome of infection in the mosquito vector. Alphavirus nsP3 interacts with the homologous proteins Rasputin (Rin) and Ras-GTPase-activating SH3-domain binding protein (G3BP1/2) in mosquito and mammalian cells, respectively (93). In both invertebrate and vertebrate cells nsP3 forms cytoplasmic granules with Rin/G3BP (Chapters 4 and 5). In mammalian cells, these nsP3-G3BP-granules inhibit the cell's response to environmental stress, as G3BP is a crucial component of stress granules (SG) (Figure 9.2)(Chapter 5). SGs contain mRNPs and stalled translation initiation complexes, and often form during viral infections. Many viruses, however, counteract the formation of SGs, suggesting antiviral activity (reviewed by (89)). In fact, a recent study showed that the formation of SGs is associated with the antiviral protein, protein kinase R (PKR)-induced phosphorylation of eukaryotic translation initiation factor 2 α (eIF2 α), which inhibits general translation (295). Moreover, a specific interaction between the PxxP domain of G3BP and PKR is known to activate PKR, suggesting that G3BP is an antiviral protein itself (175). Other antiviral RNA binding proteins, e.g. retinoic acid-inducible gene I (RIG-I) and melanoma differentiation-associated gene 5 (MDA5) also localize to SGs (296, 297). These proteins have been recognized as some of the most potent antiviral

cytoplasmic pattern recognition receptors (PRRs) (192). Together this suggests that the formation of SGs is intertwined with (the activation of) innate antiviral responses.

In both insect and mammalian cells, Rin and G3BP are sequestered into nsP3-granules via an interaction between the conserved N-terminal NTF2-like domain of Rin/G3BP and two conserved repeats in the C-terminal variable domain of alphavirus nsP3, that closely resemble the amino acid residues normally bound by NTF2-like domains (Chapter 4)(166). The central domain of nsP3 forms multimers, independent of the N-terminal macrodomain or the C-terminal variable domain. However, the variable domain is required for a granular localization (Chapter 4 and 5), but the formation of these cytoplasmic nsP3-granules does not require Rin (Chapter 4).

Further investigation of these nsP3-granules in mammalian cells revealed that these granules were devoid of other typical SG components (e.g. eIF3) and did not respond to chemical stimulations that either induce (arsenite) or disassemble (cycloheximide) normal SGs (Chapter 5). These results indicate that the interaction between Rin/G3BP and CHIKV nsP3 inhibits the formation of *bona fide* SGs.

Considering the growing evidence that SGs augment innate antiviral responses, it is not surprising that CHIKV has evolved a way to inhibit SG formation. Paradoxically, silencing of G3BP1 and G3BP2 in mammalian cell culture decreased levels of CHIKV RNA replication, CHIKV protein expression and progeny virus titers (57). Although subjected to some controversy, SINV replication was also affected by the simultaneous depletion of G3BP1/2 (57, 58). Rin depletion in insect cells *in vitro* did not alter levels of CHIKV replication and/or protein expression (Chapter 4). Depletion of Rin in live *Ae. albopictus* mosquitoes, however, significantly reduced CHIKV infection rates (Chapter 4), suggesting that the interaction between nsP3 and Rin elicits proviral effects *in vivo*. The decreased CHIKV infection rate and viral titers *in vivo* but not *in vitro* during Rin silencing in *Ae. albopictus*, suggests that Rin helps to establish a productive infection and/or affects CHIKV replication in specific insect tissues, possibly the midgut. It also suggests that results obtained in these cell lines cannot always be extrapolated to an *in vivo* model. Furthermore, siRNA-mediated gene silencing may not completely abolish the presence of Rin/G3BP, which could also explain the discrepancy between the results from the *in vitro* and *in vivo* experiments. Introducing mutations in the Rin/G3BP binding domains of nsP3 in the context of viral replication can provide more insights into the role that Rin/G3BP-nsP3 granules play during an alphavirus infection. Deletion of the C-terminal 30 amino acids, that contain the G3BP binding domains, severely reduced Semliki forest virus (SFV) replication (165), strengthening the hypothesis that the interaction between nsP3 and Rin/G3BP has a positive effect on viral replication. The exact mechanism of how Rin/G3BP enhances viral replication in both vertebrates and invertebrates

is unknown, however G3BPs are not directly involved in the translation of incoming genomes, nor genome replication. This suggests that G3BPs support the switch between viral non-structural polyprotein translation and negative-strand RNA replication (57).

Besides alphaviruses, several other viruses, including flaviviruses, induce cytoplasmic granules that sequester essential SG factors (91, 177, 178). The interaction of flaviviruses and hepatitis C virus with SG components even increased their replication efficiency (177, 179, 298). The exact effects of flavivirus infection on the composition and formation of SGs has not been properly characterized. SG components T cell intracellular antigen-1 (TIA-1) and TIA1-related protein (TIAR) did not localize to SGs during WNV infection even when SGs were induced with oxidative stress (91). In contrast, G3BP-containing granules formed during flavivirus infection (299). These contradicting results actually suggest that viral-G3BP granules inhibit the formation of *bona fide* (TIA-1 and TIAR containing) SGs. In co-ordination with this hypothesis, flavivirus sRNA was shown to bind SG components G3BP1 and G3BP2 and CAPRIN1 which repressed innate immune responses (297). Experiments using infectious WNV clones that no longer produce sRNA, as described above, combined with transient expression of transcripts that contain sequences from flavivirus 3'UTR can reveal in more detail how flaviviruses modulate the formation of SGs.

In summary, this suggests that viral-Rin/G3BP-granules inhibit the formation of *bona fide* SGs, and that this strategy has been adopted by multiple unrelated viruses, which utilize different mechanisms. In addition, viruses may utilize SG components in viral-granules (e.g. Rin/G3BP) to increase their own productivity. In *Drosophila*, Rin has been suggested to form RNase inhibitor complexes (173), which could protect CHIKV RNA replication during the initial infection in the mosquito midgut. SGs are triage centres of RNA binding proteins and AGO2 has also been found to localize to SGs (158, 300). It is tempting to speculate that arboviruses modulate the SG response in invertebrates to decrease but not completely abolish the effects of RNAi and possible other antiviral pathways to balance appropriate levels of viral replication and fitness of the vector. These observations also suggest that small molecule modulators of the stress response could be used as antiviral treatment by stimulating antiviral responses, but perhaps more effectively by reducing viral replication rates. In addition, the interaction between nsP3 and Rin can provide a novel target to interfere with the CHIKV transmission cycle.

Chikungunya virus nsP2 and the vertebrate IFN-response

It is becoming increasingly clear that SGs have an antiviral role, as PRRs (e.g. RIG-I, MDA5 and PKR) that can activate other antiviral innate immune responses localize to *bona fide* SGs (297, 301, 302). The IFN response is arguably the most potent innate antiviral response that vertebrates possess. PRRs recognize viral elements resulting in the expression and secretion of IFNs. IFNs

activate neighboring cells via transmembrane receptors, which signal through the JAK-STAT pathway. STAT1/2 dimers are activated by phosphorylation and translocate to the nucleus, resulting in the up regulation of IFN-stimulated (antiviral) genes (ISG). Modulation of the IFN-response is absolutely essential for flaviviruses and alphaviruses to establish productive infections in mammalian hosts (Figure 1.6)(68–73).

Flaviviruses inhibit the IFN response by interfering with the recognition by PRRs, IFN- β production, and multiple steps during JAK-STAT signaling (reviewed by (303)). A group of old world alphaviruses, which includes CHIKV, are notorious for the suppression of host gene expression and the induction of cytopathic effects in cell culture (83, 209). General host cell shut-off is induced by nsP2 and was reported to affect the expression of IFNs and ISGs (218).

CHIKV infected cells no longer respond to exogenous stimulation with IFNs, as viral titers and CHIKV replicon RNA replication were unaffected and ISG expression was inhibited. However, when treated with IFNs prior to infection, ISGs were readily expressed and virus replication was severely reduced (Chapter 6). Interestingly, IFNs did not induce the nuclear translocation of STAT dimers when cells were infected with CHIKV. The absence of nuclear phosphorylated STAT (pSTAT) in these cells was independent of general host shut-off as cellular levels of STAT1 were unaffected by CHIKV RNA replication and complete inhibition of protein synthesis with cycloheximide did not affect STAT nuclear translocation during the course of the experiments (Chapter 6). Transient expression of individual CHIKV nsPs revealed that nsP2 inhibited JAK-STAT signaling (Chapter 6).

NsP2 is a multifunctional protein that contains the protease that processes the non-structural polyprotein (304), has RNA helicase activity (305), NTPase activity (306) and RNA triphosphatase activity (307). Recently, nsP2 was shown to induce the ubiquitination and degradation of RNA polymerase II subunit RPB1, which results in general host cell transcriptional shut-off and cytopathic effects in mammalian cells, but not in insect cells (149). A single amino acid change in the C-terminal domain of SINV nsP2 no longer induced the degradation of RPB1, abolished the cytotoxicity of nsP2 and enabled persistent infection in mammalian cells (85, 149). A homologous mutation in a CHIKV replicon reinstated the nuclear translocation of pSTAT in cells induced with IFNs (Chapter 6). However, when mutated CHIKV nsP2 was transiently expressed in mammalian cells, nuclear accumulation of pSTAT1 was still inhibited (Chapter 7). Further investigations revealed that this mutation decreases general host shut-off and the cytotoxicity of transiently expressed nsP2, but also severely reduced CHIKV RNA replication (Chapter 7). Reduced RNA replication and subsequent viral protein expression of this less cytopathic CHIKV replicon is likely what allowed the observed nuclear accumulation of pSTAT (Chapter 6).

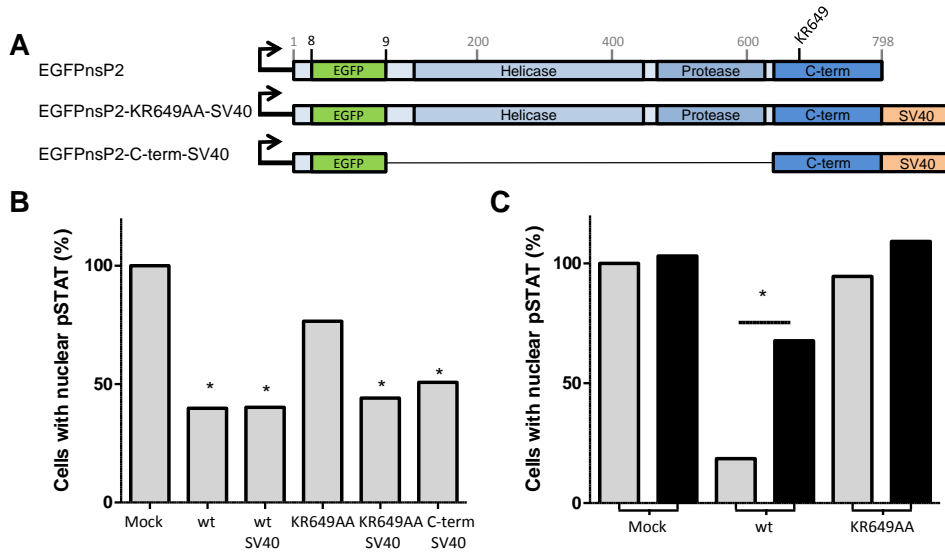


Figure 9.1. Nuclear localization of the C-terminal domain of nsP2 reduces nuclear STAT1. A. schematic representation of EGFPnsP2. Indicated are the NLS within nsP2 (KR649) and an in frame fusion with the Simian virus 40 NLS (SV40). Helicase and Protease domains were deleted and the C-terminal domain was fused in frame with EGFP. BC. NsP2 variants were transiently expressed in Vero cells and 20 hours post transfection cells received a 30 min stimulation with IFN- β (25 ng/ml). Cells were fixed permeabilized and stained for STAT1. C. cells were either mock treated (grey bars) or treated with 20nM of Leptomycin B (LMB) for 3 h (black bars) prior to IFN stimulation. Bars represent the percentage of cells with visible nuclear STAT1 relative to mock transfected IFN-induced samples. Asterisk indicates significant difference from the mock (B) or LMB induced (C) samples ($P < 0.01$, binominal test).

In contrast to SINV, additional amino acid changes were necessary to establish persistent CHIKV replication in mammalian cells (Chapter 7) (226). These mutations in CHIKV nsP2 all mapped to the homologous region of SINV nsP2 that directly binds nsP3 in the SINV replication complex (RC) (156). Changing the interaction with nsP3 could reduce the functionality of the CHIKV replication complex and therefore reduce CHIKV replication. Reduced RNA replication was necessary to establish persistent CHIKV RNA replication in mammalian cells; however, one second site mutation partly restored CHIKV replicon RNA replication. Cells expressing stable CHIKV or SFV replicon RNA replication have already been developed into an assay for the identification of inhibitors of alphavirus entry and replication (226). Finally, introducing these attenuating mutations in an infectious full-length CHIKV virus holds potential for the development of a live attenuated vaccine.

One of the mutations that contributed to the attenuation of CHIKV replicon RNA replication was inside the putative nuclear localization signal (NLS) within nsP2 (KR649-650) (223). Interestingly, substituting these residues for alanines not only kept nsP2 out of the nucleus, but also completely re-

instated the JAK-STAT signaling pathway upon stimulation with IFNs (Chapter 7). These results indicated that the inhibition of JAK-STAT signaling either occurs inside the nucleus, or is a direct consequence of mutations in the nsP2 NLS. Transiently expressed nsP2-KR649AA with an additional classical NLS fused to the C-terminus (Figure 9.1A) was redirected into the nucleus and effectively inhibited the nuclear accumulation of pSTAT upon stimulation with IFNs (Figure 9.1B). Moreover, N-terminal truncations of nsP2 revealed that only the C-terminal domain is required for the inhibition of JAK-STAT signaling (Figure 9.1B).

Only as a dimer two STAT proteins display an NLS at the STAT-STAT interface, which results in active nuclear translocation via importin- α (308). The STAT dimer has a relatively high affinity for the IFN-stimulated response element (ISRE), which promotes the transcription of down-stream ISGs. STAT proteins that are not bound to DNA are actively exported out of the nucleus by chromosome region maintenance 1 (CRM1) (309). This suggests that the JAK-STAT signaling assay, based on immunofluorescence of pSTAT proteins in fixed mammalian cells, was unable to detect nuclear pSTAT as STAT had been redirected back into the cytoplasm (Figure 9.2). Indeed, when nuclear export was chemically blocked by leptomycin B a large increase in nuclear STAT1 in nsP2 expressing IFN induced cells was observed (Figure 9.1C). These results indicate that, in the nucleus, the C-terminal domain of CHIKV nsP2 somehow induces the nuclear export of STAT.

The C-terminal domain of CHIKV nsP2 has a SAM-dependent methyltransferase fold (Chapter 7)(310), but methyltransferase activity has not been reported. Interestingly, IFN-stimulated gene expression can be silenced by hypermethylation of the promoter region (311). Genomic DNA isolation followed by sodium bisulfite treatment and PCR amplification can identify whether nsP2 expression results in alternative methylation patterns in the DNA binding sites of pSTAT dimers. Alternatively, demethylation of phosphorylated STAT1 would result in increased affinity of protein inhibitors of activated STAT1 (PIAS1) for STAT1, also reducing the binding affinity of STAT dimers (312).

In addition, CHIKV nsP2 is a highly connected and multifunctional protein, which induces nsP2-mediated ubiquitination of RPB1 (149, 217). NsP2 is associated with ubiquitin ligases RCHY1, WWP1 and a regulator of ubiquitin activity ubiquilin 4 (217). The DNA binding affinity of STAT dimers is increased by a number of co-factors, including IFN-response factor 9 (IRF9). Inducing the ubiquitination of co-factors may also decrease the DNA binding affinity of STAT dimers and consequently induce nuclear export of STAT. Similarly, rotavirus NSP1 inhibits STAT nuclear accumulation upon IFN stimulation (313). Rotavirus NSP1 also induces the proteasomal degradation of multiple IRFs, including IRF9 (314), however, both findings appear to be unrelated (315). Taken together, these results indicate that the C-terminal domain of CHIKV nsP2 specifically inhibits IFN signaling by inducing the nuclear export of STAT

proteins (Figure 9.2). Additionally, these results provide a rationale for the ineffectiveness of IFN-treatment during CHIKV infections.

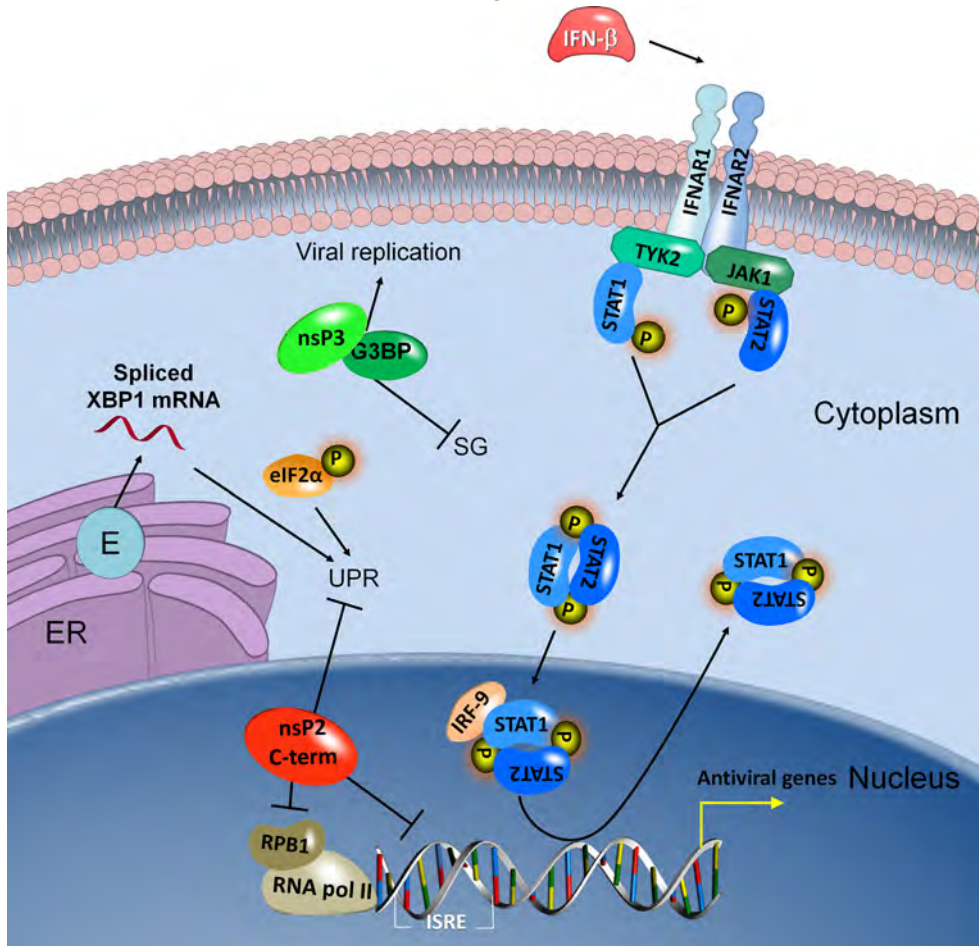


Figure 9.2. CHIKV modulation of the vertebrate host-cell. SG formation: Interaction between nsP3 and G3BP inhibits the formation of SG and contributes to effective viral replication (Chapter 4 and 5)(270). JAK-STAT signaling: STAT dimers are formed and translocate to the nucleus, but are quickly exported upon the nuclear presence of the C-terminus of nsP2. Host shut-off: RPB1 is tagged for degradation inhibiting RNA pol II transcription (145). UPR: CHIKV infection and envelope (E) proteins in the ER activate the UPR, which results in XBP1 mRNA splicing and eIF2α phosphorylation. nsP2 inhibits transcription of UPR target genes and translation of UPR transcription factors.

Chikungunya virus nsP2 and the vertebrate unfolded protein response

Once the initial cellular antiviral responses have been overcome and viral replication is underway, the vast amounts of CHIKV progeny virus that is produced poses another problem. As one of the final steps in the viral replication cycle, large amounts of viral glycoproteins are expressed which mature in the endoplasmic reticulum (ER)(Fig. 1.7). The expression of alphavirus glycoproteins

disrupts the homeostasis in the ER which in turn results in activation of the unfolded protein response (UPR) (Chapter 8)(97). There is growing evidence that the UPR enhances inflammatory and innate immune pathways (266). The UPR also increases the production of several proteins involved in protein folding, degradation and apoptosis, whilst inhibiting general protein synthesis via the phosphorylation of eIF2 α in an effort to restore homeostasis in the ER (230). Most viruses prevent the phosphorylation of eIF2 α to allow and promote the translation of viral proteins (249–251). Alphaviruses, however, allow the phosphorylation of eIF2 α during productive infection (228, 263, 264, 258). A stable hairpin loop structure in the 26S promoter of the subgenomic mRNA from SINV stalls the ribosome on the correct AUG providing resistance to eIF2 α phosphorylation (263). When the UPR was induced with a chemical inhibitor of N-linked glycosylation, in the context of a CHIKV infection or transient expression of CHIKV nsP2, the expression of UPR target genes and the eIF2 α phosphorylation insensitive activating transcription factor 4 (ATF4) was clearly inhibited. In addition, UPR transcription factor X-box binding protein 1 (XBP1) was initially activated, but was not found in the nucleus (Figure 9.2)(Chapter 8). Whether the lack of nuclear XBP1 results from a similar mechanism as STAT proteins is unknown, but investigating the subcellular distribution of activated XBP1 in cells that transiently express nsP2 and the variants thereof can provide a first indication.

The translational shut-off during alphavirus infection is independent of eIF2 α phosphorylation (228, 264), and could explain the lack of UPR transcription factors during alphavirus infection. Point mutations in nsP2 that abolish host cell (transcriptional) shut-off reversed the nsP2-mediated inhibition of the UPR. This suggests that the host-cell shut-off, governed by CHIKV nsP2, is responsible for the inhibition of the UPR. Although the mechanism of alphavirus-induced translational shut-off is not well understood, previous reports suggest SINV translational shut-off is independent of transcriptional shut-off, but both can be relieved by mutations in nsP2 (218). It is thus unclear whether indirect effects of nsP2-mediated transcriptional shut-off contribute to the observed eIF2 α -independent translational shut-off or whether there is a specific mechanism that blocks cellular translation and subsequently downstream activation of the UPR. A better understanding of the mechanisms by which alphaviruses inhibit transcription and translation will allow better understanding of how these inhibitory effects impact intracellular signaling pathways, including the UPR.

What does become apparent now is that CHIKV has evolved efficient ways to prevent or inhibit antiviral responses in vertebrates and delay apoptosis to maximize virus replication, during a rapid and lytic infection. This suggests that activating the UPR or IFN-response to treat CHIKV infections are unlikely to be effective, pressing the need for compounds that directly inhibit viral replication or alternative approaches to interrupt viral transmission cycles.

Significance and concluding remarks

In recent years, CHIKV and WNV have caused substantial outbreaks of human arthritogenic and encephalitic disease. The spread of invasive CHIKV vector species has closely been followed by CHIKV outbreaks. After the first reported autochthonous transmission on the American continent in 2013, more than a million CHIKV infections have been reported by the end of 2014. Similarly, WNV swept through the USA after its initial introduction to the continent, because it was effectively transmitted by local mosquito species. This thesis describes the epidemic potential of two pathogenic lineages of WNV within Europe and compares it to that of USUV, a related flavivirus that has only recently emerged in Europe. The results presented in chapter 2 and 3 show that European *Cx. pipiens* mosquitoes from WNV-free areas are intrinsically effective WNV and USUV vectors. This clearly indicates a risk for further spread of these arboviruses. In addition, changing climatic conditions and the adaptive nature of these small RNA viruses suggests that arbovirus outbreaks will continue to emerge. The data presented in this thesis will increase the effectiveness and accuracy of arbovirus risk assessments and calls for intensified surveillance of flavivirus activity in regions that are currently virus-free and increased awareness in clinics throughout Europe.

The molecular interactions that determine effective viral replication throughout the mosquito vector are still poorly characterized and strong inhibitors of mosquito antiviral responses (e.g. RNAi) have not been described. Arbovirus infections in the invertebrate vector are persistent and seem almost symbiotic, with little to no fitness costs for the vector. In sharp contrast, arbovirus pathogenesis in vertebrate hosts can be relatively severe and acute, which finally results in either the death of the vertebrate host or clearance of the viral infection. This is also reflected by the amount of vigorous countermeasures that arboviruses have evolved against vertebrate antiviral responses, compared to the limited and mild modulations that have been reported against the vectors antiviral responses. This thesis further describes the identification of novel molecular interactions between viral and host proteins that enable CHIKV to successfully infect both the vertebrate and invertebrate hosts (Figure 9.3).

Currently there are no vaccines or antiviral compounds available for human uses that are effective against WNV and CHIKV infections. These viruses are, however, readily cleared by an operational vertebrate innate immune response *in vivo*, which produces large amounts of IFNs (135). When IFNs are administered prior to (or very early during) infection they do effectively protect against WNV and CHIKV disease in experimental animal models (68, 71, 72, 316). IFNs are regularly used as antiviral treatment during chronic viral infections, however lack effectiveness when used to treat acute infections (e.g. WNV or CHIKV infections) (317). The results presented in Chapters 6 and 7 provide a rationale for the ineffectiveness of IFN treatment in response to clinical (acute) CHIKV infections. The combined effects of CHIKV nsP2

induced general host shut-off and the inhibition of JAK-STAT signaling are particularly effective, shutting down both general antiviral gene transcription (including the production of IFNs) and downstream signaling that is initiated by IFNs produced by other cells of the infected organism. The UPR has been proposed to strengthen and specify the IFN-response (266). This explains why CHIKV induced host shut-off has evolved to also inhibit the UPR. Indeed, the replication of several RNA viruses, including SINV, was inhibited when the UPR was activated with a small molecule deubiquitinase inhibitor (98, 267). However, these authors activated the UPR prior to infection, while our data indicate that downstream activation of the UPR is effectively inhibited during CHIKV infection. This suggests that activating either the UPR or the IFN-response (and possibly other antiviral pathways) is an ineffective strategy in the fight against these fast replicating and adaptive arboviruses. In fact, most arboviruses have adopted a similar transmission strategy, often with analogous solutions to inhibit vertebrate antiviral responses (66, 318).

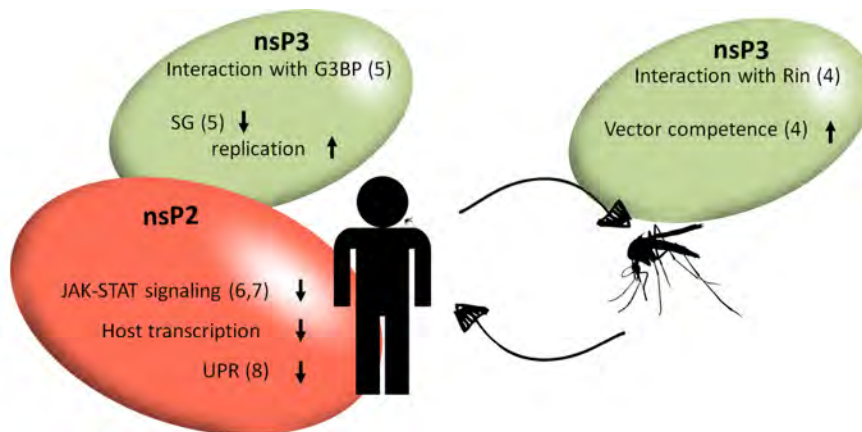


Figure 9.3. Schematic representation of the CHIKV transmission cycle with CHIKV nsP2 and nsP3 and their effect on host responses indicated. CHIKV nsP2 inhibits vertebrate RNA pol II RNA transcription in vertebrates but not in invertebrates (145). In addition it effectively inhibits the UPR and JAK-STAT signaling in vertebrates. CHIKV nsP3 interacts with vertebrate G3BP or homologous mosquito Rin, forming viral Granules and inhibiting the formation of *bona fide* SGs, with a positive, proviral effect on CHIKV replication. The respective chapters that describe these interactions are indicated within brackets and arrows indicate respective up or down regulation.

Specifically counteracting the CHIKV-induced inhibition of either the IFN-response or the UPR can provide a more effective strategy for antiviral treatments. Alternatively, compounds that directly interfere with viral replication, virion assembly or virus entry are also likely to be effective. The interaction between CHIKV nsP3 and G3BP/Rin, described in Chapters 4 and 5, may provide such a target as this interaction not only inhibits the antiviral

stress granule response, but also exerts a positive effect on viral replication both in vertebrate cells and the mosquito vector (Chapters 4 and 5)(171). Compounds that disturb the interaction between G3BP and CHIKV nsP3 have the potential to increase the antiviral response by re-establishing a functional SG response, while at the same time reducing viral replication rates. The homologous interaction between nsP3 and mosquito Rin may also provide a novel target to interfere with the CHIKV transmission cycle, e.g. by disrupting the interaction between virus and vector. It will be interesting to determine whether the interaction between alphavirus nsP3 and Rin is in fact a molecular determinant of vector competence and whether other arboviruses and RNA viruses in general, also utilize G3BP/Rin for their propagation.

This thesis thus adds to the collective knowledge of arbovirus transmission cycles by describing the risk for WNV and USUV transmission in Europe and the climatic factors that are involved. Additionally, this thesis provides novel molecular data, which suggests directing future antiviral drug development to more specific compounds that directly interfere with viral replication and transmission.

References

References

1. C. J. Finley, El mosquito hipoteticamente considerado como agente de trasmision de la fiebre amarilla. *An. la Real Acad. Ciencias Médicas, Físicas y Nat. la Habana*. **18**, 147–169 (1882).
2. S.C. Weaver, W.K.. Reissen, present and future arboviral threats. *Antiviral Res.* **85**, 1–36 (2011).
3. A. Suhrbier, M.-C. Jaffar-Bandjee, P. Gasque, Arthritogenic alphaviruses--an overview. *Nat. Rev. Rheumatol.* **8**, 420–9 (2012).
4. J. S. Mackenzie, D. J. Gubler, L. R. Petersen, Emerging flaviviruses: the spread and resurgence of Japanese encephalitis, West Nile and dengue viruses. *Nat. Med.* **10**, S98–109 (2004).
5. S. C. Weaver, A. D. T. Barrett, Transmission cycles, host range, evolution and emergence of arboviral disease. *Nat. Rev. Microbiol.* **2**, 789–801 (2004).
6. T. P. Monath, Reviews Yellow fever : an update. *Lancet Infect. Dis.* **1**, 11–20 (2001).
7. U. K. Misra, J. Kalita, Overview: Japanese encephalitis. *Prog. Neurobiol.* **91**, 108–120 (2010).
8. M. Hemungkorn, U. Thisyakorn, C. Thisyakorn, Dengue infection: a growing global health threat. *Biosci. Trends.* **1**, 90–96 (2007).
9. Y.-J. S. Huang, S. Higgs, K. M. Horne, D. L. Vanlandingham, Flavivirus-Mosquito Interactions. *Viruses.* **6**, 4703–4730 (2014).
10. B. D. Lindenbach, C. M. Rice, Molecular biology of flaviviruses. *Adv. Virus Res.* **59**:23-61 (2003).
11. S. M. Lim *et al.*, Susceptibility of European jackdaws (*Corvus monedula*) to experimental infection with lineage 1 and 2 West Nile viruses. *J. Gen. Virol.* **95**, 1320–9 (2014).
12. J. Del Amo *et al.*, Experimental infection of house sparrows (*Passer domesticus*) with West Nile virus strains of lineages 1 and 2. *Vet. Microbiol.* **172**, 542–7 (2014).
13. A. C. Brault *et al.*, Differential Virulence of West Nile Strains for American Crows. *Emerg. Infect. Dis.* **10**, 2161–2168 (2004).
14. H. S. Hurlbut, West Nile virus infection in arthropods. *Am J Trop Med Hyg.* **5**, 76–85 (1956).
15. E. B. Hayes *et al.*, Virology, pathology, and clinical manifestations of West Nile virus disease. *Emerg Infect Dis.* **11**, 1174–1179 (2005).
16. E. Donadieu *et al.*, Differential virulence and pathogenesis of West Nile viruses. *Viruses.* **5**, 2856–80 (2013).
17. R. S. Lanciotti *et al.*, Complete Genome Sequences and Phylogenetic Analysis of West Nile Virus Strains Isolated from the United States, Europe, and the Middle East. *Virology.* **298**, 96–105 (2002).
18. R. S. Lanciotti, Origin of the West Nile Virus Responsible for an Outbreak of Encephalitis in the Northeastern United States. *Science.* **286**, 2333–2337 (1999).
19. Center for Disease Control and Prevention, West Nile virus disease cases and deaths reported to CDC by year and clinical presentation, 1999–2013. (available at <http://www.cdc.gov/>).
20. D. W. C. Beasley, A. D. T. Barrett, R. B. Tesh, Resurgence of West Nile neurologic disease in the United States in 2012: what happened? What needs to be done? *Antiviral Res.* **99**, 1–5 (2013).
21. M.J. Frost *et al.*, Characterization of virulent West Nile virus Kunjin strain, Australia, 2011. *Emerg. Infect. Dis.* **18**(5):792-800 (2012).
22. A. Papa *et al.*, Genetic characterization of West Nile virus lineage 2, Greece, 2010. *Emerg. Infect. Dis.* **17**, 920–2 (2011).
23. F. Magurano *et al.*, Circulation of West Nile virus lineage 1 and 2 during an outbreak in Italy. *Clin. Microbiol. Infect.* **18**, E545–7 (2012).
24. European Centre for disease prevention and control, Distribution of West Nile fever cases by affected areas, European region/Mediterranean basin. (available at www.ecdc.europa.eu).
25. F. Cavrini *et al.*, Usutu virus infection in a patient who underwent orthotopic liver transplant transplantation, Italy, August–September 2009, *Euro surveill.* **14**, 50–53 (2009).
26. M. Pecorari *et al.*, first human case of usutu virus neuroinvasive infection, Italy, August–September 2009. *Euro Surveill.* **9–10** (2009).
27. M. Santini *et al.*, First cases of human Usutu virus neuroinvasive infection in Croatia, August–September 2013: clinical and laboratory features. *J. Neurovirol.* **2004** (2014), doi:10.1007/s13365-014-0300-4.
28. R. J. Kuhn, Togaviridae : The Viruses and Their Replication. In: Knipe DM, Howley PM, editors. *Fields' Virology*, Fifth Edition. New York: Lippincott, Williams and Wilkins. pp. 1001–1022 (2006).
29. J. H. Strauss, E. G. Strauss, The alphaviruses: gene expression, replication, and evolution. *Microbiol. Rev.* **58**, 491–562 (1994).
30. S. K. Lam *et al.*, Chikungunya infection--an emerging disease in Malaysia. *Southeast Asian J. Trop. Med. Public Health.* **32**, 447–451 (2001).

31. H. Townson, M. B. Nathan, Resurgence of chikungunya. *Trans. R. Soc. Trop. Med. Hyg.* **102**, 308–309 (2008).
32. G. Rezza *et al.*, Infection with chikungunya virus in Italy: an outbreak in a temperate region. *Lancet.* **370**, 1840–1846 (2007).
33. European Centre for disease prevention and control, ECDC Epidemiological update- autochthonous cases of chikungunya fever in France. (available at www.ecdc.europa.eu).
34. M. Grandadam *et al.*, Chikungunya virus, southeastern France. *Emerg. Infect. Dis.* **17**, 910–913 (2011).
35. I. Leparc-Goffart, A. Nougairede, S. Cassadou, C. Prat, X. de Lamballerie, Chikungunya in the Americas. *Lancet.* **383**, 514 (2014).
36. A. M. Powers, Risks to the Americas associated with the continued expansion of chikungunya virus. *J. Gen. Virol.* **96**, 1–5 (2015).
37. B. M. Nelms *et al.*, Phenotypic variation among *Culex pipiens* complex (Diptera: Culicidae) populations from the Sacramento Valley, California: horizontal and vertical transmission of West Nile virus, diapause potential, autogeny, and host selection. *Am. J. Trop. Med. Hyg.* **89**, 1168–78 (2013).
38. K. A. Bernard *et al.*, West Nile virus infection in birds and mosquitoes, New York State, 2000. *Emerg. Infect. Dis.* **7**, 679–85 (2001).
39. G. Molaei *et al.*, Vector-host interactions governing epidemiology of West Nile virus in Southern California. *Am. J. Trop. Med. Hyg.* **83**, 1269–82 (2010).
40. R. M. Moudy, M. A. Meola, L. L. Morin, G. D. Ebel, L. D. Kramer, A Newly Emergent Genotype of West Nile Virus Is Transmitted Earlier and More Efficiently by *Culex* Mosquitoes. *Am. J. Trop. Med. Hyg.* **77**, 365–370 (2007).
41. O. Engler *et al.*, European surveillance for West Nile virus in mosquito populations. *Int. J. Environ. Res. Public Health.* **10**, 4869–95 (2013).
42. J. C. Hesson *et al.*, The arbovirus vector *Culex torrentium* is more prevalent than *Culex pipiens* in northern and central Europe. *Med. Vet. Entomol.* **28**, 179–86 (2014).
43. K. A. Tsetsarkin, D. L. Vanlandingham, C. E. McGee, S. Higgs, A single mutation in chikungunya virus affects vector specificity and epidemic potential. *PLoS Pathog.* **3**, e201 (2007).
44. S. Sim, N. Jupatanakul, G. Dimopoulos, Mosquito Immunity against Arboviruses. *Viruses.* **6**, 4479–4504 (2014).
45. Z. Xi, J. L. Ramirez, G. Dimopoulos, The *Aedes aegypti* toll pathway controls dengue virus infection. *PLoS Pathog.* **4** (2008), doi:10.1371/journal.ppat.1000098.
46. H. R. Sanders *et al.*, Sindbis virus induces transport processes and alters expression of innate immunity pathway genes in the midgut of the disease vector, *Aedes aegypti*. *Insect Biochem. Mol. Biol.* **35**, 1293–1307 (2005).
47. S. Sim *et al.*, Transcriptomic Profiling of Diverse *Aedes aegypti* Strains Reveals Increased Basal-level Immune Activation in Dengue Virus-refractory Populations and Identifies Novel Virus-vector Molecular Interactions. *PLoS Negl. Trop. Dis.* **7** (2013), doi:10.1371/journal.pntd.0002295.
48. E. J. Kwon *et al.*, Transcriptional regulation of the *Drosophila* raf proto-oncogene by *Drosophila* STAT during development and in immune response. *J. Biol. Chem.* **275**, 19824–19830 (2000).
49. J. A. Souza-Neto, S. Sim, G. Dimopoulos, An evolutionary conserved function of the JAK-STAT pathway in anti-dengue defense. *Proc. Natl. Acad. Sci. U. S. A.* **106**, 17841–6 (2009).
50. I. Sanchez-Vargas *et al.*, RNA interference, arthropod-borne viruses, and mosquitoes. *Virus Res.* **102**, 65–74 (2004).
51. D. E. Brackney, J. E. Beane, G. D. Ebel, RNAi targeting of West Nile virus in mosquito midguts promotes virus diversification. *PLoS Pathog.* **5**, e1000502 (2009).
52. C. L. Campbell *et al.*, *Aedes aegypti* uses RNA interference in defense against Sindbis virus infection. *BMC Microbiol.* **8**, 47 (2008).
53. M. McFarlane *et al.*, Characterization of *Aedes aegypti* Innate-Immune Pathways that Limit Chikungunya Virus Replication. *PLoS Negl. Trop. Dis.* **8**, e2994 (2014).
54. I. Sánchez-Vargas *et al.*, Dengue virus type 2 infections of *Aedes aegypti* are modulated by the mosquito's RNA interference pathway. *PLoS Pathog.* **5**, e1000299 (2009).
55. C. C. Khoo, J. Piper, I. Sanchez-Vargas, K. E. Olson, A. W. Franz, The RNA interference pathway affects midgut infection- and escape barriers for Sindbis virus in *Aedes aegypti*. *BMC Microbiol.* **10**, 130 (2010).
56. A. M. Hess *et al.*, Small RNA profiling of Dengue virus-mosquito interactions implicates the PIWI RNA pathway in anti-viral defense. *BMC Microbiol.* **11**, 45 (2011).

References

57. E. M. Morazzani, M. R. Wiley, M. G. Murreddu, Z. N. Adelman, K. M. Myles, Production of virus-derived ping-pong-dependent piRNA-like small RNAs in the mosquito soma. *PLoS Pathog.* **8** (2012), doi:10.1371/journal.ppat.1002470.
58. A. Nayak *et al.*, Cricket paralysis virus antagonizes Argonaute 2 to modulate antiviral defense in *Drosophila*. *Nat. Struct. Mol. Biol.* **17**, 547–554 (2010).
59. H. Li, W. X. Li, S. W. Ding, Induction and suppression of RNA silencing by an animal virus. *Science*. **296**, 1319–1321 (2002).
60. L. Lakatos, G. Szittyá, D. Silhavy, J. Burgyan, Molecular mechanism of RNA silencing suppression mediated by p19 protein of tombusviruses. *EMBO J.* **23**, 876–884 (2004).
61. G. Attarzadeh-Yazdi *et al.*, Cell-to-cell spread of the RNA interference response suppresses Semliki Forest virus (SFV) infection of mosquito cell cultures and cannot be antagonized by SFV. *J. Virol.* **83**, 5735–5748 (2009).
62. H. W. Li, S. W. Ding, Antiviral silencing in animals. *FEBS Lett.* **579**, 5965–5973 (2005).
63. C. M. Cirimotich, J. C. Scott, A. T. Phillips, B. J. Geiss, K. E. Olson, Suppression of RNA interference increases alphavirus replication and virus-associated mortality in *Aedes aegypti* mosquitoes. *BMC Microbiol.* **9**, 49 (2009).
64. P. S. Mellor, Replication of arboviruses in insect vectors. *J. Comp. Pathol.* **123**, 231–247 (2000).
65. J. L. Hardy, E. J. Houk, L. D. Kramer, W. C. Reeves, Intrinsic factors affecting vector competence of mosquitoes for arboviruses. *Annu. Rev. Entomol.* **28**, 229–262 (1983).
66. B. S. Hollidge, S. R. Weiss, S. S. Soldan, The role of interferon antagonist, non-structural proteins in the pathogenesis and emergence of arboviruses. *Viruses*. **3**, 629–58 (2011).
67. M. S. Diamond, M. Farzan, The broad-spectrum antiviral functions of IFIT and IFITM proteins. *Nat. Rev. Immunol.* **13**, 46–57 (2013).
68. J. Gardner *et al.*, Chikungunya virus arthritis in adult wild-type mice. *J. Virol.* **84**, 8021–8032 (2010).
69. T. Couderc *et al.*, A Mouse Model for Chikungunya: Young Age and Inefficient Type-I Interferon Signaling Are Risk Factors for Severe Disease. *PLoS Pathog.* **4**, e29 (2008).
70. C. Schilte *et al.*, Type I IFN controls chikungunya virus via its action on nonhematopoietic cells. *J. Exp. Med.* **207**, 429–442 (2010).
71. M. A. Samuel, M. S. Diamond, Alpha/beta interferon protects against lethal West Nile virus infection by restricting cellular tropism and enhancing neuronal survival. *J. Virol.* **79**, 13350–13361 (2005).
72. J. D. Morrey *et al.*, Effect of interferon-alpha and interferon-inducers on West Nile virus in mouse and hamster animal models. *Antivir. Chem. Chemother.* **15**(2):101–9 (2004).
73. J. F. Anderson, J. J. Rahal, Efficacy of Interferon Alpha-2b and Ribavirin against West Nile Virus In Vitro. *Emerg. Infect. Dis.* **8**, 107–108 (2002).
74. M. Laurent-Rolle *et al.*, The NS5 protein of the virulent West Nile virus NY99 strain is a potent antagonist of type I interferon-mediated JAK-STAT signaling. *J. Virol.* **84**, 3503–15 (2010).
75. R. J. Lin, B. L. Chang, H. P. Yu, C. L. Liao, Y. L. Lin, Blocking of interferon-induced Jak-Stat signaling by Japanese encephalitis virus NS5 through a protein tyrosine phosphatase-mediated mechanism. *J. Virol.* **80**, 5908–5918 (2006).
76. K. Werme, M. Wigerius, M. Johansson, Tick-borne encephalitis virus NS5 associates with membrane protein scribble and impairs interferon-stimulated JAK-STAT signalling. *Cell. Microbiol.* **10**, 696–712 (2008).
77. G. S. Park, K. L. Morris, R. G. Hallett, M. E. Bloom, S. M. Best, Identification of residues critical for the interferon antagonist function of Langat virus NS5 reveals a role for the RNA-dependent RNA polymerase domain. *J. Virol.* **81**, 6936–6946 (2007).
78. J. Ashour, M. Laurent-Rolle, P. Y. Shi, A. Garcia-Sastre, NS5 of dengue virus mediates STAT2 binding and degradation. *J. Virol.* **83**, 5408–5418 (2009).
79. M. Jones *et al.*, Dengue virus inhibits alpha interferon signaling by reducing STAT2 expression. *J. Virol.* **79**, 5414–5420 (2005).
80. J. L. Munoz-Jordan *et al.*, Inhibition of alpha/beta interferon signaling by the NS4B protein of flaviviruses. *J. Virol.* **79**, 8004–8013 (2005).
81. J. T. Guo, J. Hayashi, C. Seeger, West Nile virus inhibits the signal transduction pathway of alpha interferon. *J. Virol.* **79**, 1343–1350 (2005).
82. W. J. Liu, H. B. Chen, X. J. Wang, H. Huang, A. A. Khromykh, Analysis of adaptive mutations in Kunjin virus replicon RNA reveals a novel role for the flavivirus nonstructural protein NS2A in inhibition of beta interferon promoter-driven transcription. *J. Virol.* **78**, 12225–12235 (2004).

83. N. Garmashova, R. Gorchakov, E. Frolova, I. Frolov, Sindbis virus nonstructural protein nsP2 is cytotoxic and inhibits cellular transcription. *J Virol.* **80**, 5686–5696 (2006).
84. N. Garmashova *et al.*, The Old World and New World alphaviruses use different virus-specific proteins for induction of transcriptional shutoff. *J. Virol.* **81**, 2472–2484 (2007).
85. S. A. Dryga, O. A. Dryga, S. Schlesinger, Identification of mutations in a Sindbis virus variant able to establish persistent infection in BHK cells: the importance of a mutation in the nsP2 gene. *Virology.* **228**, 74–83 (1997).
86. J. D. Simmons *et al.*, Venezuelan equine encephalitis virus disrupts STAT1 signaling by distinct mechanisms independent of host shutoff. *J Virol* (2009), doi:JVI.01041-09 [pii] 10.1128/JVI.01041-09.
87. L. Breakwell *et al.*, Semliki Forest virus nonstructural protein 2 is involved in suppression of the type I interferon response. *J. Virol.* **81**, 8677–84 (2007).
88. C. W. Burke, C. L. Gardner, J. J. Steffan, K. D. Ryman, W. B. Klimstra, Characteristics of alpha/beta interferon induction after infection of murine fibroblasts with wild-type and mutant alphaviruses. *Virology.* **395**, 121–32 (2009).
89. J. P. White, R. E. Lloyd, Regulation of stress granules in virus systems. *Trends Microbiol.* **20**, 175–183 (2013).
90. J. R. Buchan, R. Parker, Eukaryotic Stress Granules : The Ins and Out of Translation. *Mol. Cell.* **36**(6):932–41 (2009).
91. M. M. Emara, M. A. Brinton, Interaction of TIA-1/TIAR with West Nile and dengue virus products in infected cells interferes with stress granule formation and processing body assembly. *Proc. Natl. Acad. Sci. U. S. A.* **104**, 9041–6 (2007).
92. I. M. Cristea *et al.*, Tracking and elucidating alphavirus-host protein interactions. *J. Biol. Chem.* **281**, 30269–78 (2006).
93. R. Gorchakov, N. Garmashova, E. Frolova, I. Frolov, Different types of nsP3-containing protein complexes in Sindbis virus-infected cells. *J Virol.* **82**, 10088–10101 (2008).
94. M. Schröder, R. J. Kaufman, The mammalian unfolded protein response. *Annu. Rev. Biochem.* **74**, 739–89 (2005).
95. B. He, Viruses, endoplasmic reticulum stress, and interferon responses. *Cell Death Differ.* **13**, 393–403 (2006).
96. R. L. Ambrose, J. M. Mackenzie, West Nile virus differentially modulates the unfolded protein response to facilitate replication and immune evasion. *J. Virol.* **85**, 2723–32 (2011).
97. G. Barry *et al.*, Semliki Forest Virus-Induced Endoplasmic Reticulum Stress Accelerates Apoptotic Death of Mammalian Cells. *J. Virol.* **84**, 7369–7377 (2010).
98. J. W. Perry *et al.*, Antiviral activity of a small molecule deubiquitinase inhibitor occurs via induction of the unfolded protein response. *PLoS Pathog.* **8**, e1002783 (2012).
99. K. D. Saxton-Shaw *et al.*, O'nyong nyong virus molecular determinants of unique vector specificity reside in non-structural protein 3. *PLoS Negl. Trop. Dis.* **7**, e1931 (2013).
100. L. R. Petersen, A. C. Brault, R. S. Nasci, West Nile virus: review of the literature. *JAMA.* **310**, 308–15 (2013).
101. T. F. Tsai, F. Popovici, C. Cernescu, G. L. Campbell, N. I. Nedelcu, West Nile encephalitis epidemic in southeastern Romania. *Lancet.* **352**, 767–71 (1998).
102. A. E. Platonov *et al.*, Outbreak of West Nile virus infection, Volgograd Region, Russia, 1999. *Emerg. Infect. Dis.* **7**, 128–32 (2001).
103. M. Weinberger *et al.*, West Nile fever outbreak, Israel, 2000: epidemiologic aspects. *Emerg. Infect. Dis.* **7**, 686–91 (2000).
104. E. B. Hayes *et al.*, Epidemiology and transmission dynamics of West Nile virus disease. *Emerg. Infect. Dis.* **11**, 1167–73 (2005).
105. A. M. Kilpatrick, M. A. Meola, R. M. Moudy, L. D. Kramer, Temperature, viral genetics, and the transmission of West Nile virus by *Culex pipiens* mosquitoes. *PLoS Pathog.* **4**, e1000092 (2008).
106. T. Balenghien *et al.*, Vector competence of some French *Culex* and *Aedes* mosquitoes for West Nile virus. *Vector Borne Zoonotic Dis.* **8**, 589–95 (2008).
107. B. J. Blitvich *et al.*, Epitope-Blocking Enzyme-Linked Immunosorbent Assays for the Detection of Serum Antibodies to West Nile Virus in Multiple Avian Species. *J. Clin. Microbiol.* **41**, 1041–1047 (2003).
108. M. R. Haylock *et al.*, A European daily high-resolution gridded data set of surface temperature and precipitation for 1950–2006. *J. Geophys. Res.* **113**, D20119 (2008).
109. B. V. Purse *et al.*, emergence of bluetongue in Europe. *Nat. Rev. Microbiol.* **3**, 171–181 (2006).

References

110. U. Ziegler *et al.*, Monitoring of West Nile virus infections in Germany. *Zoonoses Public Health*. **59** Suppl 2, 95–101 (2012).
111. A. M. G. Klein Tank *et al.*, Daily dataset of 20th-century surface air temperature and precipitation series for the European Climate Assessment. *Int. J. Climatol.* **22**, 1441–1453 (2002).
112. M. C. Wimberly, A. Lamsal, P. Giacomo, T.-W. Chuang, Regional variation of climatic influences on west nile virus outbreaks in the United States. *Am. J. Trop. Med. Hyg.* **91**, 677–84 (2014).
113. D. M. Fonseca *et al.*, Emerging vectors in the Culex pipiens complex. *Science*. **303**, 1535–8 (2004).
114. C. Beck *et al.*, Flaviviruses in Europe: complex circulation patterns and their consequences for the diagnosis and control of West Nile disease. *Int. J. Environ. Res. Public Health*. **10**, 6049–83 (2013).
115. M.-C. Paty, Dengue fever in mainland France. *Arch. Pediatr.* **21**, 1274–8 (2014).
116. F. Schaffner, A. Mathis, Dengue and dengue vectors in the WHO European region: past, present, and scenarios for the future. *Lancet. Infect. Dis.* **14**, 1271–1280 (2014).
117. H. Weissenböck *et al.*, Emergence of Usutu virus, an African Mosquito-Borne Flavivirus of the Japanese Encephalitis Virus Group, Central Europe. *Emerg. Infect. Dis.* **8**, 652–656 (2002).
118. B. Nikolay, M. Diallo, C. S. B. Boye, A. A. Sall, Usutu virus in Africa. *Vector Borne Zoonotic Dis.* **11**, 1417–23 (2011).
119. A. Vázquez, L. Franco, V. Sambri, M. Niedrig, H. Zeller, Usutu virus – potential risk of human disease in Europe. *Euro. Surveill.* **16**, pii: 19935 (2011).
120. M.-M. Garigliany *et al.*, Detection of Usutu virus in a bullfinch (*Pyrrhula pyrrhula*) and a great spotted woodpecker (*Dendrocopos major*) in north-west Europe. *Vet. J.* **199**, 191–3 (2014).
121. S. Chvala *et al.*, Monitoring of Usutu virus activity and spread by using dead bird surveillance in Austria, 2003–2005. *Vet. Microbiol.* **122**, 237–45 (2007).
122. A. M. Kilpatrick, P. Daszak, M. J. Jones, P. P. Marra, L. D. Kramer, Host heterogeneity dominates West Nile virus transmission. *Proc. Biol. Sci.* **273**, 2327–33 (2006).
123. L. Barbic *et al.*, Demonstration of Usutu virus antibodies in horses, Croatia. *Vector Borne Zoonotic Dis.* **13**, 772–4 (2013).
124. D. Cadar *et al.*, Usutu Virus in Bats, *Emerg. Infect. Dis.* **20**, 2013–2015 (2014).
125. W. Takken, B. G. J. Knols, *Emerging pests and vector-borne diseases in Europe* Wageningen Academic Publishers, 2007; vol 1
126. L. Allering *et al.*, Detection of Usutu virus infection in a healthy blood donor from south-west Germany. *Euro. Surveill.* pii: 20341 (2012).
127. P. Gaibani *et al.*, Detection of Usutu-virus-specific IgG in blood donors from northern Italy. *Vector Borne Zoonotic Dis.* **12**, 431–3 (2012).
128. B. Nikolay, M. Diallo, O. Faye, C. S. Boye, A. a Sall, Vector competence of Culex neavei (Diptera: Culicidae) for Usutu virus. *Am. J. Trop. Med. Hyg.* **86**, 993–6 (2012).
129. K. W. R. van Cleef *et al.*, Mosquito and Drosophila entomobirnaviruses suppress dsRNA- and siRNA-induced RNAi. *Nucleic Acids Res.* **42**, 8732–44 (2014).
130. D. Blankenberg *et al.*, Manipulation of FASTQ data with galaxy. *Bioinformatics*. **26**, 1783–1785 (2010).
131. B. Langmead, C. Trapnell, M. Pop, S. L. Salzberg, Ultrafast and memory-efficient alignment of short DNA sequences to the human genome. *Genome Biol.* **10**, R25 (2009).
132. N. L. Forrester, L. L. Coffey, S. C. Weaver, Arboviral Bottlenecks and Challenges to Maintaining Diversity and Fitness during Mosquito Transmission. *Viruses*. **6**, 3991–4004 (2014).
133. C. D. Blair, Mosquito RNAi is the major innate immune pathway controlling arbovirus infection and transmission. *6*, 265–277 (2012).
134. L. Lambrechts, K. P. Paaijmans, T. Fansiri, L. B. Carrington, L. D. Kramer, Impact of daily temperature fluctuations on dengue virus transmission by Aedes aegypti. *Proc. Natl. Acad. Sci. U. S. A.* **108**, 7460–5 (2011).
135. O. Schwartz, M. L. Albert, Biology and pathogenesis of chikungunya virus. *Nat. Rev. Microbiol.* **8**, 491–500 (2010).
136. M. M. Thiboutot *et al.*, Chikungunya: a potentially emerging epidemic? *PLoS Negl. Trop. Dis.* **4**, e623 (2010).
137. Center for Disease Control and Prevention. Countries and territories where chikungunya cases have been reported (Last updated December 2014). (available at <http://www.cdc.gov/>).
138. S. W. Metz *et al.*, Effective chikungunya virus-like particle vaccine produced in insect cells. *PLoS Negl. Trop. Dis.* **7**, e2124 (2013).

139. S. W. Metz *et al.*, Chikungunya virus-like particles are more immunogenic in a lethal AG129 mouse model compared to glycoprotein E1 or E2 subunits. *Vaccine*. **9**, 6092–6 (2013).
140. A. M. Powers, Chikungunya virus control: Is a vaccine on the horizon? *Lancet*. **384**, 2008–2009 (2014).
141. D. Hallengård *et al.*, Prime-Boost Immunization Strategies against Chikungunya Virus. *J. Virol.* **88**, 13333–13343 (2014).
142. S. C. Weaver, J. E. Osorio, J. A. Livengood, R. Chen, D. T. Stinchcomb, Chikungunya virus and prospects for a vaccine. *Expert Rev. Vaccines*. **11**, 1087–101 (2012).
143. G. P. Pijlman, Enveloped virus-like particles as vaccines against pathogenic arboviruses. *Biotech J.* **10**, doi:10.1002/biot.201400427.
144. L. J. Chang *et al.*, Safety and tolerability of chikungunya virus-like particle vaccine in healthy adults: A phase 1 dose-escalation trial. *Lancet*. **384**, 2046–2052 (2014).
145. M. Solignat, B. Gay, S. Higgs, L. Briant, C. Devaux, Replication cycle of chikungunya: a re-emerging arbovirus. *Virology*. **393**, 183–97 (2009).
146. E. I. Frolova, R. Gorchakov, L. Pereboeva, S. Atasheva, I. Frolov, Functional Sindbis virus replicative complexes are formed at the plasma membrane. *J. Virol.* **84**, 11679–95 (2010).
147. J. J. Fros, E. van der Maten, J. M. Vlak, G. P. Pijlman, The C-terminal domain of chikungunya virus nsP2 independently governs viral RNA replication, cytopathicity, and inhibition of interferon signaling. *J. Virol.* **87**, 10394–400 (2013).
148. J. J. Fros *et al.*, Chikungunya virus nonstructural protein 2 inhibits type I/II interferon-stimulated JAK-STAT signaling. *J. Virol.* **84**, 10877–10887 (2010).
149. I. Akhrymuk, S. V. Kulemzin, E. I. Frolova, Evasion of the innate immune response: the Old World alphavirus nsP2 protein induces rapid degradation of Rpb1, a catalytic subunit of RNA polymerase II. *J. Virol.* **86**, 7180–91 (2012).
150. J. J. Fros *et al.*, Chikungunya virus nsP2-mediated host shut-off disables the unfolded protein response. *J. Gen. Virol.* (2014), doi:10.1099/vir.0.071845-0.
151. H. Vihinen, J. Saarinen, Phosphorylation site analysis of Semliki forest virus nonstructural protein 3. *J. Biol. Chem.* **275**, 27775–83 (2000).
152. G. P. Li, M. W. LaStarza, W. R. Hardy, J. H. Strauss, M. Rice, Phosphorylation of Sindbis Virus nsP3 in vivo and in vitro. **427**, 416–427 (1990).
153. M. W. LaStarza, J. A. Lemm, C. M. Rice, Genetic Analysis of the nsP3 Region of Sindbis Virus : Evidence for Roles in Minus-Strand and Subgenomic RNA Synthesis. **68**, 5781–5791 (1994).
154. H. Malet *et al.*, The crystal structures of Chikungunya and Venezuelan equine encephalitis virus nsP3 macro domains define a conserved adenosine binding pocket. *J. Virol.* **83**, 6534–6545 (2009).
155. J. Aaskov, A. Jones, W. Choi, K. Lowry, E. Stewart, Lineage replacement accompanying duplication and rapid fixation of an RNA element in the nsP3 gene in a species of alphavirus. *Virology*. **410**, 353–9 (2011).
156. G. Shin, S. A. Yost, M. T. Miller, E. J. Elrod, A. Grakoui, Structural and functional insights into alphavirus polyprotein processing and pathogenesis. *Proc. Natl. Acad. Sci. U. S. A.* **109**, 16534–9 (2012).
157. K. Irvine, R. Stirling, D. Hume, D. Kennedy, Rasputin, more promiscuous than ever: a review of G3BP. *Int. J. Dev. Biol.* **48**, 1065–77 (2004).
158. A. Khong, E. Jan, Modulation of stress granules and P bodies during dicistrovirus infection. *J. Virol.* **85**, 1439–51 (2011).
159. J. J. Fros *et al.*, Chikungunya Virus nsP3 Blocks Stress Granule Assembly by Recruitment of G3BP into Cytoplasmic Foci. *J. Virol.* **86**, 10873–9 (2012).
160. M. D. Panas *et al.*, Sequestration of G3BP coupled with efficient translation inhibits stress granules in Semliki Forest virus infection. *Mol. Biol. Cell.* **23**, 4701–12 (2012).
161. A. Vega-Rúa, K. Zouache, R. Girod, A.-B. Failloux, R. Lourenço-de-Oliveira, High level of vector competence of *Aedes aegypti* and *Aedes albopictus* from ten American countries as a crucial factor in the spread of Chikungunya virus. *J. Virol.* **88**, 6294–306 (2014).
162. K. Zouache *et al.*, Three-way interactions between mosquito population, viral strain and temperature underlying chikungunya virus transmission potential. *Proc. Biol. Sci.* **281** (2014), doi:10.1098/rspb.2014.1078.
163. S. W. Metz *et al.*, Functional processing and secretion of Chikungunya virus E1 and E2 glycoproteins in insect cells. *J. Virol.* **8**, 353 (2011).

References

164. E. Frolova *et al.*, Formation of nsP3-specific protein complexes during Sindbis virus replication. *J Virol.* **80**, 4122–4134 (2006).
165. M. Varjak, E. Zusinaite, A. Merits, Novel functions of the alphavirus nonstructural protein nsP3 C-terminal region. *J. Virol.* **84**, 2352–64 (2010).
166. M. D. Panas, T. Ahola, G. M. McInerney, The C-terminal repeat domains of nsP3 from the Old World alphaviruses bind directly to G3BP. *J. Virol.* **88**, 5888–93 (2014).
167. T. Vogensen, I. R. Møller, O. Kristensen, Crystal structures of the human G3BP1 NTF2-like domain visualize FxFG Nup repeat specificity. *PLoS One.* **8**, e80947 (2013).
168. T. Vogensen, O. Kristensen, Crystal structure of the Rasputin NTF2-like domain from *Drosophila melanogaster*. *Biochem. Biophys. Res. Commun.* **420**, 188–92 (2012).
169. M. D. Panas *et al.*, Viral and Cellular Proteins Containing FGDF Motifs Bind G3BP to Block Stress Granule Formation. *PLOS Pathog.* **11**, e1004659 (2015).
170. I. M. Cristea *et al.*, Host factors associated with the Sindbis virus RNA-dependent RNA polymerase: role for G3BP1 and G3BP2 in virus replication. *J. Virol.* **84**, 6720–32 (2010).
171. F. E. M. Scholte *et al.*, Stress granule components G3BP1 and G3BP2 play a proviral role early in chikungunya virus replication. *J. Virol.*, JVI.03612–14 (2015).
172. R. Baumgartner, H. Stocker, E. Hafen, The RNA-binding proteins FMR1, rasputin and caprin act together with the UBA protein lingerer to restrict tissue growth in *Drosophila melanogaster*. *PLoS Genet.* **9**, e1003598 (2013).
173. A. Costa *et al.*, Rasputin functions as a positive regulator of orb in *Drosophila* oogenesis. *PLoS One.* **8**, e72864 (2013).
174. C. Pazman, C. A. Mayes, M. Fanto, S. R. Haynes, M. Mlodzik, Rasputin, the *Drosophila* homologue of the RasGAP SH3 binding protein, functions in Ras- and Rho-mediated signaling. **1725**, 1715–1725 (2000).
175. L. C. Reineke, R. E. Lloyd, The stress granule protein G3BP1 recruits PKR to promote multiple innate immune antiviral responses. *J. Virol.* (2014), doi:10.1128/JVI.02791-14.
176. J. P. White, A. M. Cardenas, W. E. Marissen, R. E. Lloyd, Inhibition of cytoplasmic mRNA stress granule formation by a viral proteinase. *Cell Host Microbe.* **2**, 295–305 (2007).
177. Z. Yi *et al.*, Hepatitis C virus co-opts Ras-GTPase-activating protein-binding protein 1 for its genome replication. *J. Virol.* **85**, 6996–7004 (2011).
178. N. L. Baird, J. York, J. H. Nunberg, Arenavirus infection induces discrete cytosolic structures for RNA replication. *J. Virol.* **86**, 11301–10 (2012).
179. W. Li *et al.*, Cell Proteins TIA-1 and TIAR Interact with the 3' J Stem-Loop of the West Nile Virus Complementary Minus-Strand RNA and Facilitate Virus Replication. **76**, 11989–12000 (2002).
180. A. M. Powers, C. H. Logue, Changing patterns of chikungunya virus: re-emergence of a zoonotic arbovirus. *J. Gen. Virol.* **88**, 2363–77 (2007).
181. J. D. Matthews, T. K. Frey, Analysis of subcellular G3BP redistribution during rubella virus infection. *J. Gen. Virol.* **93**, 267–74 (2012).
182. P. Anderson, N. Kedersha, Stress granules. *Curr. Biol.* **19**, 397–398 (2009).
183. M. E. Lindquist, A. W. Lifland, T. J. Utley, P. J. Santangelo, J. E. Crowe, Respiratory syncytial virus induces host RNA stress granules to facilitate viral replication. *J. Virol.* **84**, 12274–12284 (2010).
184. Z. Liang, G. Li, Recombinant Sindbis virus expressing functional GFP in the nonstructural protein nsP3. *Gene Ther. Mol. Biol.* **9**, 317–324 (2005).
185. G. M. McInerney, N. L. Kedersha, R. J. Kaufman, P. Anderson, P. Liljestro, Importance of eIF2alpha Phosphorylation and Stress Granule Assembly in Alphavirus Translation Regulation. *Mol. Biol. Cell.* **16**, 3753–3763 (2005).
186. N. Kedersha *et al.*, Stress granules and processing bodies are dynamically linked sites of mRNP remodeling. *J. Cell Biol.* **169**, 871–884 (2005).
187. M. Neuvonen *et al.*, SH3 domain-mediated recruitment of host cell amphiphysins by alphavirus nsP3 promotes viral RNA replication. *PLoS Pathog.* **7** (2011), doi:10.1371/journal.ppat.1002383.
188. M. C. Robinson, An epidemic of virus disease in Southern Province, Tanganyika Territory, in 1952–53. I. Clinical features. *Trans. R. Soc. Trop. Med. Hyg.* **49**, 28–32 (1955).
189. M. Enserink, Epidemiology. Tropical disease follows mosquitoes to Europe. *Science.* **317**, 1485 (2007).
190. P. Kujala *et al.*, Monoclonal antibodies specific for Semliki Forest virus replicase protein nsP2. *J. Gen. Virol.* **78** (Pt 2), 343–351 (1997).

191. J. H. Strauss, E. G. Strauss, The alphaviruses: gene expression, replication, and evolution. *Microbiol. Rev.* **58**, 491–562 (1994).
192. R. E. Randall, S. Goodbourn, Interferons and viruses: an interplay between induction, signalling, antiviral responses and virus countermeasures. *J. Gen. Virol.* **89**, 1–47 (2008).
193. J. D. Simmons *et al.*, Venezuelan equine encephalitis virus disrupts STAT1 signaling by distinct mechanisms independent of host shutoff. *J. Virol.* **83**, 10571–10581 (2009).
194. T. Couderc *et al.*, A mouse model for Chikungunya: young age and inefficient type-I interferon signaling are risk factors for severe disease. *PLoS Pathog.* **4**, e29 (2008).
195. D. L. Vanlandingham *et al.*, Development and characterization of a double subgenomic chikungunya virus infectious clone to express heterologous genes in *Aedes aegypti* mosquitoes. *Insect Biochem. Mol. Biol.* **35**, 1162–1170 (2005).
196. N. C. Shaner *et al.*, Improved monomeric red, orange and yellow fluorescent proteins derived from *Discosoma* sp. red fluorescent protein. *Nat. Biotechnol.* **22**, 1567–1572 (2004).
197. W. J. Liu, P. L. Sedlak, N. Kondratieva, A. A. Khromykh, Complementation analysis of the flavivirus Kunjin NS3 and NS5 proteins defines the minimal regions essential for formation of a replication complex and shows a requirement of NS3 in cis for virus assembly. *J. Virol.* **76**, 10766–10775 (2002).
198. S. Heinemann, B. Biesinger, B. Fleckenstein, J. C. Albrecht, NF- κ B signaling is induced by the oncoprotein t10 through direct interaction with TRAF6. *J. Biol. Chem.* **281**, 8565–8572 (2006).
199. P. King, S. Goodbourn, The beta-interferon promoter responds to priming through multiple independent regulatory elements. *J. Biol. Chem.* **269**, 30609–30615 (1994).
200. W. J. Liu *et al.*, Inhibition of interferon signaling by the New York 99 strain and Kunjin subtype of West Nile virus involves blockage of STAT1 and STAT2 activation by nonstructural proteins. *J. Virol.* **79**, 1934–1942 (2005).
201. A. Mogal, S. A. Abdulkadir, Effects of Histone Deacetylase Inhibitor (HDACi); Trichostatin-A (TSA) on the expression of housekeeping genes. *Mol. Cell Probes.* **20**, 81–86 (2006).
202. J. Desmyter, J. L. Melnick, W. E. Rawls, Defectiveness of interferon production and of rubella virus interference in a line of African green monkey kidney cells (Vero). *J. Virol.* **2**, 955–961 (1968).
203. J. Yin, C. L. Gardner, C. W. Burke, K. D. Ryman, W. B. Klimstra, Similarities and differences in antagonism of neuron alpha/beta interferon responses by Venezuelan equine encephalitis and Sindbis alphaviruses. *J. Virol.* **83**, 10036–10047 (2009).
204. C. Scagnolari *et al.*, The synergistic interaction of interferon types I and II leads to marked reduction in severe acute respiratory syndrome-associated coronavirus replication and increase in the expression of mRNAs for interferon-induced proteins. *Intervirology.* **50**, 156–60 (2007).
205. P. V Aguilar, S. C. Weaver, C. F. Basler, Capsid protein of eastern equine encephalitis virus inhibits host cell gene expression. *J. Virol.* **81**, 3866–3876 (2007).
206. E. I. Frolova *et al.*, Roles of Nonstructural Protein nsP2 and Alpha / Beta Interferons in Determining the Outcome of Sindbis Virus Infection. *J. Virol.* **76**, 11254–11264 (2002).
207. I. Stock, Chikungunya fever--expanded distribution of a re-emerging tropical infectious disease. *Med Monatsschr Pharm.* **32**, 17–26 (2009).
208. I. Frolov, Persistent infection and suppression of host response by alphaviruses. *Arch. Virol. Suppl.*, 139–147 (2004).
209. N. Garmashova *et al.*, The Old World and New World alphaviruses use different virus-specific proteins for induction of transcriptional shutoff. *J. Virol.* **81**, 2472–2484 (2007).
210. D. L. Sawicki, R. H. Silverman, B. R. Williams, S. G. Sawicki, Alphavirus Minus-Strand Synthesis and Persistence in Mouse Embryo Fibroblasts Derived from Mice Lacking RNase L and Protein Kinase R. **77**, 1801–1811 (2003).
211. R. H. Silverman, Viral encounters with 2',5'-oligoadenylate synthetase and RNase L during the interferon antiviral response. *J. Virol.* **81**, 12720–12729 (2007).
212. M. Mazzon, M. Jones, A. Davidson, B. Chain, M. Jacobs, Dengue virus NS5 inhibits interferon-alpha signaling by blocking signal transducer and activator of transcription 2 phosphorylation. *J. Infect. Dis.* **200**, 1261–1270 (2009).
213. C. M. Rice, R. Levis, J. H. Strauss, H. V. Huang, Production of infectious RNA transcripts from Sindbis virus cDNA clones: mapping of lethal mutations, rescue of a temperature-sensitive marker, and in vitro mutagenesis to generate defined mutants. *J. Virol.* **61**, 3809–3819 (1987).
214. B. Levine, J. E. Goldman, H. H. Jiang, D. E. Griffin, J. M. Hardwick, Bcl-2 protects mice against fatal alphavirus encephalitis. *Proc. Natl. Acad. Sci. U. S. A.* **93**, 4810–4815 (1996).

References

215. C. C. Cruz *et al.*, Modulation of type I IFN induction by a virulence determinant within the alphavirus nsP1 protein. *Virology*. **399**, 1–10 (2010).
216. J. J. Fros *et al.*, Chikungunya Virus nsP3 Blocks Stress Granule Assembly by Recruitment of G3BP into Cytoplasmic Foci. *J. Virol.* **86**, 10873–9 (2012).
217. M. Bourai *et al.*, Mapping of Chikungunya virus interactions with host proteins identified nsP2 as a highly connected viral component. *J. Virol.* **86**, 3121–34 (2012).
218. R. Gorchakov, E. Frolova, I. Frolov, Inhibition of transcription and translation in Sindbis virus-infected cells. *J. Virol.* **79**, 9397–9409 (2005).
219. M. N. Rozanov, E. V. Koonin, a. E. Gorbalenya, Conservation of the putative methyltransferase domain: a hallmark of the “Sindbis-like” supergroup of positive-strand RNA viruses. *J. Gen. Virol.* **73**, 2129–2134 (1992).
220. M. Gomez De Cedron, N. Ehsani, M. L. Mikkola, J. A. Garcia, L. Kääriäinen, RNA helicase activity of Semliki Forest virus replicase protein NSP2. *FEBS Lett.* **448**, 19–22 (1999).
221. R. Gorchakov *et al.*, A new role for ns polyprotein cleavage in Sindbis virus replication. *J. Virol.* **82**, 6218–6231 (2008).
222. J. Peranen, M. Rikkonen, P. Liljestrom, L. Kaariainen, Nuclear localization of Semliki Forest virus-specific nonstructural protein nsP2. *J. Virol.* **64**, 1888–1896 (1990).
223. M. Rikkonen, J. Peranen, L. Kaariainen, Nuclear targeting of Semliki Forest virus nsP2. *Arch. Virol. Suppl.* **9**, 369–377 (1994).
224. S. Atasheva, R. Gorchakov, R. English, I. Frolov, E. Frolova, Development of Sindbis viruses encoding nsP2/GFP chimeric proteins and their application for studying nsP2 functioning. *J. Virol.* **81**, 5046–57 (2007).
225. K. Tamm, A. Merits, I. Sarand, Mutations in the nuclear localization signal of nsP2 influencing RNA synthesis, protein expression and cytotoxicity of Semliki Forest virus. *J. Gen. Virol.* **89**, 676–686 (2008).
226. L. Pohjala *et al.*, Inhibitors of alphavirus entry and replication identified with a stable Chikungunya replicon cell line and virus-based assays. *PLoS One*. **6**, e28923 (2011).
227. J. D. Simmons, A. C. Wollish, M. T. Heise, A determinant of Sindbis virus neurovirulence enables efficient disruption of Jak/STAT signaling. *J. Virol.* **84**, 11429–11439 (2010).
228. L. K. White *et al.*, Chikungunya virus induces IPS-1-dependent innate immune activation and protein kinase R-independent translational shutoff. *J. Virol.* **85**, 606–20 (2011).
229. S. G. Sawicki, G. C. Godman, On the recovery of transcription after inhibition by actinomycin D. *J. Cell Biol.* **55**, 299–309 (1972).
230. K. Zhang, R. J. Kaufman, From endoplasmic-reticulum stress to the inflammatory response. *Nature*. **454**, 455–462 (2008).
231. D. Ron, P. Walter, Signal integration in the endoplasmic reticulum unfolded protein response. *Nat. Rev. Mol. Cell Biol.* **8**, 519–529 (2007).
232. K. Kohno, Stress-sensing mechanisms in the unfolded protein response: similarities and differences between yeast and mammals. *J. Biochem.* **147**, 27–33 (2010).
233. A. Bertolotti, Y. Zhang, L. M. Hendershot, H. P. Harding, D. Ron, Dynamic interaction of BiP and ER stress transducers in the unfolded-protein response. *Nat. Cell Biol.* **2**, 326–332 (2000).
234. M. J. Gething, Role and regulation of the ER chaperone BiP. *Semin. cell Dev. Biol.* **10**, 465–472 (1999).
235. H. P. Harding, M. Calton, F. Urano, I. Novoa, D. Ron, Transcriptional and translational control in the mammalian unfolded protein response. *Annu. Rev. Cell Dev. Biol.* **18**, 575–99 (2002).
236. K. M. Vattam, R. C. Wek, Reinitiation involving upstream ORFs regulates ATF4 mRNA translation in mammalian cells. *Proc. Natl. Acad. Sci. U. S. A.* **101**, 11269–74 (2004).
237. H. P. Harding *et al.*, Regulated translation initiation controls stress-induced gene expression in mammalian cells. *Mol. Cell.* **6**, 1099–108 (2000).
238. H. Yoshida, M. Oku, M. Suzuki, K. Mori, pXBP1(U) encoded in XBP1 pre-mRNA negatively regulates unfolded protein response activator pXBP1(S) in mammalian ER stress response. *J. Cell Biol.* **172**, 565–575 (2006).
239. A.-H. Lee, N. N. Iwakoshi, L. H. Glimcher, XBP-1 Regulates a Subset of Endoplasmic Reticulum Resident Chaperone Genes in the Unfolded Protein Response. *Mol. Cell. Biol.* **23**, 7448–7459 (2003).
240. A. L. Shaffer *et al.*, XBP1, downstream of Blimp-1, expands the secretory apparatus and other organelles, and increases protein synthesis in plasma cell differentiation. *Immunity*. **21**, 81–93 (2004).

241. K. Yamamoto, H. Yoshida, K. Kokame, R. J. Kaufman, K. Mori, Differential contributions of ATF6 and XBP1 to the activation of endoplasmic reticulum stress-responsive cis-acting elements ERSE, UPRE and ERSE-II. *J. Biochem.* **136**, 343–350 (2004).
242. K. Haze, H. Yoshida, H. Yanagi, T. Yura, K. Mori, Mammalian transcription factor ATF6 is synthesized as a transmembrane protein and activated by proteolysis in response to endoplasmic reticulum stress. *Mol. Biol. Cell.* **10**, 3787–3799 (1999).
243. H. Yoshida, T. Matsui, A. Yamamoto, T. Okada, K. Mori, XBP1 mRNA is induced by ATF6 and spliced by IRE1 in response to ER stress to produce a highly active transcription factor. *Cell.* **107**, 881–891 (2001).
244. K. Yamamoto *et al.*, Transcriptional induction of mammalian ER quality control proteins is mediated by single or combined action of ATF6alpha and XBP1. *Dev. Cell.* **13**, 365–376 (2007).
245. S. Takayanagi, R. Fukuda, Y. Takeuchi, S. Tsukada, K. Yoshida, Gene regulatory network of unfolded protein response genes in endoplasmic reticulum stress. *Cell Stress Chaperones.* **18**, 11–23 (2013).
246. J. A. Isler, A. H. Skalet, J. C. Alwine, Human Cytomegalovirus Infection Activates and Regulates the Unfolded Protein Response. *J. Virol.* **79**, 6890–6899 (2005).
247. G. Barry *et al.*, Semliki forest virus-induced endoplasmic reticulum stress accelerates apoptotic death of mammalian cells. *J. Virol.* **84**, 7369–77 (2010).
248. K. D. Tardif, K. Mori, A. Siddiqui, Hepatitis C Virus Subgenomic Replicons Induce Endoplasmic Reticulum Stress Activating an Intracellular Signaling Pathway. *J. Virol.* **76**, 7453–7459 (2002).
249. H. F. Burnett, T. E. Audas, G. Liang, R. R. Lu, Herpes simplex virus-1 disarms the unfolded protein response in the early stages of infection. *Cell Stress Chaperones.* **17**, 473–83 (2012).
250. R. L. Ambrose, J. M. Mackenzie, West Nile virus differentially modulates the unfolded protein response to facilitate replication and immune evasion. *J. Virol.* **85**, 2723–32 (2011).
251. D. J. Groskreutz, E. C. Babor, M. M. Monick, S. M. Varga, G. W. Hunninghake, Respiratory Syncytial Virus Limits α Subunit of Eukaryotic Translation Initiation Factor 2 (eIF2 α) Phosphorylation to Maintain Translation and Viral Replication. *J. Biol. Chem.* **285**, 24023–24031 (2010).
252. P. F. Horwood *et al.*, Outbreak of chikungunya virus infection, Vanimo, Papua New Guinea. *Emerg. Infect. Dis.* **19**, 1535–8 (2013).
253. M. McCarthy, First case of locally acquired chikungunya is reported in US. *BMJ.* **4706**, 4706 (2014).
254. J. Jose, J. E. Snyder, R. J. Kuhn, A structural and functional perspective of alphavirus replication and assembly. replication and assembly. *Future Microbiol.* **4**, 837–56 (2009).
255. F. E. M. Scholte *et al.*, Characterization of synthetic Chikungunya viruses based on the consensus sequence of recent E1-226V isolates. *PLoS One.* **8**, e71047 (2013).
256. S. C. Chang, A. E. Erwin, A. M. Y. S. Lee, Glucose-Regulated Protein (GRP94 and GRP78) Genes Share Common Regulatory Domains and Are Coordinately Regulated by Common trans-Acting Factors. *Mol. Cell Biol.* **9**, 2153–62 (1989).
257. R. Gorchakov, E. Frolova, B. R. G. Williams, C. M. Rice, I. Frolov, Mechanisms Are Involved in Translational Shutoff during Sindbis Virus Infection PKR-Dependent and -Independent Mechanisms Are Involved in Translational Shutoff during Sindbis Virus Infection. *J. Virol.* **78**, 8455–67 (2004).
258. T. Nivitchanyong, Y. C. Tsai, M. J. Betenbaugh, G. A. Oyler, An improved in vitro and in vivo Sindbis virus expression system through host and virus engineering. *Virus Res.* **141**, 1–12 (2009).
259. A. P. S. Rathore, M.-L. Ng, S. G. Vasudevan, Differential unfolded protein response during Chikungunya and Sindbis virus infection: CHIKV nsP4 suppresses eIF2 α phosphorylation. *Virol. J.* **10**, 36 (2013).
260. J. J. Berlanga *et al.*, Antiviral effect of the mammalian translation initiation factor 2alpha kinase GCN2 against RNA viruses. *EMBO J.* **25**, 1730–40 (2006).
261. Y. S. Poo *et al.*, CCR2 Deficiency Promotes Exacerbated Chronic Erosive Neutrophil-Dominated Chikungunya Virus Arthritis. *J. Virol.* **88**, 6862–6872 (2014).
262. P. A. Rudd *et al.*, Interferon response factors 3 and 7 protect against Chikungunya virus hemorrhagic fever and shock. *J. Virol.* **86**, 9888–98 (2012).
263. I. Ventoso *et al.*, Translational resistance of late alphavirus mRNA to eIF2alpha phosphorylation: a strategy to overcome the antiviral effect of protein kinase PKR. *Genes Dev.* **20**, 87–100 (2006).
264. R. Gorchakov, E. Frolova, B. R. G. Williams, C. M. Rice, I. Frolov, PKR-dependent and -independent mechanisms are involved in translational shutoff during Sindbis virus infection. *J. Virol.* **78**, 8455–67 (2004).

References

265. P. K. Das, A. Merits, A. Lulla, Functional Cross-talk between Distant Domains of Chikungunya Virus Non-structural Protein 2 Is Decisive for Its RNA-modulating Activity. *J. Biol. Chem.* **289**, 5635–53 (2014).
266. J. A. Smith, A new paradigm: innate immune sensing of viruses via the unfolded protein response. *Front. Microbiol.* **5**, 222 (2014).
267. M. J. Gonzalez-Hernandez *et al.*, Chemical Derivatives of a Small Molecule Deubiquitinase Inhibitor Have Antiviral Activity against Several RNA Viruses. *PLoS One.* **9**, e94491 (2014).
268. P. Parola *et al.*, Novel chikungunya virus variant in travelers returning from Indian Ocean islands. *Emerg Infect Dis.* **12**, 1493–1499 (2006).
269. M. Diallo, J. Thonnon, M. Traore-lamizana, D. Fontenille, Vectors of chikungunya virus in Senegal: current data and transmission cycles. *Am. J. Trop. Med. Hyg.* **60**, 281–286 (1999).
270. T. G. Andreadis, J. F. Anderson, C. R. Vossbrinck, Mosquito Surveillance for West Nile Virus in Connecticut , 2000 : Isolation from *Culex pipiens*, *Cx. restuans*, *Cx. salinarius*, and *Culiseta melanura*. *Emerg. Infect. Dis.* **7**, 670–674 (2001).
271. M. J. Turell, M. R. Sardelis, D. J. Dohm, M. L. O. Guinn, Potential North American Vectors of West Nile Virus. *Ann. N. Y. Acad. Sci.* **951**, 317–324 (2001).
272. E. R. Jacobson *et al.*, West Nile virus infection in farmed American alligators (*Alligator mississippiensis*) in Florida. *J. Wildl. Dis.* **41**, 96–106 (2005).
273. K. Klenk *et al.*, Alligators as West Nile Virus Amplifiers. *Emerg. Infect. Dis.* **10**, 2150–5 (2004).
274. E. Ariel, Viruses in reptiles. *Vet. Res.* **42**, 100 (2011).
275. M. R. Sardelis, M. J. Turell, D. J. Dohm, M. L. O. Guinn, Vector Competence of Selected North American *Culex* and *Coquillettidia* Mosquitoes for West Nile Virus. *Emerg. Infect Dis.* **7**, 1018–1022 (2001).
276. N. Nemeth, D. Gould, R. Bowen, N. Komar, Natural and experimental West Nile virus infection in five raptor species. *J. Wildl. Dis.* **42**, 1–13 (2006).
277. N. Komar *et al.*, Experimental Infection of North American Birds with the New York 1999 Strain of West Nile Virus. *Emerg. Infect. Dis.* **9**, 311–322 (2003).
278. R. Campbell, T. C. Thiemann, D. Lemenager, W. K. Reisen, Host-selection patterns of *Culex tarsalis* (Diptera: Culicidae) determine the spatial heterogeneity of West Nile virus enzootic activity in northern California. *J. Med. Entomol.* **50**, 1303–1309 (2013).
279. M. Rudolf *et al.*, First Nationwide Surveillance of *Culex pipiens* Complex and *Culex torrentium* Mosquitoes Demonstrated the Presence of *Culex pipiens* Biotype *pipiens/molestus* Hybrids in Germany. *PLoS One.* **8**, e71832 (2013).
280. U. Ashraf *et al.*, Usutu Virus: An Emerging Flavivirus in Europe. *Virusus.* **7**, 219–238 (2015).
281. K. Pesko, C. N. Mores, Effect of Sequential Exposure on Infection and Dissemination Rates for West Nile and St . Louis Encephalitis Viruses in *Culex quinquefasciatus*. *Vector Borne Zoonotic Dis.* **9**, 281–6 (2009).
282. B. G. Bolling, L. Eisen, C. G. Moore, C. D. Blair, Insect-specific flaviviruses from *Culex* mosquitoes in Colorado, with evidence of vertical transmission. *Am. J. Trop. Med. Hyg.* **85**, 169–77 (2011).
283. C. C. Khoo, J. B. Doty, N. L. Held, K. E. Olson, A. W. Franz, Isolation of midgut escape mutants of two American genotype dengue 2 viruses from *Aedes aegypti*. *Virol. J.* **10**, 257 (2013).
284. W. K. Reisen, Y. Fang, V. M. Martinez, Effects of temperature on the transmission of west nile virus by *Culex tarsalis* (Diptera: Culicidae). *J. Med. Entomol.* **43**, 309–17 (2006).
285. T. N. Lima-Camara *et al.*, Dengue infection increases the locomotor activity of *Aedes aegypti* females. *PLoS One.* **6**, e17690 (2011).
286. K. Lerdthusnee, A. W. Vaughn, Impact of dengue virus infection on feedong of *Aedes aegypti*. **57**, 119–125 (1997).
287. L. M. Styer, M. A. Meola, L. D. Kramer, West Nile virus infection decreases fecundity of *Culex tarsalis* females. *J. Med. Entomol.* **44**, 1074–1085 (2007).
288. E. Schnettler *et al.*, Noncoding flavivirus RNA displays RNA interference suppressor activity in insect and Mammalian cells. *J. Virol.* **86**, 13486–500 (2012).
289. G. P. Pijlman *et al.*, A highly structured, nuclease-resistant, noncoding RNA produced by flaviviruses is required for pathogenicity. *Cell Host Microbe.* **4**, 579–91 (2008).
290. S. L. Moon *et al.*, A noncoding RNA produced by arthropod-borne flaviviruses inhibits the cellular exoribonuclease XRN1 and alters host mRNA stability. *RNA.* **18**, 2029–2040 (2012).
291. A. Schuessler *et al.*, West Nile virus noncoding subgenomic RNA contributes to viral evasion of the type I interferon-mediated antiviral response. *J. Virol.* **86**, 5708–18 (2012).

292. A. Funk *et al.*, RNA structures required for production of subgenomic flavivirus RNA. *J. Virol.* **84**, 11407–17 (2010).
293. E. G. Chapman *et al.*, The Structural Basis of Pathogenic Subgenomic Flavivirus RNA (sfRNA) Production. *Science*. **344**, 307–310 (2014).
294. G. Carissimo *et al.*, Antiviral immunity of *Anopheles gambiae* is highly compartmentalized, with distinct roles for RNA interference and gut microbiota. *Proc. Natl. Acad. Sci.*, 201412984 (2014).
295. L. C. Reineke, J. D. Dougherty, P. Pierre, R. E. Lloyd, Large G3BP-induced granules trigger eIF2 phosphorylation. *Mol. Biol. Cell.* **23**, 3499–3510 (2012).
296. K. Onomoto *et al.*, Critical role of an antiviral stress granule containing RIG-I and PKR in viral detection and innate immunity. *PLoS One.* **7** (2012), doi:10.1371/journal.pone.0043031.
297. K. Bidet, D. Dadlani, M. a Garcia-Blanco, G3BP1, G3BP2 and CAPRIN1 Are Required for Translation of Interferon Stimulated mRNAs and Are Targeted by a Dengue Virus Non-coding RNA. *PLoS Pathog.* **10**, e1004242 (2014).
298. M. M. Emara, H. Liu, W. G. Davis, M. a Brinton, Mutation of mapped TIA-1/TIAR binding sites in the 3' terminal stem-loop of West Nile virus minus-strand RNA in an infectious clone negatively affects genomic RNA amplification. *J. Virol.* **82**, 10657–70 (2008).
299. S. C. Courtney, S. V Scherbik, B. M. Stockman, M. a Brinton, West Nile virus infections suppress early viral RNA synthesis and avoid inducing the cell stress granule response. *J. Virol.* **86**, 3647–57 (2012).
300. J. M. Pare *et al.*, Hsp90 Regulates the Function of Argonaute 2 and Its Recruitment to Stress Granules and P-Bodies. *Mol. Biol. Cell.* **20**, 3273–3284 (2009).
301. L.C. Reineke, R. E. Lloyd, The stress granule protein G3BP1 recruits protein kinase R to promote multiple innate immune antiviral responses. *J. Virol.* **89**, 2575–89 (2014).
302. K. Onomoto, M. Yoneyama, G. Fung, H. Kato, T. Fujita, Antiviral innate immunity and stress granule responses. *Trends Immunol.* **35**, 420–428 (2014).
303. M. S. Suthar, M. S. Diamond, M. Gale, West Nile virus infection and immunity. *Nat. Rev. Microbiol.* **11**, 115–28 (2013).
304. W. R. Hardy, J. H. Strauss, Processing the nonstructural polyproteins of sindbis virus: nonstructural proteinase is in the C-terminal half of nsP2 and functions both in cis and in trans. *J. Virol.* **63**, 4653–4664 (1989).
305. P. K. Das, A. Merits, A. Lulla, Functional Crosstalk between Distant Domains of Chikungunya Virus Non-Structural Protein 2 Is Decisive For Its RNA-Modulating Activity. *J. Biol. Chem.* **28**, 5635–53 (2014).
306. M. Rikonen, J. Peranen, L. Kaariainen, ATPase and GTPase activities associated with Semliki Forest virus nonstructural protein nsP2. *J. Virol.* **68**, 5804–5810 (1994).
307. L. Vasiljeva, A. Merits, P. Auvinen, L. Kääriäinen, Identification of a novel function of the Alphavirus capping apparatus. RNA 5'-triphosphatase activity of Nsp2. *J. Biol. Chem.* **275**, 17281–17287 (2000).
308. K. M. McBride, G. Banninger, C. McDonald, N. C. Reich, Regulated nuclear import of the STAT1 transcription factor by direct binding of importin- α . *EMBO J.* **21**, 1754–1763 (2002).
309. N. Au-Yeung, R. Mandhana, C. M. Horvath, Transcriptional regulation by STAT1 and STAT2 in the interferon JAK-STAT pathway. *Jak-Stat.* **2**, e23931 (2013).
310. L. A. Kelley, M. J. E. Sternberg, Protein structure prediction on the Web: a case study using the Phyre server. *Nat. Protoc.* **4**, 363–71 (2009).
311. R. Lu, W. C. Au, W. S. Yeow, N. Hageman, P. M. Pitha, Regulation of the promoter activity of interferon regulatory factor-7 gene. Activation by interferon and silencing by hypermethylation. *J. Biol. Chem.* **275**, 31805–31812 (2000).
312. K. A. Mowen *et al.*, Arginine Methylation of STAT1 Modulates IFN α/β -Induced Transcription. *Cell.* **104**, 731–741 (2001).
313. G. Holloway, T. T. Truong, B. S. Coulson, Rotavirus antagonizes cellular antiviral responses by inhibiting the nuclear accumulation of STAT1, STAT2, and NF-kappaB. *J. Virol.* **83**, 4942–51 (2009).
314. M. M. Arnold, M. Barro, J. T. Patton, Rotavirus NSP1 mediates degradation of interferon regulatory factors through targeting of the dimerization domain. *J. Virol.* **87**, 9813–21 (2013).
315. G. Holloway, V. T. Dang, D. A. Jans, B. S. Coulson, Rotavirus inhibits interferon-induced STAT nuclear translocation by a mechanism that acts after STAT binding to importin- α . *J. Gen. Virol.* (2014), doi:10.1099/vir.0.064063-0.
316. C. Schilte *et al.*, Type I IFN controls chikungunya virus via its action on nonhematopoietic cells. *J. Exp. Med.* **207**, 429–442 (2010).

References

- 317. N. B. Finter *et al.*, The use of interferon-alpha in virus infections. *Drugs*. **42**, 749–765 (1991).
- 318. N. Le May, M. Bouloy, Antiviral escape strategies developed by bunyaviruses pathogenic for humans. *Front. Biosci.* **1**, 1065–77 (2012).
- 319. European Centre for disease prevention and control, VBORNET, mosquito maps (available at www.ecdc.europa.eu).

Summary

Samenvatting

Summary

Two highly pathogenic arthropod-borne (arbo)viruses, West Nile virus (WNV) and chikungunya virus (CHIKV), recently (re-)emerged in both Europe and the Americas. This resulted in large-scale epidemics of severe encephalitic and arthritogenic human disease, respectively. Both viruses replicate in their vertebrate hosts and mosquito vectors to complete their respective transmission cycles. In mosquitoes, arbovirus infections lead to relatively high viral titres without causing notable disease symptoms or fitness costs, whereas virus replication in the vertebrate host initiates strong antiviral responses and can be highly pathogenic and sometimes deadly.

WNV is a flavivirus (family *Flaviviridae*; genus *Flavivirus*), that finds its origin in Africa. The introduction of lineage 1 WNV into North America in 1999 caused the largest outbreak of human neuroinvasive disease to date. In southern Europe, a highly pathogenic lineage 2 strain has recently established itself in 2010, causing annual outbreaks. Additionally, the related flavivirus Usutu virus (USUV), has also emerged in Europe. Both WNV and USUV are transmitted by mainly *Culex* mosquitoes between avian amplifying hosts, but also frequently infect humans and horses. USUV and WNV co-circulate in parts of southern Europe, but the distribution of USUV extends further into central and north-western Europe.

In this thesis the potential spread of both WNV lineages through Europe is investigated by determining how effectively north-western European common house mosquitoes (*Culex pipiens*) transmit WNV. The results were compared to the transmission rates of USUV. North-western European mosquitoes were found to be highly competent vectors for both pathogenic lineages of WNV, which underscores the epidemic potential of WNV in Europe. Interestingly, American *Culex pipiens* only efficiently transmitted WNV lineage 1 but not the European lineage 2, which indicates a high degree of genotype-genotype specificity in the interaction between virus and vector. Furthermore, by comparing blood meal infection with intrathoracic injection of mosquitoes with WNV, the differential transmission rates of WNV lineage 2 could be attributed to infection barriers at the midgut level. In the vector competence studies, European mosquitoes were also found to be highly competent for USUV transmission. Interestingly, at higher temperatures USUV infected significantly more mosquitoes as compared to WNV. This indicates that mosquitoes from WNV-free areas are intrinsically capable of transmitting both pathogenic WNV lineages and explains the current localized WNV activity in southern Europe.

In addition, the infection rates of WNV and USUV were both enhanced at higher temperatures. This implies further epidemic spread of WNV and/or USUV during periods with favourable climatic conditions. Finally, as both

viruses utilize the same vector and reservoir species, the higher infection rate of USUV suggests that this virus may precede WNV transmission in Europe. This presses the need for intensified surveillance of virus activity in current WNV-free regions and warrants increased awareness in the clinic throughout Europe

In contrast to WNV, CHIKV (Family *Togaviridae*; genus *Alphavirus*) is transmitted in an urban transmission cycle involving humans and two major mosquito species: *Aedes aegypti* and *Aedes albopictus*. These invasive, originally African and Asian mosquito species are the drivers of the recent CHIKV outbreaks in Europe and the Americas. The first autochthonous CHIKV transmission on the American continent was detected in late 2013 and by the end of 2014 over a million people were diagnosed with a CHIKV infection. In humans, CHIKV can cause high fever and incapacitating arthralgia. There are no vaccines or antiviral compounds available for human use against either CHIKV (or WNV) and broad-spectrum antiviral treatments have proven ineffective. To develop novel strategies that interrupt the CHIKV transmission cycle, it is key to understand how CHIKV replicates in both vertebrates host and the mosquito vector. The molecular mechanisms that determine effective viral replication in mosquitoes are largely unknown. By studying the intracellular localization of CHIKV non-structural protein 3 (nsP3) in insect cells, an interaction between nsP3 and the endogenous mosquito protein Rasputin was uncovered and elucidated. Both proteins were found to interact via two short amino acid repeats within the C-terminus of nsP3 and the NTF2-like domain of Rasputin, forming cytoplasmic nsP3-Rin granules. Silencing of endogenous Rasputin in live *Ae. albopictus* mosquitoes revealed that this protein is essential for CHIKV to effectively establish transmissible infections. This is the first reported function of mosquito Rasputin in arbovirus infection.

Vertebrate cells express two proteins that are homologue to mosquito Rasputin, namely Ras-GAP SH3 domain-binding protein (G3BP) 1 and 2. G3BP proteins are crucial components of mammalian stress granules (SG), which are RNA triage centers that form during environmental stress, leading to impaired translation of most mRNAs. In co-localization studies in mammalian cells it is shown how CHIKV nsP3 sequesters G3BP into viral nsP3-G3BP granules. By making G3BP unavailable, nsP3 inhibits a *bona fide* SG response. The evidence obtained in these studies contributes to the growing evidence that cellular SGs possess antiviral activity, yet at the same time indicate a novel, proviral role for Rasputin during infection of the mosquito vector.

In mammalian cells, cytoplasmic pattern recognition receptors (PRR) localize to SGs. These PRRs recognize specific viral molecular patterns and upregulate the expression of interferon (IFN), activating the most potent vertebrate antiviral response, the IFN-response. The IFN-response is sufficient to clear most arbovirus infections, but administering IFN in response to CHIKV infections is ineffective. Experiments in this thesis show that CHIKV replication is resistant to IFN once RNA replication has been established, because CHIKV actively prevents IFN-induced gene expression via the inhibition of the downstream JAK-STAT signaling pathway. In response to extracellular IFNs, this

pathway activates STAT proteins, which then dimerise and translocate to the nucleus to activate antiviral gene transcription. WNV and other flaviviruses have evolved specific mechanisms to evade and inhibit the IFN-response, while alphaviruses such as CHIKV cause general host shut-off to prevent antiviral gene expression. Clear evidence is now obtained that in addition to general host shut-off, CHIKV nsP2 inhibits the JAK-STAT signaling pathway in a specific manner. Genetic evidence is presented which reveals that nsP2 independently affects RNA replication, CHIKV induced host shut-off and cytopathicity, and JAK-STAT signaling. Additional data shows that the activation and nuclear translocation of STAT is unaffected by nsP2, but that the C-terminal domain of nsP2 within the nucleus is sufficient to quickly redirect STAT dimers out of the nucleus. This host shut-off-independent inhibition of IFN signaling by CHIKV nsP2 is likely to have an important role in viral pathogenesis.

In the final phase of viral replication, viral envelope proteins mature in the endoplasmic reticulum (ER) before they translocate to the plasma membrane. When the ER-protein folding load becomes too high, unfolded and misfolded proteins in the ER will activate the unfolded protein response (UPR). Transient expression of CHIKV envelope glycoproteins are now shown to have the potential to induce the UPR. The UPR aims to reduce general protein synthesis and increase the protein-folding capacity of the ER. CHIKV infection resulted in the phosphorylation of eukaryotic translation initiation factor 2, but did not increase the expression of well-known UPR target genes. In addition, functional X-box-binding protein 1 did not translocate into the nucleus during CHIKV infection. Individual expression of CHIKV nsPs revealed that nsP2 alone was sufficient to inhibit the UPR. Mutations that rendered nsP2 unable to cause host-cell shut-off prevented nsP2-mediated inhibition of the UPR. This indicates that initial UPR induction takes place in the ER but that expression of functional UPR transcription factors and target genes is efficiently inhibited by CHIKV nsP2.

Finally, this thesis describes how effectively potential mosquito vectors transmit the flaviviruses WNV and USUV and provides novel insights on the underlying molecular mechanisms that enable CHIKV to accomplish successful infections in both its human host and mosquito vector. The effective inhibition of the JAK-STAT signaling pathway, combined with host shutoff, induced by nsP2 provides a rationale for the ineffectiveness of broad-spectrum antivirals against acute arbovirus infections and suggests directing future antiviral drug development to more specific compounds that directly interfere with viral replication and transmission. The uncovered interaction between CHIKV nsP3 and Rasputin/G3BP may provide such a target as disturbing this interaction could potentially re-instate cellular stress responses and interfere with viral replication and transmission.

Samenvatting

Het Westnijl virus (WNV) en het chikungunya virus (CHIKV) zijn twee humaan pathogene virussen die hun oorsprong vinden in Afrika, en recentelijk grote uitbraken hebben veroorzaakt op de Europese en Amerikaanse continenten. Deze door muggen overgedragen virussen kunnen in mensen respectievelijk hersen(vlies)ontsteking en artritis veroorzaken. Om succesvol verspreid te kunnen worden, vermenigvuldigen deze virussen zich in de mug tot hoge concentraties, zonder ogenschijnlijke ziekteverschijnselen te veroorzaken. Echter, virusvermenigvuldiging in mensen en andere gewervelde dieren wekt een sterke antivirale afweer op, gaat samen met ziekteverschijnselen en kan soms de dood tot gevolg hebben.

WNV is een flavivirus (familie *Flaviviridae*; genus *flavivirus*) en is onder te verdelen in een aantal stammen (of lineages). In 1999 werd WNV voor het eerst aangetroffen op het Amerikaanse continent. Een lineage 1 WNV isolaat begon in New York (VS) en verspreidde zich al snel over het gehele continent, wat resulteerde in de grootste uitbraak van hersen(vlies)ontsteking ooit waargenomen. In 2010 kreeg een pathogeen lineage 2 WNV isolaat definitief voet aan de grond in Zuid Europa, waar het sindsdien voor jaarlijkse uitbraken zorgt. Een ander flavivirus, Usutu virus (USUV) heeft zich recentelijk gevestigd in Centraal Europa. USUV en WNV circuleren beiden tussen muggen van het *Culex* genus en vogels. Naast vogels dragen geïnfecteerde muggen beide virussen regelmatig over naar mensen en andere gewervelde dieren, waarvan de (soms dodelijke) gevolgen vooral merkbaar zijn in paarden en mensen. USUV en WNV co-circuleren in delen van Zuid Europa, maar alleen USUV vertoont regelmatige activiteit in Centraal en Noordwest Europa.

Dit proefschrift begint met het onderzoeken van de potentiële verspreiding van WNV richting Noordwest Europa door te meten hoe effectief de Nederlandse huissteekmug (*Culex pipiens*) is in de overdracht van WNV. Deze resultaten werden vergeleken met die van USUV. De resultaten laten zien dat Nederlandse huissteekmuggen erg goed in staat zijn beide pathogene lineage 1 en 2 WNV isolaten over te dragen. In tegenstelling waren Amerikaanse muggen alleen geschikt voor de overdracht van het Amerikaanse lineage 1 WNV isolaat en niet het Europese lineage 2 WNV isolaat. Dit impliceert dat specifieke virus-vector genotype-genotype interacties aan dit verschil ten grondslag liggen. De eerste cellen van de mug die geïnfecteerd moeten worden zijn de endotheelcellen van de maagwand. Wanneer infectie van deze cellen werd omzeild door virus direct in het lichaam van de mug te injecteren, resulteerde 100% van alle virus-vector combinaties in een volledige infectie die zich door de mug verspreidde tot in de speekselklieren. Dit impliceert dat de verschillen in ineffectiviteit van de geteste mug-virus combinaties in het abdomen veroorzaakt

worden. Naast WNV bleek de Nederlandse huissteekmug ook in staat om USUV effectief over te dragen. Beide virussen werden beter overgedragen wanneer de geïnfecteerde muggen geïncubeerd werden bij hogere temperaturen. Bij deze hogere temperaturen was USUV effectiever in het infecteren van *Culex* muggen vergeleken met WNV. Deze resultaten kunnen verklaren waarom WNV activiteit vooralsnog gelokaliseerd is gebleven in Zuid Europa. Het impliceert ook dat deze virussen zich in de toekomst verder zouden kunnen verspreiden wanneer de weersomstandigheden gunstig zijn. Omdat USUV en WNV dezelfde vogelreservoirs en muggensoorten kunnen gebruiken voor hun respectievelijke transmissiecycli, maar USUV bij hogere temperaturen de vector effectiever kan infecteren, heeft USUV een potentieel groter bereik dan WNV. Daarom kan de prevalentie van USUV als voorbode gezien worden voor toekomstige WNV activiteit. Het feit dat muggen uit een momenteel WNV-vrije zone (c.q. Noordwest Europa) effectieve vectoren voor WNV zijn benadrukt het risico op WNV uitbraken buiten Zuid Europa en accentueert de noodzaak voor goede controles op WNV activiteit en symptoombewustzijn in de klinieken.

In tegenstelling tot WNV wordt CHIKV (family *Togaviridae*; genus *alphavirus*) hoofdzakelijk overgedragen door de Aziatische tijgermug (*Aedes albopictus*) en de gelekoortsmug (*Aedes aegypti*) in een transmissiecyclus tussen muggen en mensen. Deze respectievelijk Aziatische en Afrikaanse muggensoorten waren ook de vectoren tijdens recente CHIKV uitbraken op het Europese en Amerikaanse continent. De eerste autochtone transmissie van CHIKV op het Amerikaanse continent is waargenomen in 2013. Eind 2014 waren er al meer dan een miljoen diagnoses van CHIKV infecties geteld. CHIKV veroorzaakt onder andere hoge koorts en hevige gewrichtspijnen. Er zijn op dit moment geen vaccins of antivirale middelen tegen CHIKV beschikbaar terwijl generieke antivirale middelen ontoereikend zijn gebleken. Het is daarom van belang om nieuwe strategieën te ontwikkelen die de transmissiecyclus kunnen onderbreken, waarbij kennis van de replicatiecyclus in menselijke maar ook muggen cellen van waarde is. Voornamelijk de moleculaire mechanismen die het lot van een virus bepalen in het insect zijn nog grotendeels onbekend.

Dit proefschrift laat zien hoe het niet-structurele eiwit 3 (nsP3) van CHIKV een interactie aangaat met het endogene muggeneiwit genaamd Rasputin. Beide eiwitten lieten een interactie met elkaar zien middels twee korte aminozuurvolgordes in de C-terminus van nsP3 en het NTF2 (nucleair transport factor 2)-like domein van het Rasputin eiwit. CHIKV infecties in levende *Aedes albopictus* muggen waren minder effectief wanneer de hoeveelheid beschikbaar Rasputin eiwit in deze muggen was verminderd. Dit impliceert dat de interactie tussen nsP3 en Rasputin een cruciale functie heeft tijdens CHIKV replicatie in de mug.

Cellen van mensen en andere gewervelde dieren brengen eiwitten tot expressie die homoloog zijn aan Rasputin, genaamd Ras-GAP SH3 domain-binding protein (G3BP) 1 en 2. Deze G3BP eiwitten zijn cruciale componenten van stress granula (SG). In stressvolle situaties reageert de cel door cytoplasmatische granula te vormen van RNA bindende eiwitten zoals G3BP,

mRNAs en translatie initiatie factoren. Het resultaat hiervan is een afname van de vertaling van de meeste mRNAs. CHIKV nsP₃ zorgt ervoor dat G3BP weliswaar naar granula migreert samen met nsP₃, echter deze granula bevatten geen translatie initiatie factoren en gedragen zich niet als functionele SG. Deze experimenten laten zien dat er een antivirale rol bestaat voor SG die geremd wordt door CHIKV nsP₃, maar ook dat de interactie met homoloog Rasputin een gunstig effect heeft op virale replicatie.

In SG in cellen van gewervelden bevinden zich ook receptoren die specifieke patronen van pathogenen herkennen. Na activatie zorgen deze receptoren voor de activatie van de aangeboren immuniteit via de expressie van interferon (IFN). De IFN-respons is uiterst effectief als afweermechanisme tegen vele virussen inclusief CHIKV en WNV, maar de toediening van IFN gedurende een infectie heeft vaak weinig tot geen effect. Dit proefschrift laat zien dat CHIKV RNA replicatie-resistent is tegen IFN wanneer dit wordt toegediend na infectie en dat dit wordt veroorzaakt door onderdrukking van de JAK-STAT (Janus kinase-signal transducer and activator of transcription) signaaltransductie route door CHIKV. In een niet-geïnfecteerde cel wordt de JAK-STAT signaal transductieroute geactiveerd door IFNs en leidt dit normaliter tot de expressie van vele antivirale genen. Alphavirussen zoals CHIKV staan er om bekend de algemene genexpressie van de gastheer te verminderen. Hier laten we zien dat het nsP₂ eiwit van CHIKV ook specifiek de JAK-STAT signaal transductieroute uitschakelt. Bovendien verschaffen we genetisch bewijs dat de C-terminus van CHIKV nsP₂ een onafhankelijke rol speelt in CHIKV RNA replicatie, de inhibitie van gastheer genexpressie en de blokkade van de JAK-STAT signaal transductie route. Ook laten we zien dat de activatie en nucleaire translocatie van STAT eiwitten niet wordt aangetast door nsP₂, maar dat de aanwezigheid van de C-terminus van nsP₂ in de celkern voldoende is om STAT eiwitten voortijdig weer de celkern uit te sturen. Deze inhibitie speelt daarom hoogstwaarschijnlijk een grote rol in the pathogenese van CHIKV infecties.

Tijdens de laatste fase van virale replicatie vinden de laatste modificaties aan de virale glycoproteïnen plaats in het endoplasmatisch reticulum (ER), alvorens deze naar het celmembraan getransporteerd worden. Het ER assisteert onder andere in de correcte vouwing van deze eiwitten. Wanneer er te veel eiwitten het ER moeten passeren, kunnen verkeerd gevouwen eiwitten accumuleren in het ER en de 'ongevouwen eiwit respons' (UPR, unfolded protein response) activeren. Alphavirus glycoproteïnes kunnen de UPR ook activeren. In een poging het aantal eiwitten in het ER te verminderen wordt dan algemene translatie verminderd met uitzondering van bepaalde eiwitten die assisteren bij vouwing. CHIKV infectie resulteerde in verminderde translatie via de fosforilatie van translatie initiatie factor eIF2 α , maar zorgde niet voor de activatie van UPR-specifieke transcriptiefactoren en remde de expressie van UPR-specifieke genen. Individuele expressie van CHIKV eiwitten toonde aan dat nsP₂ op zichzelf in staat was om de UPR te remmen. Door het aanbrengen van mutaties in nsP₂ werd duidelijk dat het inhiberen van de genexpressie van de gastheer hieraan ten grondslag ligt. Samengevat laat dit zien dat de UPR in

eerste instantie geactiveerd wordt door CHIKV, maar dat nsP2 de downstream effecten van de UPR efficiënt weet te remmen.

Concluderend beschrijft dit proefschrift in welke mate potentiële muggenpopulaties WNV en USUV kunnen overdragen en geeft het nieuwe inzichten in de moleculaire interacties die ervoor zorgen dat CHIKV succesvol zijn transmissiecyclus kan doorlopen. De effectieve uitschakeling van de JAK-STAT signaal transductie route, in combinatie met het inhiberen van de gastheer genexpressie verklaart waarom generieke antivirale middelen ineffectief zijn tegen CHIKV infecties. Dit suggereert dat de ontwikkeling van nieuwe antivirale middelen beter gericht kan worden op verbindingen met een meer specifieke werking. De interactie tussen CHIKV nsP3 en de Rasputin/G3BP eiwitten van de gastheer vormt hierbij een potentieel aangrijpingspunt, aangezien het verstoren van deze interactie de stress-respons van de gastheer kan herstellen en CHIKV replicatie en transmissie remt.

Abbreviations

List of abbreviations

arbovirus	arthropod-borne virus
AGO2	argonaute-2
ATF	Activating transcription factor
Ae.	<i>Aedes</i>
ActD	actinomycin D
AP	alkaline phosphatase
BiP	Ca ²⁺ -dissociated heavy-chain binding protein
CHOP	DNA damage-inducible protein C/EBP-homologous protein 10
C	Capsid
CHIKV	chikungunya virus
CPE	cytopathic effects
Cx.	<i>Culex</i>
CHX	cycloheximide
CMV	cytomegalo virus
CRM1	chromosome region maintenance 1
DENV	Dengue virus
Dcr-2	Dicer
dpi	days post infection
dsRNA	double-stranded RNA
EIP	extrinsic incubation period
eIF2 α	eukaryotic initiation factor 2 α
EGFP	enhanced green fluorescent protein
ER	endoplasmic reticulum
E	Envelope
FBS	fetal bovine serum
Fluc	firefly luciferase
FMDV	Foot-and-mouth disease virus
G3BP	Ras-GAP SH3 domain-binding protein
gRNA	genomic RNA
GAS	gamma activating sequence
Gr'10	WNV isolate Greece 2010
GRP	glucose regulated protein
hpt	hours post transfection
hpi	hours post infection
IMD	immune deficiency pathway
IFN	interferon
IRF	IFN response factor
IFNAR	IFN alpha receptor
ISRE	IFN-stimulated response element

ISG	IFN-stimulated gene
IRE1 α	inositol-requiring 1 α
IFA	immunofluorescence assay
IU	international units
JAK	Jannus kinase
JEV	Japanese encephalitis virus
LGTV	Langat virus
LCCM	Langerhans cell conditioned medium
MDA5	melanoma differentiation-associated gene 5
mRNP	messenger ribonucleoproteins
MOI	multiplicity of infection
MEF	mouse embryonic fibroblasts
MIB	midgut infection barrier
MEB	mesenteron escape barrier
nsP	non-structural protein
NWE	north-western Europe
NA	North American
NLS	nuclear localization signal
NY'99	WNV isolate New York 1999
NTF2	nuclear transport factor 2
OAS	2'-5'-oligoadenylate synthetase 2
ONNV	O'nyong nyong virus
ORF	open reading frame
PB	processing body
PxxPxR	consensus sequence of SH3 domain-binding motif
PKR	protein kinase R
pfu	plaque forming unit
PBS	phosphate-buffered saline
PERK	protein kinase R-like ER kinase
PRR	pattern recognition receptor
PIAS	protein inhibitors of activated STAT1
RIG-I	retinoic acid-inducible gene I
Rin	Rasputin
RH	relative humidity
RNA	Ribonucleic acid
RNAi	RNA interference
RC	replication complex
RRM	RNA recognition motif
RGG	arginine glycine-rich box
Rluc	Renilla luciferase
RRV	Ross River virus
RPB1	DNA-directed RNA polymerase II subunit rpb1
RT	room temperature
RISC	RNA silencing complex

List of Abbreviations

siRNA	small-interfering RNA
SINV	Sindbis virus
SFV	Semliki Forest virus
SG	stress granule
SDS	sodium dodecyl sulfate
<i>sf</i>	<i>Spodoptera frugiperda</i>
SH-3	Src homology-3
sgRNA	subgenomic RNA
STAT	Signal Transducers and Activators of Transcription
S	spliced XBP1 mRNA
SLEV	St Louis encephalitis virus
sfRNA	subgenomic flavivirus RNA
ssRNA	single-stranded RNA
TCID	tissue culture infectious dose
tm	tunicamycin
T	total XBP1 mRNA
TIA-1	T cell intracellular antigen-1
TIAR	TIA1-related protein
TLR	Toll-like receptor
Tyk 2	Tyrosine kinase 2
TBEV	tick borne encephalitis virus
U	unspliced XBP1 mRNA
USUV	Usutu virus
UTR	untranslated region
UPR	unfolded protein response
VC	vectorial capacity
VSR	viral suppressors of RNAi
viRNA	virus-derived siRNA
VEEV	Venezuelan Equine Encephalitis virus
WNV	West Nile virus
WB	western blot
XBP1	X-box binding protein 1
YFV	yellow fever virus

Dankwoord

Dankwoord

In eerste instantie was ik niet van plan om in Wageningen te gaan promoveren, maar tijdens mijn MSc thesis bij virologie werd al snel duidelijk dat je op een hele prettige manier onderzoek kunt doen in Wageningen. De sfeer van de hele groep, de manier van werken en de mogelijkheid een eigen invulling aan het project te geven hebben me destijds toch overgehaald in Wageningen te blijven en het promotietraject in te gaan. Vier jaar zijn in rap tempo voorbij gevlogen, maar kunnen niet besloten worden voordat ik een poging heb gedaan om iedereen te bedanken voor zijn/haar bijdrage aan dit proefschrift.

Op de eerste plaats wil ik **Gorben** bedanken. Als begeleider van mijn MSc thesis was jij voor een groot deel verantwoordelijk voor de goede indruk die het laboratorium van virologie destijds bij mij heeft achtergelaten. Als klap op de vuurpijl wist je ook mijn promotieplek te creëren en mij over te halen om toch maar in Wageningen te blijven. Terugkijkend heb ik van die keuze absoluut geen spijt. De afgelopen vier jaar verliepen naar mijn mening erg soepel en onze samenwerking was wat mij betreft meer dan uitstekend. Zo creëer je voor al je AIOs de ruimte en middelen voor verdere ontwikkeling en ben je altijd te porren voor gekke nieuwe experimenten. Zet daarnaast alle internationale werkbesprekingen en conferenties, waar de vele nieuwe wetenschappelijke inzichten en contacten die alleen maar voorbijgestreefd werden door het aantal nieuwe rondjes en je bent wat mij betreft een ideale begeleider. Om maar met de bekende laatste woorden te eindigen: Bedankt Chef!

Een promotie kan natuurlijk niet zonder promotor, of in dit geval promotoren. **Just** en **Willem**, ik wil jullie dan ook hartelijk bedanken dat jullie dit project mede mogelijk hebben gemaakt. Op de momenten dat het nodig was waren jullie altijd aanwezig en met name tijdens de laatste fase, het afronden van het proefschrift, waren jullie vlot met commentaar en suggesties en was er altijd minstens één van jullie paraat. Ik hoor weleens dat er een inverse correlatie bestaat tussen het aantal begeleiders en het succes van het project, maar niets is minder waar. Beide heren professoren, heel erg bedankt!

Sander, jij hebt natuurlijk ook een grote bijdrage geleverd tijdens het opzetten van dit project en het BSL₃ laboratorium. Buiten dat om, waren de eerste twee hoofdstukken van het proefschrift nooit tot stand gekomen zonder jouw muggenlijnen en input. Succes met het vervolg van het vectoren werk en ik hoop dat ik heb kunnen bijdragen aan een vruchtbare toekomstige samenwerking tussen entomologie en virologie.

Chantal, ook jij hebt natuurlijk enorm bijgedragen aan de eerste twee

hoofdstukken van dit proefschrift. Je kreeg het altijd voor elkaar om zelfs mijn meest slecht geplande experimenten van voldoende muggen te voorzien, heel erg bedankt daarvoor. Je bent nu zelf ook al een tijdje flink uren aan het maken in het BSL₃ en ik weet zeker dat daar straks een mooi proefschrift uit komt. Succes!

Dan mevrouw de professor, **Monique**: ook al was je niet direct betrokken bij mijn project, vaak naar aanleiding van een maandagochtendseminar hebben we toch een aantal goede discussies gehad. Na de wisseling van de wacht op virologie heb je ook een aantal zaken voor mij persoonlijk heel goed weten te regelen, waarvoor veel dank!

Dan zijn we aanbeland bij de vrouw die alleen maar bestaat uit rechterhanden, **Corinne**. Niet alleen ben je een enorm efficiënte labmanager en kundige analist voor de hele arbo-groep, maar ook een goede vriendin en chauffeur. Ik kon bij jou altijd mee rijden, zelfs met racefiets en bakken yoghurt en dan in de auto nog eens heerlijk klagen over alle andere gekken (...) achter het stuur. Mislukte kloner exercities werden feilloos opgelost en titraties in het BSL₃ lab gingen twee keer zo snel met jouw hulp. Helaas voor mij kon je de laatste tijd niet meer helpen in het BSL₃, maar dat is je uiteraard vergeven. Ik wil jou en Simon dan ook nog heel veel plezier wensen met Pepino pequeño en jullie moeten maar eens snel whisky (en appelsap) komen drinken.

Mia, jij stond letterlijk altijd aan mijn zijde. Het zal wel even wennen zijn om het straks zonder dat gezellige gekakel te moeten stellen. Niet alleen op het lab, maar ook in de kroeg was je altijd goed gezelschap. Nu ik niet meer naast je sta te pipetteren moeten we maar zo vaak mogelijk in de kroeg afspreken. Maar ook de etentjes, taartjes, worstenbroodjes en reserve tandenborstels zijn absoluut niet vergeten. Hopelijk kunnen we straks de rollen omdraaien en kom je bij mij op visite en wie weet, als jij je vierkante broek aan trekt kun je misschien wel verblijven in een grote ananas. Dat er over een jaar een goed boekje ligt is zeker. Hopelijk komt daar de laatste grote knaller ook nog in, succes!

Stefan sinds jij ons hebt verlaten miste ik toch wel een bepaald soort humor op de werkvloer. Ook de scherpe discussies, de lekkere nummertjes en de galmende stem van Elvis in het lab hebben enorm bijgedragen aan dit proefschrift. Je bent al lekker aan het knallen in het beloofde land, maar mocht je in de buurt zijn, staat er altijd een goed glas whisky klaar.

Double doctor **Amaya**, when you took Stefan's desk, officially surrounding me with only women, I must admit, I feared the worst (notice the correct use of the word worst), but you proved to be a wonderful addition to our corner. You have become a good friend and I hope to see you more often either in the Netherlands, Scotland or Spain!

Giel, ik weet zeker dat de arbo-groep met jou weer een paar jaar aan de weg kan

timmeren. Daarnaast ben je ook een gezellige aanwinst en heb je de vrouwelijke ban van de arbo-groep weten te doorbreken. Natuurlijk ben ik niet alleen maar altruïstisch, ik ben ook heel blij dat zo'n goed opgeleide MSc een aantal van mijn lopende projecten en pilot proeven een goed vervolg kan gaan geven. Heel veel succes, maar dat komt vast wel goed.

Dryas, Athos, Paulus, Han, Stineke and **Patrick**, you all have been around the virology lab together with me for a substantial amount of time. You are an incredibly colourful bunch and I had lots of fun making movies, playing soccer, having drinks, or just chit-chatting around the lab and coffee table. **Athos**; you are particularly colourful, with your dark humour. I have really enjoyed all of your complaining. I guess you're up next, so good luck mate. **Corien** en **Bob**, onze tijd samen is erg kort geweest, maar ik vond het leuk om toch nog even de nieuwe viro leden te hebben leren kennen.

De rest van de vaste staf, **Vera, Richard, Jan, Marleen, Dick, Dick, Els** en **Hanke**, er is niemand van jullie die niet heeft bijgedragen in gezelligheid of wetenschap. Dus heel erg bedankt daarvoor.

Dan wil ik al mijn MSc en BSc studenten bedanken. Jullie hebben in meer of mindere mate je steentje bijgedragen aan dit proefschrift. Helaas heb ik niet al jullie werk kunnen opnemen, maar het wordt daarom niet minder gewaardeerd. **Erika, Hetty, Jeroen, Christel, Ruud, Sabine, Sabine, Sjoerd, Wouter, Leontien** en **Daniël** heel erg bedankt. In addition I have to thank three other ex-MSc students of virology: **Jacky, Jim** en **Natalia**. Your work has greatly contributed to this thesis, it is still fruitful today, and without it we would have never been on the cover of JVI!

Besides the people at virology and entomology in Wageningen I cannot forget the growing list of collaborators, from which I just want to highlight **Martijn, Florine, Andreas, Lee, Alex, Ronald, Pascal, Ab, Byron, Anna-Bella** and **Karima**. Thanks for all your experimental contributions, input, and discussions and I am looking forward to more collaborations in the future.

Then I would also like to thank all the people who made my time in Wageningen enjoyable. With a special mentioning of **Olaf, Pier, Marco** and partners. The sexy pasta, dinner parties, Mario cart and our poor choice in action movies will not be forgotten. **Bart, Bas, Bosse** en de **Wajos** met barbecues, fietstochtjes en de laatste jaren vooral het jaarlijkse Wajo weekend als hoogtepunt. Volgende keer in Schotland! The members of the tripod, **Jeroen, Peter** en **Marcela**. We have already been to most continents together sharing some great experiences and sometimes tiny little tents. Marcelita you are the fourth, smallest and most talkative member of the tripod and I have the deepest respect for your ability to withstand our company and still smile as much as you do! Jeroen bij jou stond de deur altijd voor me open en Peter, wie had ooit gedacht dat we nog eens als coauteurs op een manuscript zouden staan. Wat ik vooral wil zeggen

is enorm bedankt voor alle fitness, bier en bitterballen sessies, het was niet het zelfde geweest zonder jullie. You guys will keep hearing from me when I visit the Netherlands, and I propose that we keep doing what we do best, Cheers!

Lieve **Pa** en **Ma**, de wetenschap werd er thuis al vroeg ingebracht, of we nu een hut wilden bouwen of weer een maf huisdier wilden onderhouden, zolang er van te voren voldoende onderzoek naar gedaan werd was bijna alles mogelijk. Jullie onvoorwaardelijke steun heeft er voor gezorgd dat (ik nog altijd denk dat) nog steeds bijna alles mogelijk is. Daarnaast heeft de Fros farm zich de laatste jaren ontwikkeld tot een rustiek landhuis waar ik altijd mijn toevlucht kon zoeken als ik weer eens te lang in het lab had gestaan of niet meer naar huis kon rijden na een uit de hand gelopen vrijdagmiddagborrel. Ik wil jullie en ook de rest van de familie daar dan ook heel erg voor bedanken. In het bijzonder, **Fenke**, jij hebt fantastisch werk geleverd om mijn ideeën om te zetten in een, naar mijn mening, hele mooie cover.

Annelientje, ik mag van geluk spreken dat je het al zo lang met mij uit weet te houden, dat is pas een echte prestatie. Ontzettend bedankt voor de leuke tijd die we hebben gehad en ik weet zeker dat er nog veel zullen volgen. Ook je familie mag ik niet vergeten, jullie stonden altijd paraat voor taalkundig advies, een goed glas wijn, barbecue of andere gezelligheid. Bedankt allemaal!

Curriculum Vitae

About the author

Jelke Jan Fros was born on December 25th, 1985 in Ede. After attending primary and high school in Wageningen, he started his studies in Psychology at the University of Groningen in 2004. After completion of the first year, he switched to Life Sciences and Technology in 2005, whereupon he completed his Bachelor's degree with an internship at TNO in 2008. He then returned to Wageningen for his Master's degree in Biotechnology at Wageningen University. He researched and wrote his thesis on 'the inhibition of the JAK-STAT pathway by chikungunya virus non-structural proteins' at the laboratory of virology in Wageningen, for which he won the MSc thesis award from the Wageningen University Fund. After this he started an internship at the QIMR Berghofer medical research institute in Brisbane, Australia, under the supervision of prof. A. Suhrbier, working on chikungunya virus and the unfolded protein response. He graduated *cum laude* in 2010 and continued his research on arboviruses in a collaborative PhD between the laboratories of Virology and Entomology at Wageningen University, under the supervision of prof. J.M. Vlak, prof. W. Takken and dr. G.P. Pijlman. During this time, he performed experiments with chikungunya and West Nile virus infections in both mammalian and insect cell culture systems as well as in live mosquitoes. His research led to various publications, and was presented at several international scientific conferences, including the chikungunya 2013 conference for which he received the young investigators award. After receiving his doctoral degree, Jelke will spend four weeks in Sierra Leone, contributing to diagnostics for the detection of ebola virus. He will then start his post-doctoral research at the Roslin Institute in Edinburgh, under supervision of prof. P. Simmonds.

List of Publications

Fros, Jelke J, Lee D Major, Florine E M Scholte, Joy Gardner, Martijn J van Hemert, Andreas Suhrbier, and Gorben P Pijlman. 2014. "**Chikungunya Virus nsP2-Mediated Host Shut-off Disables the Unfolded Protein Response.**" *The Journal of General Virology* 96 (Pt 3): 580-9.

Van Cleef, Koen W R, Joël T van Mierlo, Pascal Miesen, Gijs J Overheul, **Jelke J Fros**, Susan Schuster, Marco Marklewitz, Gorben P Pijlman, Sandra Junglen, and Ronald P van Rij. 2014. "**Mosquito and Drosophila Entomobirnaviruses Suppress dsRNA- and siRNA-Induced RNAi.**" *Nucleic Acids Research* 42 (13): 8732-44.

Fros, Jelke J, Erika van der Maten, Just M Vlak, and Gorben P Pijlman. 2013. "**The C-Terminal Domain of Chikungunya Virus nsP2 Independently Governs Viral RNA Replication, Cytopathicity, and Inhibition of Interferon Signaling.**" *Journal of Virology* 87 (18): 10394-400.

Fros, Jelke J, Natalia E Domeradзка, Jim Baggen, Corinne Geertsema, Jacky Flipse, Just M Vlak, and Gorben P Pijlman. 2012. "**Chikungunya Virus nsP3 Blocks Stress Granule Assembly by Recruitment of G3BP into Cytoplasmic Foci.**" *Journal of Virology* 86 (19): 10873-9.

Fros, Jelke J, Wen Jun Liu, Natalie A Prow, Corinne Geertsema, Maarten Ligtenberg, Dana L Vanlandingham, Esther Schnettler, Just M Vlak, Andreas Suhrbier, Alexander A Khromykh, and Gorben P Pijlman. 2010. "**Chikungunya Virus Nonstructural Protein 2 Inhibits Type I/II Interferon-Stimulated JAK-STAT Signaling.**" *Journal of Virology* 84 (20): 10877-87.

Fros, Jelke J, Corinne Geertsema, Chantal B Vogels, Peter P Roosjen, Anna-Bella Failloux, Just M Vlak, Constantianus J Koenraadt, Willem Takken and Gorben P Pijlman. "**West Nile virus: High chance of transmission by north-western European mosquitoes warrants increased surveillance and awareness.**" *Submitted.*

Fros, Jelke J, Chantal B Vogels, Constantianus J Koenraadt, Willem Takken and Gorben P Pijlman. "**Usutu virus, highly transmissible by common house mosquitoes and a prelude to WNV activity in Europe.**" *Manuscript in prep.*

Fros, Jelke J, Corinne Geertsema, Karima Zouache, Jim Baggen, Natalia Domeradзка, Jacky Flipse, Just M Vlak, Anna-Bella Failloux and Gorben P Pijlman. "**Mosquito Rasputin interacts with chikungunya virus nsP3 and determines the infection rate in Aedes albopictus.**" *Manuscript in prep.*

Training activities



Review of literature and writing of the project proposal

Arbovirus-host interactions

Post-graduate courses, competence strengthening and laboratory training

Safe handling of radioactive materials and sources

Hands-on molecular graphics

ISGlobal course on arboviral diseases

Bedrijfschulperlening

Making great scientific illustrations

Working with mosquitoes under biosafety level 3 conditions at the Institute Pasteur

Invited review of (unpublished) journal manuscript

Archives of Virology

Journal of Virology

PLoS NTD

International conferences and other scientific meetings

American society of virology 31 annual conference, USA (2012)*

22nd Annual meeting of the society for virology, Germany (2012)*

Gordon conference, viruses and cells, Italy (2013)**

Chikungunya, Malaysia (2013)*

American society of virology 33 annual conference, USA (2014)*

Yearly entomology laboratory research exchange meeting (2011)*

FP7 Vectorie meetings (2011-2013)

Dutch annual virology symposium (2011-2014)

FP7 Vectorie workshop (2013)

PE&RC Days (2011-2015)

Teaching activities

Cell biology and health (2011, 2012)

Molecular virology (2011-2013)

Immunotechnology (2013, 2014, 2015)

Supervision of 10 MSc and 2 BSc students during their thesis

* Oral, ** Poster

The research described in this thesis was carried out at the Laboratories of Virology and Entomology at Wageningen University, The Netherlands, and was financially supported by the European 195 Community's Seventh Framework Programme (FP7 VECTORIE project number 261466).

Cover

Fotographs: Mosquitoes Hans Smid (Bugsinthepicture.com), Microscopy Jelke J. Fros. Design: Fenke N. Fros and Jelke J. Fros

Printed by Gildeprint Drukkerijen, Enschede, The Netherlands

